BMI-1598

PROPERTIES OF FUELS FOR HIGH-TEMPERATURE REACTOR CONCEPTS

BATTELLE MEMORIAL INSTITUTE

DISCLAIMER

CORRIGENDA

BMI-1598, PROPERTIES OF FUELS FOR HIGH-TEMPERATURE REACTOR CONCEPTS

July 1, 1963

Please attach to report or make the following changes on the appropriate pages.

Page

6 Fuel Comparison Table: Substitute the following values for the thermal conductivities for UO_2 in cal/(sec)(cm)(C): 0.026 at 20 C, 0.008 at 600 C, 0.005 at 1200 C.

11 Section C6: Rupture time for 1600 F should be 60.2 instead of 602.

17 Section C6: Revise as follows:

Temperature, F	Stress for Creep Rate Shown, psi			Rupture Data	
	0.001 Per Cent per Hr	0.01 Per Cent per Hr	0.1 Per Cent per Hr	Stress, psi	Rupture Time, hr
1600	9,800	14,900	22,000	30,000	38.7
1800	7,800	10,000	13,000	20,000	27.2
				15,000	169.7

53 Table G2: Add the superscript (b) to the 4.8 entry, last line in first column, and place the following footnote below the table:

(b) Reaction between UC and tantalum container resulted in the large density change shown, and also affected the fission-gas release.

65 Section B6a: Vaporization equation for above 2000 K should read :

$$\log p \text{ (mm Hg)} = 13.298 - \frac{3.7195 \times 10^4}{T} + \frac{3.5612 \times 10^6}{T^2} + \frac{2.6178 \times 10^9}{T^3}$$

77 Figure D2b: Chalk River curve should be labeled "UO_2"; thermal-conductivity unit on ordinate should read: w/(cm)(C).

82 Section F2e should read: Stainless steel No reaction at 2400 F.
Tungsten fast reaction at 2065 C.

84 Section G2b(3) should have appended at the end of the sentence: "...at temperatures up to 3000 F."

84 Section G2c: Next to last line on the page insert "observed" between the words differences and between and "(for in-pile release)" between the words models and is.

109 Section A3, second line correction: "characteristics" instead of "characreristics".

111 Table C5 correction: "BeO" instead of "Beo".

CORRIGENDA (Continued)

Page

117 Section G5a: Delete from next-to-last sentence: . . . "and UO_2 loses its crystallinity in the range of 36 to 64 x 10^{20} fission fragments per cm^3".

118 Table G1: Last two entries in column headed "Comments" should read, respectively: $Be(OH)_2$-UO_2 and BeO-UO_3.

121 & 122 Tables G5a, G5b, and G5c: Unit for column headed "Fission Burnup" should read a/o U.

127 Reference (2): First author should read: Stubbs, F. J. instead of Stubbs, T. J.

128 Table 1: Footnote (a) should be changed to read "Capsule probably leaked".

162 Table G1: Add superscript (f) to Core-to-Cladding Ratio$^{(f)}$ column heading and add the following footnote:

(f) Ratio of core dimension to total cladding dimension for each indicated dimension.

194 Fourth line: Change "Table 2 contains" to "Tables 2A and 2B contain".

195 Table 2: Change title to "Table 2A" and delete "Nominal" in Irradiation Temperature column heading. Add to the bottom of Table 2A on page 195 the following footnotes:

(a) Listed in order of preparation in the case of multiple coatings.
(b) Rate of isotope release divided by rate of generation. Values listed are the release ratios at the end of the indicated time.

196 Table 2 (Continued): Delete entire page and replace with Table 2B.

197 Line 4, sixth paragraph: Replace "the" with "some" in the phrase "the pyrolytic-carbon-coated particles".

197 Last line of sixth paragraph should carry a citation for reference (8).

202 Add Reference (8): Oak Ridge National Laboratory, "Gas-Cooled Reactor Program Quarterly Progress Report for Period Ending December 31, 1961", ORNL-3254 (April 6, 1962), pp 161-165.

203 Volume Conversions: ft^2 should be ft^3.

204 Add the following conversion to list of fission units:

$$\text{Fissions per } cm^3 \text{ of alloy} = \left(\frac{\text{a/o burnup of uranium atoms present}}{100}\right)\left(\frac{\text{w/o uranium in the alloy}}{100}\right)\left(\text{density of the alloy}\right)\left(\frac{6.02 \times 10^{23}}{\text{atomic weight of the uranium present}}\right)$$

Note: Burnup is by fission.

Density, in g per cm^3, is the gross or macro density of the alloy and includes porosity.

COATED PART.

TABLE 2B. SUMMARY OF FISSION-GAS-RELEASE DATA FROM COATED-PARTICLE FUELS

Lot	Fuel Diameter, μ	Kind	Coating Thickness, μ	Coating Kind	Irradiation Temperature, C	Accumulated Irradiation Time, hr	Uranium Burnup, a/o	R/B at 820 F[a] Kr^{88}	R/B at 820 F[a] Xe^{135}	R/B at 820 F[a] Xe^{133}
HTM-1	200	UC_2	82	Col-PyC	745-900	1390	12.1	3×10^{-5}	6×10^{-5}	3×10^{-4}
3M-SP-2	250	UC_2	82	Lam-PyC	620-990	1510	14.9	2×10^{-4}	2×10^{-4}	5×10^{-4}
NCC-AD	300	UC_2	80	Duplex-PyC	315-925	2110	14.7	4×10^{-6}	9×10^{-6}	3×10^{-5}
3M-101-U	228	UC_2	0	None	500-820	980	4.3	5×10^{-3}	1×10^{-2}	7×10^{-2}

(a) Rate of release of isotope divided by rate of generation.

Report No. BMI-1598

UC-25 Metals, Ceramics,
and Materials
(TID-4500, 18th Ed.)

Contract No. W-7405-eng-92

PROPERTIES OF FUELS FOR HIGH-TEMPERATURE REACTOR CONCEPTS

Edited by

Roy W. Endebrock

Prepared at the request of
Oak Ridge National Laboratories
Gas-Cooled Reactor Program

November 1, 1962

BATTELLE MEMORIAL INSTITUTE
505 King Avenue
Columbus 1, Ohio

TABLE OF CONTENTS

PREFACE

This compilation was prepared especially to aid design engineers in the selection of potential fuels for advanced high-temperature reactors. It was undertaken at the request of Oak Ridge National Laboratory in support of the ORNL Gas-Cooled Reactor Program. The compilation presents available data on critical properties for all fuels believed to be potentially capable of operating at surface temperatures of at least 650 C. Fuels of recent interest with this capability are included even though sufficient data for their final evaluation are not yet available.

The compilation is broken down into sections devoted to particular types of fuels. Property data for all these materials are arranged in a standardized format designed for rapid consultation. In addition to these data sheets, a master table that permits comparison of all fuels covered in the compilation on the basis of four properties considered essential in an initial fuel evaluation is presented. Also, a compilation of appropriate conversion units has been included for the design engineer's convenience.

ACKNOWLEDGMENT

The Editor wishes to express his gratitude to the Battelle personnel who assisted in the preparation of the sourcebook. Particularly appreciated were the efforts of the specialists who compiled the data sheets: M. C. Brockway, M. F. Browning, R. J. Burian, W. Chubb, J. A. De Mastry, M. S. Farkas, M. Kangilaski, D. L. Keller, D. E. Kizer, J. B. Melehan, N. E. Miller, J. H. Oxley, R. L. Ritzman, F. A. Rough, E. O. Speidel, D. L. Stoltz, V. W. Storhok, A. B. Tripler, and R. A. Wullaert. Grateful acknowledgment is made to J. J. Breslin for his assistance in editing the manuscript. Invaluable, also, was the assistance given by ORNL personnel, especially by J. H. Coobs, G. Samuels, Jr., and A. E. Goldman.

GUIDE FOR THE USE OF THE DATA SHEETS

The format used in data sheets of the various fuels contained in this sourcebook was arranged so that the properties compiled for each fuel material are consistent and are presented in a standard code. In those instances where needed data are not yet available for a specific property, this lack of information is pointed out; however, where a particular property designation is not applicable to the material of interest, it is omitted. Any given letter-number combination identifies the same property throughout the sourcebook. The code employed is listed below:

A. Composition Limits

1. Chemical composition
2. Phase diagram
3. Effect of impurities

B. Physical Properties

1. Density (room temperature)
2. Density versus temperature
3. Uranium or plutonium content*
4. Liquidus temperature
5. Solidus temperature
6. Vapor pressure
7. Thermal expansion (linear)
8. Recrystallization temperature range

C. Mechanical Properties

1. Hardness (room temperature)
2. Hot hardness
3. Ultimate tensile strength
4. Yield strength
5. Compressive strength
6. Creep strength
7. Young's modulus
8. Shear modulus
9. Bulk modulus, B $B = \frac{E}{3(1 - 2\sigma)}$, where E = Young's modulus and σ = Poisson's ratio
10. Poisson's ratio
11. Elongation

D. Thermal Properties

1. Specific heat
2. Thermal conductivity

E. Electrical Properties

1. Electrical resistivity

F. Chemical Properties

1. Reactions with coolants
   a. Steam
   b. Helium
   c. Carbon dioxide
   d. Nitrogen
   e. Hydrogen
   f. Liquid metals (limited to sodium, NaK, and lithium)
   g. Air
2. Reactions with claddings or structural materials

*Computed on the basis of the U^{238} or Pu^{239} to make application of the data to particular enrichments most convenient.

G. Irradiation Properties

1. Dimensional stability during irradiation
2. Fission-gas-release data
3. Swelling-temperature data
4. Unusual nuclear properties
5. Property changes as a result of irradiation

H. References

FUEL COMPARISON TABLE

Fuel Material	Contained Uranium or Plutonium		Melting Point		Thermal Conductivity, cal/(sec)(cm)(C)			Fission-to-Absorption Cross Section Ratio
	w/o	G per Cm^3	C	F	At 20 C	At 600 C	At 1200 C	
Alloys								
Nb-10 w/o U	10 U	0.955 (U)	2400	4350	--	0.0936	--	0.12
Nb-20 w/o U	20 U	1.82 (U)	2300	4175	--	0.0774	--	0.22
Compounds								
PuC	95.6-96.1 Pu	13.0 to 13.1 (Pu)	1650	3000	--	--	--	--
PuO_2	88.2 Pu	10.1 (Pu)	2280	4130	--	--	--	--
$(Th_9U)B_4$	10 U	--	--	--	--	0.891	--	--
$(Th_9U)C$	10 U	--	--	--	--	0.0375	--	--
$(Th_9U)C_2$	10 U	--	--	--	--	0.0566	--	--
UC	95.2 U	12.9 (U)	2400	4350	0.08	0.055	0.055	0.55
UN	94.4 U	13.5 (U)	2630	4770	0.032	0.046	0.058	0.44
UO_2	88.2 U	9.67 (U)	2760	5000	0.11	~0.035	0.022	0.55
U_3Si_2	86.2 U	11.3 (U)	1665	3030	0.035	--	--	0.53
Ceramic Dispersions								
20 w/o UO_2-80 w/o Al_2O_3	17.6 U	--	~2030	~3700	--	--	--	0.33
30 w/o UO_2-70 w/o Al_2O_3	26.5 U	--	~2030	~3700	--	--	--	0.45
10 w/o UO_2-90 w/o BeO	8.8 U	0.26 (U)	~2450	~4440	0.25	--	--	0.48
80 w/o UO_2-20 w/o Be	70.6 U	--	--	--	--	--	--	0.53
95 w/o UO_2-5 w/o MgO	83.8 U	--	--	--	--	--	--	0.54
2.57 w/o UO_2-7.3 w/o ThO_2-90 w/o BeO	2.24 U	--	--	--	--	--	--	0.13
25 w/o UO_2-35.5 w/o ThO_2-39.1 w/o BeO	22.1 U	--	--	--	--	--	--	0.22
UO_2-graphite	19 U	0.38 (U)	--	--	0.052 to 0.073	--	--	0.54
UO_2-graphite	45 U	1.21 (U)	--	--	0.035 to 0.051	--	--	0.58
UC_2-graphite	10 U	0.19 (U)	--	--	~0.13	--	--	0.51
UC_2-graphite	20 U	0.40 (U)	--	--	~0.14	--	--	0.53
Metallic Dispersions								
20 w/o UO_2-stainless steel	17.6 U	1.43 (U)	1400 to 1460	2550 to 2650	0.017	0.037	0.067	0.064
40 w/o UO_2-stainless steel	35.3 U	3.06 (U)	1400 to 1460	2550 to 2650	0.022	0.028	0.034	0.13
50 w/o UO_2-stainless steel	44.1 U	3.95 (U)	1400 to 1460	2550 to 2650	0.022	0.027	0.032	0.18
Cermets								
Mo-80 volume per cent UC	76.16 U	9.44 (U)	2625	4760	0.039	0.036	0.071	0.47
Mo-80 volume per cent UN	75.55 U	9.79 (U)	2625	4760	~0.05	0.055	--	0.39
Mo-80 volume per cent UO_2	70.48 U	7.32 (U)	2625	4760	~0.05	0.045	--	0.44

ALLOYS

URANIUM ALLOYS - GENERAL

M. S. Farkas

The minimum surface temperature of 650 C (indicating a center temperature of over 700 C) specified by ORNL eliminates uranium, alpha-phase uranium alloys, and most gamma-phase uranium alloys from consideration in this compilation.

Experimental data have shown that irradiation swelling occurs above about 500 C.

NIOBIUM-10 W/O URANIUM ALLOY

Compiled by J. A. DeMastry

A1. Chemical composition[1]

Niobium-10 w/o uranium

2. Phase diagram[2]

The diagram shown in Figure A2 is from Rogers and Browne, and represents essential confirmation of work of earlier investigators, although revisions in certain boundaries have been made.

The complete solubility of gamma uranium and niobium is agreed on by all investigators, although there is disagreement as to the extent of the $gamma_1$-plus-$gamma_2$ region. Sawyer reports the region as extending from about 11 to 78 a/o at 645 C, while Rogers and Browne report the monotectoid to occur at 16 ± 1 a/o niobium and 645 C, but give values of 73 and 70 a/o, respectively, for the niobium-rich limit of the $gamma_1$-plus-$gamma_2$ region at this temperature. Dwight reports the monotectoid as occurring at 19 a/o niobium and 634 C, the latter temperature being in agreement with its determination by Bauer.

On the basis of a tetragonal structure observed in quenched alloys containing 14 to 20 a/o niobium and thermal arrests ranging in temperature from 675 to 725 C for alloys containing 9.6 to 17 a/o niobium, Dwight suggests an ordering of the gamma phase in the region of the monotectoid. While additional investigation is required, the tetragonal structure may be ascribed to a transition structure in the metastable-gamma decomposition.

There is some question concerning the nature of the alpha-to-beta transformation at the uranium-rich end of the system. Although most investigators agree that the reaction occurs peritectoidally, alpha has also been described as forming in a eutectoid reaction. A shift of less than ±5 C in the alpha-to-beta transition temperature is agreed to by all investigators.

Solubilities in the alpha and beta phase are reported to be extremely limited. Browne gives the maximum solubility in each phase as being between 1 and 2 a/o niobium.

3. Effect of impurities[3]

Oxygen in excess of 1000 ppm results in increased tensile and creep strength and severe losses in ductility.

B1. Density (room temperature)[4]

9.55 g per cm^3

2. Density versus temperature

No data available

3. Uranium content

0.955 g per cm^3

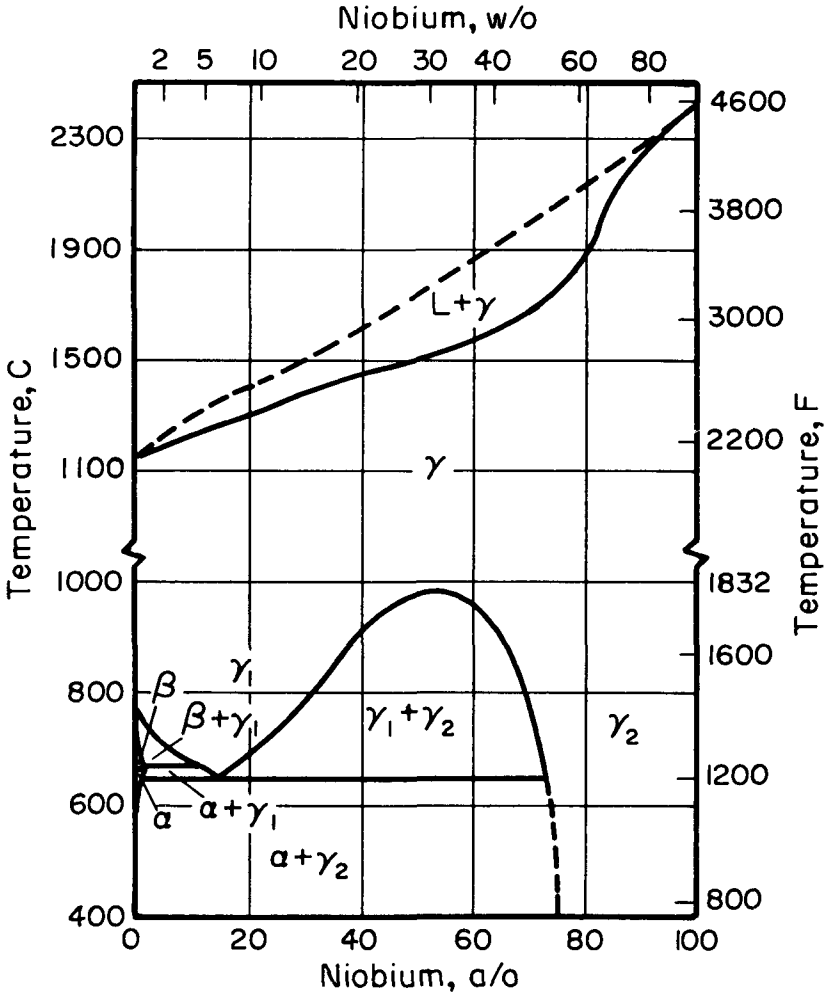

FIGURE A2. URANIUM-NIOBIUM PHASE DIAGRAM[2]

AEA-43204

4. Liquidus temperature[2]

2400 ± 50 C

5. Solidus temperature[2]

2400 ± 50 C

6. Vapor pressure

No data available

7. Thermal expansion (linear)[3]

Temperature, F	Coefficient, 10^{-6} per F
68-200	4.1
200-400	4.1
400-600	4.3
600-800	4.5
800-1000	4.8
1000-1200	4.9
1200-1400	5.0
1400-1600	5.2
1600-1800	5.2
68-1800	4.7

8. Recrystallization temperature range[4]

1100 to 1200 C

C1. Hardness (room temperature)[1]

164 kg per mm^2

2. Hot hardness[1]

Temperature, C	Hardness, kg per mm^2
400	143
500	138
600	119
700	113
800	108
900	95
1000	75
1100	63

3. Ultimate tensile strength[1,3]

Temperature, F	Ultimate Tensile Strength, psi[a]
68	72,900
1600	72,000
1800	52,000
2000	35,000
2200	24,000

(a) Alloy contained 3100 ppm oxygen.

4. Yield strength[1,3]

Temperature, F	Yield Strength, psi
68	55,900
1800	45,000
2000	25,000

5. Compressive strength

No data available

6. Creep strength[3]

Stress for Creep Rate Shown, psi				Rupture Data	
Temperature, F	0.001 Per Cent per Hr	0.01 Per Cent per Hr	0.1 Per Cent per Hr	Stress, psi	Rupture Time, hr
1600	17,000	25,000	37,000	30,000	602
				25,000	381
1800	8,800	12,000	15,000	20,000	28.9
				14,000	54

Note: Alloy contained 3100 ppm oxygen which accounts for unusual strength.

7. Young's modulus

No data available

8. Shear modulus

No data available

9. Bulk modulus

No data available

10. Poisson's ratio

No data available

11. Elongation[1,3]

Temperature, F	Elongation in 1-In. Gage Length (Flat Specimens), per cent
68	3
1600	1
1800	4
2000	9
2200	10

Note: Alloy contained 3100 ppm oxygen.

D1. Specific heat

No data available

2. Thermal conductivity[3]

Temperature, F	Thermal Conductivity, Btu/(hr)(ft)(F)
200	14.0
400	16.0
600	18.0
800	19.9
1000	21.7
1200	23.6
1400	25.4
1600	27.1
1800	28.7

E1. Electrical resistivity[3]

Temperature, F	Resistivity, microhm-cm
68	36
200	39
400	43
600	47
800	51
1000	54
1200	57

F1. Reactions with coolants

a. Steam[1]
Minus 13.3 mg per cm^2 in 1000 hr at 750 F (399 C)

b. Helium[4]
No attack after 100 hr at 1800 F (982 C)

c. Carbon dioxide[1]
Plus 0.23 mg per cm^2 in 50 hr at 600 F (982 C)

d. Nitrogen
No data available

e. Hydrogen
No data available

f. Liquid metals[3]
Plus 0.15 mg per cm^2 in sodium in 1500 hr at 1500 F (816 C)
Plus 0.14 mg per cm^2 in NaK in 1000 hr at 1600 F (871 C)

g. Air[1]
Plus 2.34 mg per cm^2 in 100 hr at 750 F (400 C)

2. Reactions with claddings or structural materials

No data available

G1. Dimensional stability during irradiation[4]

Minus 2.1 per cent change in density, 5.6×10^{20} fission per cm^3, 1200 F
Minus 2.3 per cent change in density, 2.8×10^{20} fission per cm^3, 1900 F

2. Fission-gas-release data

No data available

3. Swelling-temperature data

No data available

4. Unusual nuclear properties

No data available

5. Property changes as a result of irradiation

No data available

H. References

(1) De Mastry, J. A., Shober, F. R., and Dickerson, R. F., "Metallurgical Studies of Niobium-Uranium Alloys", BMI-1400 (December 7, 1959).

(2) Rough, F. A., and Bauer, A. A., "Constitution of Uranium and Thorium Alloys", BMI-1300 (June 2, 1958).

(3) De Mastry, J. A., Moak, D. P., Epstein, S. G., Bauer, A. A., and Dickerson, R. F., "Development of Niobium-Uranium Alloys for Elevated-Temperature Fuel Applications", BMI-1536 (August 9, 1961).

(4) De Mastry, J. A., Unpublished Data.

NIOBIUM-20 W/O URANIUM ALLOY

Compiled by J. A. DeMastry

A1. Chemical composition[1]

Niobium-20 w/o uranium

2. Phase diagram[2]

The diagram shown in Figure B2 is from Rogers and Browne, and represents essential confirmation of work of earlier investigators, although revisions in certain boundaries have been made.

The complete solubility of gamma uranium and niobium is agreed on by all investigators, although there is disagreement as to the extent of the $gamma_1$-plus-$gamma_2$ region. Sawyer reports the region as extending from about 11 to 78 a/o at 645 C, while Rogers and Browne report the monotectoid to occur at 16 ± 1 a/o niobium and 645 C, but give values of 73 and 70 a/o, respectively, for the niobium-rich limit of the $gamma_1$-plus-$gamma_2$ region at this temperature. Dwight reports the monotectoid as occurring at 19 a/o niobium and 634 C, the latter temperature being in agreement with its determination by Bauer.

On the basis of a tetragonal structure observed in quenched alloys containing 14 to 20 a/o niobium and thermal arrests ranging in temperature from 675 to 725 C for alloys containing 9.6 to 17 a/o niobium, Dwight suggests an ordering of the gamma phase in the region of the monotectoid. While additional investigation is required, the tetragonal structure may be ascribed to a transition structure in the metastable-gamma decomposition.

There is some question concerning the nature of the alpha-to-beta transformation at the uranium-rich end of the system. Although most investigators agree that the reaction occurs peritectoidally, alpha has also been described as forming in a eutectoid reaction. A shift of less than ±5 C in the alpha-to-beta transition temperature is agreed to by all investigators.

Solubilities in the alpha and beta phase are reported to be extremely limited. Browne gives the maximum solubility in each phase as being between 1 and 2 a/o niobium.

3. Effect of impurities[3]

Oxygen in excess of 1000 ppm results in increased tensile and creep strength and severe losses in ductility.

B1. Density (room temperature)[4]

9.1 g per cm^3

2. Density versus temperature

No data available

3. Uranium content

1.82 g per cm^3

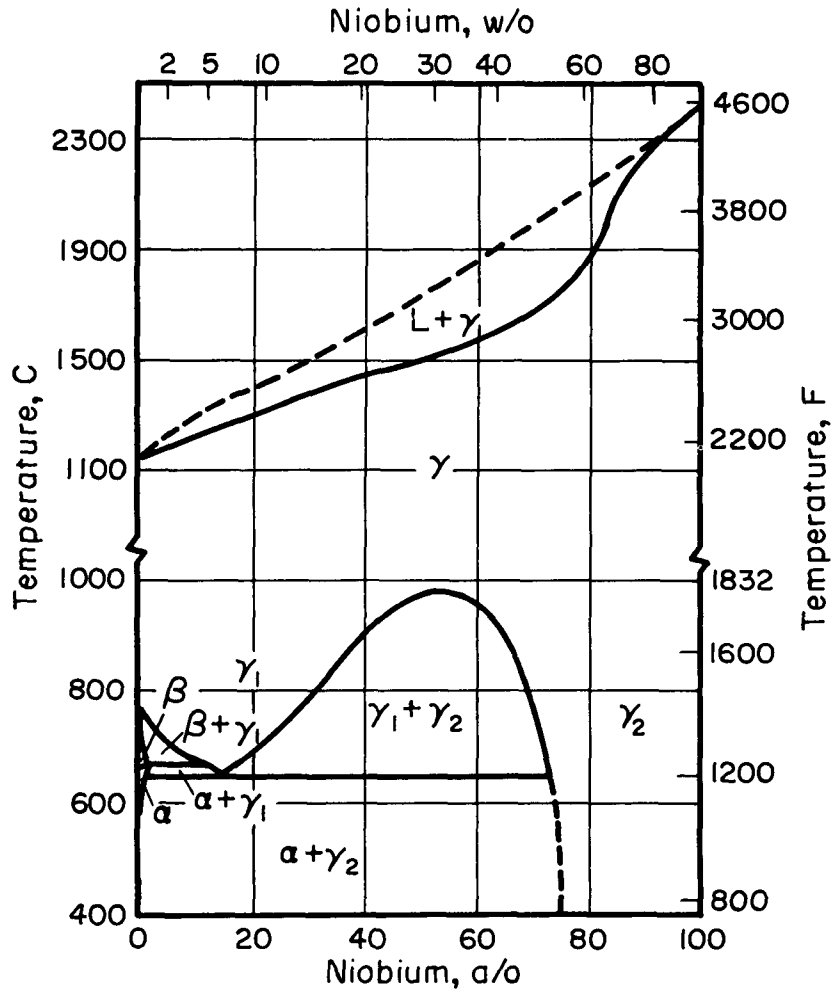

FIGURE A2. URANIUM–NIOBIUM PHASE DIAGRAM [2]

AEA-43203

4. **Liquidus temperature**[2]
   2325 ± 50 C

5. **Solidus temperature**[2]
   2325 ± 50 C

6. **Vapor pressure**
   No data available

7. **Thermal expansion**[3]

Temperature, F	Coefficient, 10^{-6} per F
68-200	4.2
200-400	4.4
400-600	4.6
600-800	4.7
800-1000	5.0
1000-1200	5.1
1200-1400	5.3
1400-1600	5.5
1600-1800	5.7
68-1800	5.0

8. **Recrystallization temperature range**[4]
   1100 to 1200 C

C1. **Hardness (room temperature)**[1]
   213 kg per mm^2

2. **Hot hardness**[1]

Temperature, C	Hardness, kg per mm^2
400	163
500	155
600	145
700	143
800	140
900	133
1000	113
1100	92

3. **Ultimate tensile strength**[1,3]

Temperature, F	Ultimate Tensile Strength, psi
68	102,000
1600	68,000
1800	52,000
2000	38,000

4. Yield strength[1,3]

Temperature, F	Yield Strength, psi
68	93,000
1600	58,000
1800	43,000
2000	29,000

5. Compressive strength

No data available

6. Creep strength[3]

Temperature, F	Stress for Creep Rate Shown, psi			Rupture Data	
	0.001 Per Cent per Hr	0.01 Per Cent per Hr	0.1 Per Cent per Hr	Stress, psi	Rupture Time, hr
1600	17,000	25,000	37,000	30,000	38.7
1800	8,800	11,500	15,000	20,000	27.2
				51,000	169.7

7. Young's modulus

No data available

8. Shear modulus

No data available

9. Bulk modulus

No data available

10. Poisson's ratio

No data available

11. Elongation[1,3]

Temperature, F	Elongation in 1-In. Gage Length, per cent
68	7
1600	10
1800	34
2000	74

D1. Specific heat

No data available

2. Thermal conductivity[3]

Temperature, F	Thermal Conductivity, Btu/(hr)(ft)(F)
200	10.2
400	11.8
600	13.6
800	15.5
1000	17.6
1200	19.8
1400	22.2
1600	24.6
1800	27.2

E1. Electrical resistivity[3]

Temperature, F	Resistivity, microhm-cm
68	54
200	56
400	59
600	63
800	66
1000	68
1200	71

F1. Reactions with coolants

a. Steam[1]
Minus 2.45 mg per cm^2 in 1000 hr at 750 F (400 C)

b. Helium[4]
No attack after 100 hr at 1800 F (980 C)

c. Carbon dioxide[1]
Plus 0.13 mg per cm^2 in 50 hr at 600 F (315 C)

d. Nitrogen
No data available

e. Hydrogen
No data available

f. Liquid metals
Plus 0.10 mg per cm^2 in sodium in 1500 hr at 1500 F (815 C)
Plus 0.69 mg per cm^2 in NaK in 1000 at 1600 F (870 C)

g. Air[1]
Plus 20.0 mg per cm^2 in 100 hr at 750 F (400 C)

2. Reactions with claddings or structural materials

No data available

G1. Dimensional stability during irradiation[4]

Minus 2.5 per cent change in density, 5.0×10^{20} fissions per cm^3, 1200 F
Minus 1.7 per cent change in density, 2.49×10^{20} fissions per cm^3, 1900 F

2. Fission-gas-release data

No data available

3. Swelling-temperature data

No data available

4. Unusual nuclear properties

No data available

5. Property changes as a result of irradiation

No data available

H. References

(1) DeMastry, J. A., Shober, F. R., and Dickerson, R. F., "Metallurgical Studies of Niobium-Uranium Alloys", BMI-1400 (December 7, 1959).

(2) Rough, F. A., and Bauer, A. A., "Constitution of Uranium and Thorium Alloys", BMI-1300 (June 2, 1958).

(3) DeMastry, J. A., Moak, D. P., Epstein, S. G., Bauer, A. A., and Dickerson, R. F., "Development of Niobium-Uranium Alloys for Elevated-Temperature Fuel Applications", BMI-1536 (August 9, 1961).

(4) DeMastry, J. A., Unpublished Data.

THORIUM-URANIUM ALLOYS - GENERAL

M. S. Farkas

The specification of a minimum surface-temperature of 650 C eliminates thorium-uranium alloys from consideration for ORNL high-temperature reactor concepts.

Little information on irradiation swelling exists, but there are strong indications that the limiting temperature for known alloys is below the 650 to 700 C minimum service temperature limitation. One study has shown that thorium-11 w/o uranium swells at 650 C*.

*Reactor Core Materials, 3 (1), 8 (February, 1960).

COMPOUNDS

PLUTONIUM CARBIDE

Compiled by V. W. Storhok

A1. Chemical composition[1]

PuC, 95.22 w/o plutonium, 4.78 w/o carbon

2. Phase diagram[1]

See Figure A2

3. Effect of impurities

No data available

B1. Density (room temperature)[2]

13.6 g per cm^3

2. Density versus temperature

No data available

3. Plutonium content

13.0 to 13.1 g per cm^3

4. Liquidus temperature[1]

~1800 C

5. Solidus temperature[1]

1654 C

6. Vapor pressure

No data available

7. Thermal expansion (linear)[3]

10×10^{-6} per C from RT to 900 C (presumed from text of reference)

8. Recrystallization temperature range

No data available

C1. Hardness (room temperature)[4]

Carbon, a/o	DPH
44.4	480
47.1	700
50.4	770

2. Hot hardness

No data available

3. Ultimate tensile strength

No data available

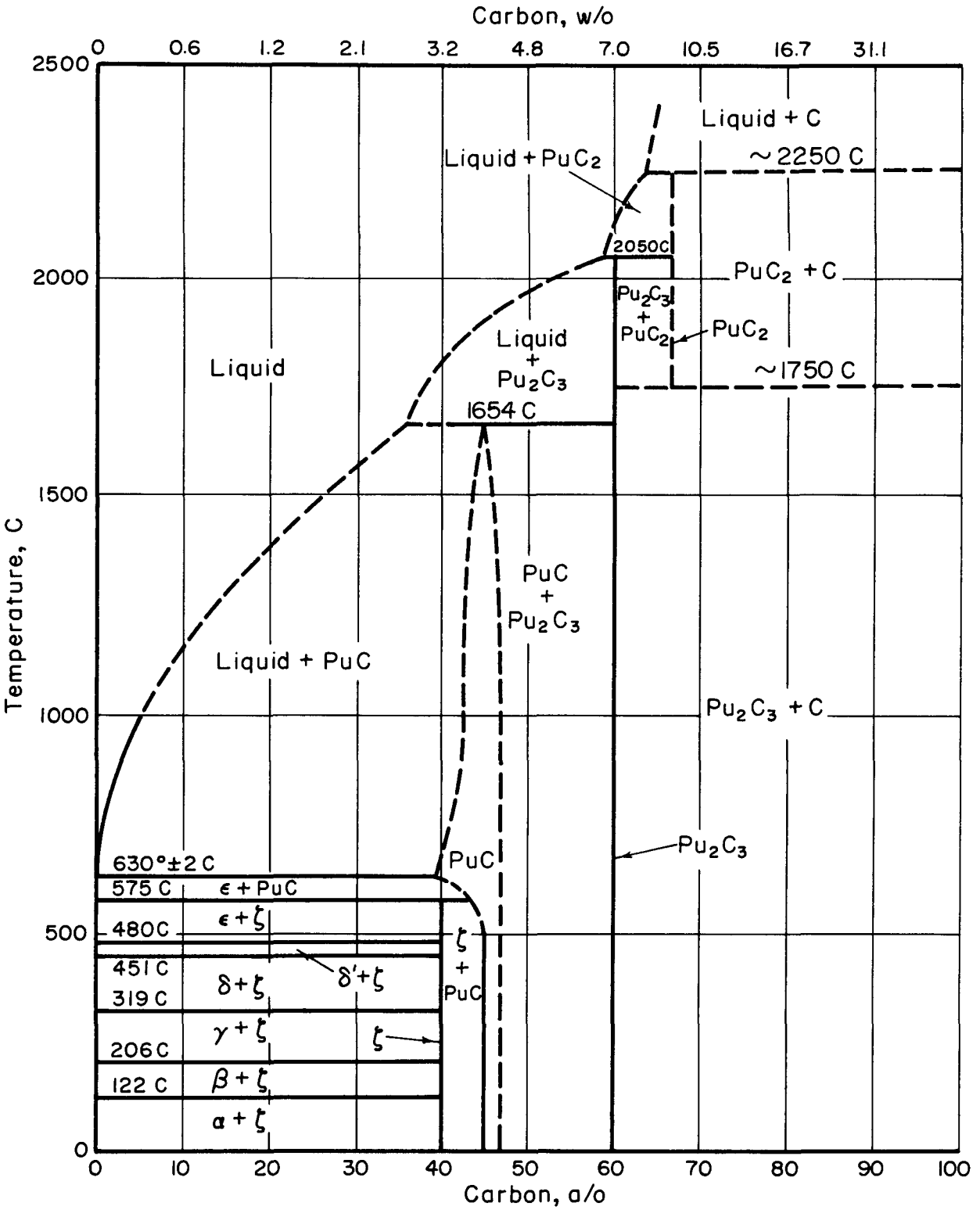

FIGURE A2. PLUTONIUM - CARBON PHASE DIAGRAM[1]

AEA-43205

4. Yield strength
No data available

5. Compressive strength
No data available

6. Young's modulus
No data available

7. Shear modulus
No data available

8. Bulk modulus
No data available

9. Poisson's ratio
No data available

10. Elongation
No data available

D1. Specific heat
No data available

2. Thermal conductivity
No data available

E1. Electrical resistivity[5]
266 microhm-cm

F1. Reactions with coolants

a. Steam[6]
Probably very rapid attack - effervesces in hot water, producing methane and hydrogen.

b. Helium
Apparently no reaction at room temperature, as helium is often employed as PuC glove-box atmosphere; no high-temperature data.

c. Carbon dioxide
No data available

d. Nitrogen
No data available

e. Hydrogen
No data available

f. Liquid metals
NaK[4]
Apparently compatible to at least 430 C

g. Air[7]
Oxidizes slowly at 300 C

2. Reactions with claddings or structural materials

Graphite[8]
Carbon content of PuC (4.57 w/o) increased to 6.72 w/o when heated in graphite for 14 days at 1500 C. Product was mainly Pu_2C_3.

Molybdenum[8]
No reaction at 1400 C

Niobium[8]
Reacts at 1400 C

Stainless steel[4]
PuC (44.4 a/o carbon) penetrated 8.54 mils in 3 days at 1000 C.

Tantalum[4]
PuC (44.4 a/o carbon) penetrated 1.67 mils in 3 days at 1000 C.

Vanadium[8]
Reacts at 1400 C

Tungsten[8]
No reaction at 1400 C

Zirconium[8]
Reacts at 1400 C

G1. Dimensional stability during irradiation[9]
Of four specimens irradiated to a burnup of 3.28×10^{19} fissions per cm^3 at a maximum central temperature of 430 C, three decreased in density with the maximum decrease being 1.44 per cent. One specimen cracked.

2. Fission-gas-release data
No data available

3. Swelling-temperature data
No data available

4. Unusual nuclear properties
No data available

5. Property changes as a result of irradiation
No data available

H. References

(1) Mulford, R. N. R., Ellinger, F. H., Hendrix, G. S., and Albrecht, E. D., "The Plutonium-Carbon System", Plutonium 1960, Edited by Grison, E., Lord, W. B. H., and Fowler, R. D., Cleaver-Hume Press Ltd., London, pp 301-311.

(2) Coffinberry, A. S., Schonfeld, F. W., Waber, J. T., Kelman, C. R., and Tipton, C. R., Jr., "Plutonium and Its Alloys", Reactor Handbook, Materials, 2nd Edition, Edited by Tipton, C. R., Jr., Interscience Publishers, New York (1960), pp 248-290.

(3) "Reactor Development Program Progress Report, August, 1960", ANL-6215 (September 16, 1960).

(4) "Metallurgy Division Annual Report for 1960", ANL-6330.

(5) Unpublished LASL Data.

(6) Drummong, J. L., McDonald, B. J., Dikenden, H. M., and Welch, G. A., "The Preparation and Properties of Some Plutonium Compounds, Part VII Plutonium Carbides", J. Chem. Soc., pp 4785 (December, 1957).

(7) Strasser, A., "Uranium Carbide As a Fuel, A Revision of Current Knowledge", Nuclear Eng., 5 (51), 353-357 (August, 1960).

(8) Waldren, M., Unpublished U. K. Data.

(9) Hilberry, N., "Reactor Development Program Progress Report", ANL-6355 (April, 1961).

PLUTONIUM DIOXIDE

Compiled by V. W. Storhok

A1. Chemical composition[1]

PuO_2, 88.19 w/o plutonium, 11.81 w/o oxygen

2. Phase diagram[1]

See Figure A2

3. Effect of impurities

No data available

B1. Density (room temperature)[2]

11.46 g per cm^3

2. Density versus temperature

No data available

3. Plutonium content

10.1 g per cm^3

4. Liquidus temperature[3]

2280 ± 30 C (pseudomelting temperature)

5. Solidus temperature[3]

2280 ± 30 C (pseudomelting temperature)

6. Vapor pressure[4]

Temperature, C	Vapor Pressure, atm		
	Oxygen	Argon	Air
1450	--	2.1×10^{-9}	1.1×10^{-9}
1500	5.0×10^{-10}	--	3.1×10^{-9}
1525	--	4.4×10^{-9}	--
1550	8.9×10^{-10}	3.1×10^{-9}	--
1575	9.9×10^{-10}	--	--
1600	2.0×10^{-9}	5.3×10^{-9}	1.3×10^{-8}
1650	2.1×10^{-9}	1.7×10^{-8}	6.4×10^{-9}
1675	--	1.1×10^{-8}	--
1700	2.8×10^{-9}	8.7×10^{-9}	2.0×10^{-8}
1725	1.9×10^{-8}	1.3×10^{-8}	--
1750	1.6×10^{-8}	2.7×10^{-8}	--
1775	3.8×10^{-8}	--	3.8×10^{-8}

Conclusions: (1) PuO_2 congruently vaporizes in oxygen.
(2) PuO_2 vaporizes as $PuO_2(g) + PuO(g)$ in neutral gases.

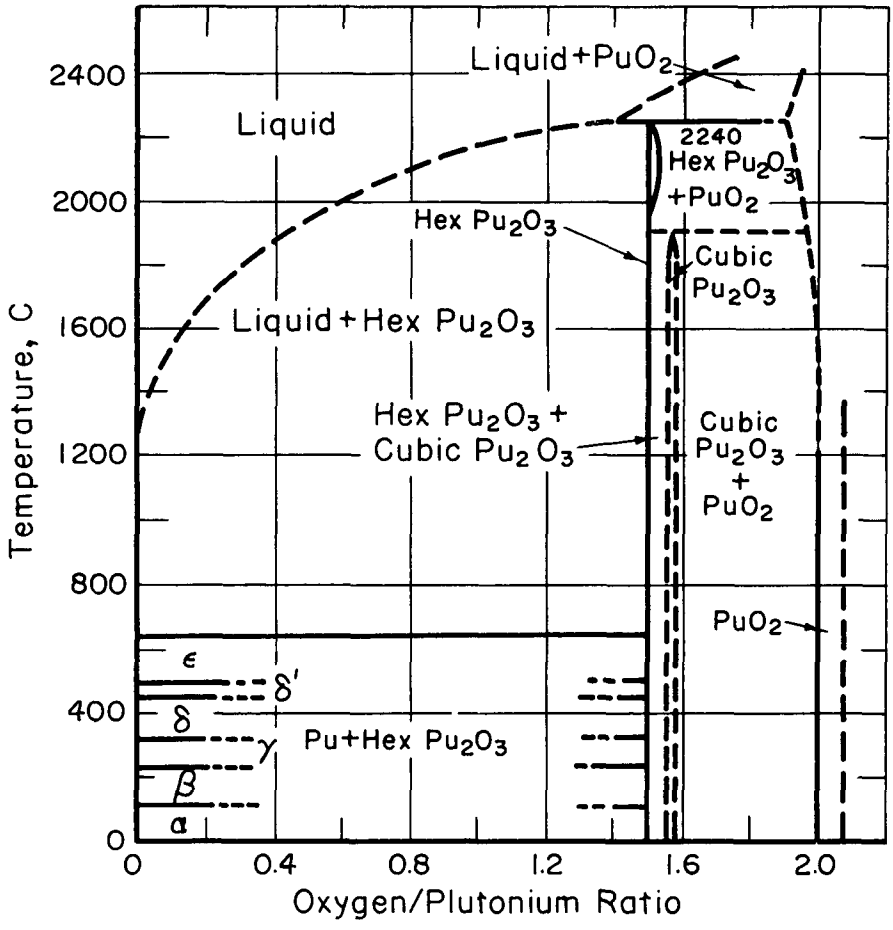

FIGURE A2. PLUTONIUM - OXYGEN SYSTEM [1]

AEA-43207

7. Thermal expansion (linear)(5)

Temperature, C	Coefficient, 10^{-6} per C
20-300	8.2
20-600	9.9
20-800	10.5
20-1000	11.4

8. Recrystallization temperature range
No data available

C1. Hardness (room temperature)
No data available

2. Hot hardness
No data available

3. Ultimate tensile strength
No data available

4. Yield strength
No data available

5. Compressive strength
No data available

6. Creep strength
No data available

7. Young's modulus
No data available

8. Shear modulus
No data available

9. Bulk modulus
No data available

10. Poisson's ratio
No data available

11. Elongation
No data available

D1. Specific heat
No data available

2. Thermal conductivity
No data available

E1. Electrical resistivity

No data available

F1. Reactions with coolants

a. Steam

No data available

b. Helium[6]

Slight reduction of PuO_2 occurs to yield oxygen-to-plutonium ratio of about 1.97.

c. Carbon Dioxide[7]

Apparently no serious reaction occurs, as CO_2 has been employed as a sintering atmosphere at temperatures up to 1650 C.

d. Nitrogen

No data available

e. Hydrogen[6]

PuO_2 begins to reduce to Pu_2O_3 at about 1400 C.

f. Liquid metals

NaK[8]

Apparently compatible to at least 680 C

g. Air[6]

Lower oxides to $PuO_{2.00}$ at temperatures as low as 200 C.

2. Reactions with claddings or structural materials

Iron and austenitic stainless steel[9]

Slight reduction of PuO_2 to Pu_2O_3 occurs after 100 hr at 1400 C.

Inconel[10]

No reaction up to 1370 C

Chromium[10]

No reaction up to 1370 C

Molybdenum[10]

No reaction up to 1370 C

Niobium[9]

Slight reduction of PuO_2 to Pu_2O_3 curves after 100 hr at 1400 C.

Titanium[10]

Reacts at 1370 C

Tungsten[10]

Reacts at 1370 C

Vanadium[10]
No reaction at 1370 C

Zircaloy-2[10]
Reacts at 1370 C

Al_2O_3
Reacts at 1590 C

MgO[10]
No reaction at 1590 C

ZrO_2[10]
Alloyed at 1590 C

G1. Dimensional stability during irradiation
See Table G1.

2. Fission-gas-release data
See Table G1.

3. Swelling-temperature data
No data available

TABLE G1. EFFECTS OF IRRADIATION[a] ON PuO_2-40 w/o $U^{235}O_2$-40 w/o $U^{238}O_2$[8]

Burnup[b], 10^{20} fissions per cm^3	Maximum Surface Temperature[c], C	Average Heat Flux, 10^6 Btu/(hr)(ft^2)	Fission-Gas Release, per cent	Length Increase, per cent	Central Void Formation	
					Per Cent of Cross Section	Per Cent of Postirradiation Length
1.93[d]	468	0.37	27.8	11.2	No void	--
2.67[e]	532	0.55	52.4	4.2	4 to 5.4	>43
3.96[d]	435	0.36	71.3	0	3.0	15
5.98[e]	621	0.54	49.6	4.0	No void	--
20.3[e]	638	1.30	28.8	5.7	2 to 4	51
20.3[d]	680	1.27	48.1	9.0	9.8 to 19.5	75

(a) Irradiation properties of PuO_2 should be reasonably similar.
(b) Calculated assuming 9000 MWD/2000 lb of plutonium and uranium = 2.47×10^{20} fissions per cm^3 in the fuel material.
(c) No central temperature given.
(d) Swaged specimen.
(e) Pelletized specimen.

4. Unusual nuclear properties
No data available

5. Property changes as a result of irradiation
No data avilable

H. References

(1) Schonfeld, F. W., "Plutonium Phase Diagrams Studied at Los Alamos", The Metal Plutonium, Edited by Coffinberry, A. S., and Miner, W. N., University of Chicago Press, pp 241-254 (1961).

(2) Coffinberry, A. S., Schonfeld, F. W., Waber, J. T., Kelman, C. R., and Tipton, C. R., Jr., "Plutonium and Its Alloys", Reactor Handbook, Materials, 2nd Edition, Edited by Tipton, C. R., Jr., Interscience Publishers, New York, pp 248-290 (1960).

(3) Chikalla, T. D., "The Liquidus for the System UO_2-PuO_2", HW-69832 (June, 1961).

(4) Pardue, W. M., unpublished BMI data.

(5) Arthur, G., "Ceramics Properties", Nuclear Eng., 6, 253-257 (June 1, 1961).

(6) Goldsmith, S., Editor, "Plutonium Recycle Program Annual Report, Fiscal Year 1961", HW-70000 (August 11, 1961).

(7) Harrison, J. D. L., "The Sintering Behavior of Mixed UO_2 and PuO_2 Powders", AERE-R-3765 (July, 1961).

(8) Gerhart, J. M., Siltanen, J. H., and Cochran, J. S., "The Irradiation and Examination of a Plutonium Uranium Oxide Fast Reactor Fuel", Symposium on Radiation Effects in Refractory Fuel Compounds, ASTM Special Technical Publication No. 306 (1962).

(9) Poole, D. M., Critchly, J. K., Davidson, J. A. C., French, P. M., Hodkin, E. N., and Notley, M. J. F., "Properties of Some Plutonium Fuels", Plutonium 1960, Edited by Grison, E., Lord, W. B. H., and Fowler, R. D., Cleaver-Hume Press, Ltd, London (1961), pp 627-649.

(10) Paprocki, S. J., Keller, D. L., and Pardue, W. M., "The Chemical Reactivity of PuO_2 with Reactor Materials", BMI-1580 (May 29, 1962).

THORIUM URANIUM BORIDE

Compiled by J. A. DeMastry

A1. Chemical composition

$(Th_9U)B_4$

2. Phase diagram

No data available

3. Effect of impurities

No data available

B1. Density (room temperature)

No data available

2. Density versus temperature

No data available

3. Uranium content

No data available

4. Liquidus temperature

No data available

5. Solidus temperature

No data available

6. Vapor pressure

No data available

7. Thermal expansion (linear)[1]

Temperature, F	Coefficient, 10^{-6} per F
68-200	3.5
68-400	3.7
68-600	3.8
68-800	4.0
68-1000	4.1
68-1200	4.2
68-1400	4.3
68-1600	4.3
68-1800	4.4

8. Recrystallization temperature range

No data available

C1. Hardness (room temperature)[2]

2700 Knoop (100-g load)

C2. Hot hardness
No data available

3. Ultimate tensile strength
No data available

4. Yield strength
No data available

5. Compressive strength[1,3]

Temperature, F	Compressive Strength, psi
68	45,000
1200	48,000
1800	33,000

6. Creep strength
No data available

7. Young's modulus
No data available

8. Shear modulus
No data available

9. Bulk modulus
No data available

10. Poisson's ratio
No data available

11. Elongation
No data available

D1. Specific heat
No data available

2. Thermal conductivity[4]

Temperature, C	Thermal Conductivity, cal/(sec)(cm)(C)
200	0.0652
400	0.0731
600	0.0810
800	0.0891
900	0.0932

E1. Electrical resistivity
No data available

F1. Reactions with coolants

a. Steam
No data available

b. Helium
No data available

c. Carbon Dioxide[2]
Plus 0.03 mg/(cm^2)(hr) at 590 C

d. Nitrogen
No data available

e. Hydrogen
No data available

f. Liquid metals
No data available

g. Air[5]

Temperature, F	Total Weight Gain in 24 Hr, mg per cm^2
1100	0.42
1600	4.8
1700	6.8
2100	14.5
2200	24.6

2. Reactions with claddings or structural materials
No data available

G1. Dimensional stability during irradiation
No data available

2. Fission-gas-release data
No data available

3. Swelling-temperature data
No data available

4. Unusual nuclear properties
No data available

5. Property changes was a result of irradiation
No data available

H. References

(1) Dayton, R. W., and Tipton, C. R., Jr., "Progress Relating to Civilian Applications During January, 1962", BMI-1565 (February 1, 1962).

(2) Farkas, M. S., Bauer, A. A., and Dickerson, R. F., "Evaluation of Thorium and Thorium-Uranium Compounds As Thermal Breeder Fuels", BMI-1568 (February 15, 1962).

(3) Dayton, R. W., and Dickerson, R. F., "Progress Relating to Civilian Applications During February, 1962", BMI-1569 (March 1, 1962).

(4) Dayton, R. W., and Dickerson, R. F., "Progress Relating to Civilian Applications During July, 1962", BMI-1589 (August 1, 1962).

(5) Dayton, R. W., and Dickerson, R. F., "Progress Relating to Civilian Applications During March, 1962", BMI-1574 (April 1, 1962).

THORIUM URANIUM CARBIDE

Compiled by J. A. DeMastry

A1. Chemical composition

$(Th_9U)C$

2. Phase diagram

No data available

3. Effect of impurities

No data available

B1. Density (room temperature)

No data available

2. Density versus temperature

No data available

3. Uranium content

No data available

4. Liquidus temperature

No data available

5. Solidus temperature

No data available

6. Vapor pressure

No data available

7. Thermal expansion (linear)[1]

Temperature, F	Coefficient, 10^{-6} per F
68-200	3.5
68-400	3.6
68-600	3.6
68-800	3.8
68-1000	3.8
68-1200	3.9
68-1400	3.9
68-1600	4.1
68-1800	4.1

8. Recrystallization temperature range

No data available

C1. Hardness (room temperature)[2]

520 Knoop (100-g load)

C2. Hot hardness

No data available

3. Ultimate tensile strength

No data available

4. Yield strength

No data available

5. Compressive strength[1,3]

Temperature, F	Compressive Strength, psi
68	23,000
1200	17,000
1800	67,000

6. Creep strength

No data available

7. Young's modulus

No data available

8. Shear modulus

No data available

9. Bulk modulus

No data available

10. Poisson's ratio

No data available

11. Elongation

No data available

D1. Specific heat

No data available

2. Thermal conductivity[4]

Temperature, C	Thermal Conductivity, cal/(sec)(cm)(C)
200	0.0308
400	0.0342
600	0.0375
800	0.0411
900	0.0426
1000	0.0442

E1. Electrical resistivity

No data available

F1. Reactions with coolants

a. Steam[2]
Catastrophic

b. Helium
No data available

c. Carbon dioxide
No data available

d. Nitrogen
No data available

e. Hydrogen
No data available

f. Liquid metals[2]
Minus 4.5×10^{-2} mg/(cm^2)(day) at 1200 F in NaK.

g. Air[2]
Dry: plus 17 mg/(cm^2)(hr) at 1300 F
Wet: catastrophic

F2. Reactions with claddings or structural materials
No data available

G1. Dimensional stability during irradiation
No data available

2. Fission-gas-release data
No data available

3. Swelling-temperature data
No data available

4. Unusual nuclear properties
No data available

5. Property changes as a result of irradiation
No data available

H. References

(1) Dayton, R. W., and Tipton, C. R., Jr., "Progress Relating to Civilian Applications During January, 1962", BMI-1565 (February 1, 1962).

(2) Farkas, M. S., Bauer, A. A., and Dickerson, R. F., "Evaluation of Thorium and Thorium-Uranium Compounds as Thermal Breeder Fuels", BMI-1568 (February 15, 1962).

(3) Dayton, R. W., and Dickerson, R. F., "Progress Relating to Civilian Applications During February, 1962", BMI-1569 (March 1, 1962).

(4) Dayton, R. W., and Dickerson, R. F., "Progress Relating to Civilian Applications During July, 1962", BMI-1589 (August 1, 1962).

THORIUM URANIUM DICARBIDE

Compiled by J. A. DeMastry

A1. Chemical composition

$(Th_9U)C_2$

2. Phase diagram

No data available

3. Effect of impurities

No data available

B1. Density (room temperature)

No data available

2. Density versus temperature

No data available

3. Uranium content

No data available

4. Liquidus temperature

No data available

5. Solidus temperature

No data available

6. Vapor pressure

No data available

7. Thermal expansion (linear)[1]

Temperature, F	Coefficient, 10^{-6} per F
68-200	4.1
68-400	4.2
68-600	4.3
68-800	4.4
68-1000	4.4
68-1200	4.6
68-1400	4.7
68-1600	4.8
68-1800	5.0

8. Recrystallization temperature range

No data available

C1. Hardness (room temperature)[2]

460 Knoop (100-g load)

2. Hot hardness

No data available

3. Ultimate tensile strength

No data available

4. Yield strength

No data available

5. Compressive strength[1,3]

Temperature, F	Compressive Strength, psi
68	59,000
1200	15,000
1800	23,000

6. Creep strength

No data available

7. Young's modulus

No data available

8. Shear modulus

No data available

9. Bulk Modulus

No data available

10. Poisson's ratio

No data available

11. Elongation

No data available

D1. Specific heat

No data available

2. Thermal conductivity[4]

Temperature, C	Thermal Conductivity, cal/(sec)(cm)(C)
200	0.0483
400	0.0528
600	0.0566
800	0.0607
900	0.0629
950	0.0637

E1. Electrical resistivity

No data available

F1. Reactions with

a. Steam[2]
Catastrophic

b. Helium
No data available

c. Carbon dioxide
No data available

d. Nitrogen
No data available

e. Hydrogen
No data available

f. Liquid metals[2]
Minus 1.5×10^{-2} mg/(cm^2)(day) in 1200 F NaK

g. Air[2]
Dry: plus 17 mg/(cm^2)(hr) at 1300 F
Wet: catastrophic

2. Reactions with claddings or structural materials
No data available

G1. Dimensional stability during irradiation
No data available

2. Fission-gas-release data
No data available

3. Swelling-temperature data
No data available

4. Unusual nuclear properties
No data available

5. Property changes as a result of irradiation
No data available

H. References

(1) Dayton, R. W., and Tipton, C. R., Jr., "Progress Relating to Civilian Applications During January, 1962, BMI-1565 (February 1, 1962).

(2) Farkas, M. S., Bauer, A. A., and Dickerson, R. F., "Evaluation of Thorium and Thorium-Uranium Compounds As Thermal Breeder Fuels", BMI-1568 (February 15, 1962).

(3) Dayton, R. W., and Dickerson, R. F., "Progress Relating to Civilian Applications During February, 1962", BMI-1569 (March 1, 1962).

(4) Dayton, R. W., and Dickerson, R. F., "Progress Relating to Civilian Applications During August, 1962", BMI-1593 (September 1, 1962).

URANIUM CARBIDES

Compiled by W. Chubb

A1. Chemical composition

Uranium monocarbide, UC, 4.8 w/o carbon
Uranium sesquicarbide, U_2C_3, 7.0 w/o carbon
Uranium dicarbide, UC_2, 9.1 w/o carbon

2. Phase diagram[1]

See Figure A2.

3. Effect of impurities

The melting point of UC is lowered by all known impurities except HfC, NbC, TaC, ThC, UN, and ZrC. See Reference (2) for additional details of ternary constitution.

Most impurities tend to increase the room-temperature hardness and strength of UC.

B1. Density (room temperature)

As-cast uranium-carbon alloys[3]: see Figure B1.
U_2C_3: 12.8 g per cm^3.[4]

2. Density versus temperature

No data available: see B-7.

3. Uranium content

Compound	Fuel Density, g per cm^3
UC	12.9
U_2C_3	11.9
UC_2	10.2

4. Liquidus temperature

See Figure A2.

5. Solidus temperature

See Figure A2.

6. Vapor pressure[5,6]

The vapor species over uranium carbides are not known precisely. A congruently vaporizing composition exists at approximately $UC_{1.07}$. Higher carbon alloys lose carbon preferentially by vaporization. Assuming the vapor species over UC_2 saturated with carbon (actually about $UC_{1.86}$) to be uranium atoms and carbon atoms, the following expressions for the vapor pressure of uranium have been obtained:

From 1930 to 2365 K[5]:

$$\ln P_U = -\frac{67,164}{T} - 0.111\left(\ln T + \frac{2000}{T}\right) + 12.140.$$

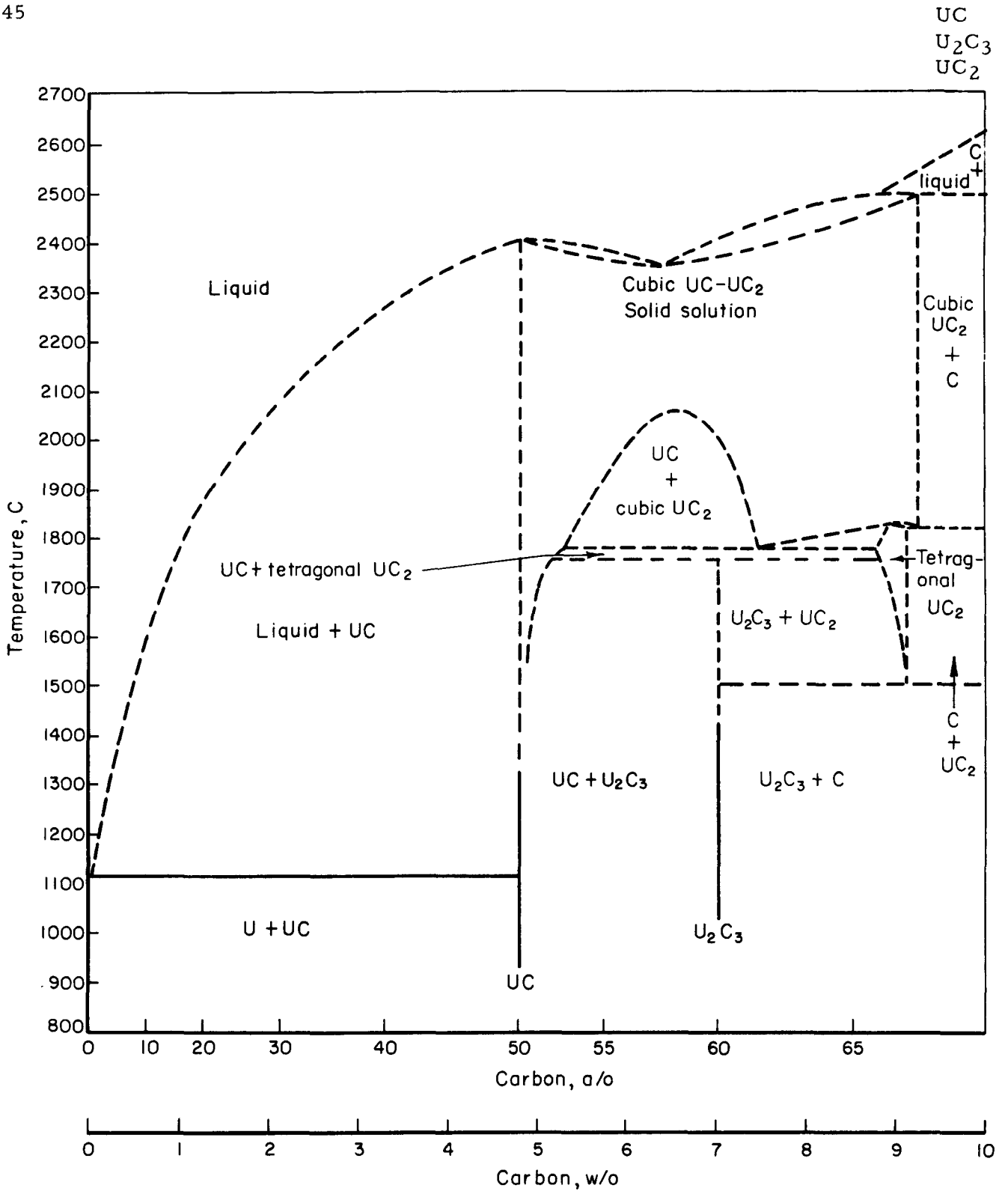

FIGURE A2. URANIUM-CARBON CONSTITUTIONAL DIAGRAM[1]

AEA-43208

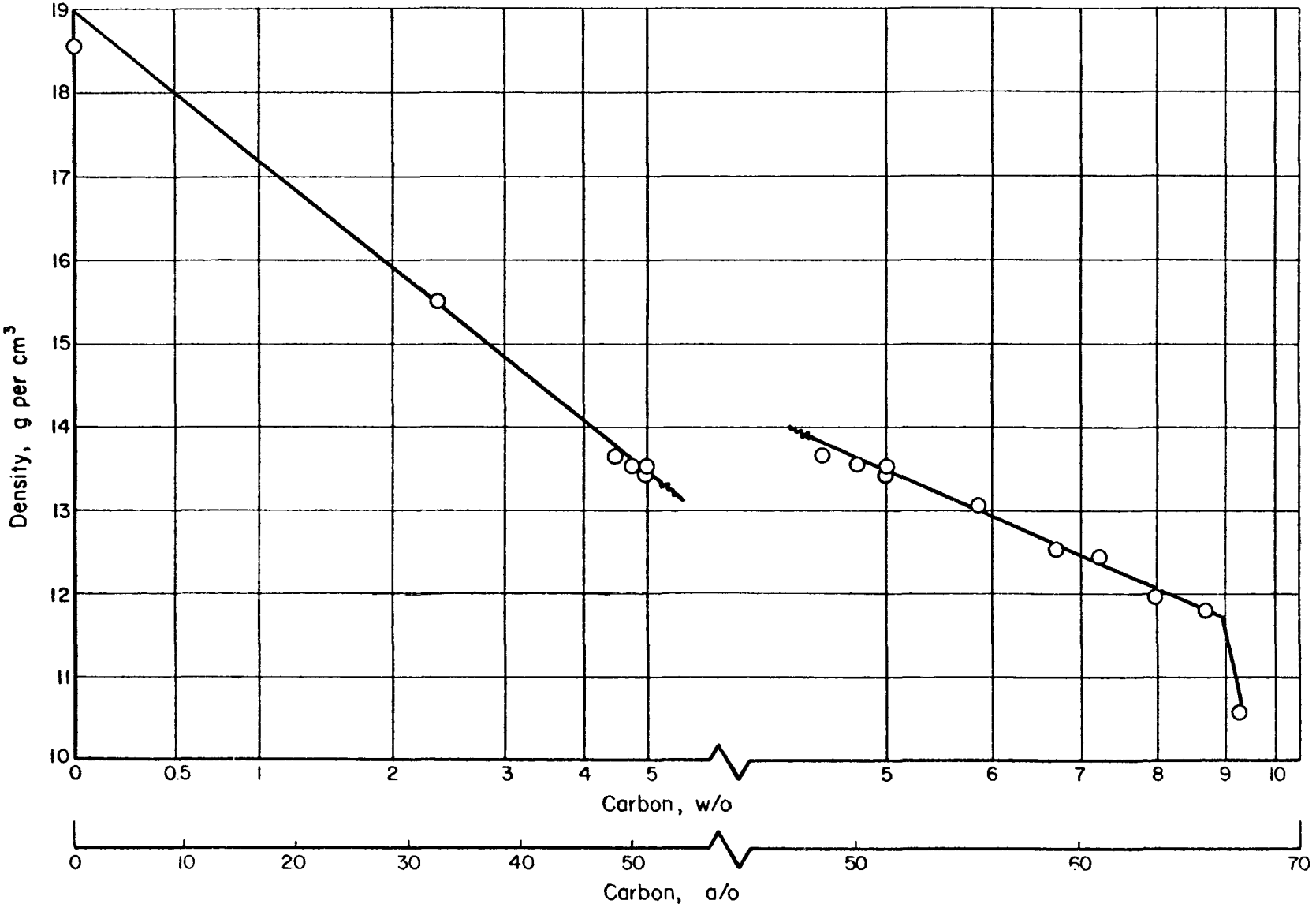

FIGURE BI. DENSITY OF AS-CAST URANIUM-CARBON ALLOYS[3]

From 2448 to 2731 K[6]:

$$\log P_U \text{ (atm)} = -30,600/T + 6.36.$$

7. Thermal expansion

As-Cast Alloys	Coefficient[a] from 20 to 1600 C, 10^{-6} per C
Uranium - 4.8 w/o carbon	11.0
Uranium - 7.0 w/o carbon	12.0
Uranium - 9.0 w/o carbon	15.8

(a) Calculated from dilation curves in Reference (1).

8. Recrystallization temperature range[7,8]

Grain growth in UC is very slow at 1100 C and relatively rapid at 1700 C.

The diffusion rate of uranium in UC is less than 10^{-11} cm^2 per sec at 1400 C. See also C-2.

C1. Hardness (room temperature)[4]

Material	Typical Room-Temperature Hardness, DPH, kg per mm^2
Uranium - 4.8 w/o carbon alloy, as cast, UC	700
Uranium - 7.0 w/o carbon alloy, as cast, UC + UC_2	750
Uranium - 7.0 w/o carbon alloy, annealed, U_2C_3	1100
Uranium - 9.0 w/o carbon alloy, as cast, UC_2	500

2. Hot hardness[1]

The hardness of the uranium carbides begins to decrease rapidly at about 1000 C and falls below 100 kg per mm^2 for all compositions between 5 and 9 w/o carbon at about 1200 C.

3. Ultimate tensile strength

No data available

4. Yield strength[4]

No data available; transverse rupture strengths range from 10,000 ± 4,000 psi for uranium - 4.8 w/o carbon alloy to 12,000 ± 4,000 psi for uranium - 7.0 w/o carbon alloy.

5. Compressive strength[4]

Material	Compressive Rupture Strength, psi
Uranium - 4.8 w/o carbon alloy, as cast, UC	51,000
Uranium - 7.0 w/o carbon alloy, as cast, UC + UC_2	66,000

6. Creep strength[9]

Grain-growth, hot-pressing, and hot-hardness studies show that recovery processes are active in uranium carbides at temperatures near 1100 C.

In the temperature range from 1500 to 1900 C, plastic strain rates in arc-cast UC follow a relation of the type:

$$\text{Strain Rate} = kf(\sigma) \exp(-37{,}500/RT),$$

where k is a constant, $f(\sigma)$ is a functional relation of stress,

σ is the stress (about 2000 psi) at 0.001 strain, R is the gas constant, and T is the absolute temperature.

7. Young's modulus

Material	Temperature, C	Young's Modulus, 10^6 psi	Reference
Uranium - 4.8 w/o carbon alloy	20	29.5	(4)
Uranium - 7.0 w/o carbon alloy	20	29.0	(4)
Uranium - 5.0 w/o carbon alloy	20	29.6	(10)
Uranium - 5.0 w/o carbon alloy	500	28.8	(10)
Uranium - 5.0 w/o carbon alloy	1000	27.2	(10)
Uranium - 5.0 w/o carbon alloy	1500	20.7	(10)
Uranium - 5.0 w/o carbon alloy	1700	14.8	(10)

8. Shear modulus

No data available

9. Bulk modulus

No data available

10. Poisson's ratio

No data available

11. Elongation

No data available

D1. Specific heat[11]

The specific heat of a uranium-4.8 w/o carbon alloy sintered to a density of 10.2 g per cm^3 (75 per cent of theoretical) was found to be 0.048 cal/(g)(C) at 125 C and 0.053 cal/(g)(C) at 250 C.

2. Thermal conductivity[2]

The thermal conductivity of UC (uranium-4.8 w/o carbon alloy) is 0.055 cal/(sec)(cm)(C) from 200 to 1000 C.

UC
U_2C_3
UC_2

E1. Electrical resistivity[1,3,4]

The resistivity at room temperature[3] of as-cast uranium carbon alloys is shown in Figure E1. The resistivity of a uranium-7 w/o carbon alloy transformed to U_2C_3 by heat treatment[4] is about 210 microhm-cm at room temperature.

The resistivity of three different uranium carbon alloys as a function of temperature[1] is shown in Figure E2.

F1. Reactions with coolants

a. Steam[12,13,14]

Uranium carbides react with steam, water, and water vapor at room temperature and above to form hydrogen, hydrocarbons, and hydrated uranium oxides. The rate is significant at room temperature and becomes catastrophic at about 100 C.

b. Helium

Uranium carbides are decarburized or oxidized depending upon the partial pressure of the oxygen imposed on the system at temperatures of about 1000 C or above as an impurity in helium.

c. Carbon dioxide[15]

The rate of oxidation of uranium monocarbide is very rapid in carbon dioxide at 500 C and above.

d. Nitrogen[2]

Uranium monocarbide dissolves nitrogen at high temperatures, forming the solid solution, U(C,N), and the higher carbides and nitrides found in the ternary uranium-carbon-nitrogen system.

e. Hydrogen[16]

Hydrogen reacts with uranium dicarbide to produce uranium monocarbide and methane at 700 C.

f. Liquid metals[17,18]

Uranium carbides are oxidized by the oxygen normally present as an impurity in sodium and NaK at temperatures of 600 C and above.

g. Air[19]

Bulk uranium carbide begins to oxidize in oxygen at about 300 C. An initial rapid reaction is followed by a slower reaction. Apparently the first oxide to form is adherent and somewhat protective.

2. Reactions with claddings or structural materials

The reactions of uranium carbides with solids are characterized by a temperature range below which no perceptible reaction occurs and above which reaction occurs at a catastrophic rate. The approximate location of this temperature range is indicated by the remarks noted in Table F2.

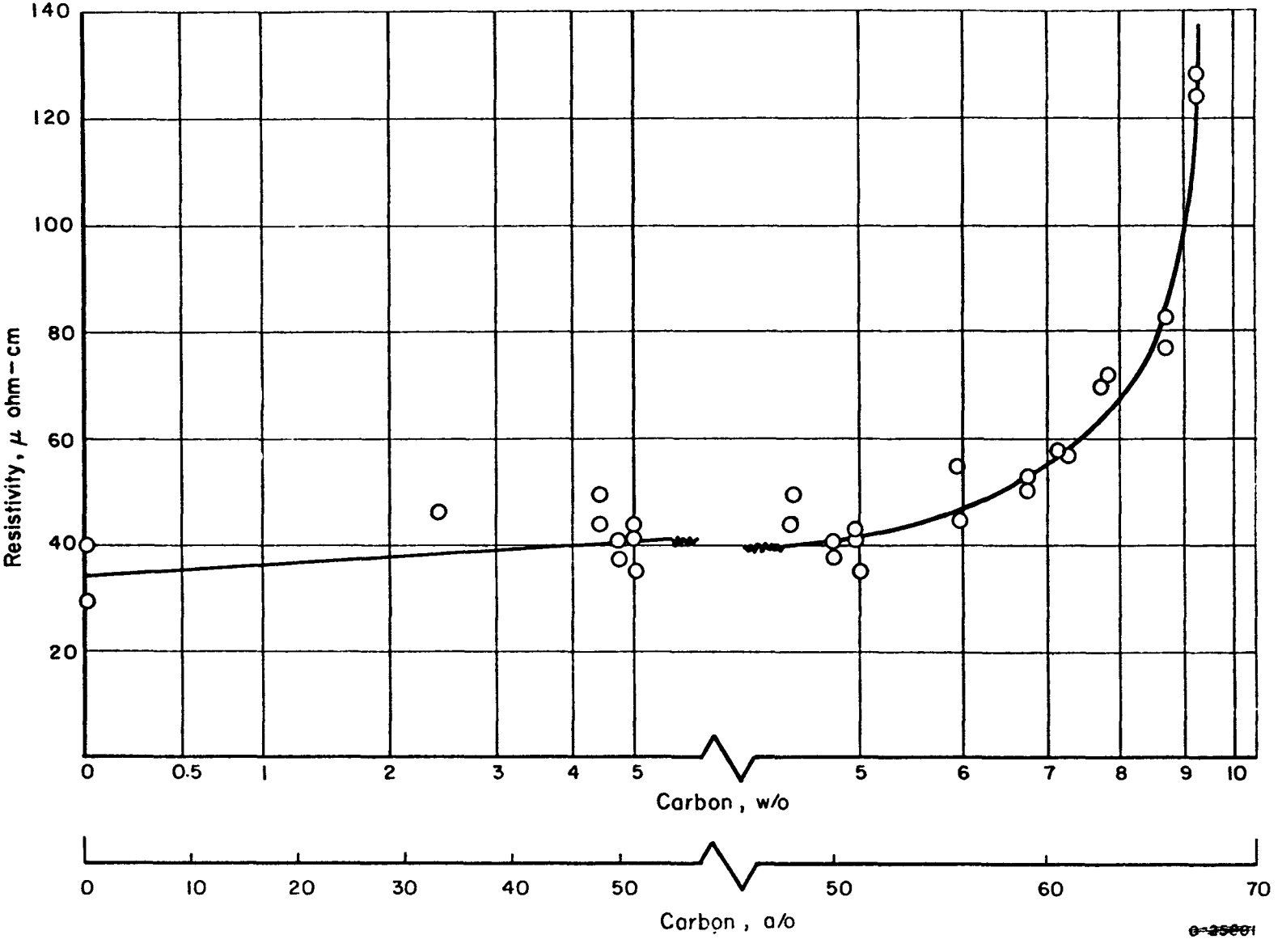

FIGURE E1. RESISTIVITY OF AS-CAST URANIUM-CARBON ALLOYS [3]

AEA-43214

UC
U_2C_3
UC_2

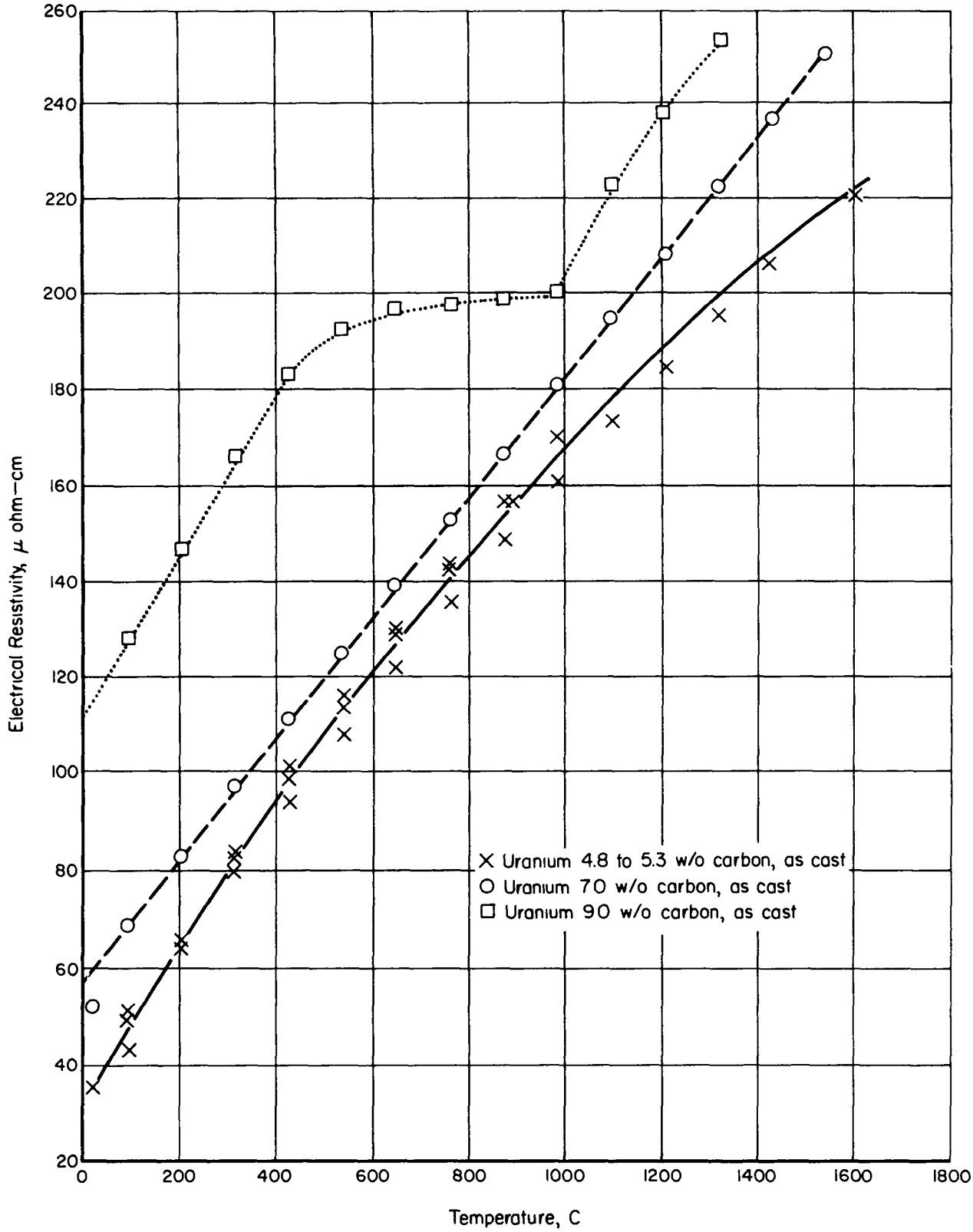

FIGURE E2. EFFECT OF TEMPERATURE ON THE ELECTRICAL RESISTIVITY OF URANIUM-CARBON ALLOYS[1]

AEA-43247

TABLE F2. COMPATIBILITY OF URANIUM CARBIDES WITH SOLIDS

Solid Material	Remarks	Reference
Aluminum	Slight reaction at 600 C and above	(4,20)
Beryllium	Reacts to form UBe_{13} at 700 C and above	(21)
Copper	No reaction at 1000 C	(4)
Graphite	Slight reaction at 1600 C	(8)
Inconel	Slight reaction at 800 C	(4)
Inconel X	Formed liquid eutectic at 820 C	(22)
Magnesium	No reaction at 600 C	(4)
Molybdenum	Slight reaction at 1200 C	(4,23)
Nickel	Rapid reaction at 1000 C (see Inconel X)	(11)
Nichrome V	Melted at 1100 C (see Inconel X)	(23)
Niobium	Slight reaction at 1100 C	(24)
Niobium-40 a/o titanium	Formed a liquid phase at 1200 C	(23)
Silicon	Reacts to form USi_3 at 1000 C	(11)
Mild steel	Slight reaction at 1000 C	(4)
Type 304 stainless	No reaction with stoichiometric UC to 870 C	(25)
Type 304 stainless	Slight carburization of stainless by U_2C_3 and UC_2 at 550 C	(25)
Tantalum	Rapid reaction at 1800 C	(26)
Titanium	Slight reaction at 1100 C	(27)
Tungsten	Rapid reaction at 1800 C	(26)
Zirconium	Slight reaction at 800 C	(4)
Zircaloy-2	Slight reaction at 820 C	(22)

G1. Dimensional stability during irradiation

As shown in Table G2, the dimensional stability of uranium carbides at moderate temperatures is excellent during irradiation.

2. Fission-gas-release data[1,17,28]

At temperatures up to 800 C, the fission gas released by bulk uranium carbide may be attributed entirely to fission recoils. See Table G2.

3. Swelling-temperature data

The swelling temperature of uranium carbides has not been located exactly, but appears to be over 1000 C [See Reference (29), Table G2]. See also C6.

4. Unusual nuclear properties

No unusual nuclear properties of the uranium carbides have been observed.

5. Property changes as a result of irradiation

Increases in resistivity[1,30] and in lattice strain[1] have been observed in uranium monocarbide. An increase in resistivity of 2.5 per cent was observed at a flux of 6×10^{17} thermal nvt. An increase in resistivity of over 150 per cent was observed at a burnup of 1.3×10^{18} fissions per cm^3.

TABLE G2. IRRADIATION DATA ON URANIUM CARBIDES

Material		Central Core Temperature, C	Average Heat-Generation Rate, 10^3 Btu/(ft^2)(hr)	Surface Temperatures During Irradiation, C	Approximate Burnup, fissions per cm^3	Density Change, per cent	Fission-Gas-Release Fraction[a]	Reference
Carbon Content (Balance Uranium), w/o	Fabrication Condition							
5.2	As cast	590-870	680	340-480	5×10^{19}	0.8	--	(17)
5.2	As cast	370-590	850	270-350	6.5×10^{19}	2.5	4×10^{-4}	(17)
5.3	As cast	490-1000	880	330-580	2×10^{20}	2.0	--	(17)
5.1	As cast	380-800	940	270-480	3×10^{20}	2.5	5×10^{-4}	(17)
5.0	As cast	580-640	700	330-410	4.5×10^{20}	1.8	--	(28)
5.2	As cast	530-680	--	300-400	6.5×10^{20}	3.4	--	(28)
5.3	As cast	430-560	670	240-310	9×10^{20}	4.4	--	(28)
5.0	Annealed	--	--	680-810	2.5×10^{20}	0.6	3×10^{-3}	(1)
6.7	Annealed	--	--	600-740	2×10^{20}	1.3	--	(1)
4.8	As cast	930-1300	--	Over 1000	0.5 to 2×10^{20}	Over 10	0.05-0.30	(29,31)

(a) Amount released/amount produced.

UC
U_2C_3
UC_2

H. References

(1) Rough, F. A., and Chubb, W., "Progress on the Development of Uranium Carbide-Type Fuels", BMI-1554 (November 17, 1961).

(2) Rough, F. A., and Chubb, W., "An Evaluation of Data on Nuclear Carbides", BMI-1441 (May 31, 1960).

(3) Rough, F. A., and Chubb, W., "Progress on the Development of Uranium Carbide-Type Fuels", BMI-1370 (August 21, 1959).

(4) Rough, F. A., and Chubb, W., "Progress on the Development of Uranium Carbide-Type Fuels", BMI-1488 (December 27, 1960).

(5) Leitnaker, J. M., and Witteman, W. G., "The Dissociation Pressure of Uranium Dicarbide", TID-13629 (September, 1961).

(6) Fujishiro, S., "The Dissociation Pressure of UC_2 ...", Nippon Genshiryoku Gakkaishi, Vol. 3, pp 913-917 (December, 1961).

(7) Accary, A., and Lucas, R., "The Effect of Heat Treatment on Uranium Monocarbide and U-UC Cermets", Rev. met., 58, 383-387 (May, 1961).

(8) Chubb, W., Townley, C. W., and Getz, R. W., "Diffusion Coefficients of Uranium and Carbon in Uranium Monocarbide", BMI-1551 (November 6, 1961).

(9) Chang, R., "The Flow and Recovery of Uranium Monocarbide ...", J. Appl. Phys., 33, 858-863 (March, 1962).

(10) "Annual Technical Progress Report, Atomics International", NAA-SR-5350 (August, 1960, p VII-26.

(11) Boettcher, A., and Schneider, G., "Some Properties of Uranium Monocarbide", Proceedings of the Second United Nations International Conference on The Peaceful Uses of Atomic Energy, Geneva (1958), Vol. 6, pp 561-563.

(12) Litz, L. M., "Uranium Carbides, Their Preparation, Structure, and Hydrolysis", The Ohio State University, Ph. D. Thesis (1948), USAEC Document No. NP-1453.

(13) Engle, G. B., Goeddel, W. V., and Luby, C. S., "Reaction-Rate Studies of Thorium-Uranium Dicarbides in Moist Air", GA-2195 (April 20, 1961).

(14) Blanco, R. E., "Quarterly Progress Report for Chemical Development Section B, April-June, 1961", ORNL-TM-1 (November 15, 1961).

(15) Antill, J. E., Peakall, K. A., Crick, N., and Smart, E., "Compatibility of UO_2, UC, and U with CO_2", AERE-M/M-168 (1957).

(16) Silverman, L., "The High Temperature Chemical Reactivities of the Uranium Carbides", NAA-SR-memo-4269 (August, 1959).

(17) Rough, F. A., Hare, A. W., Price, R. B., and Alfant, S., "Irradiation of Uranium Monocarbide", Nuclear Sci. Eng., 7, 111-121 (February, 1960).

(18) Gordon, E., "Quarterly Progress Report, Fuel Cycle Development Program, Oct. to Dec., 1961", UNC-3001 (February 1, 1962).

(19) Murbach, E. M., "The Oxidation of Uranium Carbide", NAA-SR-memo-5494 (July, 1960).

(20) Thurber, W. C., and Beaver, R. J., "Dispersions of Uranium Carbides in Aluminum Plate-Type Research Reactor Fuel Elements", J. Nuclear Mat., 1, 226-232 (October, 1959).

(21) "Metallurgy Division Annual Progress Report", ORNL-3160 (August 17, 1961).

(22) Sheridan, W., Strasser, A., Anderson, J., and Taylor, K., "Carbide Fuel Development Phase Report", NDA-2162-5 (Sept. 30, 1961).

(23) Sheinhartz, I., "Dispersion Type Materials for Fuel Elements, Part II, Uranium Carbide and Uranium Sulfide Dispersion Materials", SCNC-273 (March, 1959).

(24) Finley, J. J., Korchynsky, M., and Sarian, S., "Columbium Alloy Clad Uranium Carbide Fuel Element", ORO-366 (September 1, 1960).

(25) "Annual Technical Progress, Fiscal Year 1961", NAA-SR-6370 (August 15, 1961).

(26) Carpenter, F. D., "Investigations of Carbides as Cathodes for Thermionic Space Reactors", GA-2670 (December, 1961).

(27) Nichols, R. W., "Ceramic Fuels - Properties and Technology", Nuclear Eng., 3, 327-333 (August, 1958).

(28) Hare, A. W., and Rough, F. A., "The Effect of High-Burnup Irradiation on Massive Uranium Carbide", BMI-1491 (January 6, 1961).

(29) "Gas-Cooled Reactor Program Progress Report", ORNL-3166 (August 28, 1961), pp 136-148.

(30) Griffiths, L. B., "The Effect of Irradiation and Post Irradiation Annealing on The Electrical Resistivity of Uranium Monocarbide", J. Nuclear Mat., 4, 336 (1961).

(31) Manly, W. D., "Gas-Cooled Reactor Program Progress Report", ORNL-3302 (July 16, 1961), pp 265-266.

URANIUM MONONITRIDE

Compiled by E. O. Speidel

A1. Chemical composition

UN, 5.56 w/o nitrogen, 94.44 w/o uranium

2. Phase diagram[1]

No diagram has been constructed for the uranium-nitrogen system. Three compounds, UN, U_2N_3, and UN_2, are known to exist. The system is two-phase between the mononitride, UN, and the sesquinitride, U_2N_3. The solubility of nitrogen in uranium is limited. The solubility of uranium in the mononitride, UN, is also limited.

The sesquinitride, U_2N_3, is stable only to 1300 C, where it decomposes to form UN plus nitrogen at low pressures.

3. Effect of impurities[2]

No data available; variations in the lattice constant of UN have been attributed to the presence of carbon or oxygen instead of solubility of nitrogen in UN.

B1. Density (room temperature)[2]

14.32 g per cm^3 (X-ray)

2. Density versus temperature

No data available

3. Uranium content

13.5 g per cm^3

4. Liquidus temperature

No data available; see B5.

5. Solidus temperature[3]

The observed melting temperature of five samples varied from 2575 to 2710 C under an atmosphere of NH_3 (UN probably decomposes since the decomposition temperature is strongly pressure dependent).

6. Vapor pressure

No data available

7. Thermal expansion (linear)[4,5]

Temperature, C	Coefficient, 10^{-6} per C
20-1200	9.7
20-1600	10.1

8. Recrystallization temperature range

No data available; see Reference (6) for possible data.

C1. **Hardness (room temperature)**[7,8]

600 ± 50 KHN

2. **Hot hardness**[4]

Temperature, C	DPH
650	280
760	220
870	160
980	130
1090	120

3. **Ultimate tensile strength**

No data available

4. **Yield strength**

No data available

5. **Compressive strength**

No data available

6. **Creep strength**

No data available

7. **Young's modulus**

33×10^6 psi [extrapolated to 100 per cent density from data in References (4) and (5)]

8. **Shear modulus**

16×10^6 [extrapolated to 100 per cent density from data in Reference (5)]

9. **Bulk modulus**

25×10^6

10. **Poisson's ratio**

0.28 [extrapolated to 100 per cent density from data in Reference (5)]

D1. **Specific heat**

No data available

2. **Thermal conductivity**[9]

Temperature, C	Thermal Conductivity[a], cal/(sec)(cm)(C)
25	0.032[b]
200	0.037
300	0.040
400	0.042
500	0.044
600	0.046
700	0.048
800	0.049

(a) Measured on a 97 per cent dense specimen. (b) Extrapolated.

E1. Electrical resistivity[9]

Temperature, C	Resistivity[a], microhm-cm
25	161[b]
200	176
300	184
400	190
500	196
600	201
700	205
800	208

(a) Measured on a 97 per cent dense specimen.
(b) Extrapolated.

F1. Reactions with coolants

a. Steam
No data available

b. Helium
No data available

c. Carbon dioxide
No data available

d. Nitrogen
Will probably form higher nitrides up to 1300 C; see A2 above.

e. Hydrogen[9]
No reaction up to 800 C

f. Liquid metals
No data available

g. Air[10]
Catastrophic above 150 C

2. Reactions with claddings or structural materials

No engineering data available

G1. Dimensional stability during irradiation[11]

Estimated Burnup, fissions per cm^3	Estimated Temperature, F				Density Decrease, per cent
	Surface		Center Line		
	Start	End	Start	End	
1.2×10^{21}[a]	1070	400	2600	900	3.5[b]

(a) Estimated from reactor data.
(b) Based on dimensional measurements of cladding.

2. Fission-gas-release data

No data available

3. Swelling-temperature data

No data available

4. Unusual nuclear properties

$N^{14}(n,p)C^{14}$ reaction

5. Property changes as a result of irradiation[12]

Effects of neutron radiation on crystal structure:

$$\frac{\Delta a}{a} = 1.67 - 1.67 \exp(-7 \times 10^{-18} n),$$

where $\frac{\Delta a}{a}$ is fractional increase in unit-cell size, and n is neutron dose in n per cm^2. Specimens used were irradiated in the BEPO reactor in a flux of about 10^{12} $n/(cm^2)(sec)$ at ambient temperature.

H. References

(1) Rough, F. A., and Bauer, A. A., "Constitution of Uranium and Thorium Alloys", BMI-1300 (June 2, 1958)

(2) Rundle, R. E., Baenziger, N. C., Wilson, A. S., and McDonald, R. A., "The Structures of the Carbides, Nitrides and Oxides of Uranium", J. Am. Chem. Soc., 70, 99-105 (1948).

(3) Chiotti, P., "Experimental Refractory Bodies of High Melting Nitrides, Carbides, and Uranium Dioxide", J. Am. Ceram. Soc., 35, 123-130 (1952).

(4) Keller, D. L., "Development of Uranium Mononitride", Quarterly Progress Report for July-September, 1961, to Joint U. S.-Euratom Research and Development Board, BMI-X-178 (EUR/AEC-169) (October 1, 1961).

(5) Taylor, K. M., and McMurtry, C. H., "Synthesis and Fabrication of Refractory Uranium Compounds, Summary Report for May, 1959 through December, 1960", ORO-400 (February, 1961).

(6) Accary, A., and Marchal, M., "Behavior of Uranium Mononitride Under Heat Treatment", Mem. Sci. Rev. Met., 59, 57-70 (January, 1962).

(7) Epstein, H. M., and Keller, D. L., "Quarterly Progress Report to Joint U. S.-EURATOM Research and Development Board on Battelle Assistance to AEC-EURATOM Program for the Period Ending December 31, 1960", TID-11928 (EUR/AEC-75).

(8) Epstein, H. M., and Keller, D. L., "Quarterly Progress Report to Joint U.S.-EURATOM Research and Development Board on Battelle Assistance to AEC-EURATOM Program for the Period Ending March 31, 1961", TID-12551 (EUR/AEC-76).

(9) Keller, D. L., "Quarterly Progress Report to Joint US-EURATOM Research and Development Board on Development of Uranium Mononitride for the Period Ending June 30, 1961", (EUR/AEC-77).

(10) Speidel, E., Battelle Memorial Institute, Unpublished Information.

(11) Keller, D. L., "Development of Uranium Mononitride, Quarterly Progress Report for January-March, 1962 to Joint U.S.-EURATOM Research and Development Board", EUR/AEC-348 (April 1, 1962).

(12) Adams, J., and Rogers, M. D., "X-Ray Diffraction Studies of Fission Fragment Damage in Uranium Carbide and Nitride", J. Nuclear Energy, Pts. A & B., Reactor Sci. Technol., 14, 51-53 (April, 1961)

URANIUM OXIDES

Compiled by J. B. Melehan, F. A. Rough, and M. Kangilaski

A1. Chemical composition

a. Stoichiometric UO_2, 88.15 w/o uranium, 11.85 w/o oxygen

b. U_4O_9, 86.86 w/o uranium, 13.14 w/o oxygen

c. U_3O_7, 86.44 w/o uranium, 13.56 w/o oxygen

d. U_3O_8, 84.80 w/o uranium, 15.20 w/o oxygen

e. UO_3, 83.22 w/o uranium, 16.78 w/o oxygen

2. Phase diagram[1]

See Figure A2

3. Effect of impurities

The principal impurity of interest is oxygen. The addition of excess oxygen results in decreased lattice parameters of UO_2 (a = 5.4691 ± 0.005 A) until the U_4O_9 (a = 5.4411 A) composition is attained. The cubic fluoride-type UO_2 is modified gradually in the UO_2-U_4O_9 phase region and is finally converted to the cubic U_4O_9 structure. The U_3O_7 structure is tetragonal with a = 5.447 ± 0.003 A, c = 5.400 ± 0.002 A, and is only stable below 200 C and at compositions less than $UO_{2.33}$. U_3O_8 is orthorhombic with the lattice constants a = 6.91 ± 0.01 A, b = 11.96 ± 0.03 A, and c = 4.15 ± 0.01 A. The UO_3 exists in two modifications, alpha UO_3 with a hexagonal structure (a = 3.971 ± 0.004 A and c = 4.168 ± 0.008 A) and beta UO_3 with an orthorhombic structure (a = 13.01 A, b = 10.92 A, c = 9.51 A). There has been no systematic study of the effect of ternary, metallic, or nonmetallic additions on the composition limits.

B1. Density (room temperature)[1-7]

a. Theoretical density of stoichiometric UO_2 (based on X-ray diffraction analysis) is 10.95 to 10.97 g per cm^3.

b. Change of density with oxygen content is shown in Figure B1.[1]

2. Density versus temperature

See B7.

3. Uranium content

9.67 g per cm^3

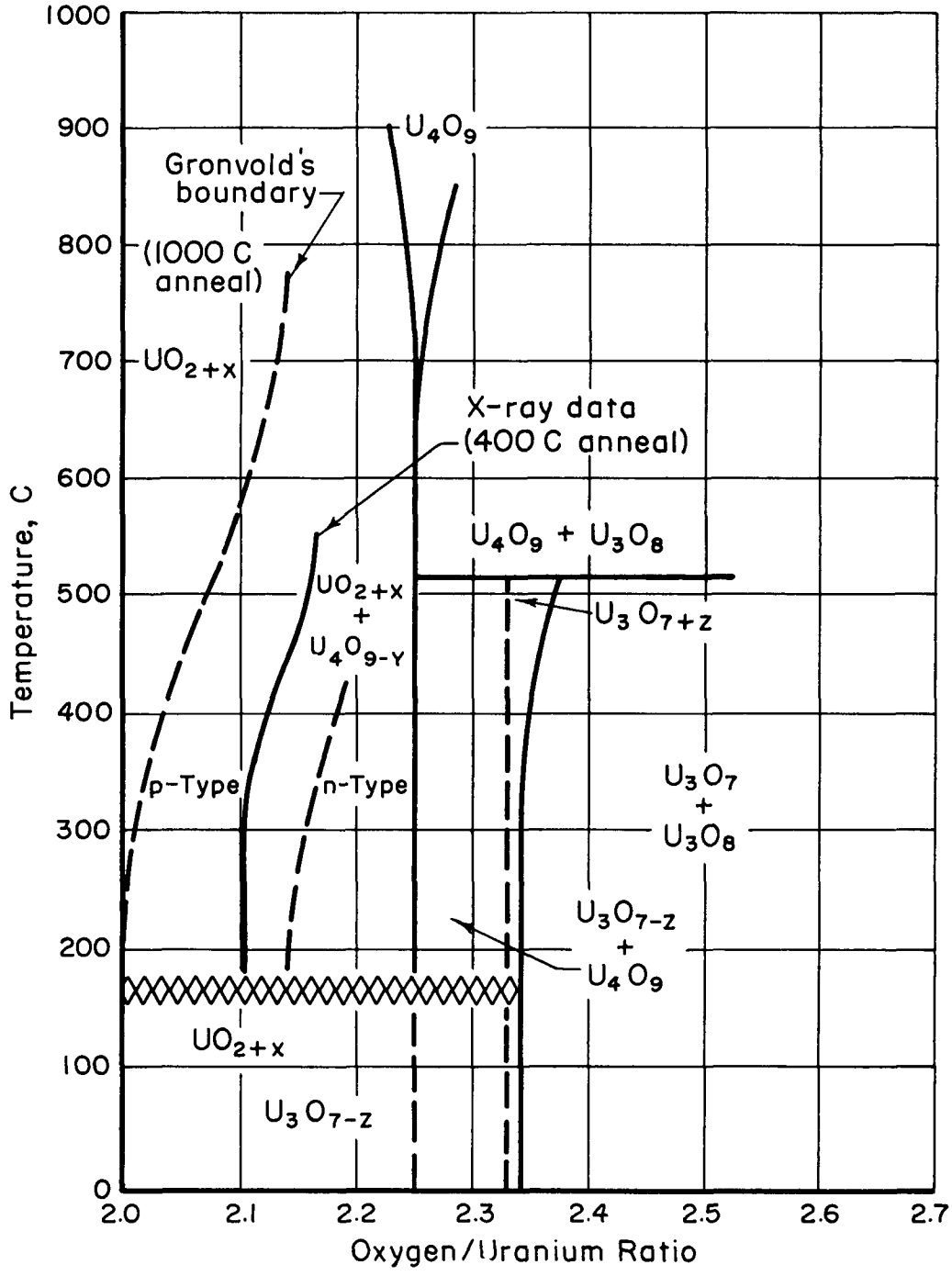

FIGURE A2. UO_2-U_3O_7 PHASE DIAGRAM[1]

AEA-43209

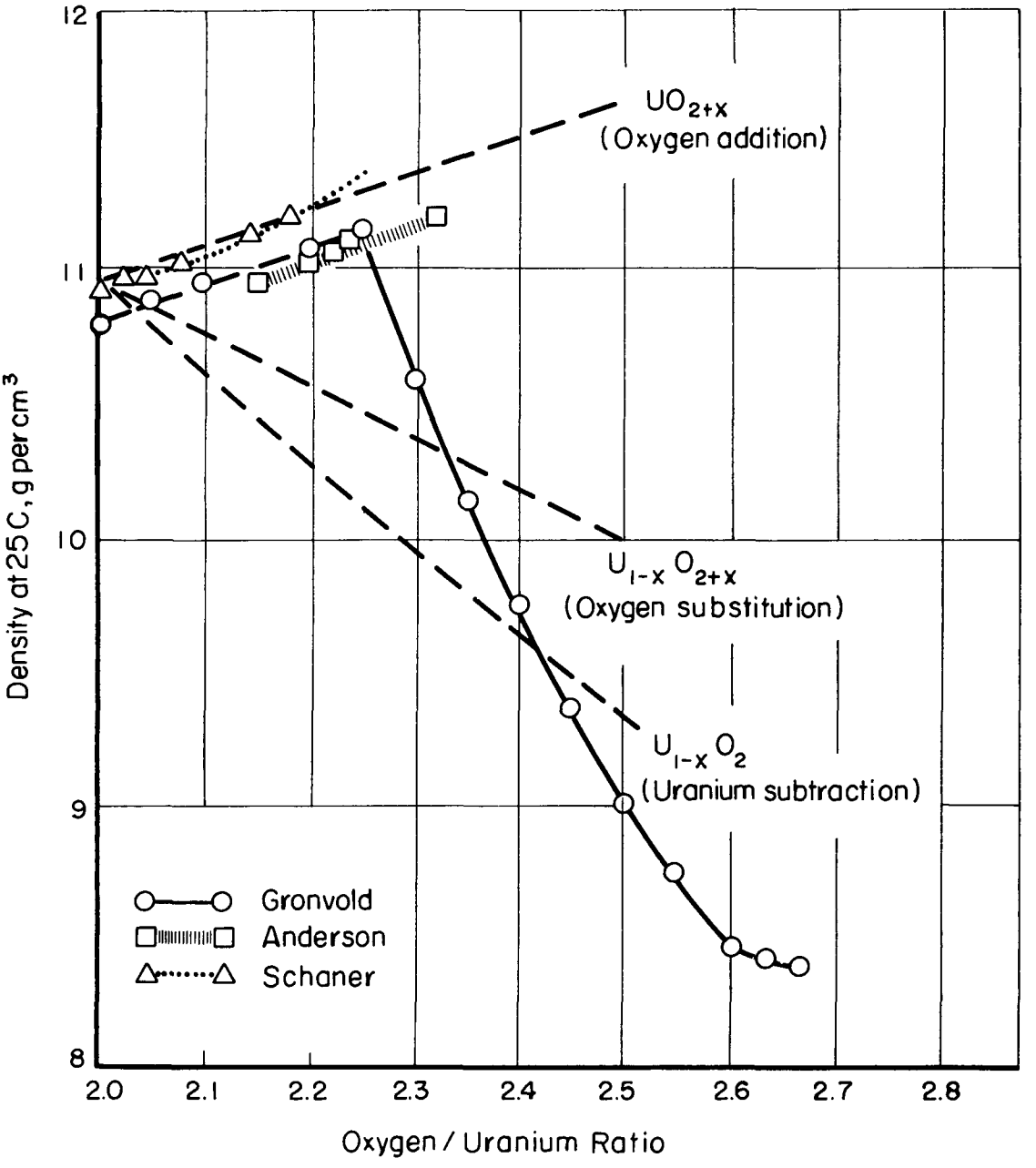

FIGURE BI. URANIUM OXIDE DENSITY AS A FUNCTION OF COMPOSITION[1]

AEA-43000

4. Liquidus temperature[8-11]

a. In helium atmosphere using a tungsten crucible: 2800 C ± 20 C

b. In vacuum: 2405 C ± 20 C

c. In hydrogen, argon, or helium: 2760 ± 30 C

5. Solidus temperature

Same as liquidus temperature

6. Vapor pressure[12,13]

a. Vaporization of stoichiometric UO_2

From 1600-2000 K:

$$\log p_{(mmHg)} = -\frac{33,115}{T} - 4.026 \log T + 25.686.$$

Above 2000 K:

$$\log p_{(mmHg)} = 13.298 - \frac{3.7195 \times 10^4}{T} \quad \frac{3.5612 \times 10^6}{T^2} \quad \frac{2.6178 \times 10^9}{T^3}.$$

b. Vapor pressure of UO_3 from thermodynamic data for crystalline UO_2 and gaseous UO_3.

Below 2000 K:

$$\log p_{(atm)} = -\frac{13,100}{T} + 4.73 + 1/2 \log p_{O_2}, \text{ where}$$

p_{O_2} = partial pressure of oxygen over UO_3.

7. Thermal expansion (linear)[7,14,15]

a. Dilatometric linear thermal expansion to the melting point of UO_2 (93 per cent of theoretical density): $l = l_o (1 + 6.0 \times 10^{-6} T + 2.0 \times 10^{-9} T^2 + 1.7 \times 10^{-12} T^3)$, where T = temperature, K.

b. X-ray diffraction measurements of UO_2 cell size give expansion coefficients of 9.9×10^{-6} to 10.8×10^{-6} per C.

8. Recrystallization temperature range

No data available

9. Grain growth[16]

See Figure B9.

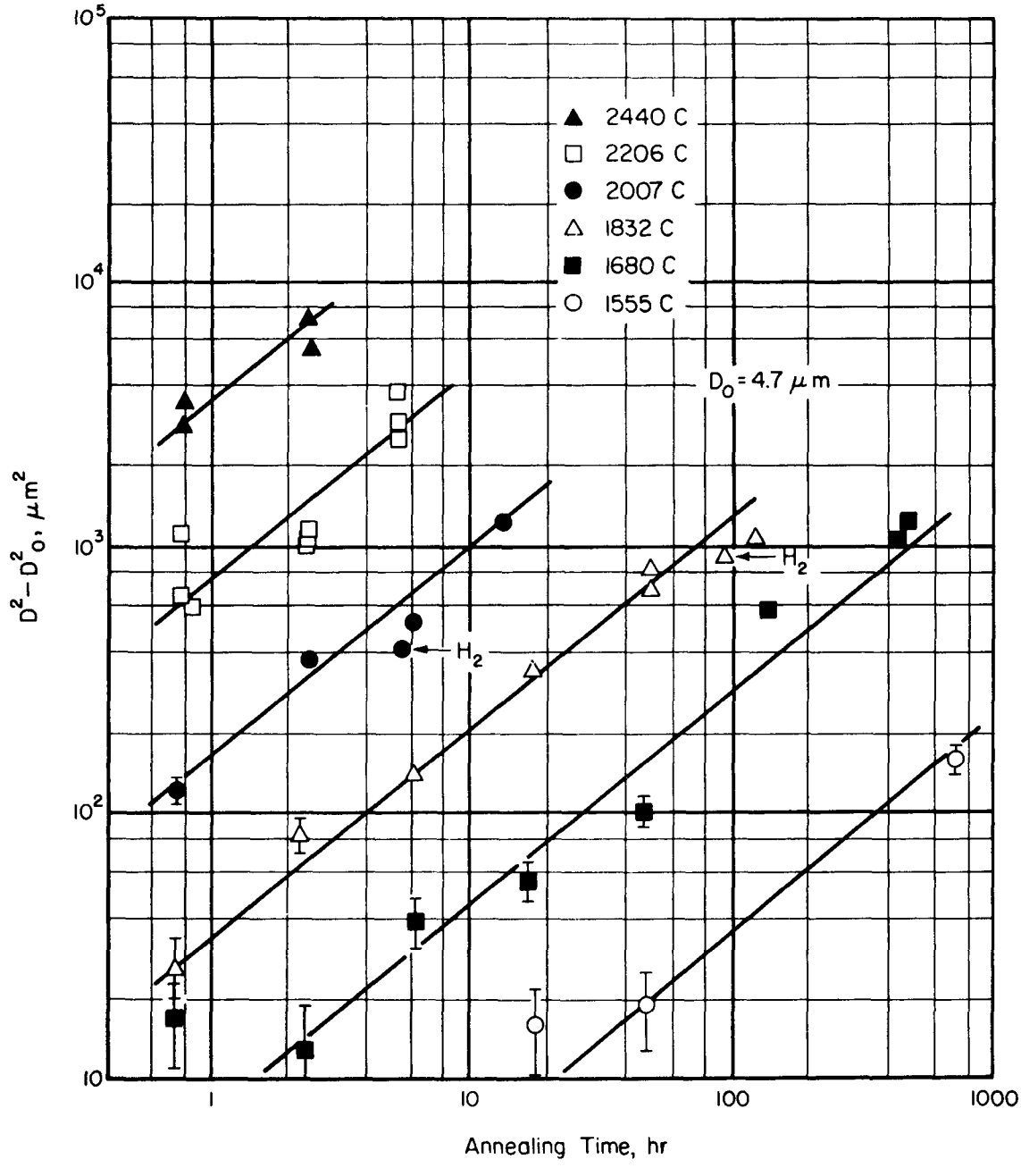

FIGURE B9 VARIATION OF GRAIN SIZE WITH ANNEALING TIME AND TEMPERATURE[16]

D is the new diameter and D_o is the old diameter.

AEA-43237

C1. Hardness (room temperature)[9,17]

a. The load and crystal direction has considerable effect on the microhardness. See Figures C1a[18].

b. Effect of oxygen/uranium ratio on hardness of single-phase UO_{2+x} is shown in Figure C1b.[1]

2. Hot hardness

No data available

3. Ultimate tensile strength[17,19,20]

a. Modulus of rupture is shown in Table C3.

b. Fracture strength ranges from 2300 to 5400 psi (determined indirectly from compressive strength perpendicular to the axis of specimen).

5. Compressive strength[17]

See Table C5.

TABLE C5. COMPRESSIVE STRENGTH OF FUSED UO_2 AT ROOM TEMPERATURE[17]

Grain Size, μ	Length/Diameter Ratio	Average Compressive Strength, psi
0-5	2:1	140,000
10-15	2:1	70,000
15-20	2:1	60,000

6. Creep strength[20]

Three-point loading test data are presented in Figures C6a, C6b, and C6c.

7. Young's modulus[21,22]

a. See Table C7.

b. Effect of nonstoichiometry on Young's modulus

96 per cent dense $UO_{2.16}$: $E = 18 \times 10^6$ psi
After hydrogen reduction at 1200 C: $E = 27 \times 10^6$.

8. Shear modulus[21]

See Table C7.

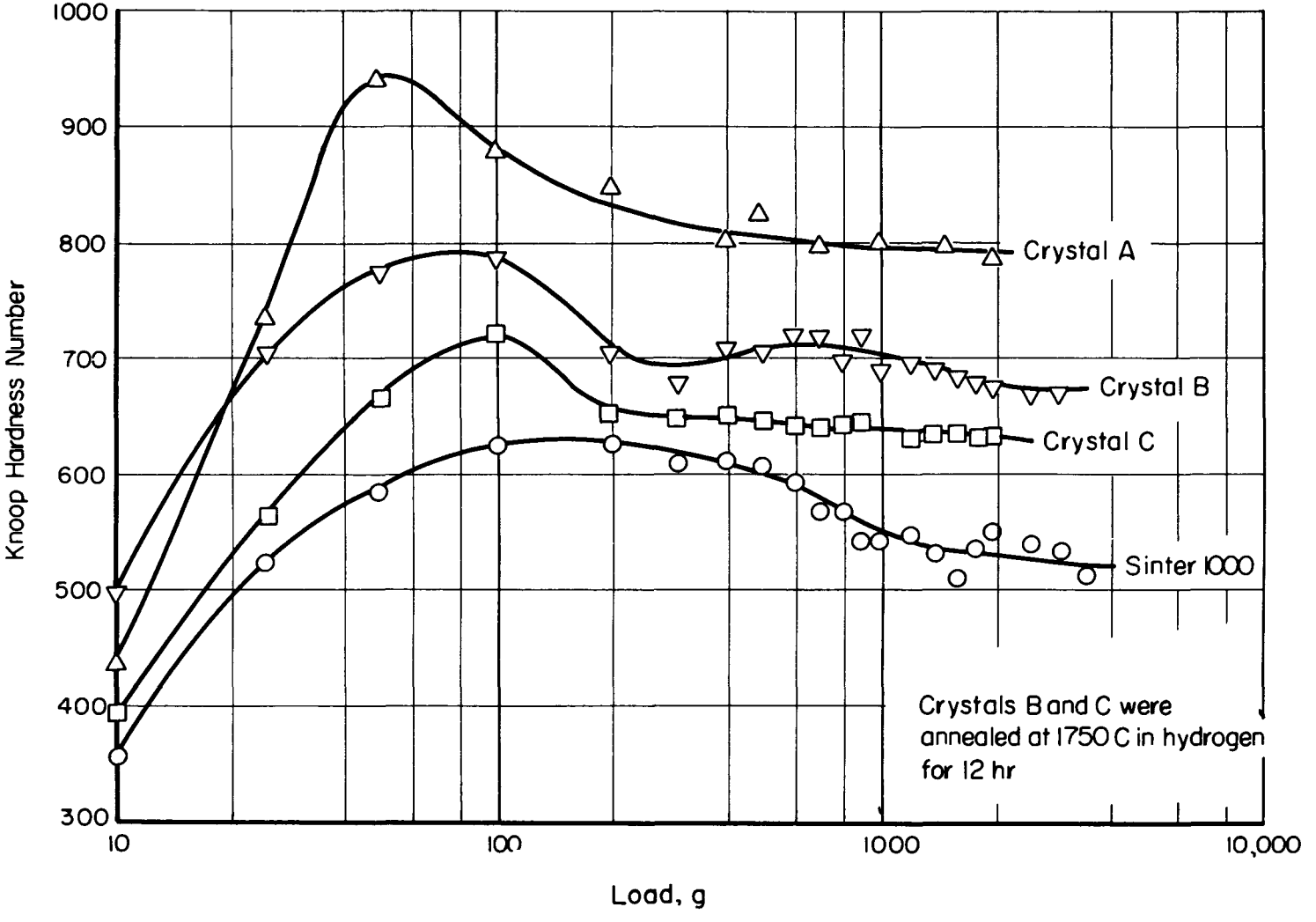

FIGURE C1a. MICROHARDNESS OF URANIUM DIOXIDE[18]

AEA-43238

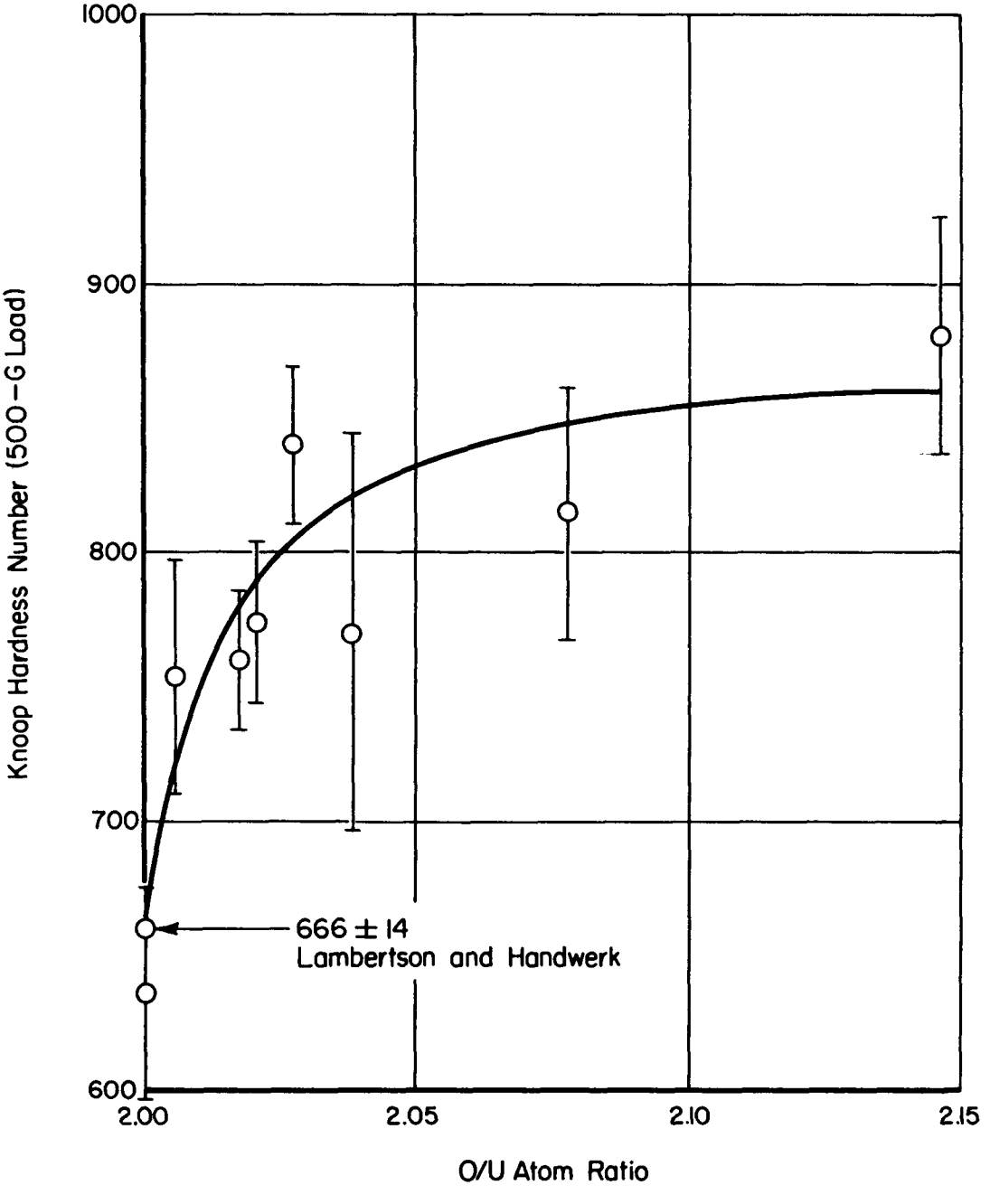

FIGURE CIb. EFFECT OF OXYGEN CONTENT ON HARDNESS OF UO_{2+x} SOLID SOLUTION

Samples were annealed at 900 C for 67 hr and quenched to room temperature.[1, 18]

AEA-43239

TABLE C3. BEND STRENGTH AND BULK DENSITY OF DIFFERENT UO_2 CERAMICS[1]

Starting UO_2 Powder	Sintering Conditions[a]			Strength Data			
	Atmosphere	Temperature, C	Time, hr	Number of Specimens	Average Modulus of Rupture, psi	Standard Deviation, psi	Bulk Density, g per cm^3
At Room Temperature							
Fused, 0 to 5 μ[b]	Argon	2000	1/2	4	11,990	2,370	10.10
Fused, 5 to 10 μ	Argon	2000	1/2	4	9,480	1,180	9.68
Fused, 10 to 15 μ	Argon	2000	1/2	6	10,270	1,040	9.14
Fused, 15 to 20 μ	Argon	2000	1/2	4	8,610	1,380	8.48
Fused, 0 to 5 μ	Helium	2000	1/2	9	12,920	1,261	9.89
Steam oxidized[c]	Helium	2000	1	8	7,340	560	8.34
Hydrogenated steam oxidized[c]	Helium	2000	1	7	9,580	637	8.82
Peroxide precipitated[c]	Helium	2000	1	6	12,400	1,610	10.04
Ammonia precipitated[c]	Helium	1900-2000	1	12	11,100	1,230	9.84
Steam oxidized + 0.75 w/o TiO_2	Helium	1900	1	7	12,700	2,180	9.66
Hydrogenated steam oxidized + 0.50 w/o TiO_2	Helium	1800	1	6	14,500	3,180	10.10
Peroxide precipitated + 0.25 w/o TiO_2	Helium	1600	1	7	10,400	2,800	10.39
Peroxide precipitated + 0.2 w/o aluminum stearate	Helium	2000	1	8	12,700	1,730	10.37
Ammonia precipitated + 0.2 w/o aluminum stearate	Helium	2000	1	11	10,870	1,164	10.26
At 1000 C							
Fused, 0 to 5 μ	Argon	2000	1/2	3	17,980	900	10.02
Fused, 5 to 10 μ	Argon	2000	1/2	4	15,790	1,050	9.56
Fused, 10 to 15 μ	Argon	2000	1/2	6	12,590	3,170	9.17
Fused, 15 to 20 μ	Argon	2000	1/2	4	8,280	1,080	8.48
Fused, 0 to 5 μ	Helium	2000	1/2	9	14,900	2,020	9.89
Steam oxidized	Helium	2000	1	7	7,700	897	8.34
Hydrogenated steam oxidized	Helium	2000	1	8	10,800	1,210	8.81
Peroxide precipitated	Helium	2000	1	7	21,700	3,770	10.05
Ammonia precipitated	Helium	1900-2000	1	12	9,380	1,440	9.85
Steam oxidized + 0.75 w/o TiO_2	Helium	1900	1	7	15,600	846	9.62
Hydrogenated steam oxidized + 0.50 w/o TiO_2	Helium	1800	1	8	19,500	1,480	10.13
Peroxide precipitated + 0.25 w/o TiO_2	Helium	1600	1	6	13,600	3,060	10.39
Peroxide precipitated + 0.2 w/o aluminum stearate	Helium	2000	1	15	11,800	1,820	10.36
Ammonia precipitated + 0.2 w/o aluminum stearate	Helium	2000	1	16	9,380	1,770	10.30

(a) Forming. Preformed in a steel mold and then hydrostatically repressed at 45,000 psi, no binder used.
Sintering Tungsten setter plates, inductively heated, graphite susceptor furnace.
Finishing Specimens ground and lapped to 1/8 x 1/4 x 1-1/4 in.

(b) Norton Company electric-arc fused UO_2.

(c) Prepared by ORNL.

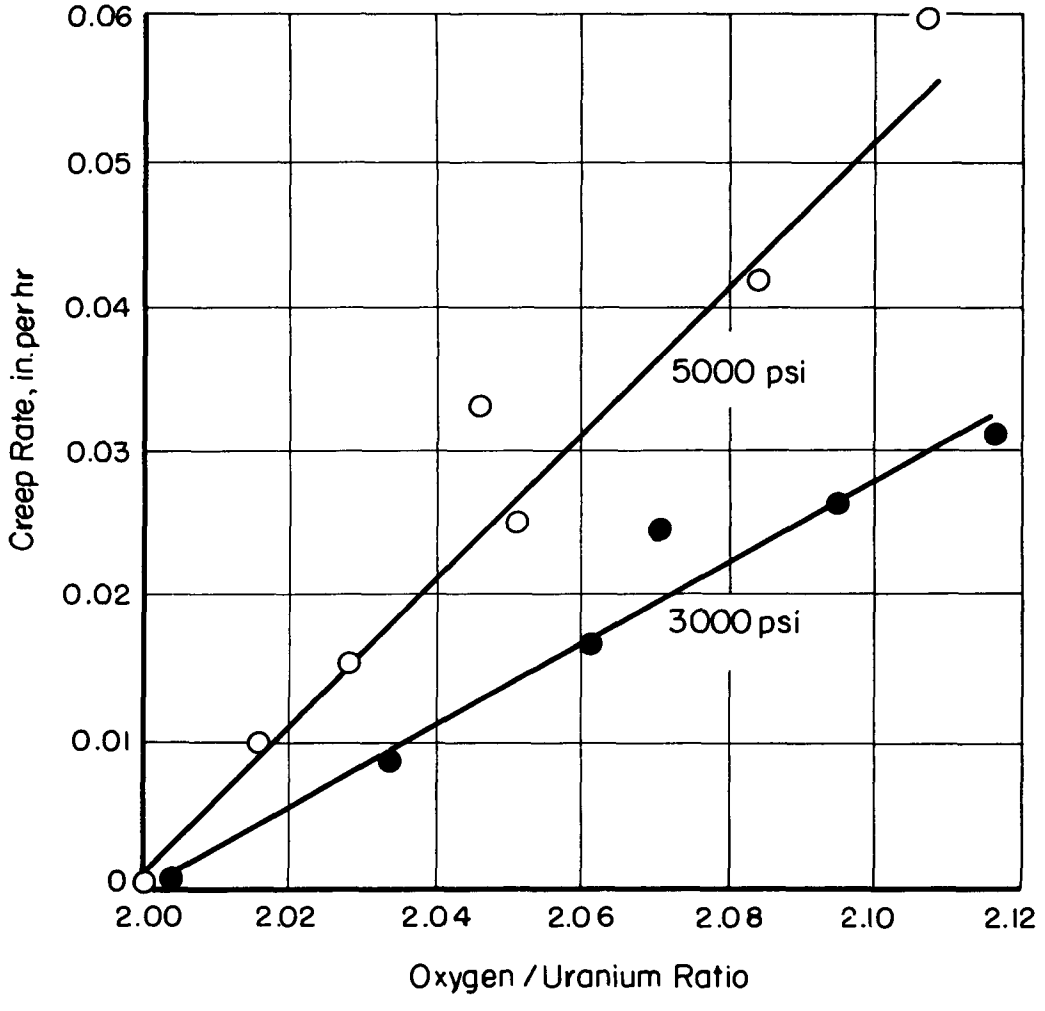

FIGURE C6a. DEPENDENCE OF CREEP RATES ON EXCESS OXYGEN AT 1300 C FOR MAXIMUM (INITIAL) STRESSES OF 5000 AND 3000 PSI [20]

AEA-43240

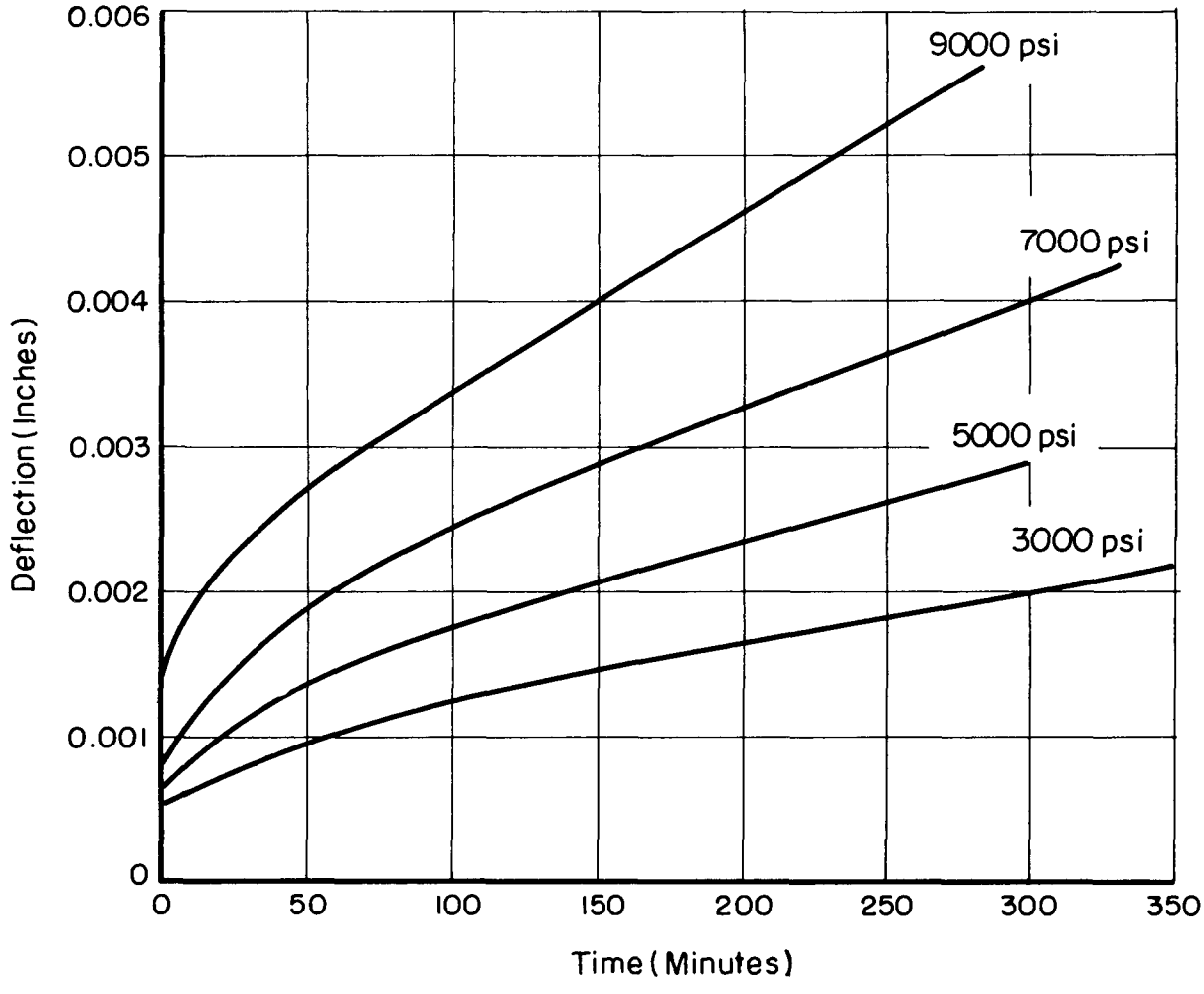

FIGURE C6b. CREEP CURVES FOR $UO_{2.00}$ AT 1300 C [20]

AEA-43241

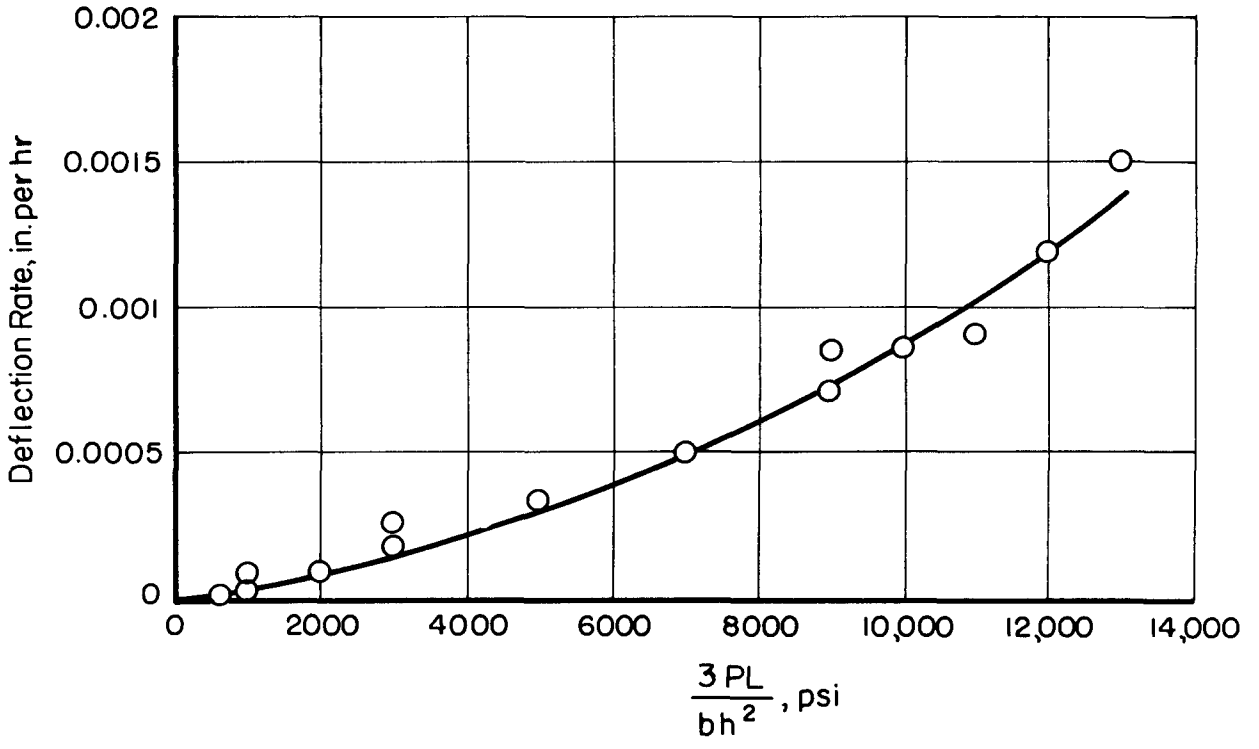

FIGURE C6c. DEFLECTION-RATE DEPENDENCE ON APPLIED STRESS FOR UO_2 AT 1300 C IN HYDROGEN[20]

AEA-43242

TABLE C7. ELASTIC PROPERTIES OF UO_2 AT ROOM TEMPERATURE[21]

Type of UO_2	Bulk Density, % TD	Young's Modulus[a], 10^6 psi			Shear Modulus[b], 10^6 psi	Poisson's Ratio		Bulk Modulus[d], 10^6 psi	
		E_L	E_{FW}	E_{FL}		μ_L	μ_{FW}	K_L	K_{FW}
MCW cold-pressed UO_2 sintered at 1750 C in hydrogen (oxygen/uranium ratio = 2.02)	94.6	28.0	28.1	28.0	10.8	0.302	0.306	23.5	24.1
NH_3-precipitate cold-pressed UO_2 sintered at 1750 C in hydrogen	93.0	26.4	25.2	26.7	10.2	0.291	--	21.1	--

(a) E_L = Young's modulus calculated from the longitudinal resonant frequency.
E_{FW} = Young's modulus calculated from the flatwise flexural vibration.
E_{FL} = Young's modulus calculated from the edgewise flexural vibration.

(b) Shear modulus calculated from the torsional resonant frequency.

(c) $\mu = \frac{E}{2G} - 1.$

(d) $K = \frac{E}{3(1-2\mu)}.$

9. Bulk modulus[21]

See Table C7.

10. Poisson's ratio[21]

See Table C7.

D1. Specific heat[3,23]

a. Heat capacity at constant pressure:
$C_p = 18.45 + 2.431 \times 10^{-3} T - 2272 \times 10^5 T^{-2}$ cal/(g mole)(C).

b. Table of specific heats calculated from above expression:

Temperature, C	Specific Heat, cal/(g)(C)
100	0.063
200	0.067
500	0.074
1000	0.078
1500	0.082

2. Thermal conductivity[1,24-34]

a. See Figures D2a and D2b and Tables D2a and D2b.

b. An empirical equation for thermal conductivity of 100 per cent dense UO_2 from 800 to 2100 C is as follows:

$$K = \frac{1}{17.3 + 0.016\ T}\ w/(cm)(C),$$

where T = Temperature, K.

E1. Electrical resistivity[1]

a. Typical values of electrical conductivity are shown in Figure E1a.

b. Effect of nonstoichiometry on electrical conductivity is shown in Figure E1b.

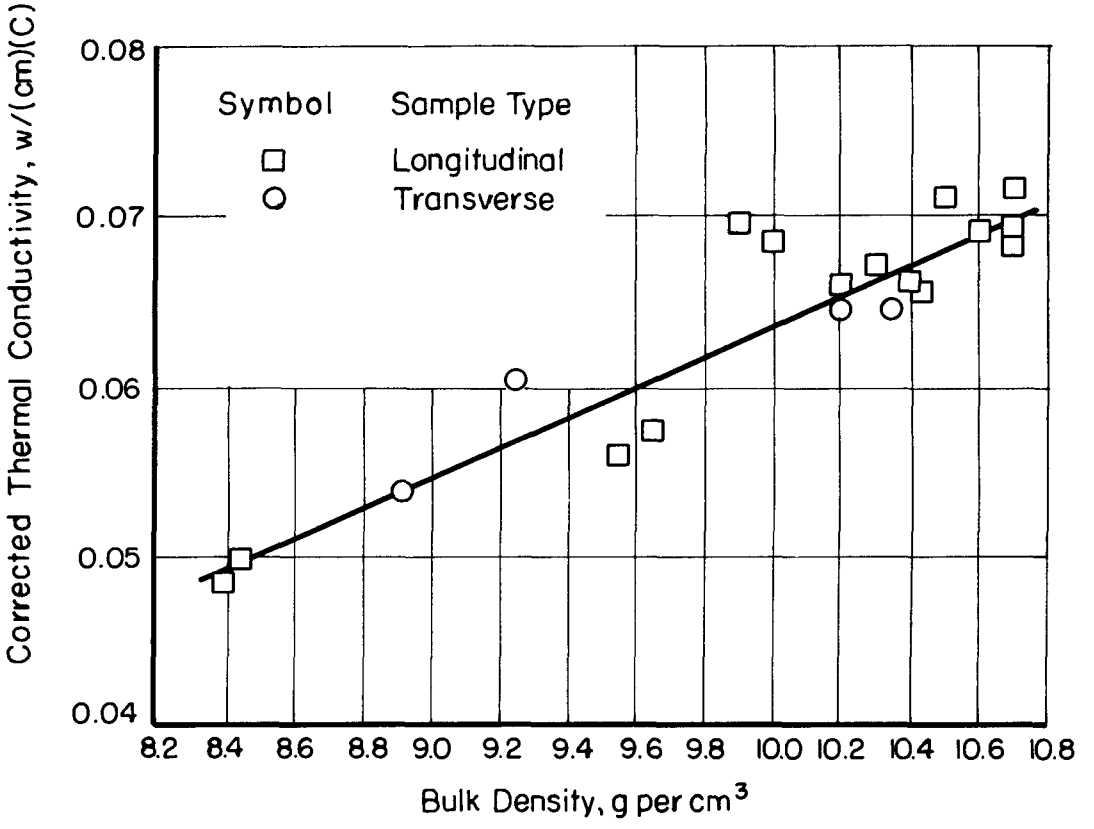

FIGURE D2a. VARIATION OF THERMAL CONDUCTIVITY (CORRECTED TO ZERO POROSITY) WITH BULK DENSITY[24]

AEA-43222

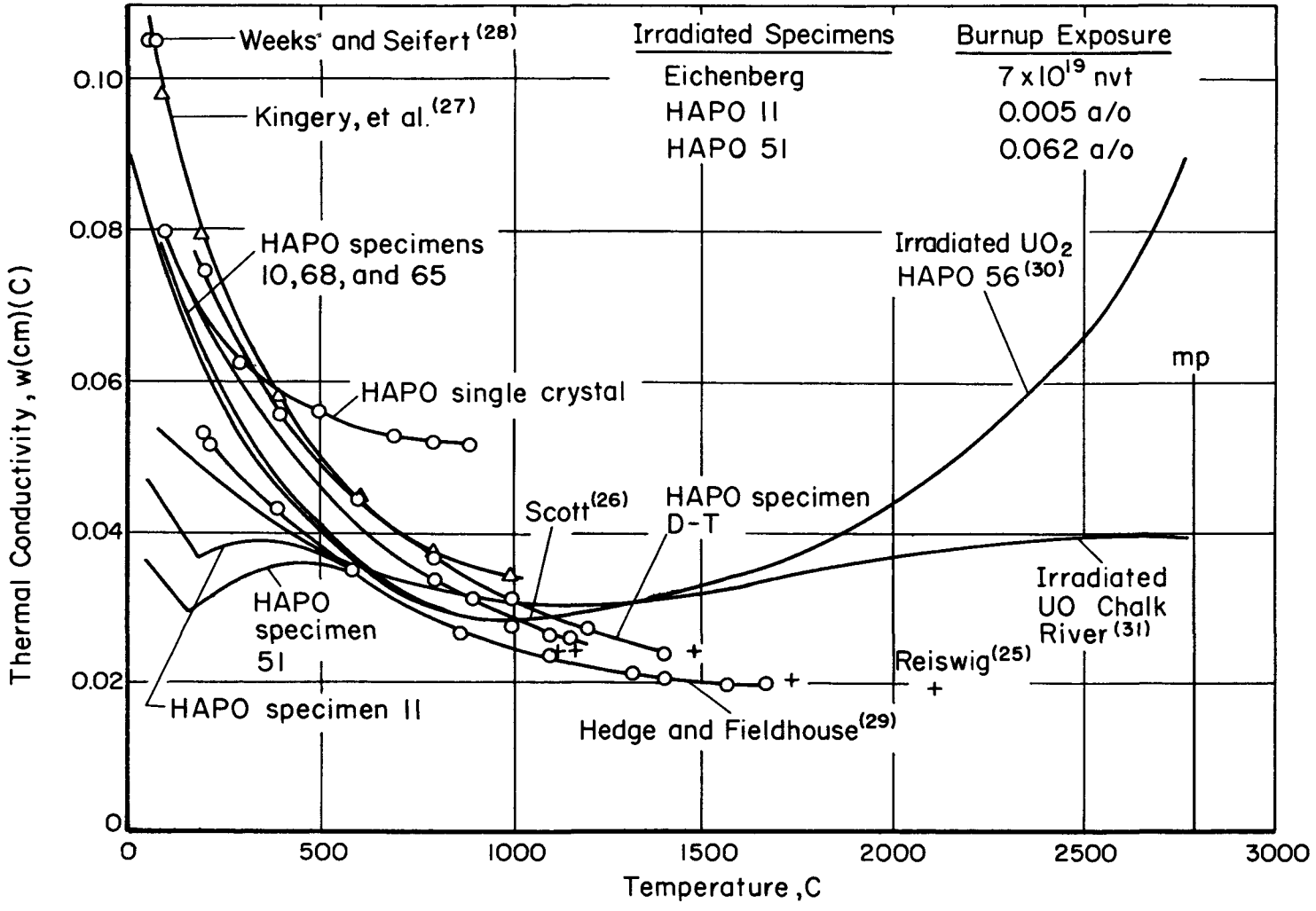

FIGURE D2b. THERMAL CONDUCTIVITY OF UO_2 [30,32]

All values have been adjusted linearly with density to 100 per cent theoretical.

A-43223

TABLE D2a. THERMAL CONDUCTIVITY FOR STOICHIOMETRIC UO_2[1]

Oxygen/Uranium Ratio	Density, g per cm^3	Atmosphere	Temperature, C	Thermal Conductivity for 100 Per Cent Dense UO_2 (Calculated), w/(cm)(C)	Reference
2.00	8.00	Vacuum	200	0.0815	(27)
			400	0.0590	
			600	0.0452	
			800	0.0376	
			1000	0.0351	
2.00	10.08	Vacuum	100	0.105	(33)
			150	0.0908	
2.00 reduced from 2.09	10.55	Vacuum	60	0.115	(33)
			70	0.114	
			80	0.114	
2.00	8.17	Helium	200	0.0524	(29)
			215	0.0510	
			390	0.0428	
			640	0.0348	
			870	0.0264	
			1100	0.0234	
			1320	0.0209	
			1400	0.0199	
			1560	0.0190	
			1670	0.0193	
2.00	10.5	Hydrogen	800	0.0340	(26)
			900	0.0310	
			1000	0.0275	
			1100	0.0260	
			1150	0.0255	

TABLE D2b. EFFECT OF COMPOSITION ON THERMAL CONDUCTIVITIES OF URANIUM OXIDES[1]

Uranium/Oxygen Ratio	Density, g per cm^3	Theoretical Density, g per cm^3	Conductivity for 100 Per Cent Dense UO_2[a], w/(cm)(C)	Relative Conductivity, per cent	Reference
2.00	10.55	10.96	0.115[b]	100	(33)
2.00	10.00	10.96	0.092	100	(34)
2.01	10.30	10.97	0.071	100	(24)
2.01[c]	10.25	10.97	0.0535	100	(24)
2.04	10.30	11.02	0.064	90	(24)
2.055	10.30	11.03	0.061	86	(24)
2.055[c]	10.25	11.03	0.043	80	(24)
2.07	10.30	11.06	0.054	76	(24)
2.08	10.30	11.07	0.0495	67	(24)
2.09[c]	10.25	11.08	0.031	58	(24)
2.09	10.55	11.08	0.071[d]	62	(33)
2.095	10.30	11.09	0.0395	53	(24)
2.11	10.30	11.11	0.033	46.5	(24)
2.14[c]	10.25	11.15	0.0225	42	(24)
2.16	10.8	11.18	0.035	38	(34)
2.19	9.83	11.22	0.035[e]	30	(33)
2.21	10.6	11.25	0.018[f]	25	(24)
2.26[c,g]	8.05	8.4	0.018	25	(24)

(a) Measurements at 60 C except where noted.
(b) 58 C.
(c) 0.1 w/o TiO_2 addition.
(d) 57 C.
(e) 53 C.
(f) Average of three specimens.
(g) U_3O_8 plus trace amount of UO_2.

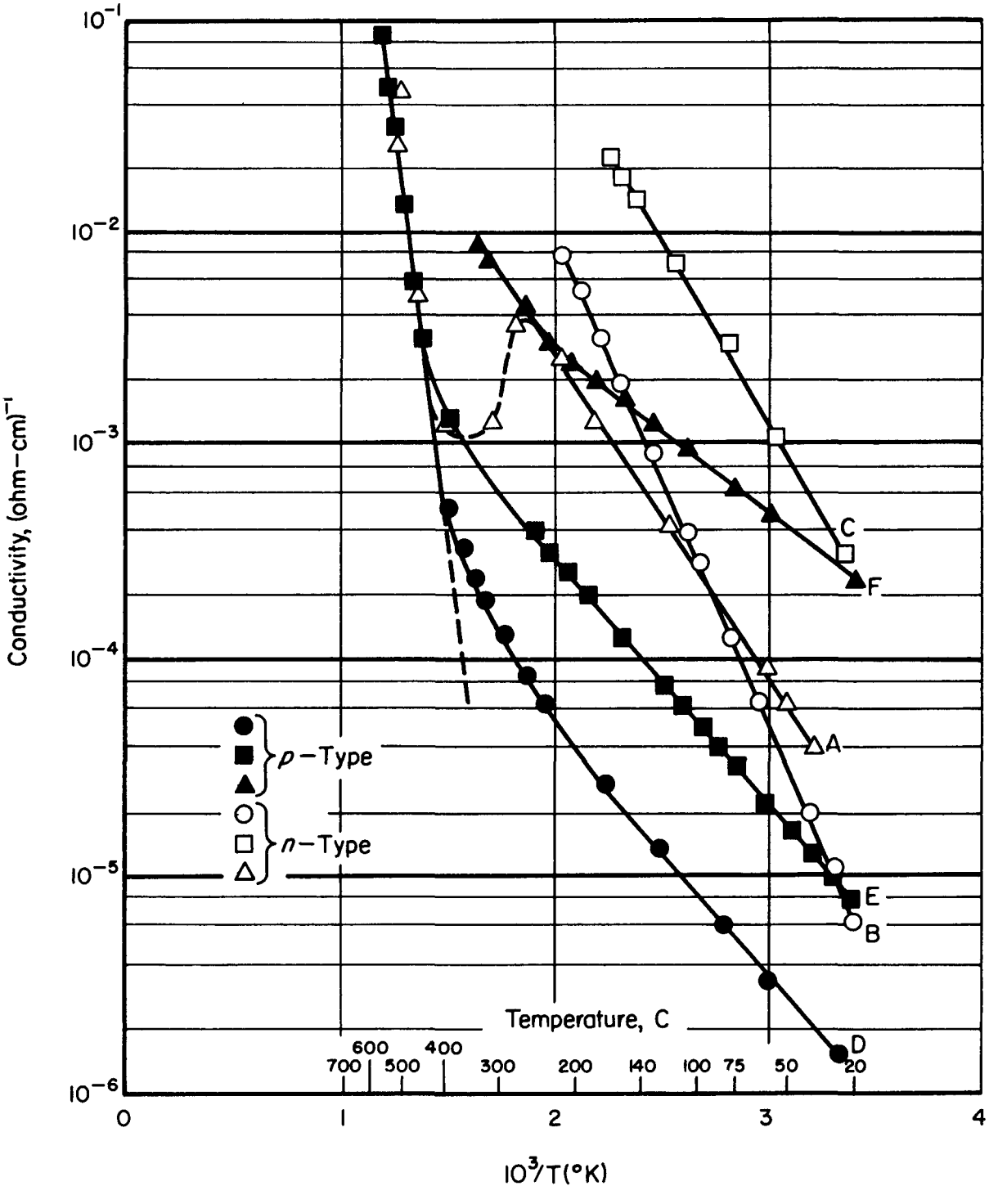

FIGURE E1a. CONDUCTIVITY OF SINTERED SPECIMENS OF *n*-AND *p*-TYPE UO_2[1]

AEA-43245

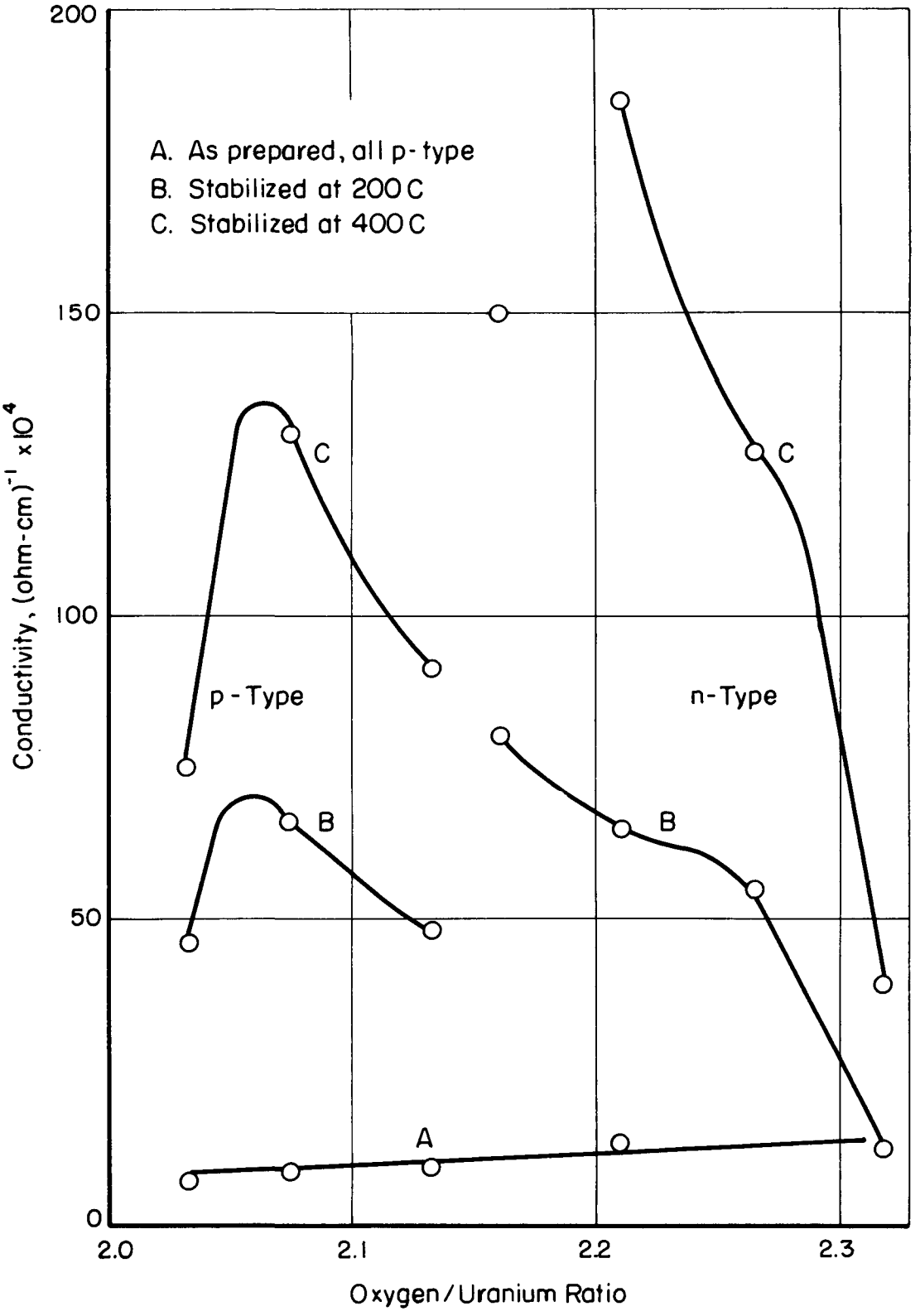

FIGURE E1b. ROOM-TEMPERATURE ELECTRICAL CONDUCTIVITY AS A FUNCTION OF OXYGEN/URANIUM RATIO OF PRESSED SPECIMENS OF UO_2 [1]

AEA-43246

F1. Reaction with coolants[1,11,35-37]

a. Steam

Specimen	Test Conditions	Average Weight Loss, per cent	U(VI) Content After Test, w/o
Cold pressed and sintered	302 hr in degassed steam at 750 F and 2000 psig	0.04	0.27 0.64 0.50
Hot pressed	302 hr in degassed steam at 750 F and 2000 psig	0.42	0.43

b. Helium

No reaction occurs from room temperature to the UO_2 melting point.

c. Carbon dioxide

At 1292 F, UO_2 (ρ = 9.6 g per cm^3) exhibited a weight change of 0.008 $mg/(cm^2)(hr)$.

d. Hydrogen

No reaction up to the melting point of UO_2 occurs.

2. Reactions with cladding or structural materials[34,38,39]

Material	Reaction With UO_2
a. Niobium-base alloys	None to 2300 F
b. Zirconium	Reaction at 1500 F
c. Nickel-base alloys	No reaction at 2000 F; reaction at 2500 F
d. Iron-base alloys	No reaction at 2000 F
e. Stainless steel	No reaction at 600 F
f. Chromium-base alloys	No reaction at 2000 F
g. Tungsten	First reaction at 1785 C; fast reaction at 2065 F
h. Tantalum	First reaction at 2295 C; fast reaction at 2420 C
i. Molybdenum	First reaction at 2155 C
j. Rhenium	First reaction at 925 C; fast reaction at 2295 C

G1. Dimensional stability during irradiation[40-42]

a. A density decrease of 0.33 per cent per a/o of burnup resulted at a burnup of 53 per cent.[40,41]

b. A density decrease of 0.5 per cent per a/o of burnup was observed in water cooled flat plate fuels.[42]

2. Fission-gas-release data

a. Postirradiation diffusion

(1) At low burnup, or by neutron activation, diffusion coefficients in sintered UO_2 are found to depend upon the experimental conditions, and are believed to depend upon the oxygen/uranium ratio, although the latter has not been proved.

(a) In reducing atmosphere (helium-5 volume per cent hydrogen) the following data have been obtained for sintered UO_2:[1,43]

$$D_{Xe} = 6.6 \times 10^{-6} e^{(-71,700/RT)}$$

$$D_{Xe} = 7.8 \times 10^{-6} e^{(-71,000/RT)}$$

D_{Kr} data are similar.[1]

(b) Other data for a neutral atmosphere, a gettered atmosphere, and a gettered (in presence of tantalum) vacuum gave variable activation energies for xenon diffusion, the activation energy increasing apparently with increased gettering or as the oxygen/uranium ratio approaches 2.00.

Neutral atmosphere:[44]

$$D_{Xe} = 1.5 \times 10^{-8} e^{(-46,000/RT)}.$$

Gettered atmosphere:[45]

Activation energy = 115,000 cal per g mole

D_{Xe} at 1400 C = 2×10^{-15} cm^2 per sec.

Gettered vacuum:[46]

Activation energy = 125,000 cal per g mole

D_{Xe} at 1400 C = 5×10^{-16} cm^2 per sec.

(c) For other data see Reference (1).

(2) Effects of increasing burnup upon gas release do not appear to be serious for water-cooled pin-type fuel elements up to 25,000 MWD/T. For example[1], comparison between calculated (based on diffusion measurements) and observed Kr^{85} releases for sintered oxides of 86 to 96 per cent density, exposed at heat fluxes of 40,000 to 300,000 Btu/(hr)(ft^2) for burnups between 1,000 and 13,000 MWD/T are shown in Figure G2a. Similarly, the variation of $D'_{Xe} = D/a^2$ (where $a = \frac{3d}{s}$, d = fraction of theoretical density, s = surface area in cm per cm^3) with burnup is also shown in Figure G2b for gas-cooled reactor conditions.[47] No significant increase is believed to occur for burnups up to 16,400 MWD/T, the scatter being largely accounted for by the uncertainties in the surface areas. (Correlation was established by assuming an activation energy of 70,000 cal per g mole and correcting D′ to 1400 C. Specimens with temperature above 1600 C were not considered.) On the other hand, flat-plate specimens irradiated at average temperatures well below 1000 C showed an apparent large increase in diffusion coefficient of Kr^{85} at 1000 C with increasing burnup, as shown in Figure G2c.[1] These results were obtained by postirradiation heating and show significant burnup effects at burnups above 25,000 MWD/T for these conditions. Similar effects may or may not occur when irradiations are conducted at higher temperatures.

b. In-pile diffusion

Low-burnup in-pile measurements of fission-gas release from UO_2 in helium-5 volume per cent hydrogen yield the following conclusions[48]:

(1) Xenon and krypton diffusion are about equal at temperatures up to 3000 F.

(2) Iodine diffusion rates are about equal to xenon for the above temperatures, and iodine is not a significant contributor in a practical fuel element. Bromine effects on krypton are nil.

(3) Diffusion coefficients obtained by neutron activation are adequate to characterize the low-burnup behavior of rare gases in UO_2.

c. Model for diffusion

The model for diffusion release of xenon and krypton from sintered UO_2 is adequately represented by assuming a spherical geometry with the appropriate surface-to-volume ratio.[1] It is likely that a flat-plate geometry of appropriate surface-to-volume ratio would be more precise in some cases, but the maximum differences between the two models is only 14 per cent of the predicted release.[48]

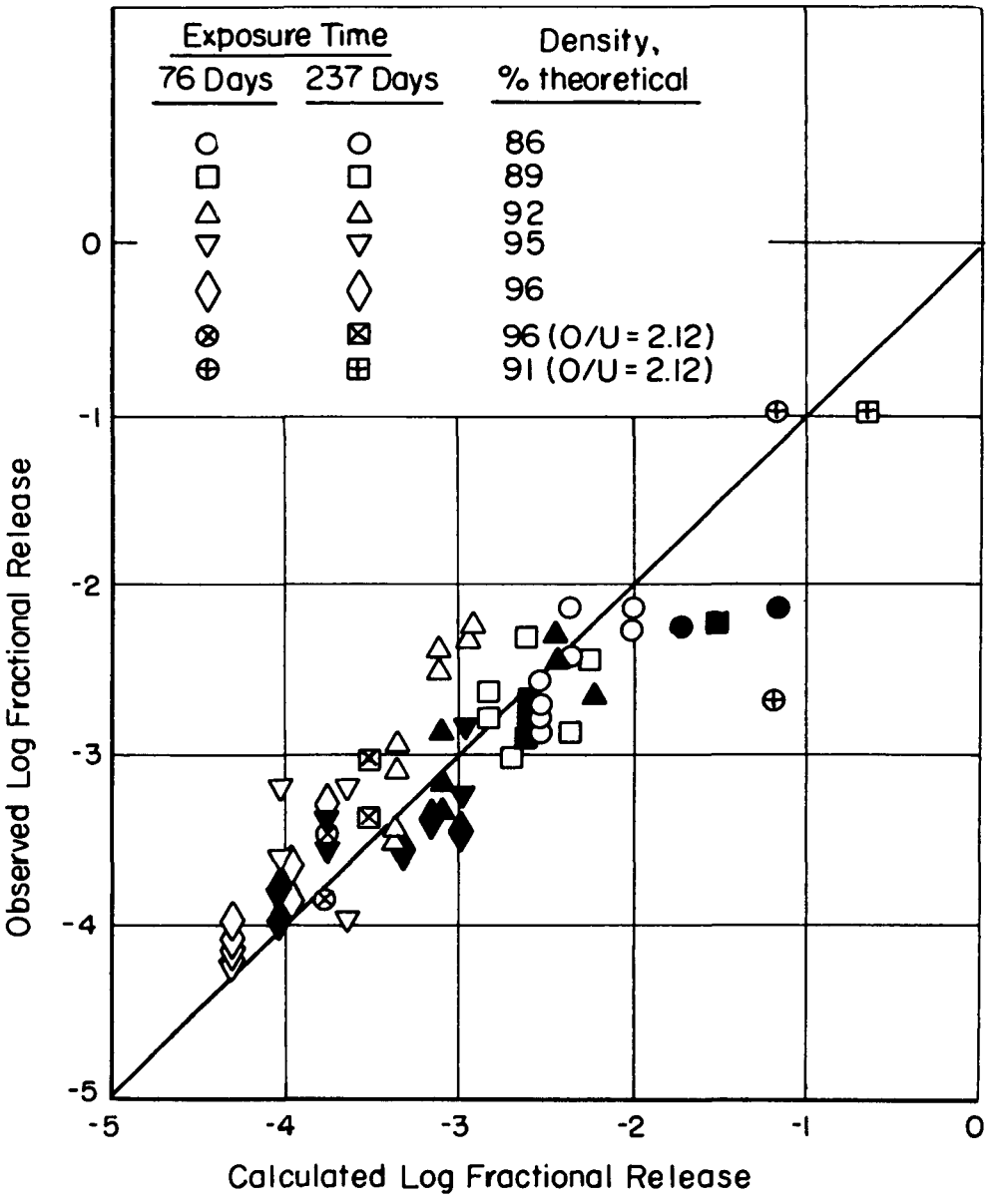

FIGURE G2a. CALCULATED AND OBSERVED FRACTIONAL FISSION-GAS RELEASE (Kr^{85})[1]

AEA-43248

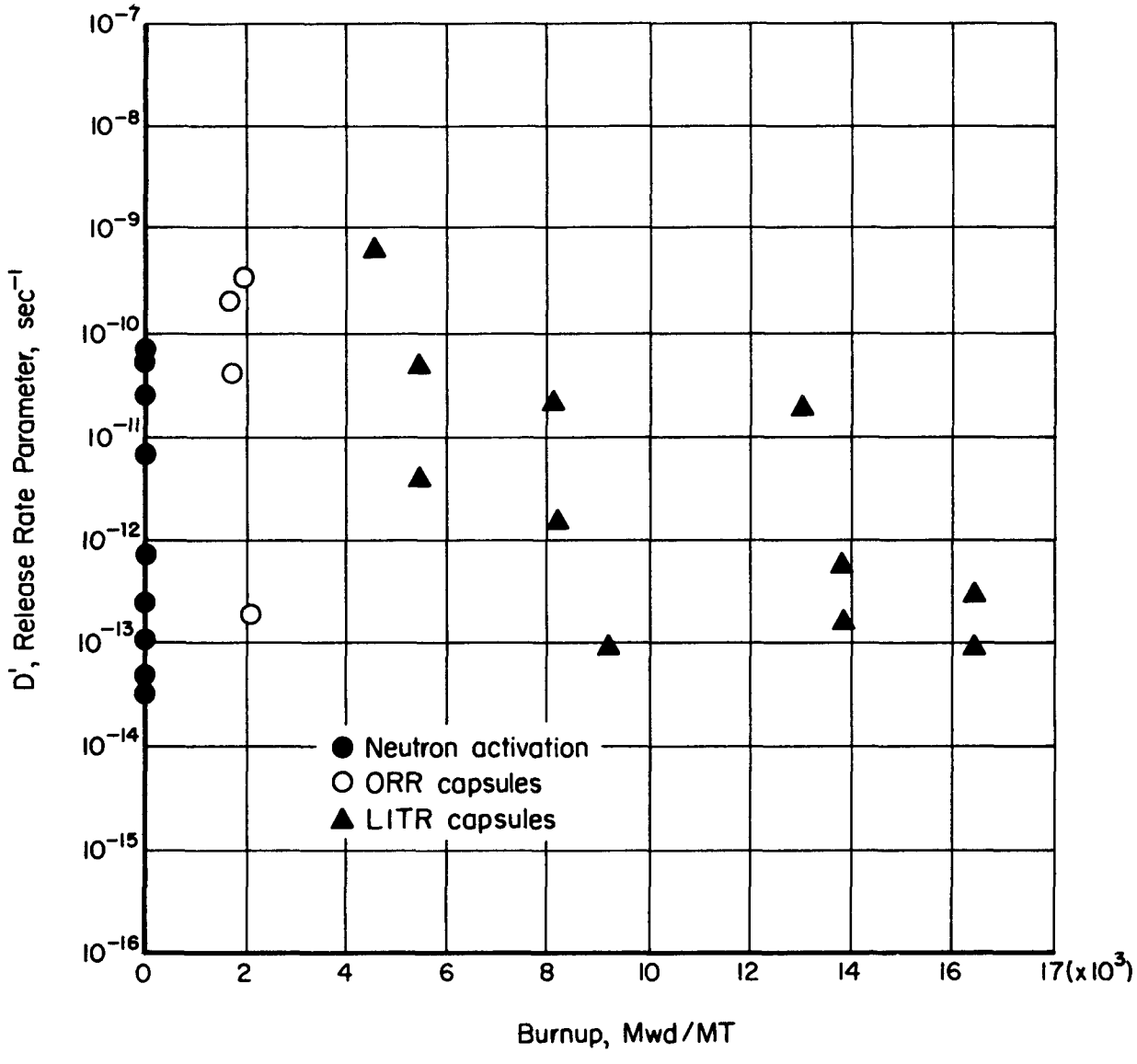

FIGURE G2b. RELATIONSHIP BETWEEN D' VALUES AT 1400 C AND BURNUP FOR UO_2 SAMPLES WITH DENSITIES ABOVE 10 g per cm^3

AEA-43249

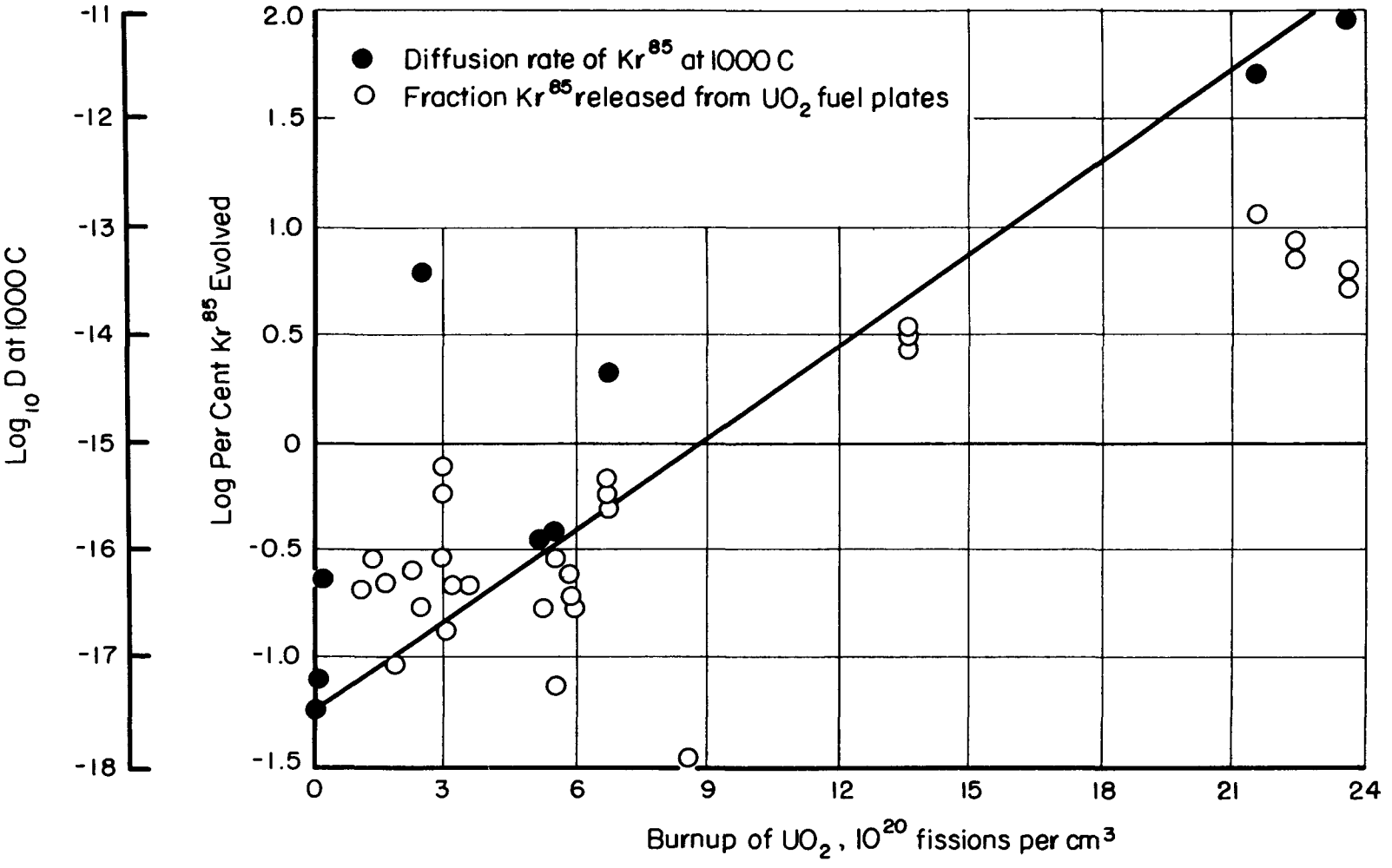

FIGURE G2c. VARIATION OF DIFFUSION RATE AND RELEASE OF Kr^{85} FROM DENSE UO_2 [1]

AEA-43250

d. Other mechanisms of gas release

It appears, especially in high-heat rating elements, that many mechanisms other than diffusion are acting. Some of these mechanisms are significant, indicating that correlation between diffusion-model predictions and observed releases are fortuitous. Further discussions of other mechanisms of gas release are in the literature.(1,30,49-51). See also the correlation of gas release with heat rating below.

e. Correlation of gas release with heat rating

A surprising agreement between predictions by a simple diffusion model and observed releases at low burnup as a function of heat generation is illustrated in Figure G2d.(31) Selection of only one arbitrary parameter was necessary to obtain a good fit between calculated and experimental data.

3. Swelling-temperature data

Swelling has been observed in bulk UO_2 water-cooled fuels as indicated in Figure G3. The center temperatures are in dispute, but it is apparent that swelling will result when large accumulations of gases occur. The behavior of UO_2 fuel elements at gas-cooled reactor conditions, however, may be much different. Additional data are needed for such conditions. The plastic behavior of UO_2 at elevated temperatures has been demonstrated.(1,20,22)

4. Unusual nuclear properties

None

5. Property changes as a result of irradiation(1,17)

a. Thermal conductivity: a 33 per cent decrease at 60 C after 1.1×10^{19} fissions per cm^3. See Figure D2b.(32)

The difference in the Chalk River and HAPO data on irradiated UO_2 at above 1500 C is probably due to the differences in irradiation times. The HAPO data are based on long irradiation times during which the thermal conductivity was improved by sintering and grain growth. The Chalk River data are based on short irradiations. Additional data have been reported by Eichenberg.(52)

b. Hardness: an increase from 625 to 830 KHN after 2×10^{20} fissions per cm^3 has been reported.(1)

c. Melting point: an increase of 125 C after 1.5×10^{19} fissions per cm^3 and a significant reduction after 2×10^{21} fissions per cm^3 have been reported.(18,53,54) See Figure G5c.

d. Electrical conductivity(18)

See Figure G5d.

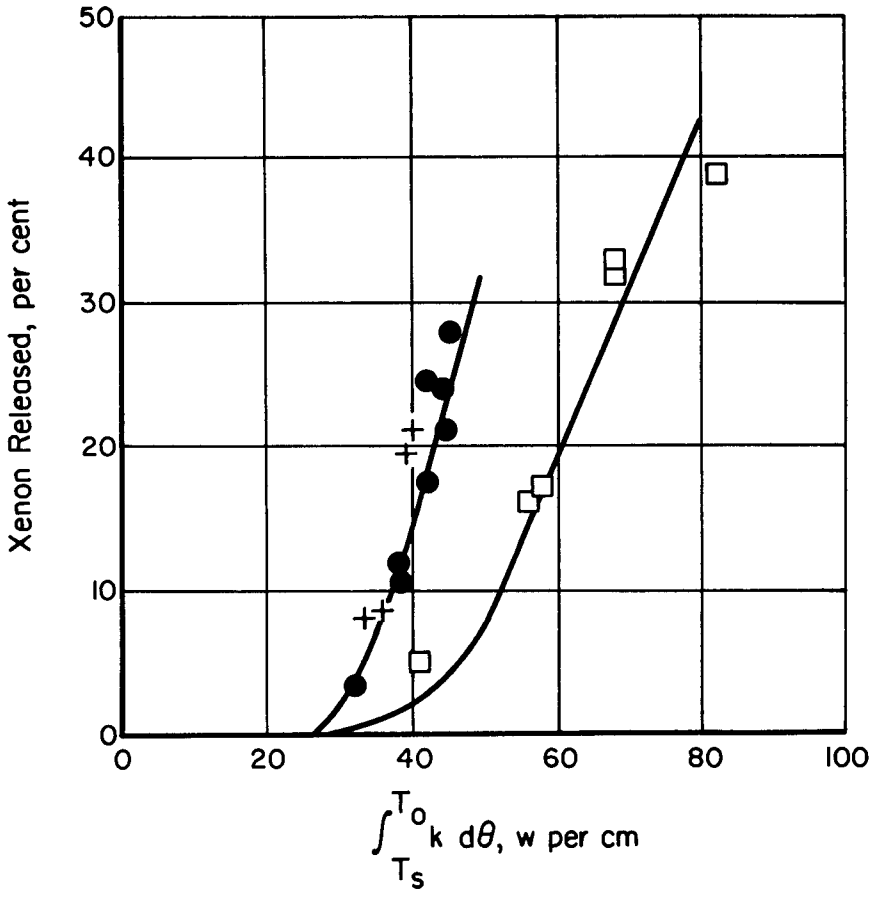

FIGURE G2d THE PERCENTAGE OF FISSION XENON RELEASED FROM SINTERED UO_2 DURING IRRADIATION AS A FUNCTION OF THE FUEL'S HEAT RATING[31]

AEA-43251

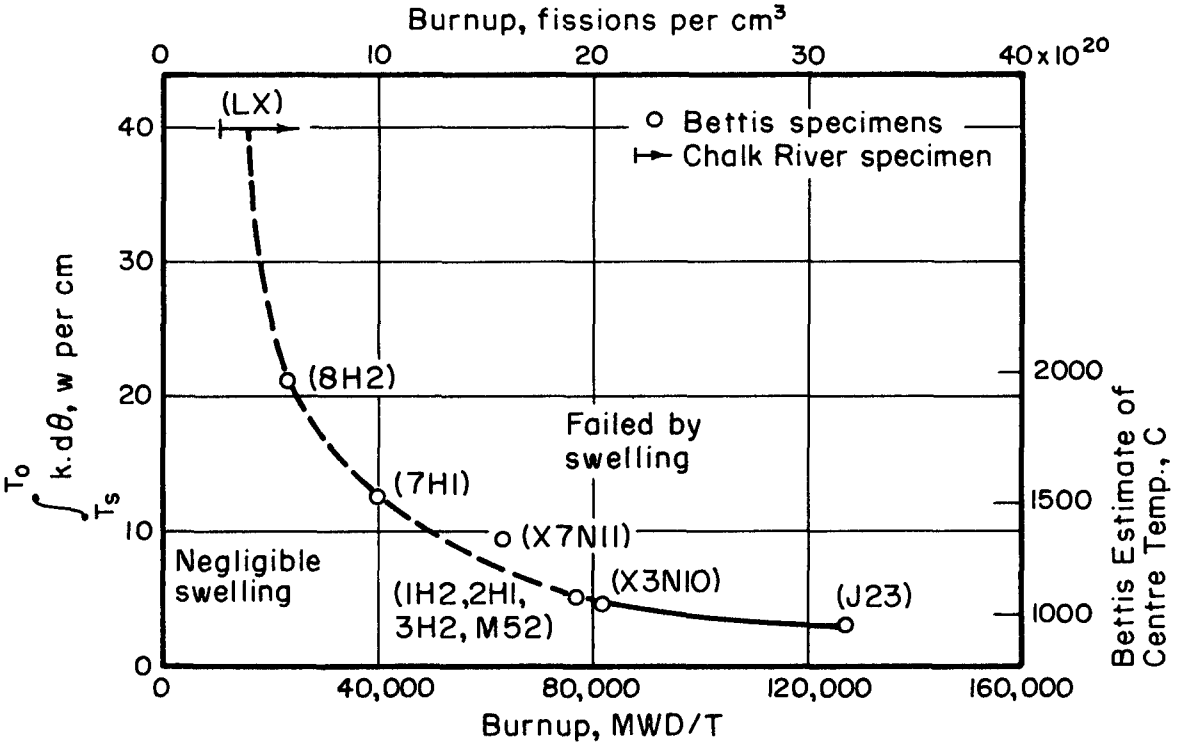

FIGURE G3. THE CORRELATION BETWEEN BURNUP AND HEAT RATING FOR UO_2 SPECIMENS THAT FAIL BY SWELLING OF THE FUEL[31]

All specimens were subject to a total restraint of about 200 kgf per cm (3000 psi).

AEA-43252

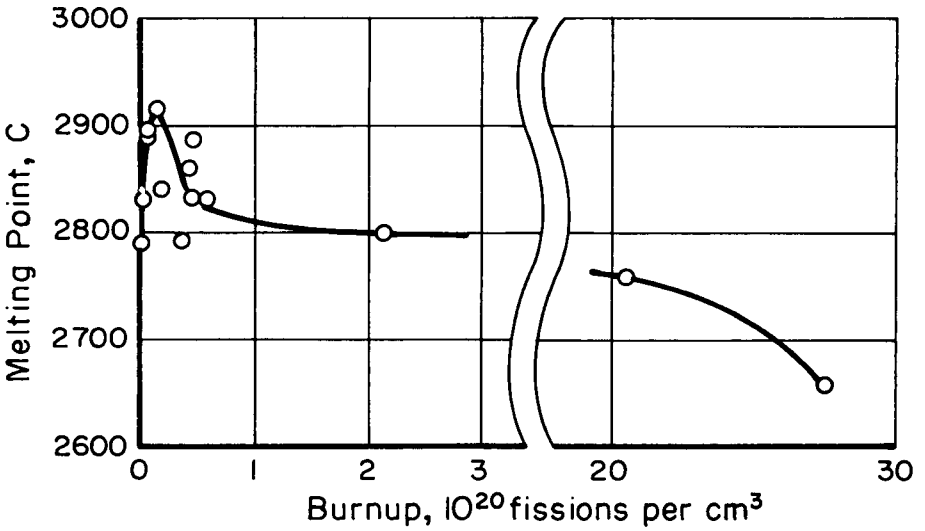

FIGURE G5c. MELTING TEMPERATURE OF IRRADIATED UO_2[18]

AEA-43253

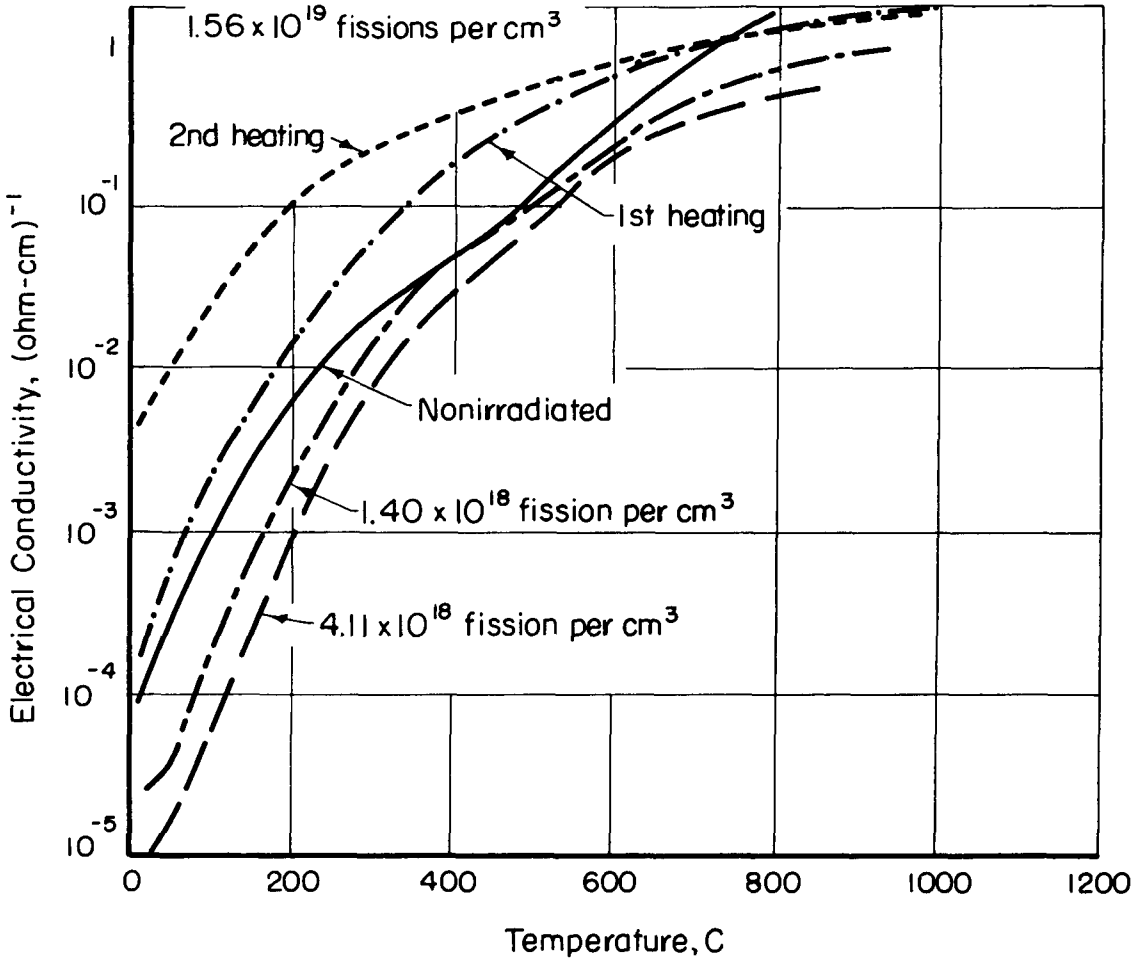

FIGURE G5d. ELECTRICAL CONDUCTIVITY OF POLYCRYSTALLINE UO_2[18]

AEA-43254

H. References

(1) Belle, J., Editor, Uranium Dioxide: Properties and Nuclear Applications, Naval Reactors, Division of Reactor Development, USAEC (July, 1961).

(2) Anderson, J. S., Harper, E. A., Moorbath, S., and Roberts, L. E. J., "The Properties and Microstructure of Uranium Dioxide; Their Dependence on the Mode of Preparation", AERE C/R 886 (August 19, 1952).

(3) Katz, J. J., and Rabinowitch, E., The Chemistry of Uranium, National Nuclear Energy Series, Div. VIII, Vol. 5, McGraw-Hill Book Company, New York (1951).

(4) Johnson, J. R., Fulkerson, S. D., and Taylor, A. J., "Technology of Uranium Dioxide, A Reactor Material", Am. Ceram. Soc. Bull., 36, 12 (1957).

(5) Johnson, J. R., "Uranium Dioxide", Progress in Nuclear Energy, Series V, Metallurgy and Fuels, Vol. 2, Howe, J. P., and Finnister, H. M., Editors, Pergamon Press, New York (1950), pp 209-222.

(6) Johnson, J. R., and Curtis, C. E., "The Technology of UO_2 and ThO_2", Proceedings of the International Conference on the Peaceful Uses of Atomic Energy, New York (1956), Vol. 9, pp 169-173.

(7) Gronvold, F., "High Temperature X-Ray Study of Uranium Oxides in UO_2-U_3O_8 Region", J. Inorg. Nuclear Chem., 1, 357-370 (1955).

(8) Loch, L. D., and Quirk, J. F., "Ceramics", Reactor Handbook, Volume 1, Materials, C. R. Tipton, Jr., Interscience Publishers, Inc., New York (1960).

(9) Lambertson, W. A., and Handwerk, J. H., "The Fabrications and Physical Properties of Uranium Bodies", ANL-5053 (February, 1956).

(10) Ackerman, R. J., "The High Temperature High-Vacuum Vaporization and Thermodynamic Properties of Uranium Dioxide", ANL-5482 (September 14, 1955).

(11) Wisuzi, L. G., and Pijanowski, S. W., "The Thermal Stability of Uranium Dioxide", KAPL-1902 (November 1, 1959).

(12) Ackerman, R. J., Gilles, P. W., and Thom, R. J., "High Temperature Thermodynamic Properties of Uranium Dioxide", J. Chem. Phys., 25, 1089-1097 (1956).

(13) Ackerman, R. J., Thom, R. J., Alexander, C. A., and Tetenbaum, M., "Free Energies of Formation of Gaseous Molybdenum, Tungsten and Uranium Trioxide", Presented at the Am. Chem. Soc. Meeting, April, 1959.

(14) Vaughan, D. A., Bridge, J. R., and Schwartz, C. M., "Comparison of Active and Inactive Uranium Dioxide-Oxygen Systems", BMI-1241 (December 10, 1957).

(15) Kempter, C. P., and Elliott, R. O., "Thermal Expansion of UN, UO_2, UO_2-ThO_2 and ThO_2, J. Chem. Phys., 30, 1524-1526 (1959).

(16) MacEwan, J. R., "Grain Growth in Sintered Uranium Dioxide", AECL-1184 (January, 1961).

(17) Burdick, M. D., and Parker, H. S., "Effect of Particle Size on Bulk Density and Strength Properties of Uranium Dioxide Specimens", J. Am. Ceram. Soc., 39, 181-187 (1956).

(18) Roake, W. E., "Irradiation Alteration of Uranium Dioxide", HW-73072 (March, 1962).

(19) Knudsen, F. P., Parker, H. S., and Burdick, M. D., "Flexural Strength of Specimens Prepared From Several Uranium Dioxide Powders; Its Dependence on Porosity and Grain Size and the Influence of Additions of Titania", J. Am. Ceram. Soc., 43, 641-647 (1960).

(20) Armstrong, W. M., and Irvine, W. R., "The Plastic Deformation of Uranium Dioxide at Elevated Temperatures", 63rd Annual Convention of the American Ceramic Society, Toronto, Ontario, Canada, 1961.

(21) Lang, S. M., "Properties of High Temperature Ceramics and Cermets, Elasticity and Density at Room Temperatures", Nat. Bur. Standards (U. S.) Monograph 6 (March 1, 1960).

(22) Scott, R., Hall, A. R., and William, J., "The Plastic Deformation of Uranium Oxides Above 800 C", J. Nuclear Materials, 1, 39-48 (1959).

(23) Hausner, H. H., and Mills, R. G., "Uranium Dioxide for Fuel Elements", Nucleonics, 15 (7), 94-103 (1957).

(24) Ross, A. M., "The Dependence of Thermal Conductivity of Uranium Dioxide on Density Microstructure, Stoichiometry, and Thermal Neutron Irradiation", CRFD-817 (September, 1960).

(25) Reiswig, R. D., "Thermal Conductivity of UO_2 to 2100 C", J. Am. Ceram. Soc., 44 (1), 48-49 (1961).

(26) Scott, R., "Thermal Conductivity of UO_2", AERE M/R-2526 (March, 1958).

(27) Kingery, W. D., Francl, J., Coble, R. L., and Vasilos, T., "Thermal Conductivity: X, Data For Several Pure Oxide Materials Corrected to Zero Porosity, J. Am. Ceram. Soc., 37, 107-110 (1954).

(28) Weeks, J., and Seifert, R., "Apparatus for the Measurement of the Thermal Conductivity of Solids", ANL-4938 (1952).

(29) Hedge, J. C., and Fieldhouse, I. B., "Measurement of Thermal Conductivity of Uranium Oxide", AECU-3881 (September 20, 1956).

(30) Roake, W. E., "Irradiation Alteration of Uranium Dioxide", HW-73072 (March, 1962).

(31) Robertson, J. A. L., "High Temperature Properties of Ceramic Fuels: Their Significance and Measurement", AECL-1529 (June, 1962).

(32) Matolich, J., Jr., and Deem, H. W., BMI, Unpublished Data.

(33) Kingery, W. D., "Thermal Conductivity: XIV, Conductivity of Multi-component Systems", J. Am. Ceram. Soc., 42, 617-627 (1959).

(34) Nichols, R. W., "Ceramic Fuels - Properties and Technology", Nuclear Eng., 3, 327-333 (1958).

(35) Anderson, J. S., Sawyer, J. O., Worner, H. W., Willis, G. M., and Bannister, M. J., "Decomposition of Uranium Dioxide at its Melting Point", Nature, 185, 915-916 (1960).

(36) Power Reactor Technology, 3 (2), 49-50 (March, 1960).

(37) Anderson, J. S., and Sawyer, J. O., "The Stability of Uranium Dioxide in Hydrogen at High Temperature", Proc. Chem. Soc., 145-146 (1960).

(38) Dickerson, R. F., "Reactor Materials Properties", Nucleonics, 18 (11), 154-161 (1960).

(39) "Metallurgy Division Annual Progress Report for Period Ending September 1, 1959", ORNL-2839 (December 16, 1959).

(40) Barney, W. K., and Wemple, B. D., "Metallograph of UO_2-Containing Fuel Elements", KAPL-1836 (January 15, 1958).

(41) Barney, W. K., "Irradiation Effects in UO_2", Proceedings of the Second United Nations International Conference on the Peaceful Uses of Atomic Energy, Geneva (1958), Vol. 6, pp 677-680.

(42) Bleiberg, M. L., Yeniscavich, W., and Gray, R. G., "Effects of Burnup on Certain Ceramic Fuel Materials", Radiation Effects In Refractory Fuel Compounds, ASTM, S. T. P. No. 306 (March 1962), p 64.

(43) Long, G., Davies, D., and Findley, J. R., "Diffusion of Fission Products in Uranium Dioxide and Uranium Monocarbide", Paper presented at The First Conference in Nuclear Reactor Chemistry, Gatlinburg (October 12-14, 1960).

(44) Booth, A. H., and Rymer, G. T., "Determination of the Diffusion Constant of Fission Xenon in UO_2 Crystals and Sintered Compacts", CRDC-720 (August, 1958).

(45) Barnes, R. H., Kangilaski, M., Melehan, J. B., and Rough, F., "Xenon Diffusion in Single-Crystal and Sintered UO_2", BMI-1533 (August 1, 1961).

(46) Stevens, W. B., MacEwan, J. R., and Ross, A. M., "The Diffusion Behavior of Fission Xenon in Uranium Dioxide", Paper presented at The First Conference on Nuclear Reactor Chemistry, Gatlinburg (October 12-14, 1960).

(47) Toner, D. F., and Scott, J. L., "Study of Factors Controlling the Release of Xenon-133 from Bulk UO_2", Radiation Effects in Refractory Fuel Compounds, ASTM, S. T. P. No. 306 (March, 1962), p 86.

(48) Melehan, J. B., and Rough, F. A., Unpublished Data (August, 1962).

(49) Lewis, W. B., "Behavior of Fission Gases in UO_2 Fuel", DL-45 (November, 1961).

(50) Cottrell, W. B., Culver, H. N., Scott, J. L., and Yarosh, M. M., "Fission Product Release From UO_2", ORNL-2935 (September 13, 1960).

(51) Robertson, J. A. L., "High Temperature Properties of Ceramic Fuels: Their Significance and Measurement", AECL-1529 (June, 1962).

(52) Eichenberg, J. D., "An In-Pile Measurement of the Effective Thermal Conductivity of UO_2", WAPD-200 (March 28, 1958).

(53) Christensen, J. A., and Bates, J. L., "High Temperature Microscopy of Irradiated UO_2", paper presented at Am. Cer. Soc. Meeting, Toronto, Ontario, 23-27, April 1961; Abstract in Cer. Bull., 40, 4 (1961).

(54) Bates, J. L., Christensen, J. A., and Daniel, J. L., "Irradiation of Uranium Dioxide Single Crystal", paper presented at ANS Meeting, Boston, 17-21 June, 1962; Abstract in Trans. ANS, 5, 1 (1962).

URANIUM SILICIDE

Compiled by M. Kangilaski

A1. Chemical composition

U_3Si_2, 92.7 w/o uranium, 7.3 w/o silicon

2. Phase diagram[1]

See Figure A2.

3. Effect of impurities

No data available

B1. Density (room temperature)[2]

12.20 g per cm^3

2. Density versus temperature

No data available

3. Uranium content

11.3 g per cm^3

4. Liquidus temperature[1]

1665 C

5. Solidus temperature[1]

1665 C

6. Vapor pressure

No data available

7. Thermal expansion (linear)[3]

14.6×10^{-6} per C at 20 to 1000 C

8. Recrystallization temperature range

No data available

C1. Hardness (room temperature)[4]

659 DPH

2. Hot hardness

No data available

3. Ultimate tensile strength

No data available

4. Yield strength

No data available

5. Compressive strength

No data available

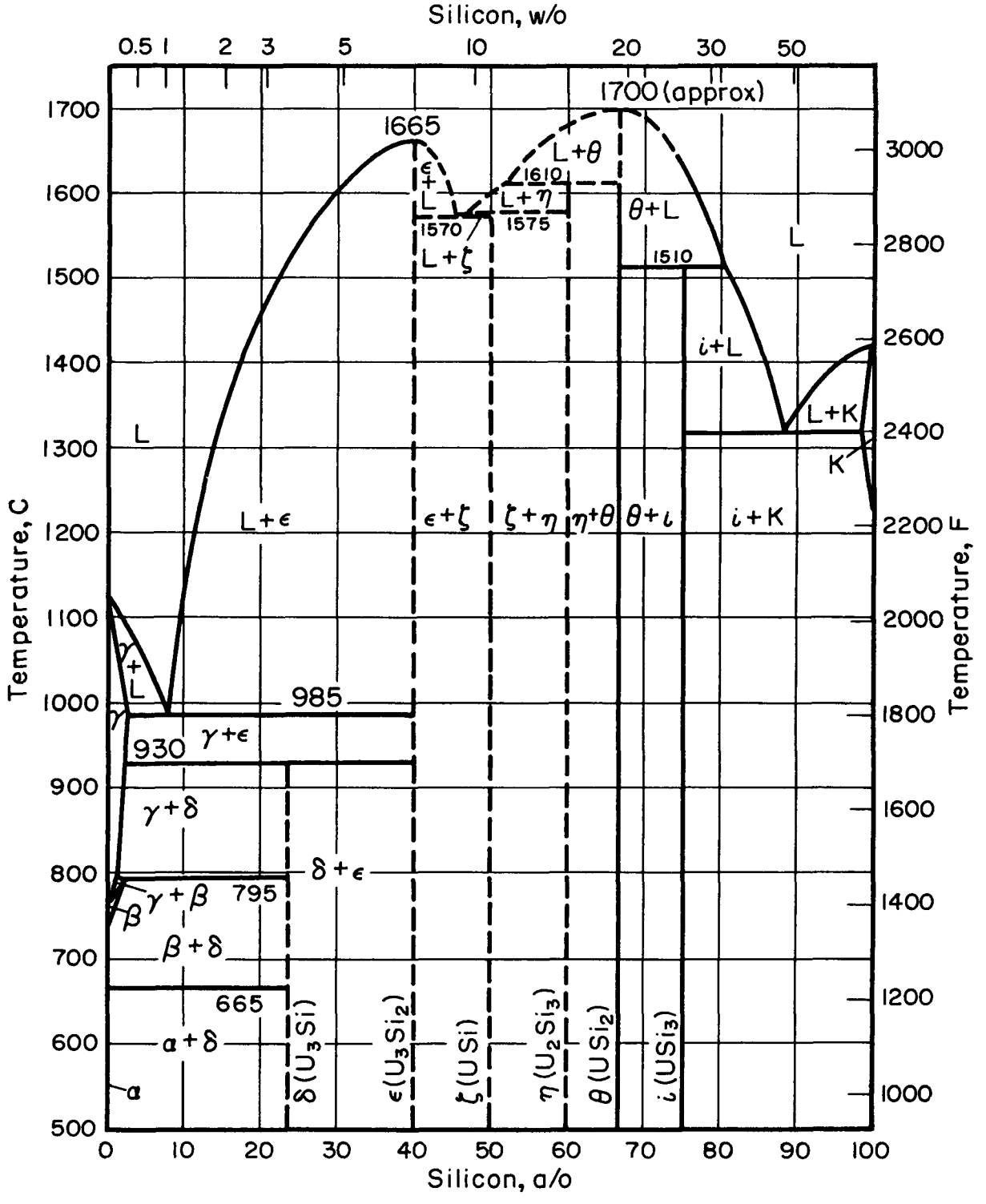

FIGURE A2. URANIUM - SILICON PHASE DIAGRAM [1]

AEA-43206

6. Creep strength
No data available

7. Young's modulus[5]
7.5×10^6 psi

8. Shear modulus
No data available

9. Bulk modulus
No data available

10. Poisson's ratio
No data available

11. Elongation
No data available

D1. Specific heat[6]
0.0416 cal/(mole)(C), (calculated value)

2. Thermal conductivity[7]
0.035 cal/(sec)(cm)(C) at room temperature

E1. Electrical resistivity[6]
112 microhm-cm at 100 C; 124 microhm-cm at 300 C

F1. Reactions with coolants

a. Steam
No data available

b. Helium
No data available

c. Carbon dioxide[7]
Similar to uranium

d. Nitrogen[8]
Reaction slower than with oxygen, initially parabolic, faster than uranium-nitrogen reaction

e. Hydrogen[7]
Probably incompatible

f. Liquid metals[7]
No attack by NaK after 1 week at 800 C; no other data available

g. Air
No data available

2. Reactions with claddings or structural materials
No data available

G1. Dimensional stability during irradiation[9]

A decrease of 6 to 7 per cent in density after burnup of 1.8×10^{20} fissions per cm^3 at a surface temperature of 690 C and a center temperature of 910 C has been observed.

2. Fission-gas-release data[9]

2.5 per cent of the fission gases were released under the above conditions.

3. Swelling-temperature data

No data available

4. Unusual nuclear properties

No data available

5. Property changes as a result of irradiation

No data available

H. References

(1) Kaufmann, A. R., Cullity, B. D., Bitsianes, G., "Uranium Silicon Alloys", J. Metals, 9, 23-27 (January 1957).

(2) Rough, F. A., and Bauer, A. A., "Constitution of Uranium and Thorium Alloys", BMI-1300 (June 2, 1958).

(3) Loch, L. D., Engle, G. B., Snyder, M. J., and Duckworth, W. H., "Survey of Refractory Uranium Compounds", BMI-1124 (1956).

(4) Unpublished information from AI.

(5) "Annual Technical Progress Report, AEC Unclassified Programs, Fiscal Year 1960", NAA-SR-5350.

(6) Cape, J. A., and Taylor, R. E., "Thermal Properties of Refractory Materials, Quarterly Progress Report No. 3, February 1, 1961 to April 31, 1961", AI-6358.

(7) Nichols, R. W., "Ceramic Fuels, Properties, and Technology", Nuclear Eng., 3, 29, 1958.

(8) Snyder, M. J., and Duckworth, W. H., "Properties of Some Refractory Uranium Compounds", BMI-1223 (September 9, 1957).

(9) Kangilaski, M., BMI, Unpublished Data.

UO_2-Al_2O_3 DISPERSIONS

Compiled by R. A. Wullaert

A1. Chemical composition

See Figure A2, phase diagram.

2. Phase diagram[1]

See Figure A2.
A eutectic occurs at 1900 ± 10 C, 48.3 w/o UO_2-51.7 w/o Al_2O_3.

3. Effect of impurities[2,3]

Impurities (potassium, sodium) cause fuel migration during sintering.[2] Additions of MgO and SiO_2 allow fabrication of pellets with higher densities.[3]

B1. Density (room temperature)

Theoretical density of UO_2-Al_2O_3 dispersions = (w/o UO_2) (10.97) + (w/o Al_2O_3) (4.00).

2. Density versus temperature

No data available

3. Uranium content

The UO_2 fuel particles contain 88 w/o uranium.

4. Liquidus temperature

See Figure A2.

5. Solidus temperature

See Figure A2.

6. Vapor pressure

No data available

7. Thermal expansion (linear)

No data available

8. Recrystallization temperature range

No data available

C1. Hardness (room temperature)

No data available

2. Hot hardness

No data available

3. Ultimate tensile strength[4]

The modulus of rupture for a 33 w/o UO_2-Al_2O_3 is in the range of 1900 to 3300 psi (data are for 60 per cent dense material).

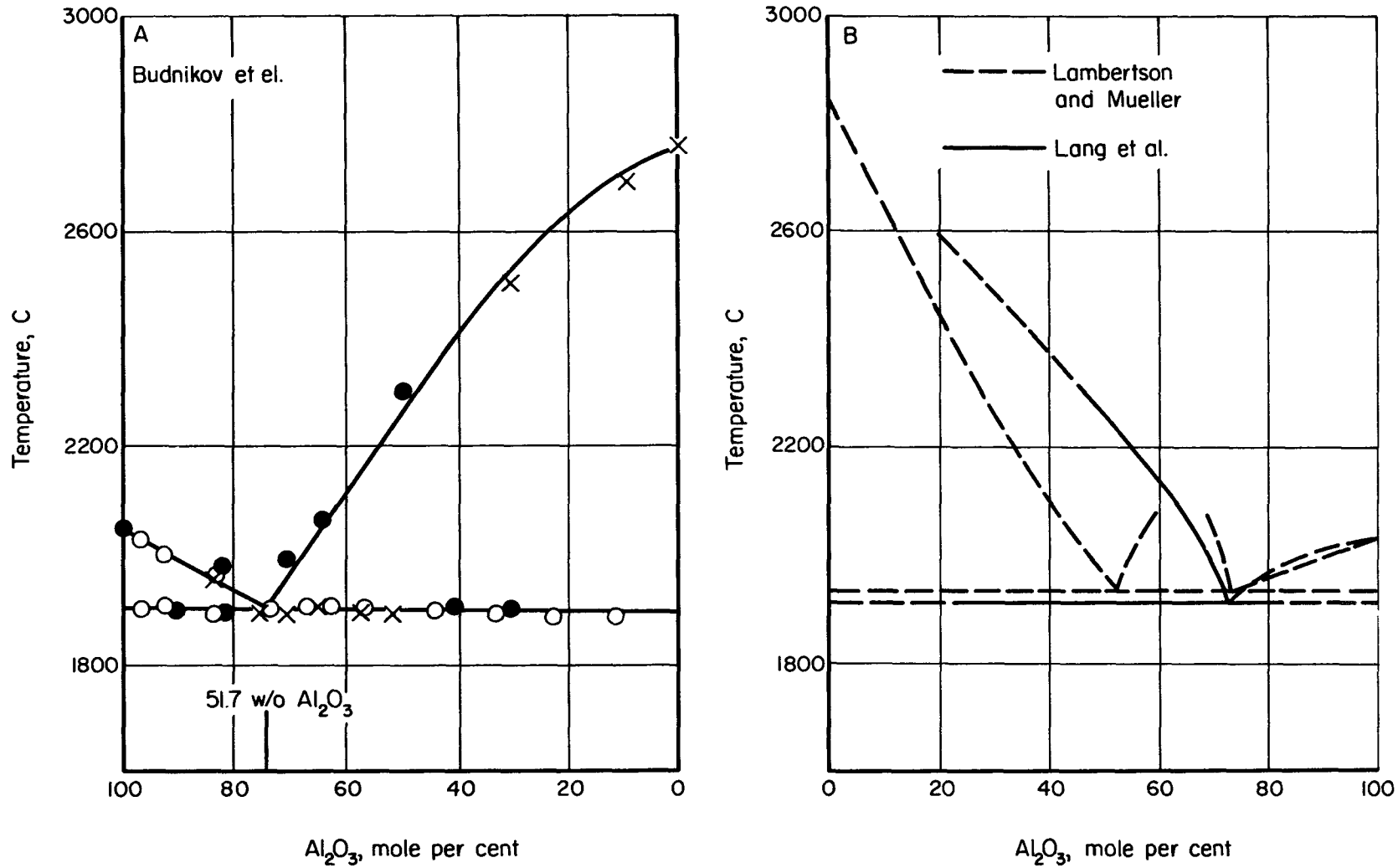

AEA-43202

FIGURE A-2 PROPOSED PHASE DIAGRAMS OF THE UO_2—Al_2O_3 SYSTEM[1]

4. Yield strength

No data available

5. Compressive strength

No data available

6. Creep strength

No data available

7. Young's modulus

No data available

8. Shear modulus

No data available

9. Bulk modulus

No data available

10. Poisson's ratio

No data available

11. Elongation

No data available

D1. Specific heat

No data available

2. Thermal conductivity

No data available

E1. Electrical resistivity[5]

Electrical resistance is a function of the fuel content and fuel particle size, as shown in Figure E1.

F1. Reactions with coolants

a. Steam[4,6]

Calcined Al_2O_3 is attacked appreciably by water at 650 F, but fused Al_2O_3 is comparatively stable (see Table F1a). Al_2O_3 exhibits losses of ~1 mg per hr at 1200 C and 3 mg per hr at 1400 C in a gas stream of water vapor.[6]

b. Helium

There is no reaction with Al_2O_3.

c. Carbon dioxide[7]

There is no reactivity of Al_2O_3 in carbon dioxide in the temperature range of 400 to 800 C.

d. Nitrogen

Al_2O_3 exhibits losses of ~1 mg per hr at 1200 C and 3 mg per hr at 1400 C in a nitrogen gas stream.[6]

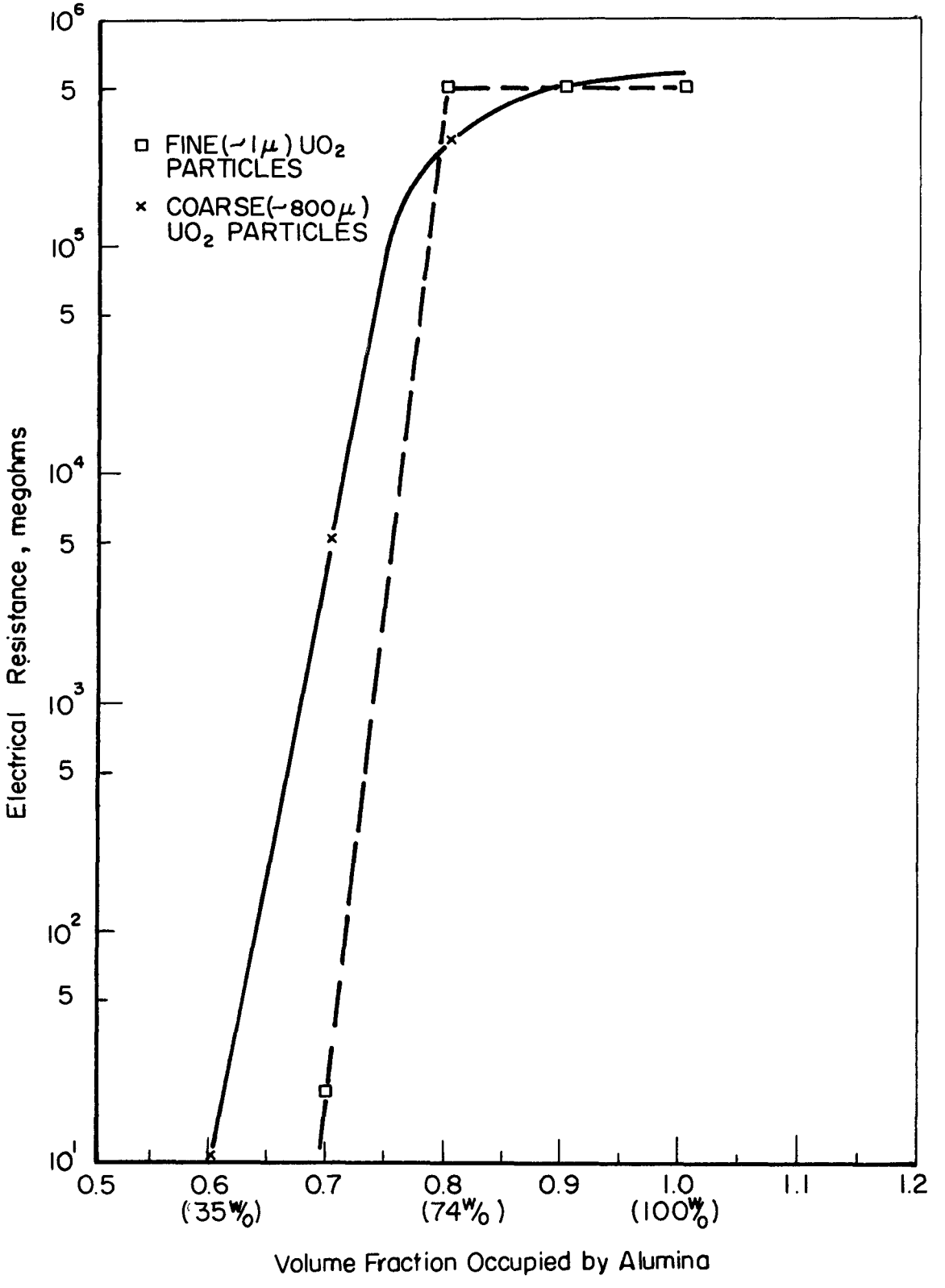

FIGURE EI. RELATIONSHIP BETWEEN ELECTRICAL RESISTANCE AND COMPOSITION FOR Al_2O_3-UO_2 PELLETS[5]

AEA-43213

TABLE F1a. WATER CORROSION TEST[a] ON 33 w/o UO_2-Al_2O_3[4]

Sample	Total Loss in Weight[b], g per dm^2	Total Time, hr	Weight Loss, g/(dm^2)(hr)
33 w/o UO_2-Al_2O_3 (10-μ UO_2)	48.7	250	0.195
	56.8	565	0.100
	67.1	1000	0.067
	100.0	2000	0.050
33 w/o UO_2-Al_2O_3 (100-μ UO_2)	33.2	250	0.133
	36.1	510	0.071
	72.0	1000	0.072

(a) Test performed in static autoclaves with water at 680 F under 2000 psi and containing LiOH at pH 10.0.

(b) The area is the product of the dimensions and not the true surface area.

e. Hydrogen
There is no reaction with Al_2O_3.

f. Liquid metals
No data available

g. Air
There is no reactivity of Al_2O_3 in air in the temperature range of 400 to 800 C.[7]

2. Reactions with claddings or structural materials
No data available

G1. Dimensional stability during irradiation[8-10]
(See Table G1, Figure G1)

2. Fission-gas-release
(See Table G1)

3. Swelling-temperature data
No data available

4. Unusual nuclear properties
No data available

5. Property changes as a result of irradiation

a. Fission fragments appear to produce different and larger effects in Al_2O_3, as compared to UO_2 and BeO. The fission-fragment damage in Al_2O_3 is more like that which occurs in U_3Si, U_3O_8, and ZrO_2. Al_2O_3 appears to store large amounts of fission-fragment kinetic energy.[8]

TABLE G1. DIMENSIONAL STABILITY AND GAS RELEASE OF IRRADIATED UO_2-Al_2O_3

Composition, w/o		Estimated Temperature, C		Burnup,		Physical Change, per cent		Fission-Gas Release,		
UO_2	Al_2O_3	Fuel Surface	Fuel Center Line	10^{20} fissions per cm^3	a/o U Fiss.	Diameter	Density	per cent	Comment	Reference
26	74	800	--	0.45	1 (U-235)	+0.78	--	--	--	(10)
21	79	260	--	2.74		--	-18.5	--	See Figure G1	(9)
		220	--	2.33		--	-19.9	--		
		110	--	1.25		--	-17.9	--		
		390	--	10.8		--	-19.7	--		
		210	--	6.92		--	-18.8	--		
		290	--	5.25		--	-17.4	--		
		300	--	0.92		--	-22.5	--		
		300	--	0.92		--	-16.3	--		
80 (depleted)	20	40	--	0.002		--	--	--	Loss of Al_2O_3 structure	(9)
21	79	620	740	4	19	--	--	0.6-1.4 Kr^{85}	In-pile	(8)

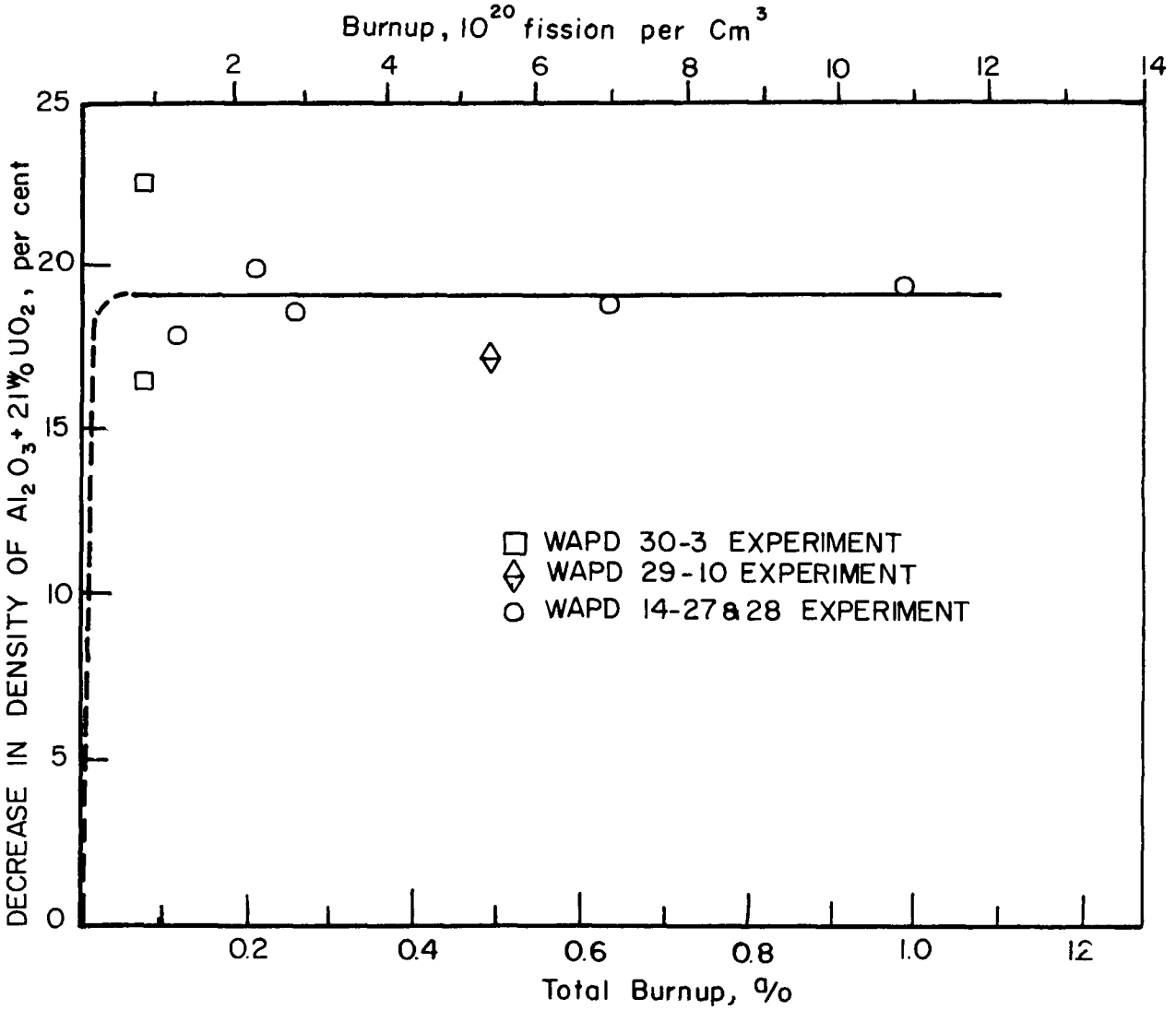

FIGURE GI. INCREASE IN VOLUME OF 21% UO_2– Al_2O_3 ON IRRADIATION[9]

AEA-43221

b. Property changes in 21 w/o UO_2-Al_2O_3 (see Table G1 for irradiation conditions) have been reported.[9] The original porosity in the specimens disappeared, and there were no grain boundaries visible in the Al_2O_3 matrix. Collapsed voids appeared in the UO_2 particles. The crystal structure of the Al_2O_3 was destroyed, but not that of the UO_2. The fission-fragment range in the dispersion was sufficient to reach all of the Al_2O_3. Annealing for 8 hr at 1000 C in vacuum completely recrystallized the Al_2O_3.[9]

H. References

(1) Budnikov, P. P., Tresvyatsky, S. G., and Kushakovsky, V. I., "Binary Phase Diagrams for UO_2-Al_2O_3, UO_2-BeO, and UO_2-MgO", Proceedings of the Second United Nations International Conference on the Peaceful Uses of Atomic Energy, Geneva (1958), A/Conf. 15/P/2193, Vol 6, p 125.

(2) "Maritime Gas Cooled Reactor Program, Quarterly Progress Report for Period Ending December 31, 1959", GA-1195.

(3) Livey, D. T., and Murray, P., "The Stability of Beryllia and Magnesia In Different Atmospheres at High Temperatures", J. Nuc. Energy, 2, 202 (1956).

(4) Winsnyi, L. G., and Taylor, K. M., "Fabrication and Evaluation of Urania-Alumina Fuel Elements and Boron Carbide Burnable Poison Elements", ASTM Special Publication No. 276 (1960).

(5) Johnson, D. E., and Tobin, J. M., "Proceedings of the Beryllium Oxide Meeting Held at Oak Ridge National Laboratory, Oak Ridge, Tennessee, December 1-2, 1960", TID-7602 (Pt 1), (1960).

(6) Wickert, K., "Deposits on Heating Surfaces in Steam Generators, II", Brennstoff-Wärme-Kraft, 16, 101 (1958).

(7) Berleman, M. G., and Simon, S. L., "The Volatilization of Beryllia in Water Vapor", ANL 4177 (1948).

(8) Bleiberg, M. L., Yeniscavich, W., and Gray, R. G., "Effect of Burnup on Certain Ceramic Fuel Materials", WAPD-T-1274 (1961).

(9) Berman, R. M., Bleiberg, M. L., and Yeniscavich, W., "Fission Fragment Damage to Crystal Structures", WAPD-T-1125 (February 2, 1960).

(10) Johnson, D. E., and Tobin, J. M., Nuclear Reactor Chemistry, First Conference, Gatlinburg, Tennessee, October 12-14, 1960, TID-7610.

UO_2-BeO DISPERSIONS

Compiled by R. A. Wullaert

A1. Chemical composition

UO_2-BeO dispersions containing from 2 w/o UO_2 to 80 w/o UO_2 have been successfully fabricated and irradiated.

2. Phase diagram

A eutectic occurs at 2170 ± 20 C, 83.6 w/o UO_2- 16.4 w/o BeO.[1] See Figure A2.

3. Effect of impurities

Variations of impurities and fuel-particle size will produce variable sintering characreristics.[2] Carbon in BeO is responsible for gas-bubble formation along grain boundaries during heat treatment.[3]

B1. Density (room temperature)

Theoretical density of UO_2-BeO dispersion = (w/o UO_2) (10.97) + (w/o BeO) (3.03).

2. Density versus temperature

No data available

3. Uranium content

The UO_2 fuel particles contain 88 w/o uranium.

4. Liquidus temperature

No data available

5. Solidus temperature

No data available

6. Vapor pressure

No data available

7. Thermal expansion[4]

70.9 w/o UO_2-29.1 w/o BeO has a coefficient of thermal expansion of 8.84×10^{-6} per C for the temperature range between 100 and 400 C

8. Recrystallization temperature range[5,6]

Grain growth of both components of UO_2-BeO dispersions has been reported to occur above 1600 C. There is marked recrystallization of BeO above 2050 C.[7]

C1. Hardness (room temperature)

No data available

2. Hot hardness

No data available

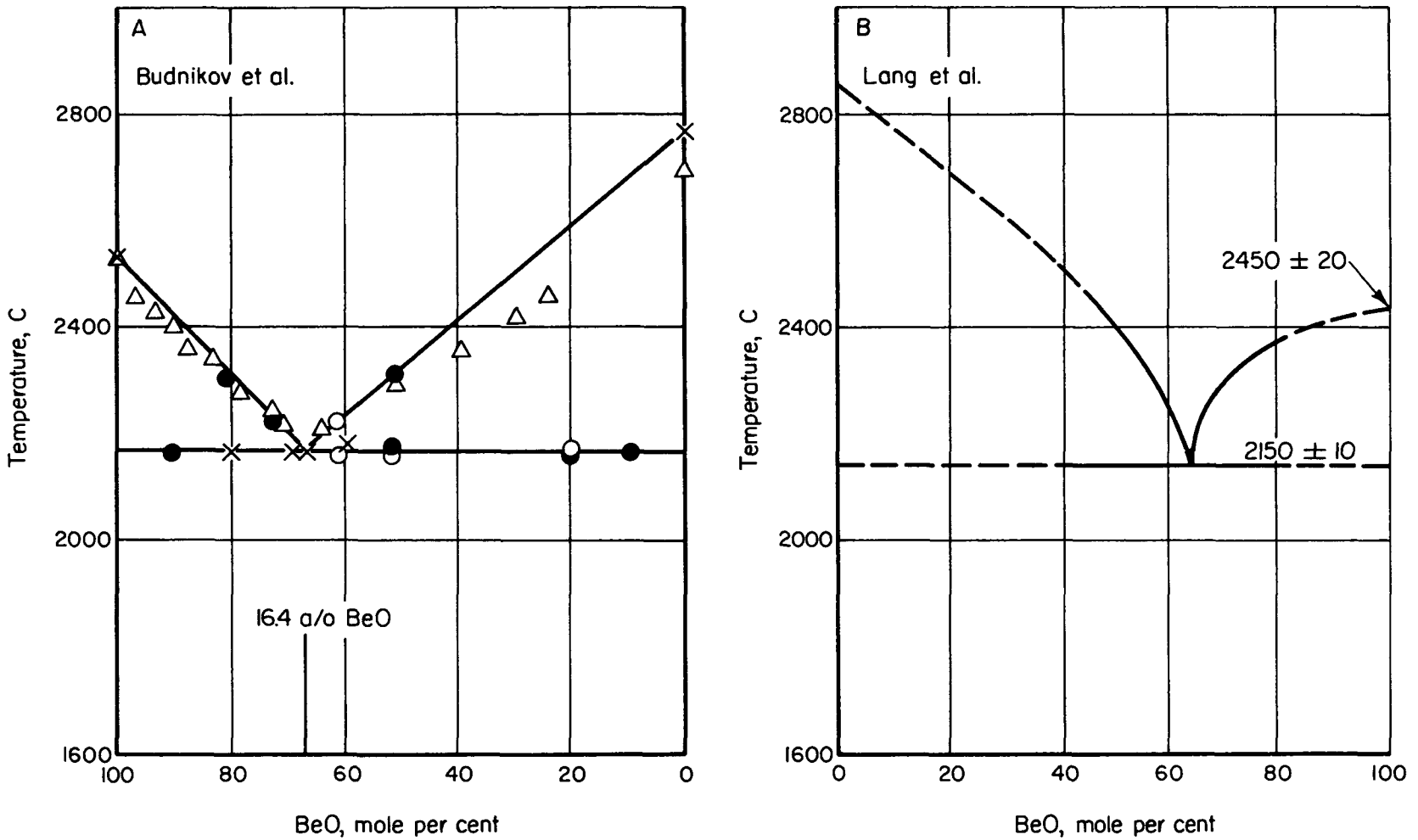

FIGURE A-2 PROPOSED PHASE DIAGRAMS OF THE UO_2–BeO SYSTEM[1]

AEA-43201

3. Ultimate tensile strength[8]

Composition	Bending Strength, psi	Density, per cent of theoretical
2 w/o UO_2-BeO	27,600	98
10 w/o UO_2-BeO	32,800	98

4. Yield strength

No data available

5. Compressive strength

Crushing strength of 48.3 w/o UO_2-BeO is 83,300 ± 8,000 psi.[9, 10] Compressive strength is sensitive to the density and fuel content, as shown in Table C5.[11]

TABLE C5. SOME PROPERTIES OF HOT-PRESSED BeO AND BeO-10 w/o UO_2 COMPACTS[11]

Material	Density, g per cm^3	Elastic Modulus, 10^{10} dynes per cm^2	Compressive Strength, 10^3 psi	Thermal Conductivity (25 C), cal/(cm)(sec)(C)
Beo	2.7	270	125	0.25
	2.9	350	175	0.25
BeO-10 w/o UO_2	2.9	305	155	0.20-0.25
	3.0	340	188	0.20-0.25

6. Creep strength

No data available

7. Young's modulus

Young's modulus is sensitive to the density and fuel content of the dispersion (see Table C5).[11]

8. Shear modulus

No data available

9. Bulk modulus

No data available

10. Poisson's ratio

No data available

11. Elongation

No data available

D1. Specific heat

No data available

2. Thermal conductivity

Greater than 35 volume per cent UO_2 (66 w/o) results in a great loss in the thermal conductivity.[12] Thermal conductivity is sensitive to the density and fuel content as shown in Table C5[11] and Figures D2a and D2b[13].

E1. Electrical resistivity

No data available

F1. Reactions with coolants

a. Steam

Beryllia reacts with water vapor to form a volatile compound believed to be beryllium hydroxide. The rate-controlling process is the diffusion of the gaseous beryllium hydroxide through the laminar boundary layer produced at the BeO surface by the flowing gases.[14] The results of various investigators for the corrosion of BeO in moist air are given in Table F1a(1).[13, 15, 16] For similar experimental conditions, there appears to be some divergence of results. The reaction in moist air is strongly influenced by surface phenomena,[17] which may account for the variations in results. The corrosion of BeO as a function of exposure temperature is illustrated in Tables F1a(2) and F1a(3).[16, 17] Sintered BeO suffers no apparent attack by humid air (water content - 23.1 mg per liter) after exposures of up to 250 hr at 1100 C.[17] At temperatures above this, the corrosion would become significant under reactor conditions. The data indicate that moist air will not cause excessive corrosion of sintered BeO, but the effects of higher gas velocities and radiation on the process have not been taken into account. Additions of Al_2O_3 to BeO have not reduced the volatility of BeO sufficiently to decrease the corrosion rates.[18]

b. Helium

Structural failure and color changes occur in BeO when it is heated to 2100 C in helium. See Table F1b.[19]

c. Carbon dioxide

No data available

d. Nitrogen

There is no reaction with BeO.

e. Hydrogen

The presence of hydrogen induced a reaction between BeO and carbon at 1600 C. See Table F1b.[19]

f. Liquid metals

No data available

g. Air

There is no reaction of dry air with BeO below 2000 C.[7]

2. Reactions with claddings or structural materials

56-59 w/o UO_2-BeO: There was no reaction with Hastelloy X or Type 316 stainless steel after irradiation at temperatures up to 940 C.[20]

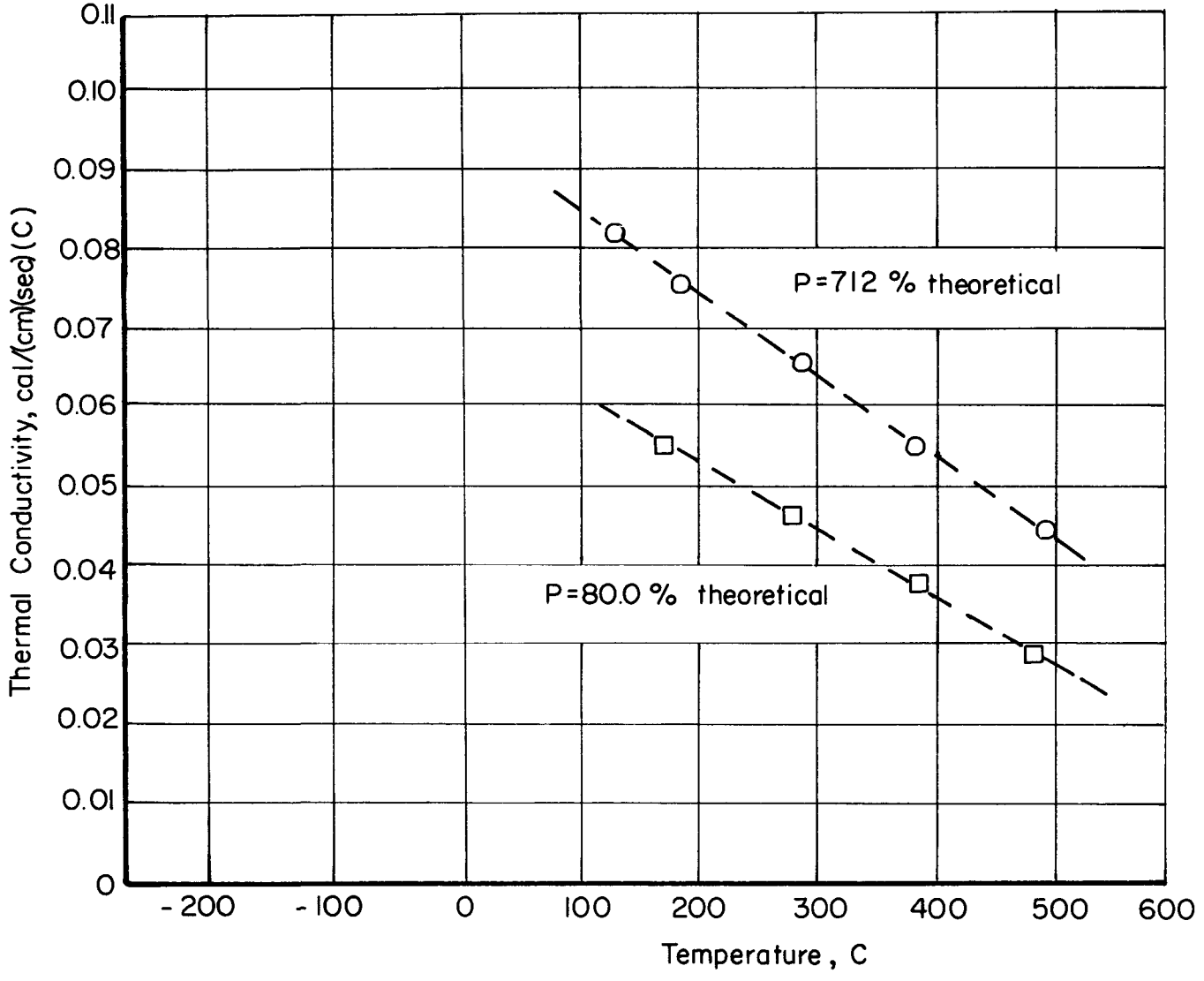

FIGURE D2a. Thermal Conductivity of 47 w/o UO_2 BeO [13]

AEA-43243

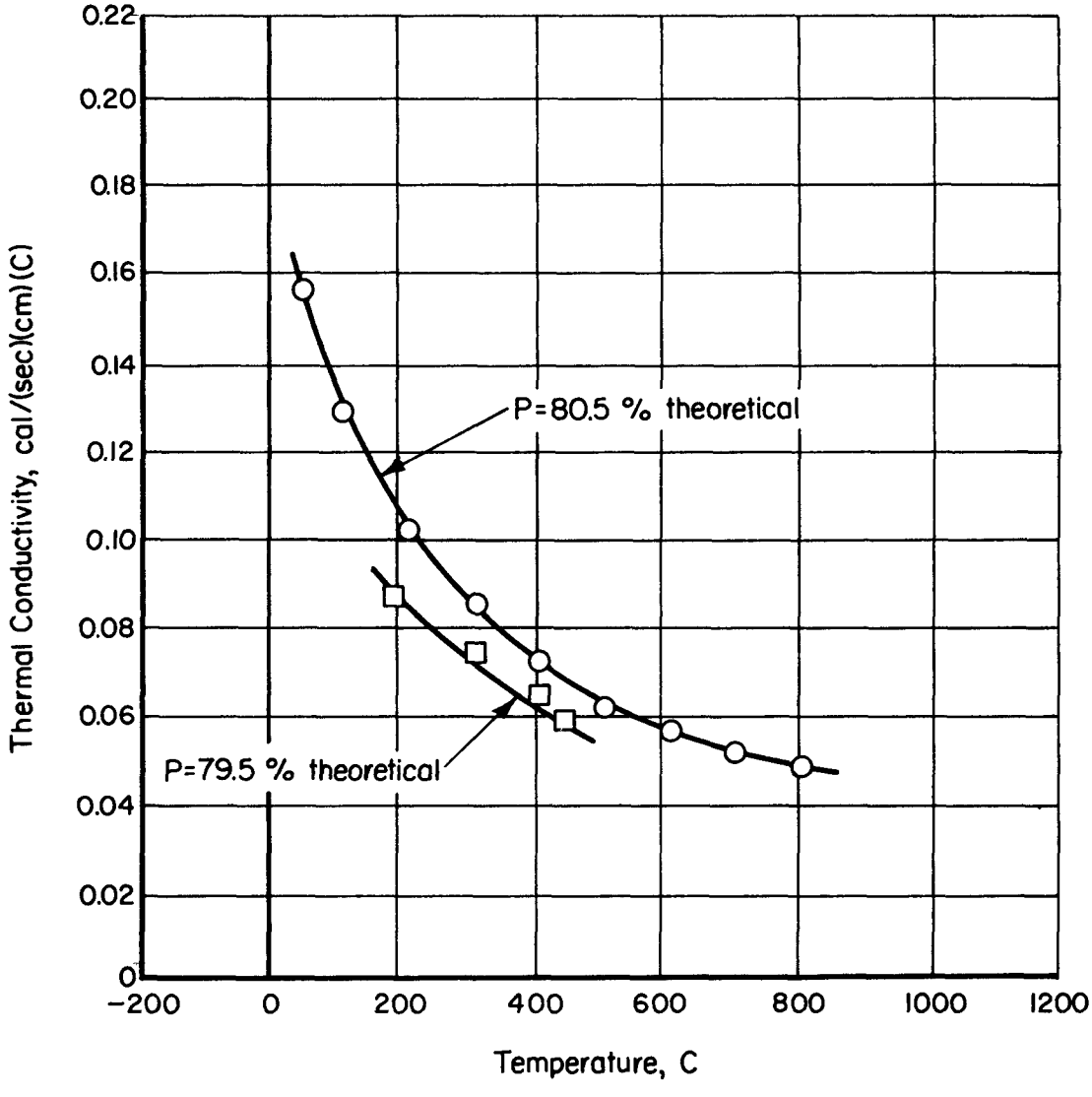

FIGURE D2B. THERMAL CONDUCTIVITY OF 70.9 w/o UO_2–BeO[13]

AEA-43244

TABLE Fla(1). THE CORROSION OF BeO IN MOIST AIR[a]

Temperature, C	Gas Velocity, m per hr	Weight Loss, mg/(cm^2)(hr)	Loss Rate, μ per year	References
1550	994	10.2	2.2×10^5	(15)
1550	994	2.6	5.8×10^4	(16)
1535	3620	0.23	5.1×10^3	(13)

(a) Experiments were of the standard transpiration type in which moist air saturated at 25 and 50 C (with moisture contents of 23.13 and 93.12 mg per liter of air) was passed over BeO.

TABLE Fla(2). CORROSION OF BeO IN PURE STEAM[16]

Temperature, C	Weight Loss, mg/(cm^2)(hr)
1000	0.01
1250	0.22
1400	0.76
1500	1.83
1550	2.60

TABLE F1a(3). CORROSION RATES FOR SINTERED BeO IN HUMID AIR[17]

Air Saturation Temperature, C	Sample Temperature, C	Geometric Specific Gravity	Duration of Individual Exposures, hr	Corrosion Rate, g/(cm^2)(hr)
25	1100	2.97	Var.[a]	<0.02
		2.51	Var.	<0.02
	1200	2.99	24	1.0
		2.60	24	2.2
	1300	2.69	24	2.3
		2.86	24	2.4
		2.99	Var.	1.1
		2.98	24	2.5
		2.25	Var.	1.4
		2.36	24	3.0
50	1300	2.27	24	10.4
		2.98	24	6.3

(a) Variable exposures, in integral multiples of 24 hr.

TABLE F1b. WEIGHT LOSS OF BeO[a] IN HYDROGEN AND HELIUM AT ELEVATED TEMPERATURES[19]

Temperature, C	Weight Loss, per cent	
	In Hydrogen	In Helium
1575	2	--
1600	--	0.5
1900	8	2.5
2100	46	8
2300	--	13

(a) BeO was fabricated by sintering at 1890 C for 30 min in air. The impurity content was less than 1 per cent. The specimen was mounted on carbon.

61 w/o UO_2-BeO: There was no reaction with ThO_2 spacers during irradiation at ~ 1000 C.[21]

G1. Dimensional stability during irradiation[9,10,12,20-26]

See Table G1.

2. Fission-gas-release data

The rate of release of Xe^{133} from neutron-activated samples of 61 w/o UO_2-BeO was determined at 1200, 1400, 1600, and 1800 C. At 1200 and 1400 C, a small initial burst of Xe^{133} was observed with subsequent release by a diffusion mechanism. At 1600 C, the initial release was much higher, but apparently diffusion controlled. The pellets released nearly all of their fission gas in approximately 30 hr at 1800 C, and there appeared to have been a microstructural change in the BeO matrix.[5,6]

3. Swelling-temperature data

No data available

4. Unusual nuclear properties

BeO has excellent moderating properties. The slowing-down power ($\xi\Sigma_s$) is 0.13, and the moderating ratio $\left(\frac{\xi\Sigma_s}{\Sigma_a}\right)$ is 180.[7] Helium and tritium are produced in BeO mainly by the (n, 2n) and (n, α) reactions with beryllium. The reactions involved are the following:

a. (n, 2n) reaction:

$Be^9 + n \rightarrow Be^8 + 2n$ (threshold energy = 2.7 Mev),

$Be^8 \rightarrow 2He^4$ (half-life = 10^{-14} sec).

b. (n, α) reaction:

$Be^9 + n \rightarrow He^6 + He^4$ (threshold energy = 0.71 Mev),

$He^6 \rightarrow Li^6 + \beta$ (half-life = 0.82 sec),

$Li^6 + n \rightarrow He^4 + H^3$ (thermal-neutron capture)

5. Property changes as a result of irradiation

a. Radiation may accelerate the corrosion rate of BeO in moist air by introducing hydrogen into the air stream.[27] A few investigators[11,28] have reported a radiation-induced reaction between water vapor and carbon contained in BeO. It has been estimated that 3 to 5 w/o fission-fragment impurity content in UO_2 will destroy its lattice, whereas only 2 w/o is necessary in BeO. This may be due to greater irradiation stability of cubic lattice (UO_2) over hexagonal (BeO). The threshold value for lattice destruction in BeO is 11 to 27 x 10^{20} fission fragments per cm^3, and UO_2 loses its crystallinity in the range of 36 to 64 x 10^{20} fission fragments per cm^3. The estimates depend on lattice restraint, burnup rate, and temperature.[22]

TABLE G1. DIMENSIONAL STABILITY AND GAS RELEASE OF IRRADIATED UO_2-BeO

Composition	Estimated Fuel Temperature[a], C		Burnup		Physical Change, per cent		Fission Gas Released, per cent	Comments	Reference
	T_s	T_c	10^{20} Fissions per Cm^3	Uranium, a/o	Diameter	Density			
25.3 w/o UO_2-BeO	499	504	11.1	54.5	+27[b]	--	19.9(Kr^{85})	25-μ-size UO_2	(22)
28 7 w/o UO_2-BeO	516	521	12.1	54.3	+6[b]	--	6.9(Kr^{85})	150-μ-size UO_2	(22)
30.1 w/o UO_2-BeO	454	460	10 7	44.4	+8[b]	--	--	150-μ-size UO_2, UO_2 leached from surface of plate	(22)
65 w/o UO_2-BeO	682	688	10 8	14.2	+4[b]	--	0.1(Kr^{85})	25-μ-size UO_2	(22)
53.2 w/o UO_2-BeO	840	--	--	1.5	--	Nil	0.1-0.15(Kr^{85})	--	(12)
59.2 w/o UO_2-BeO	1250	--	0.7	--	Nil	Nil	0.4(Kr^{85})	--	(23)
48.3 w/o UO_2-BeO	1250	--	~2.0	--	Nil	Nil	--	125-μ-size UO_2	(9,10)
			5	--	--	-3	--	--	(9,10)
56 w/o UO_2-BeO	780-940	>1000	1.3	--	--	-1.0 to -2.4	--	44-μ-size UO_2	(20,24)
59 w/o UO_2-BeO	780-940	>1000	1.3	--	--	-1.0 to -2.4	--	150-μ-size UO_2	(20,24)
58.9 w/o UO_2-BeO	--	(1010)	--	~4.2	+0.5 to 1.6	--	0.3(Kr^{85})	<5-μ-size UO_2	(21)
		(1200)	--	~4.2	+1.5 to 2.4	--	0.3(Kr^{85})	--	(21)
		(1090)	--	~5.1	+0.2 to 1.5	--	0.2(Kr^{85})	--	(21)
70 w/o UO_2-BeO	930	1700	5-6.4	--	No change	--	0.59-2.7(Kr^{85})	--	(25)
80 w/o UO_2-Beo	930	1700	5-6.4	--	No change	--	0.59-2.7(Kr^{85})	--	(25)
2 w/o UO_2-BeO	--	(250)	--	0.53	+0.50	--	--	--	(11)
					+0.62	--	--	--	(11)
				1.08	+0.90	--	--	--	(11)
					+0.52	--	--	--	(11)
				1.86	+0.60	--	--	--	(11)
					+0.65	--	--	--	(11)
10 w/o UO_2-BeO	--	(650)	--	0.53	+0.44	--	--	<2-μ-size UO_2	(11)
					+0.61	--	--	--	(11)
				1.08	+0.71	--	--	<2-μ-size UO_2	(11)
					+0.46	--	--	--	(11)
				1.86	+0.62	--	--	<2-μ-size UO_2	(11)
					+0.65	--	--	--	(11)
47.4 w/o UO_2-BeO	--	--	--	7.25×10^{-7}	--	--	1.06(Xe^{137}), 1.87(I^{131})	BeO and UO_2[c]	(26)
				7.21×10^{-7}	--	--	4.10(Xe^{133}), 8.22(I^{131})	$Be(OH)_2$-OH_2[c]	(26)
				6.44×10^{-7}	--	--	5.28(Xe^{133}), 8.52(I^{131})	BeO-UO_2[c]	(26)

(a) Temperatures in brackets not specified whether located on surface or centerline.

(b) Loop (external) pressure on specimens was 2200 psi. Specimens under external pressure of 14 psi under similar irradiation conditions exhibited up to three times the thickness increase.

(c) Starting materials. Fission products were collected during a postirradiation anneal at 1800 F for 24 hr.

b. In 53.2 w/o UO_2-BeO (see Table G1 for irradiation conditions) there was no change in microstructure. Annealing at 1370 C for 4 hr produced no changes in dimensions.[12]

c. In 48.3 w/o UO_2-BeO (see Table G1) there was no evidence of destruction of BeO grain structure or formation of gas bubbles or voids. Crushing strength was reduced by as much as one-third, with an average value after irradiation of 68,500 psi.[9] The pellets resistance to abrasion decreased. X-ray diffraction studies showed no change in the c-spacing of the irradiated BeO matrix, whereas the a-spacing increased 0.74 per cent. Thus the c/a ratio decreased from 1.62 to 1.61 (a 0.62 per cent change). The high irradiation temperature (1250 C) may account for the small amount of damage as compared to low-temperature irradiations (like WAPD experiments). The average fission-fragment density in the BeO shell around the UO_2 particles was calculated to be 2×10^{20} fission fragments per cm^3, or 0.15 per cent of the total number of beryllium and oxygen atoms present. It was also calculated that each of the beryllium and oxygen atoms within the recoil range of the fuel (10 μ) was displaced at least once.[10]

d. In 25.3 w/o UO_2, 28.7 w/o UO_2, 30.1 w/o UO_2-BeO (see Table G1) the UO_2 exhibited high degree of porosity (fission-gas bubbles). Bubbles were also observed at the UO_2-BeO interface. Cracks were observed in undamaged regions of the BeO matrix. It was concluded that the BeO matrix was destroyed by an impurity effect of fission fragments, rather than through displacement effects. Coarse and fine dispersions had approximately the same fissions per cm^3, but the BeO matrix of the coarse dispersion was not completely destroyed. Calculations showed that ~44 per cent of the BeO was damaged using 25-μ UO_2 particles, whereas only ~5 per cent was damaged using 150-μ UO_2 particles. The amount of swelling per fission (swelling rate) is calculated to be 4.8×10^{-23} cm^3 per fission. The fine dispersion had greater gas release because the BeO matrix became amorphous, thus being less dense and allowing higher gas-diffusion rates.[29]

e. In 56 w/o UO_2, 59 w/o UO_2-BeO (see Table G1) the amount of fission gas released was approximately equal to that expected to be released by recoil, although slightly larger amounts were released from lower density specimens. Postirradiation heating for 4 hr at 1300 C produced no swelling, cracking, or crumbling. There appeared to be no visible deterioration of pellets due to irradiation. The microstructure was unaffected.[20, 24]

f. In 58.9 w/o UO_2-BeO (see Table G1) the fuel no longer had a definite microstructure.[21]

g. In 70 w/o UO_2-BeO (see Table G1) metallographic examination revealed no voids in the center of the fuel, but spherical voids appeared at the outer edge of fuel particles. Large voids were present at the UO_2-BeO interface. X-ray diffraction showed very little change in the crystal structure of UO_2. BeO showed a slight lattice strain (0.44 per cent). The UO_2 lattice contracted 0.07 to 0.26 per cent and showed lattice strains of 0.12-0.18 per cent.[25]

h. In 2 w/o UO_2-BeO and 10 w/o UO_2-BeO (see Table G1 for irradiation conditions) the effects of irradiation on crushing strength have been determined and are shown in Table G5a. The 2 w/o UO_2-BeO pellets had lower densities and more variations in strength. The 10 w/o UO_2-BeO appears to saturate at a 30 per cent decrease. The elastic modulus also appears to saturate at about a 30 per cent decrease, as shown in Table G5b and Figure G5a. The thermal conductivity decreased by a factor of 4 to 6, as shown in Table G5c and Figure G5b. Recovery of the thermal conductivity started at annealing temperatures of ~600 C. Heating for 7 hr at 1000 C in vacuo decreased the thermal-resistivity ratio of 10 w/o UO_2-BeO from 6.75 to 2.5. It is concluded that 2 w/o UO_2-BeO and 10 w/o UO_2-BeO dispersions behaved about the same for equal neutron-exposure times, even though fraction of total atoms fissioned was five times greater in the 10 w/o UO_2 specimens.[11]

TABLE G5a. EFFECT OF IRRADIATION ON THE CRUSHING STRENGTH 0.25 BY 0.25-IN. BeO-UO_2 CYLINDERS[11]

Material	Density, g per cm^3	Fission Burnup, a/o	Average Crushing Strength[a]	
			Value Obtained, 10^3 psi	Percentage of Unirradiated Value
BeO-2 w/o UO_2	2.4	0	57.1	--
		0.53	53.9	94
		1.08	75.6	132
		1.86	65.0	114
	2.6	0	131.7	--
		0.53	106.6	81
		1.08	115.5	88
		1.86	108.1	82
BeO-10 w/o UO_2	2.9	0	155.1	--
		0.53	105.2	68
		1.08	109.0[b]	70
		1.86	111.8	72
	3.0	0	188.3	--
		0.53	137.2	73
		1.08	144.1	77
		1.86	135.8	72

(a) All values based on at least five samples.

(b) The average deviation in this case was 16.3 per cent. In all other cases the average deviation was less than 15 per cent.

TABLE G5b. EFFECT OF IRRADIATION ON THE ELASTIC MODULUS OF BeO-UO_2 PRISMS[11]

Material	Density, g per cm^3	Fission Burnup, a/o	Decrease in Elastic[a] Modulus, per cent
BeO-2 w/o UO_2	2.79	0.53	21.6
		1.08	20.2, 29.8(25.0)
		1.86	31.6, 24.9(28.3)
	2.84	0.53	17.8
		1.08	25.3, 29.7(27.5)[b]
		1.86	26.5, 29.2(27.9)[b]
BeO-10 w/o UO_2	2.84	0.53	23.6
		1.08	25.3, 24.9(25.1)
		1.86	30.3, 26.2(28.3)
	3.02	1.08	18.4, 28.2(23.3)
		1.86	30.3, 31.1(30.7)

(a) Average values are given in parentheses.

(b) Preirradiation values unavailable; values are approximations based on similar material.

TABLE G5c. EFFECT OF IRRADIATION ON THE THERMAL RESISTIVITY OF BeO-UO_2 PRISMS[11]

Material	Density, g per cm^3	Fission Burnup, a/o	Irradiated/Unirradiated Resistivity Ratio[a]
BeO-2 w/o UO_2	2.78	0.53	4.75
		1.08	5.25
		1.86	5.92
	2.85	0.53	5.74
		1.08	6.04
		1.86	6.56
BeO-10 w/o UO_2	2.85	0.53	4.14
		1.08	4.65
		1.86	5.66
	3.01	1.08	5.54
		1.86	6.16

(a) All values are averages of several runs, usually on two irradiated and two similar unirradiated prisms.

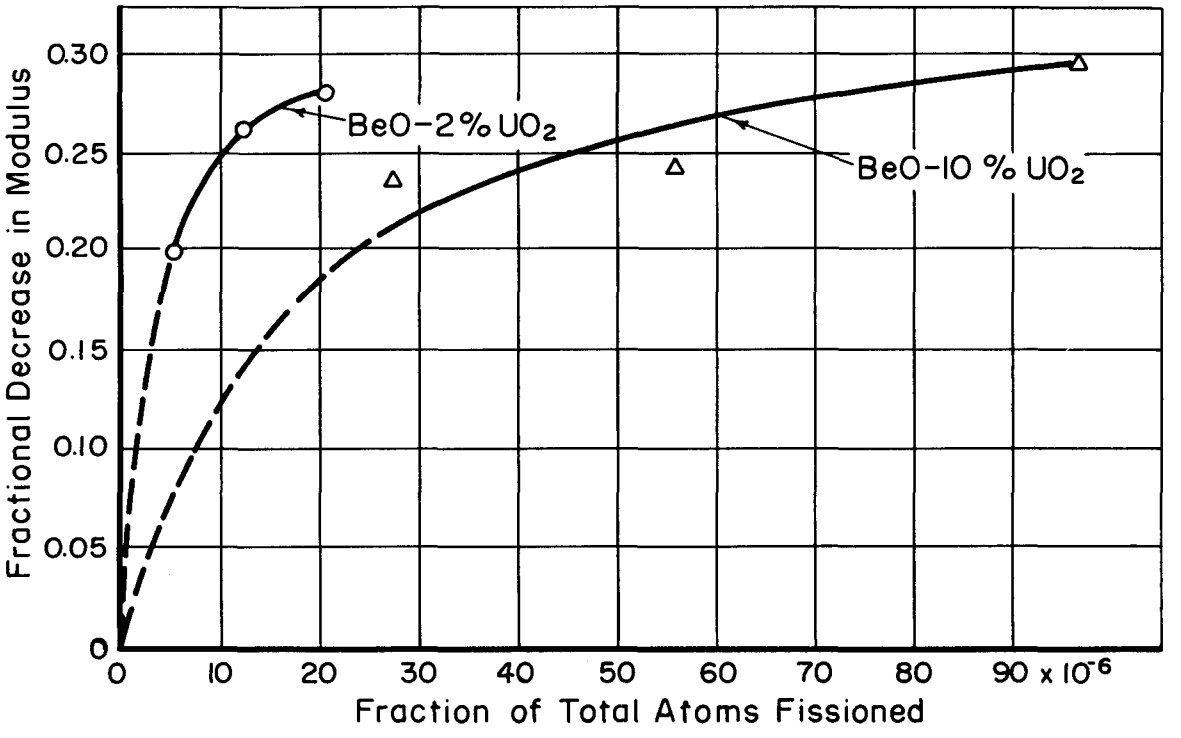

FIGURE G5a. EFFECT OF PILE IRRADIATION ON THE ELASTIC MODULUS OF BeO-UO COMPACTS[11]

AEA-43231

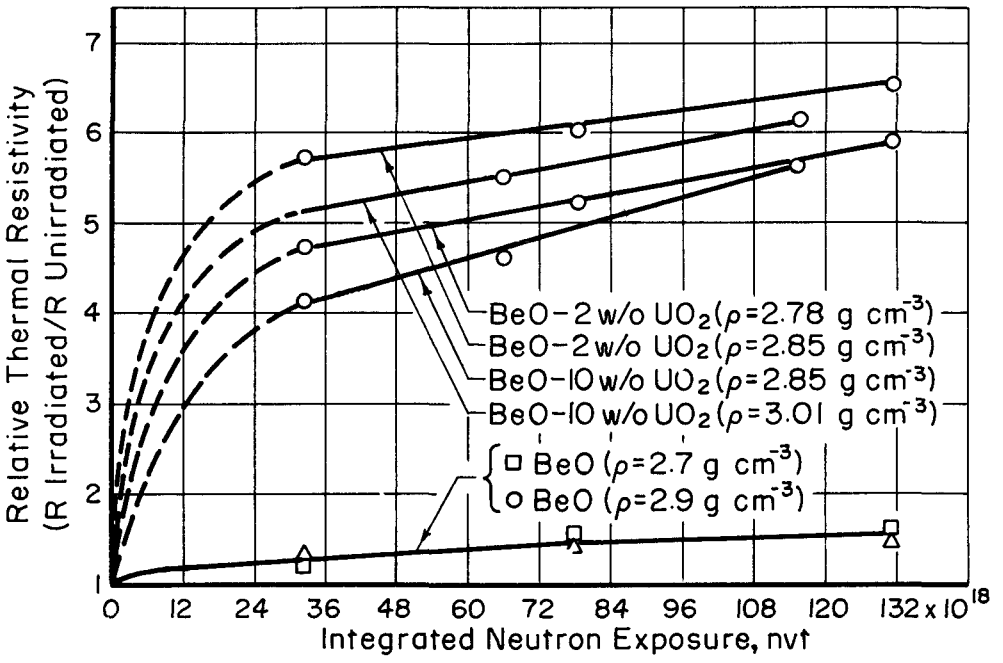

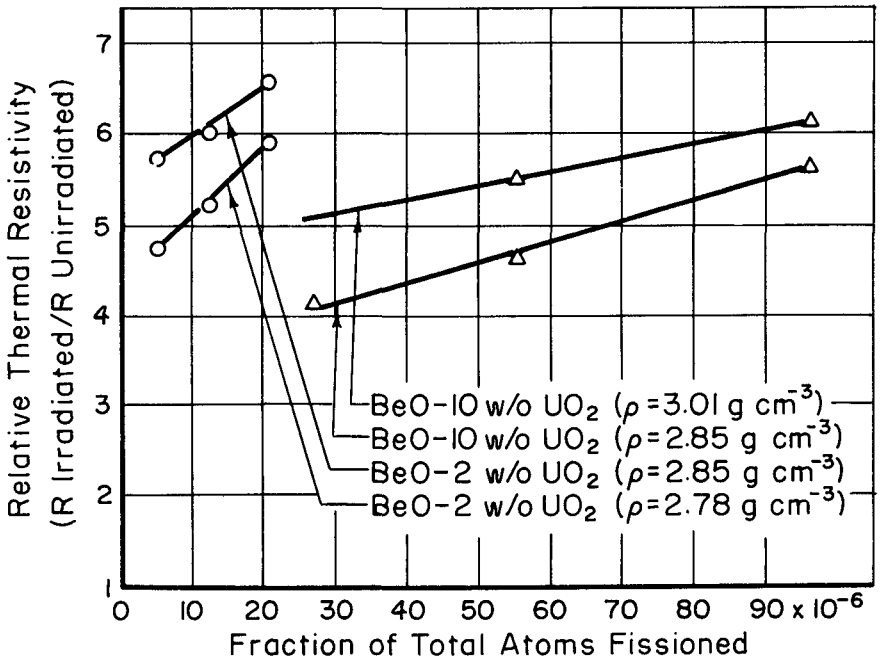

FIGURE G5b. EFFECT OF PILE IRRADIATION ON THE RELATIVE THERMAL RESISTIVITY OF BeO-UO_2 COMPACTS[11]

H. References

(1) Budnikov, P. P., Tresvyatsky, S. G , and Kushakovsky, V. I., "Binary Phase Diagrams for UO_2-Al_2O_3, UO_2-BeO, and UO_2-MgO", Proceedings of the Second United Nations International Conference on the Peaceful Uses of Atomic Energy, Geneva (1958), A/Conf. 15/P/2193, Vol 6, p 125.

(2) Ward, J. F., and Funk, C. W., "Proceedings of the Beryllium Oxide Meeting Held at Oak Ridge National Laboratory, Oak Ridge Tennessee, December 1-2, 1960", TID-7602 (Pt. 1), (1960).

(3) Bisson, A., and Frisby, H., "Electron Microscope Observation of Porosities, Carbon Inclusions, and Dislocations in Beryllium Oxide Sintered Under Load", J. Nuclear Materials, 4 (2), 133 (1961).

(4) McCreight, L. R., "Thermal Expansion Measurement of Six Fuel Materials", KAPL-M-LRM-7 (1952, Declassified 1957).

(5) "Gas-Cooled Reactor Project, Quarterly Progress Report for Period Ending December 31, 1960", ORNL-3049 (1961).

(6) "Gas-Cooled Reactor Project, Quarterly Progress Report for Period Ending March 31, 1961", ORNL-3102 (1961).

(7) Rothman A. J., "Beryllium Oxide – It's Properties and Applications in Nuclear Reactors", UCRL-6502-T (1961).

(8) Kida, K., Nishigaki, S., and Ueda, R., "A Study of the Fabrication of BeO-UO_2 by Means of Vacuum Hot Pressing", NP-Tr-804 (1961).

(9) Johnson, D. E., and Tobin, J. M., "Proceedings of the Beryllium Oxide Meeting Held at Oak Ridge National Laboratory, Oak Ridge, Tennessee, December 1-2, 1960", TID-7602 (Part 1).

(10) Johnson, D. E., "Stability of BeO-UO_2 Reactor Fuel Materials During Irradiation", GA-2065 (1961).

(11) Gilbreath, J. R., and Simpson, O. C., "The Effect of Reactor Irradiation on the Physical Properties of Beryllium Oxide", Proceedings of the Second United Nations International Conference on the Peaceful Uses of Atomic Energy, Geneva (1958), A/Conf. 15/P/621, Vol 5, p 367.

(12) Johnson, D. E., and Tobin, J. M., "Nuclear Reactor Chemistry, First Conference, Gatlinburg, Tennessee", October 12-14, 1960, TID-7610.

(13) Goldsmith, A., Waterman, T. E., and Hirshhorn, H. O., Handbook of Thermophysical Properties of Solid Materials, Macmillan Co., New York (1961), Vol 3.

(14) McKisson, R. L., "An Evaluation of the Beryllia-Water Vapor Reaction in an Open-Cycle Air Cooled Reactor", J. Nuclear Materials, 1, 196 (1959).

(15) Grossweiner, L. I., and Seifert, R. L., "The Reaction of Beryllium Oxide With Water Vapor", J. Am. Chem. Soc., 74, 2701 (1952).

(16) Berleman, M. G., and Simon, S. L., "The Volatilization of Beryllia in Water Vapor", ANL-4177 (1948).

(17) Elston, J., and Caillat, R., "Corrosion of BeO", Proceedings of the Second United Nations International Conference on the Peaceful Uses of Atomic Energy, Geneva (1958), A/Conf. 15/P/1147, Vol 5, p 334.

(18) Young, W. A., "The Reactions of Water Vapor With Beryllia and Beryllia-Alumina Compounds", NAA-SR-4446 (1960).

(19) Ohlinger, L. A., "Stability of Beryllium Oxide in Hydrogen at Elevated Temperatures in the Program on the Stability of Refractory Elements and Compounds in a Hydrogen Atmosphere at Elevated Temperatures", NEPA-598 (1948).

(20) Gates, J., "Proceedings of the Beryllium Oxide Meeting Held at Oak Ridge National Laboratory, Oak Ridge, Tennessee, December 1-2, 1960", TID-7602 (Part 1) (1960).

(21) "Gas-Cooled Reactor Program, Quarterly Progress Report for Period Ending December 31, 1961", ORNL-3254 (1961).

(22) Bleiberg, M. L., Yeniscavich, W., and Gray, R. G., "Effect of Burnup on Certain Ceramic Fuel Materials", WAPD-T-1274 (1961).

(23) Johnson, D. E., Koretzky, J., and Smalley, A. K., "Irradiation of BeO-UO_2 Ceramics", GA-2268 (1961).

(24) Freas, D. G., Saling, J. H., Sheets, H. D., Stang, J. H., Gates, J. E., and Dickerson, R. F., "A Study of the Radiation Stability of UO_2 Dispersions in BeO", BMI-1484 (1960).

(25) Saling, J. H., BMI Private Communication (1962).

(26) "Maritime Gas Cooled Reactor Program, Quarterly Progress Report for Period Ending December 31, 1959", GA-1195.

(27) Levy, A., and Foster, J. F., "The Compatibility of Gas Coolants and Ceramic Materials in Coated-Particle Nuclear Fuels", BMI-1530 (1961).

(28) Clarke, F. J. P., and Williams, J., "The Stability of BeO Under Reactor Conditions", AERE-M/M-229 (1959).

(29) Yeniscavich, W., and Bleiberg, M. L., "The Effect of Irradiation on BeO + UO_2, ThO_2 + UO_2, and ZrO_2 + CaO + UO_2", WAPD-BT-20 (1960).

UO_2-MgO DISPERSIONS

Compiled by R. A. Wullaert

Uranium dioxide and magnesium oxide form a limited region of solid solutions in air. The solid solutions have the UO_2 crystal structure and contain up to 37 mole per cent of MgO at temperatures of 1600 to 1750 C. The UO_2-MgO system is not a true condensed system, but some section of the triple UO_2-MgO-O system.[1] Thus the UO_2-MgO system does not give a true dispersion if the temperature is sufficiently high and the MgO becomes soluble in the UO_2.

The fission-gas release of 28.9 w/o $UO_{2.08}$-71.1 w/o MgO has been investigated.[2] Gas release was appreciable and nearly constant at temperatures up to 500 C, and increased sharply above 600 C. A "burst" release effect was observed, and was very marked at high temperatures. It was concluded that the dispersion was of little use in high-temperature gas-cooled reactor applications because of the high gas release.

References

(1) Budnikov, P. P., Tresvyatsky, S. G., and Kushakovsky, V. I., "Binary Phase Diagrams for UO_2-Al_2O_3, UO_2-BeO, and UO_2-MgO", Proceedings of the Second United Nations International Conference on the Peaceful Uses of Atomic Energy, Geneva (1958), A/Conf. 15/P/2193, Vol 6, p 125.

(2) Stubbs, T. J., Silver, P. J., and Webster, C. B., "The Release of Fission Product Rare Gases From Some Ceramic Materials", AERE-C/M-343 (1958).

UO_2/ThO_2-BeO DISPERSIONS

Compiled by R. A. Wullaert

One of the main purposes of a fuel dispersion is to provide a matrix material that will give greater radiation stability than that furnished by the dispersed fuel particles alone. Under irradiation, the matrix will restrain the swelling of the fuel particles and retain much of the fission gases released. The additional advantage of a UO_2/ThO_2-BeO dispersion is that the UO_2 is diluted by the ThO_2, and for a given burnup of uranium, the fissions per cm^3 in the UO_2/ThO_2 fuel particles are reduced. This is important because there is a critical number of fissions per cm^3 (depending on irradiation conditions) that will cause UO_2 to lose its crystal structure and thus its radiation stability.

There has been very little work done on UO_2/ThO_2-BeO dispersions. In general, the preirradiation properties are probably similar to UO_2-BeO dispersions, since the UO_2 particles are "replaced" by UO_2/ThO_2 particles.

The eutectics of the binary systems UO_2-BeO and ThO_2-BeO do not occur at the same temperature or relative composition, so the UO_2-ThO_2-BeO system will not show a true eutectic. However, since the binary eutectic temperatures and compositions are not very different, the UO_2-ThO_2-BeO system exhibits a quasibinary eutectic at 60 to 80 mole per cent BeO at approximately 2100 C. Therefore, the maximum operating temperature for this type of dispersion is 2100 C. UO_2 and ThO_2 form a complete series of solid solutions, thus providing dilution of the UO_2 fuel. (1)

A few irradiations of UO_2/ThO_2-BeO dispersions have been conducted. The irradiation conditions, dimensional changes, and fission-gas releases are listed in Table 1. Both the dimensional changes and fission-gas release are quite small.

TABLE 1. DIMENSIONAL STABILITY AND GAS RELEASE OF IRRADIATED UO_2/ThO_2-BeO

Composition, w/o			Estimated Fuel Temperature,	Uranium	Diameter Change,	Fission-Gas Release,		
UO_2	ThO_2	BeO	C	Burnup, a/o	per cent	per cent	Comments	References
25.4	35.5	39.1	800-1,100	7.1-10.1	+0.6	0.3 (Kr^{85})	< 5-μ-size UO_2	(2)
			800-1,100	7.1-10.1	+1.5[a]	--		(2)
2.57	7.3	90.1	610	13.0	+0.25	0.25	100 to 185-μ UO_2-ThO_2	(3)
3.67	10.4	85.9	610	13.4	+0.15	0.1		(3)
3.67	10.4	85.9	600	11.8	+0.29	0.1	< 10-μ UO_2-ThO_2	
6.43	18.3	75.3	650	13.0	+0.15	0.15	100 to 185-μ UO_2-ThO_2	(3)
7.34	6.8	85.9	690	11.8	+0.26	0.1	--	(3)
11.5	2.7	85.8	670	9.4	+0.25	0.25	--	(3)
14.8	42.0	43.2	750	9.4	+0.15	0.3	--	(3)
16.3	29.3	60.4	620	11.7	+0.21	0.35	--	(3)

(a) Irradiated in air.

References

(1) Reeve, K. D., "An Exploratory Study of the BeO-UO_2-ThO_2 System", AERE-M/R-2727 (1958).

(2) "Gas-Cooled Reactor Program, Quarterly Progress Report for Period Ending December 31, 1961", ORNL-3254 (1961).

(3) Hickman, B. S., and Hilditch, R. J., AAEC, "The Irradiation Behavior of Beryllium Oxide Based Dispersion Fuels", To Be Published.

DISPERSIONS OF UNCOATED FUEL IN GRAPHITE

Compiled by M. C. Brockway, and A. B. Tripler

A1. Chemical composition

Property data versus uranium content are given in succeeding sections for fuel loadings up to 50 w/o uranium as either UO_2 or UC_2.

3. Effect of impurities

a. Graphite is not a single material but a family of materials whose properties may vary broadly depending on choice of production materials and processing. The properties of fueled graphite depend also on the form of dispersed fuel and the loadings. Thus, no single set of properties can be representative of graphite matrix fuel dispersions in general.

b. Impurity content of graphite (carbon) matrices is strongly dependent upon the maximum process temperature as shown in Tables A3a and A3b.

TABLE A3a. TYPICAL TRACE IMPURITY CONTENTS OF FUELED GRAPHITE[1]

Element	Impurity Content[a][b], ppm	
	2800 C Graphitization	1400 C Bake
Iron	20	200
Boron	1	2
Silicon	<0.5	120
Magnesium	<0.01	20
Copper	<0.05	20
Aluminum	<0.1	10
Titanium	1	10
Vanadium	<1	60
Silver	<0.01	1
Calcium	5	50
Sodium	2	5
Potassium	20	25
Chromium	<3	4
Manganese	<1	40
Nickel	<1	200

(a) Other elements if present were less than the following minimum detectable concentration (ppm): Pb(<1), Zn(<1), As(<30), Sn(<1), Zr(<3), Sb(<1), Bi(<1), P(<30), Co(<3), Mo(<3), and Ba(<1).

(b) Data were obtained from fueled graphite containing 5 w/o UO_2 spheroids processed to the maximum indicated temperatures. Final fuel form for the 1400 C bake was UO_2; for the 2800 C graphitization, UC_2.

TABLE A3b. HYDROGEN CONTENT OF FUELED GRAPHITE AS RELATED TO MAXIMUM HEAT TREATMENT[1]

Maximum Baking[a] Temperature, C	Hydrogen Content, ppm		
	Average	Maximum	Minimum
700	6200	6370	6080
1000	1030	1110	840
1400	230	300	200
1800	25	30	10
2200	56	110	20
2400	98	150	50
2800	68	170	10

(a) Fueled graphite was prepared by addition of ceramic-grade UO_2 to a carbonaceous mix which was then formed and baked to the maximum indicated temperature. The considerable range of hydrogen content found for temperatures between 1800 and 2800 C correlated with the extent of fueled-compact exposure to the atmosphere between heat treatment and analysis. The lower values should be attainable by thorough protection of the carbide fuel from hydrolysis.

B1. Density (room temperature)[2]

See Table B1.

TABLE B1. ROOM-TEMPERATURE DENSITY AS RELATED TO FUEL LOADING IN UO_2-GRAPHITE AND UC_2-GRAPHITE COMPACTS[2]

UO_2-Graphite Compacts			UC_2-Graphite Compacts		
Uranium, w/o	Compact Density[a], g per cm^3	Fuel Content[c], g per cm^3	Uranium, w/o	Compact Density[b], g per cm^3	Fuel Content[c], g per cm^3
0	1.69	0	0	1.79	0
2.9	1.72	0.05	10	1.89	0.19
9.8	1.83	0.18	20	1.99	0.40
19	2.01	0.38	25	2.07	0.52
29	2.22	0.64	31	2.16	0.67
36	2.44	0.88	40	2.33	0.93
45	2.69	1.21	50	2.53	1.27

(a) Maximum bake temperature 1425 C.
(b) Maximum graphitization temperature 2800 C.
(c) Maximum theoretical fuel density based on U^{238}.

2. Density versus temperature

No data available

3. Uranium content

See Table B1.

4. Liquidus temperature

The upper operating limit of the fueled composite will be dependent on reaction of fuel phase with the graphite or on fuel migration. Studies at ORNL[3] showed the reaction between minus 60 plus 80-mesh UO_2 and graphite at pressures of 1×10^{-3} to 1×10^{-4} mm of mercury fit the rate equation,

$$x = kt^{1/2},$$

where x is the fraction of UO_2 converted to carbide, k is the temperature-dependent rate constant, and t is time in hours, at temperature. The values of k obtained were 0.18, 0.33, and 0.44 at 1275, 1325, and 1375 C, respectively. Comparison of these results with those obtained for minus 325-mesh UO_2, indicated that the reaction rate was insensitive to particle size below about 1325 C and relatively insensitive above this temperature.

6. Vapor pressure

No data available on fueled graphite.

7. Thermal expansion (linear)[1,2]

See Table B7a and Table B7b.

TABLE B7a. THERMAL EXPANSION VERSUS FUEL LOADING OF UO_2-GRAPHITE COMPACTS[2]

Uranium[a], w/o	Mean Thermal-Expansion Coefficient (25-600 C), 10^{-6} per C	
	With the Grain[b]	Across the Grain[b]
0	2.81	4.75
2.9	2.37	4.37
9.8	2.26	3.94
19	2.48	3.85
29	2.47	4.19
36	2.56	4.06
45	2.40	4.07

(a) Fueled compacts baked to 1425 C.

(b) "With the grain" and "across the grain" correspond to directions perpendicular and parallel, respectively, to the direction of applied force in molding the green compacts.

TABLE B7b. THERMAL EXPANSION VERSUS FUEL LOADING OF UC_2-GRAPHITE COMPACTS [1]

Uranium[a], w/o	Mean Thermal-Expansion Coefficient (25-540 C)[b], 10^{-6} per C	
	With the Grain	Across the Grain
0	3.06	4.54
2.9	3.06	4.85
9.8	3.50	5.48
20	3.44	5.11
31	3.58	5.09
40	3.92	5.70
50	5.01	8.34[c]

(a) Maximum graphitization temperature, 2350 C.
(b) Measured in vacuo (~4 x 10^{-5} mm of mercury), or in purified helium.
(c) Doubtful value, slight oxidation of UC_2 fuel may have occurred in this case.

C1. Hardness (room temperature)

No data for fueled graphite

3. Ultimate tensile strength

a. Room-temperature flexural (bend) strength values are shown in Tables C3a(1) and C3a(2)

TABLE C3a(1). FLEXURAL STRENGTH VERSUS FUEL LOADING OF UO_2-GRAPHITE COMPACTS [2]

Uranium[a], w/o	Flexural Strength[b], psi	
	With the Grain	Across the Grain
0	10,200	6,340
2.9	12,000	7,560
9.8	9,450	6,600
19	7,600	6,160
29	9,740	6,940
36	8,490	5,550
45	6,830	4,890

(a) Fueled compacts baked to 1425 C.
(b) The strength data were determined using single-point loading at a rate of 42 lb per min with a 0.625-in. span.

TABLE C3a(2). FLEXURAL STRENGTH VERSUS FUEL LOADING OF UC_2-GRAPHITE COMPACTS [2]

Uranium[a], w/o	Flexural Strength[b], psi	
	With the Grain	Across the Grain
0	8090	5900
10	5670	4060
20	4350	2840
25	3790	2670
31	3430	2790
40	3230	2270
50	2240	2080

(a) Fueled compacts baked to 2800 C.
(b) The strength data were determined using single-point loading at a rate of 42 lb per min with a 0.625-in. span.

b. Elevated-temperature tensile strength data have been reported by Wagner[4] for an unfueled experimental grade, CK, three fueled grades (fuel added to the base CK grade), LDH, LDC, LDP, and a commercial unfueled grade, H4LM. Figure C3 presents these data.

4. Yield strength

No data available

5. Compressive strength[5]

See Tables C5a and C5b.

TABLE C5a. COMPRESSIVE STRENGTH VERSUS FUEL LOADING OF URANIUM CARBIDE-GRAPHITE COMPACTS [5]

Uranium, w/o	Compressive Strength[a], psi
0	10,070
3.9	9,060
11.7	8,300
20.8	5,570
23.7	5,520
30.3	5,940

(a) Compacts baked to 2800 C. Strength was probably measured against the grain but reference is not specific.

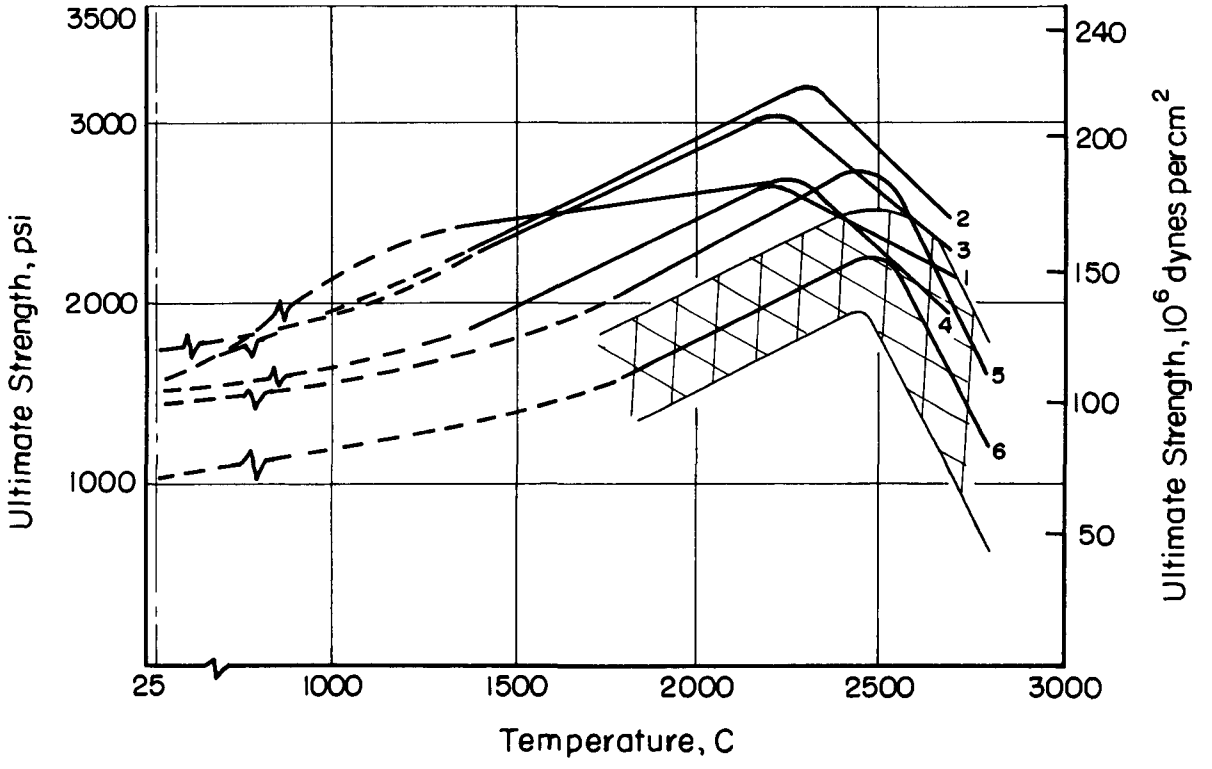

FIGURE C3. GRAPHITE ULTIMATE TENSILE STRENGTH AS A FUNCTION OF TEMPERATURE[4]

1 CK
2 LDH ($\frac{1}{8}$ g per cm^3 U)
3 LDC ($\frac{1}{4}$ g per cm^3 U)
4 LDP (0.35 g per cm^3 U)
5 H4LM
6 H4LM (perpendicular to grain, all others parallel)

AEA-43226

TABLE C5b. COMPRESSIVE STRENGTH VERSUS FUEL LOADING OF URANIUM OXIDE-GRAPHITE COMPACTS [5]

Uranium, w/o	Compressive Strength[a], psi
0	15,800
3.8	18,600
11.7	18,990
19.9	14,100

(a) Compacts baked to 1450 C. Strength was probably measured against the grain.

6. Creep strength

a. The creep of carbon (graphite) bodies depends not only on the stress applied and the temperature, but also on the previous thermal history of the material, and the form of carbon from which the body was made. In the case of fueled graphite, the effect of fuel loading is added.

b. Wagner[4] has published high-temperature creep data for both fueled and unfueled graphites. Under constant temperature and stress, two types of compressive-creep curves were observed. Type A consisted of an initial rapid creep, a second-stage "steady state", and an accelerated third stage terminating in fracture. Type B exhibited a rapid initial creep followed by a "steady-state" second stage extending to fracture. Type B was most commonly observed, and an approximate correlation of the "steady-state" region of the compressive-creep curves was obtained by the empirical equation:

$$\frac{d\epsilon}{dt} = \dot{\epsilon} = K(\sigma/\sigma_B) \exp n_e - E_a/RT, \qquad \text{(Equation 1)}$$

where $\dot{\epsilon}$ is negative in compression and

ϵ = steady-state (second-stage) creep rate, sec^{-1}

K,n = empirical constants, K in sec^{-1}

σ = stress applied to produce $\dot{\epsilon}$, dynes per cm^2

σ_B = stress required to produce failure of the particular sample being tested, dynes per cm^2

E_a = activation energy, cal per mole

R = universal gas constant, cal/(mole)(C)

T = temperature, K.

All the Type B data (failure without third-stage creep) were correlated by a single set of constants. The final working equation was

$$\dot{\epsilon} = -40\ (\sigma/\sigma_B)\ \exp\ 3.8_e - 50{,}000/RT.$$

Creep data for five types of graphite reported by Wagner are given in Table C6b(1).

TABLE C6b(1). SUMMARY OF STEADY-STATE CREEP RATES OF GRAPHITE IN COMPRESSION. COMPARISON OF EXPERIMENTAL CREEP RATES AND CREEP RATES CALCULATED BY EQUATION 1 [4]

Sample	Graphite Type	Grain Orientation	Temperature, K	$\frac{\sigma}{\sigma_B}$	Creep Rate, $\dot{\epsilon}$, 10^{-5} per Sec	
					Measured	Calculated[a]
1	H4LM[b]	Parallel	2270	0.67	-0.89	-0.60
				0.81	-0.89	-1.1
2	H4LM	Parallel	2530	0.78	-4.9	-3.3
				0.86	-5.2	-4.8
3	H4LM	Perpendicular	2570	0.70	-1.2	-2.5
			2570	0.78	-2.3	-3.8
4	CK-57[c]	Parallel	2400	0.80	-2.3	-2.1
				0.93	-3.1	-3.7
				1.00	-4.3	-4.9
5	CK-56	Parallel	2760	0.84	-5.2	-9.8
6	CK-56	Parallel	2760	1.00	-25.	-19.
7	LDH-10[d]	Parallel	2280	0.75	-1.3	-0.96
				0.91	-5.8	-2.0
8	LDH-10	Parallel	2560	1.00	-3.2	-9.5
9	LDH-10	Parallel	2750	0.76	-3.9	-6.6
				0.90	-11.	-12.5
10	LDH-12	Parallel	2760	1.00	-19.	-19.
11	LDH-12	Parallel	2760	0.78	-9.2	-7.4
12	LDC-16[e]	Parallel	2430	0.61	-0.80	-0.86
				0.70	-1.4	-1.4
				0.90	-18.	-3.8
13	LDC-15	Parallel	2570	1.00	-9.5	-9.8
14	LDC-15	Parallel	2720	0.83	-8.2	-8.3

(a) Calculated by Equation 1 (see C6b in text).
(b) An unfueled commercial grade of graphite.
(c) CK is unfueled experimental graphite.
(d) LDH is CK-type graphite fueled with 125 mg of uranium per cm^3 of carbon.
(e) LDC is CK-type graphite fueled with 250 mg of uranium per cm^3 of carbon.

In the case of tensile creep, the rate was found to depend upon the uranium content in addition to the other variables. The empirical equation used to correlate the "steady-state" region of these creep curves was

$$\dot{\epsilon} = f(U)\ K(\sigma/\sigma_B)\ \exp\ n_e - E_a/RT\ .$$

Within the conditions studied, f(U) took the form

$$f(U) = a + bU + CU^2\ .$$

Inserting the empirically determined constants, the correlation for "steady-state" tensile creep was:

$$\epsilon = (4 + 80U - 125U^2)\,(\sigma/\sigma_B)\exp 3.8_e - 69{,}000/RT\,. \quad \text{(Equation 2)}$$

Table C6b(2) lists creep data obtained for four unfueled and three fueled graphites.

Green[6] has published creep data for the same types of fueled graphites at stress levels of 1630, 2130, or 2540 psi, and temperatures of 2000, 2200, and 2400 C. These data were not correlated by an empirical equation.

7. Young's modulus

No data available

8. Shear modulus

No data available

9. Bulk modulus

No data available

10. Poisson's ratio

No data available

TABLE C6b(2). SUMMARY OF STEADY-STATE CREEP RATES OF GRAPHITE IN TENSION AND COMPARISON OF C6b EXPERIMENTAL CREEP RATES AND CREEP RATES CALCULATED BY EQUATION 2[4]

Sample	Graphite Type	Grain Orientation	Temperature, K	$\frac{\sigma}{\sigma_B}$	Creep Rate, $\dot{\epsilon}$, 10^{-5} per Sec	
					Measured	Calculated[a]
1	H4LM[b]	Parallel	2270	0.73	0.13	0.27
2	H4LM	Parallel	2380	0.77	0.18	0.70
3	H4LM	Perpendicular	2730	0.82	0.36	0.42
4	H4LM	Parallel	2770	0.77	0.16	0.57
5	H4LM	Parallel	2770	1.0	1.2	1.5
6	H4LM	Parallel	2800	0.83	1.0	0.81
7	H4LM	Parallel	3270	0.55	1.5	1.0
8	H4LM	Perpendicular	3270	0.75	2.3	3.4
9	CK-68[c]	Parallel	2360	0.80	0.06	0.07
				0.94	0.12	0.13
10	LDH-19[d]	Parallel	2350	0.76	0.13	0.16
				0.90	0.35	0.32
11	LDC-38[e]	Parallel	2350	0.64	0.12	0.10
				0.79	0.21	0.22
				0.93	0.34	0.41
12	LDP-41[f]	Parallel	2350	0.73	0.11	0.13
				0.84	0.13	0.22
				1.0	0.27	0.43
13	CK-68	Parallel	2700	0.63	0.39	0.19
				0.84	0.66	0.57
				0.98	0.90	1.0
14	LDH-19	Parallel	2680	0.56	0.46	0.35
				0.75	0.57	1.0
				0.88	0.83	1.8
				1.0	1.1	3.0
15	LDC-38	Parallel	2730	0.54	0.51	0.41
				0.62	0.86	0.71
				0.74	1.6	1.4
				0.82	2.3	2.1
				1.0	5.4	4.3
16	LDP-41	Parallel	2700	0.75	0.62	1.0
				0.81	0.79	1.4
				0.97	1.7	3.0
17	ATJ[b]	Parallel	2770	0.68	1.2	0.35
18	ATJ	Perpendicular	2770	0.68	1.5	0.35
19	ATJ	Parallel	2770	0.74	3.4	0.46
20	CS-312[b]	Parallel	2270	0.81	0.024	0.042
21	CS-312	Parallel	3270	1.0	4.8	9.6
22	CS-312	Perpendicular	3270	0.89	5.5	6.4

(a) Calculated by Equation 2 (see C6b in text).
(b) H4LM, ATJ, and CS are three commercial grades of unfueled graphite.
(c) CK is an unfueled experimental grade.
(d) LDH is Grade CK fueled with 125 mg of uranium per cm^3 of carbon.
(e) LDC is Grade CK fueled with 250 mg of uranium per cm^3 of carbon.
(f) LDP is Grade CK fueled with 350 mg of uranium per cm^3 of carbon.

D1. Specific heat[3,7]

Data obtained for TREAT[3] urania fueled graphite indicate a linear relation between temperature and C_p over the temperature range 200 to 1000 C, as shown by the data in Table D1. This fueled graphite contained 0.211 w/o uranium. The dispersed fuel particles were 44 μ in diameter, and the maximum processing (bake) temperature was 900 C.

TABLE D1. SPECIFIC HEAT OF FUELED GRAPHITE[7]

Temperature, C	Specific Heat, cal/(g)(C)
205	0.304
315	0.331
425	0.358
540	0.385
650	0.412
760	0.439
870	0.466
980	0.493

2. Thermal conductivity[2,4,5]

a. Data for fueled graphite are shown in Tables D2a(1) and D2a(2).

TABLE D2a (1). THERMAL CONDUCTIVITY VERSUS FUEL CONTENT OF UO_2-GRAPHITE COMPACTS[2]

Uranium, w/o	Thermal Conductivity[a], cal/(sec)(cm)(C)	
	With the Grain	Across the Grain
0	0.0984	0.0740
2.9	0.0806	0.0521
9.8	0.0798	0.0529
19	0.0732	0.0521
29	0.0634	0.0500
36	0.0595	0.0430
45	0.0508	0.0351

(a) Compacts were baked to 1425 C. Room-temperature conductivity data are given.

TABLE D2a (2). THERMAL CONDUCTIVITY VERSUS FUEL LOADING OF URANIUM CARBIDE-GRAPHITE COMPACTS[5]

Uranium, w/o	Thermal Conductivity[a], cal/(sec)(cm)(C)
0	0.11
3.9	0.11
11.7	0.13
20.8	0.14
23.7	0.15

(a) Compacts were baked to 2800 C. Conductivity was measured against the grain at room temperature.

b. Wagner[4] has reported thermal conductivity as a function of temperature for two unfueled graphites (H4LM, a commercial graphite, and CK, an experimental grade), and for two fueled graphites (I DH containing 0.125 g of uranium per cm^3, LDC containing 0.250 g of uranium per cm^3). The data, as shown in Figure D2b, indicate apparent lack of dependence of conductivity on fuel loading for these fuels and loading levels.

E1. Electrical resistivity[2]

See Tables E1a and E1b.

TABLE E1a. ELECTRICAL RESISTIVITY VERSUS FUEL LOADING OF UO_2-GRAPHITE COMPACTS[2]

Uranium, w/o	Specific Resistance[a], microhm-cm	
	With the Grain	Across the Grain
0	2122	3006
2.9	2094	2912
9.8	2243	2807
19	2466	3051
29	2485	3392
36	2787	3640
45	3194	4220

(a) Compacts were baked to 1425 C. Room-temperature resistance data are given.

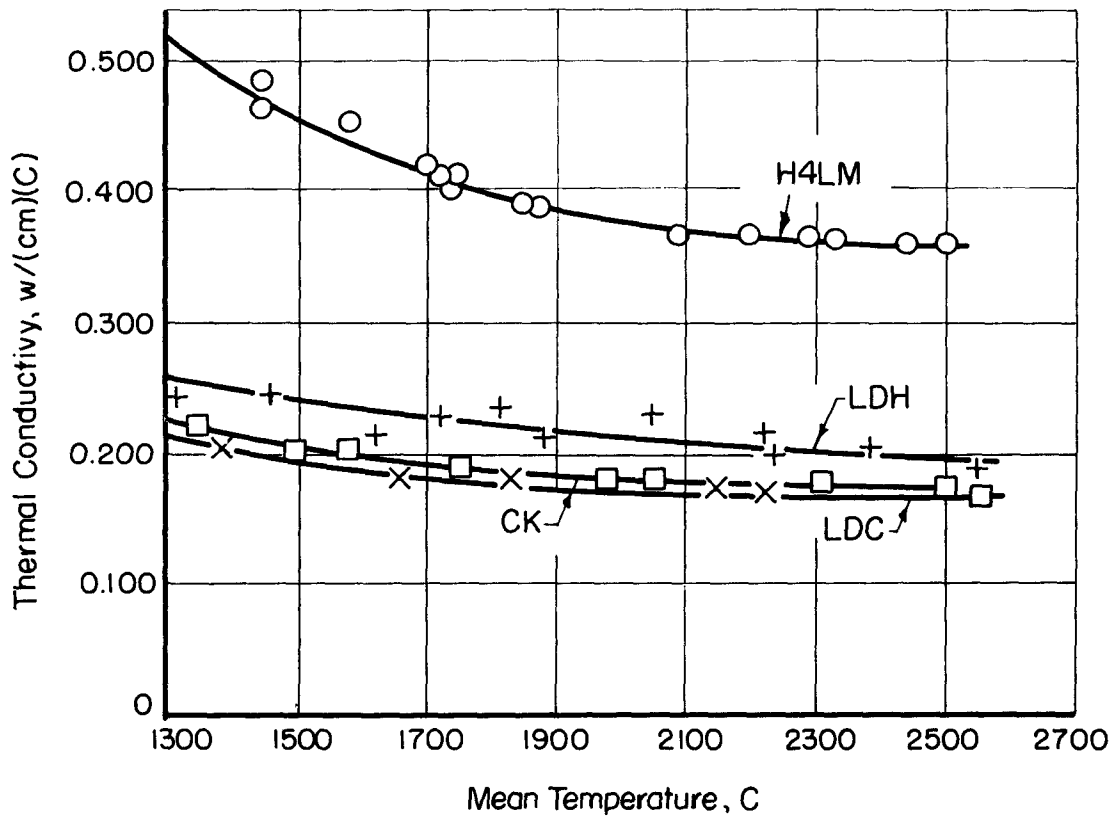

FIGURE D2b. THERMAL CONDUCTIVITY OF GRAPHITE PARALLEL TO GRAIN [4]

AEA-43255

TABLE E1b. ELECTRICAL RESISTIVITY VERSUS FUEL LOADING OF UC_2-GRAPHITE COMPACTS[2]

Uranium, w/o	Specific Resistance[a], microhm-cm	
	With the Grain	Across the Grain
0	1842	2960
10	1432	1971
20	840	1736
25	782	1443
31	531	892
40	437	682
50	463	670

(a) Compacts were baked to 2800 C. Data are for room-temperature resistance.

F1. Reactions with coolants (data are for unfueled graphite)

a. Steam[8,9]

(1) 2.8 volume per cent H_2O in helium using "fuel-element graphite":

(a) Minus 6.4 mg per cm^2 in 80 hr at 900 C

(b) Minus 20 mg per cm^2 in 80 hr at 1000 C

(2) Varying amounts of H_2O in helium under gamma irradiation using TSX graphite[9]

H_2O Concentration, ppm	Weight Loss, 10^{-7} g/g/hr	
	At 600 C	At 700 C
50	2.18	6.17
90	--	7.12
155	5.29	8.90
300	5.42	10.13

b. Helium

No data available

c. Carbon dioxide[10]

See Table F1c.

TABLE F1c. REACTION OF GRAPHITE WITH CARBON DIOXIDE FLOWING AT 1.5 FT^3 PER HR[10]

Geometry	Type of Graphite	Manufacturer	Temperature, C	Weight Loss, g/g/hr
		Thermal Experiments		
0.426-in.-diameter by 2-in.-high solid cylinder	CSF	NCC	650	1.09×10^{-5}
			700	$3.34 - 4.50 \times 10^{-5}$
			750	$1.24 - 2.09 \times 10^{-4}$
			825	9.21×10^{-4}
	GL-10	GLC	750	$6.24 \times 10^{-5} - 1.42 \times 10^{-4}$
	CO	NCC	750	$1.78 - 6.37 \times 10^{-4}$
	RX 1	NCC	750	5.03×10^{-4}
	RX 2	NCC	750	$2.75 - 2.82 \times 10^{-4}$
	RX 3	NCC	750	$2.83 - 2.84 \times 10^{-4}$
	SP22	SCC	750	1.02×10^{-4}
	SP28	SCC	750	7.72×10^{-5}
0.426-in.-OD, 0.250-in.-ID by 2-in.-high hollow cylinder	CSF	NCC	626	7.67×10^{-6}
			676	$1.83 - 1.97 \times 10^{-5}$
			726	$5.24 - 9.56 \times 10^{-5}$
			776	$1.93 - 3.39 \times 10^{-4}$
			826	5.04×10^{-4}
0.628-in.-diameter sphere	CSF	NCC	650	2.32×10^{-5}
			700	5.70×10^{-5}
			726	8.47×10^{-5}
			776	3.42×10^{-4}
			850	2.23×10^{-3}
		Microwave Experiments[a]		
	CSF	NCC	150	10^{-4} (1 in. from glow)
			150	10^{-2} (directly in glow)

(a) These data are included to indicate possibility of a very rapid reaction at higher temperature and with irradiation. Experiments were conducted at 125 W at 2450 megacylces in 1.5-cfh CO_2.

d. Nitrogen

No engineering data available

e. Hydrogen

No engineering data available

f. Liquid metals[11]

Dilation of TSP graphite parallel to extrusion axis after 500 hr, in 650 C sodium was 0.90 per cent. Reaction of graphite with 950 F sodium during 100 hr was as follows:

Graphite Type	Density g per cm^3	Dilation, per cent: Parallel to Extrusion Axis	Dilation, per cent: Perpendicular to Extrusion Axis
SA25	1.60	1.40	1.46
TSP	1.70	0.82	1.00
CCN	1.89	0.60	0.84

g. Air[12]

The threshold temperature (temperature at which 1 per cent loss occurs in 24 hr in stagnant air) for pure graphite is 540 C. At 700 C, the loss is 1 per cent in 35 min for pure graphite and 1 per cent in 10 min for commercial graphite.

2. Reactions with claddings or structural materials[13]

See Table F2.

TABLE F2. ELEVATED-TEMPERATURE REACTIONS OF GRAPHITE WITH SOME CLADDING AND STRUCTURAL METALS[13]

Metal	Exposure		Carbon, w/o		Ultimate Strength, 1000 psi		Elongation, per cent		Remarks
	Time, hr	Temperature, F	Before	After	Before	After	Before	After	
Zirconium	1000	1750	0.04	0.09	70.0	70.2	44.0	8.0	Metallographic examination showed negligible carburization
Zircaloy-2	1000	1750	0.01	0.06	101.0	89.8	28.0	22.0	Metallographic examination showed negligible carburization
Zirconium	1500	1850	0.04	0.40	70.0	53.0	44.0	32.0	Carburization case observed, 0.0015-in. average, 0.0023-in. maximum thickness
Zirconium (oxidized surface)	1500	1850	0.04	0.66	69.6	80.2	32.0	8.0	Carburization case observed, 0.0015-in. average, 0.0036-in. maximum thickness
Zirconium (oxidized surface)	1500	1850	0.04	0.78	69.6	76.8	32.0	6.0	Carburization case observed, 0.0010-in. average, 0.0013-in. maximum thickness
"A"Nickel	1500	1850	0.05	0.21	67.2	55.3	37.0	36.0	Metallographic examination showed no carburization case or second-phase carbon precipitation
"A"Nickel	1500	1850	0.05	0.18	69.2	64.3	37.0	36.0	Metallographic examination showed no carburization case or second-phase carbon precipitation
"K"Monel	1500	1850	0.16	0.17	99.4	89.3	44.0	52.0	Metallographic examination showed no carburization case or second-phase carbon precipitation
"K"Monel	1500	1850	0.16	0.18	99.4	95.5	44.0	52.0	Metallographic examination showed no carburization case or second-phase carbon precipitation

G1. Dimensional stability during irradiation[1,14-16]

a. Investigations defining the dimensional stability of a fueled graphite as a function of fission-fragment exposure, irradiation temperature, and fuel-particle type and size have not been published.

b. General Atomic has published high-burnup data for graphite fueled with $(Th,U)C_2$ (6.5 w/o uranium, 15.5 w/o thorium). These elements experienced a burnup equal to about 60 per cent of the HTGR design lifetime of 3 years, or 6.9×10^{19} fissions per cm^3. Dimensional stability of these is given in Table G1b. Increased matrix change produced by the greater fission-fragment damage to fuel of smaller particle size is evident.

TABLE G1b. DIMENSIONAL CHANGES OF FUEL COMPACTS IRRADIATED TO 6.9×10^{19} FISSIONS PER CM^3[15]

Compact	Fuel-Particle Size, μ	Average Temperature of Graphite Can, C	Fuel-Body Center-Line Temperature, Calculated C	Dimensional Changes, per cent	
				Diameter	Length
1	250-500	650-760	1200	0	+0.2
2	110-250	730-840	1300	-0.2	+0.2
3	<50	840-900	1400	-1.7	+2.2
4	<50	900-925	1480	-2.2	+3.0
5	110-250	760-840	1200	-0.3	<-0.1
6	250-500	700-790	1150	0	<+0.1

c. Data by ORNL[14] for similar fission levels but for different graphite matrices, fuels, and temperatures indicate greater dimensional change. Graphite compacts[1,16] containing 9.55 w/o uranium and baked to 2800 C were irradiated with a central fuel temperature of approximately 1850 C, dropping to a can-wall temperature of approximately 850 C. Burnup was 5.05×10^{19} fissions per cm^3. Dimensional changes of the specimens were -3.1 to -4.2 per cent on diameter, and +2.7 to +5.2 on length, or a bulk density change of +2.5 per cent.

2. Fission-gas-release data[17-19]

a. Fission-gas release from fueled graphite is dependent upon dispersed-fuel form (and particle size), temperature, and the physical properties of the matrix graphite.

b. Extensive data on xenon and krypton release from $(U,Th)C_2$-graphite fuel compacts have been reported by General Atomic. The steady-state release of these gases as a function of temperature and half-life were determined in out-of-pile photofissioning experiments. The results[17] are shown in Figures G2b(1) and G2b(2). Xenon-release data have also been obtained during heating of preirradiated fueled graphite.[18] Figure G2b(3) presents release data from fuel-impregnated graphite. Figure G2b(4) gives release from fueled elements prepared by different methods containing $(Th,U)C_2$ fuel. Release was obtained for broken as well as whole

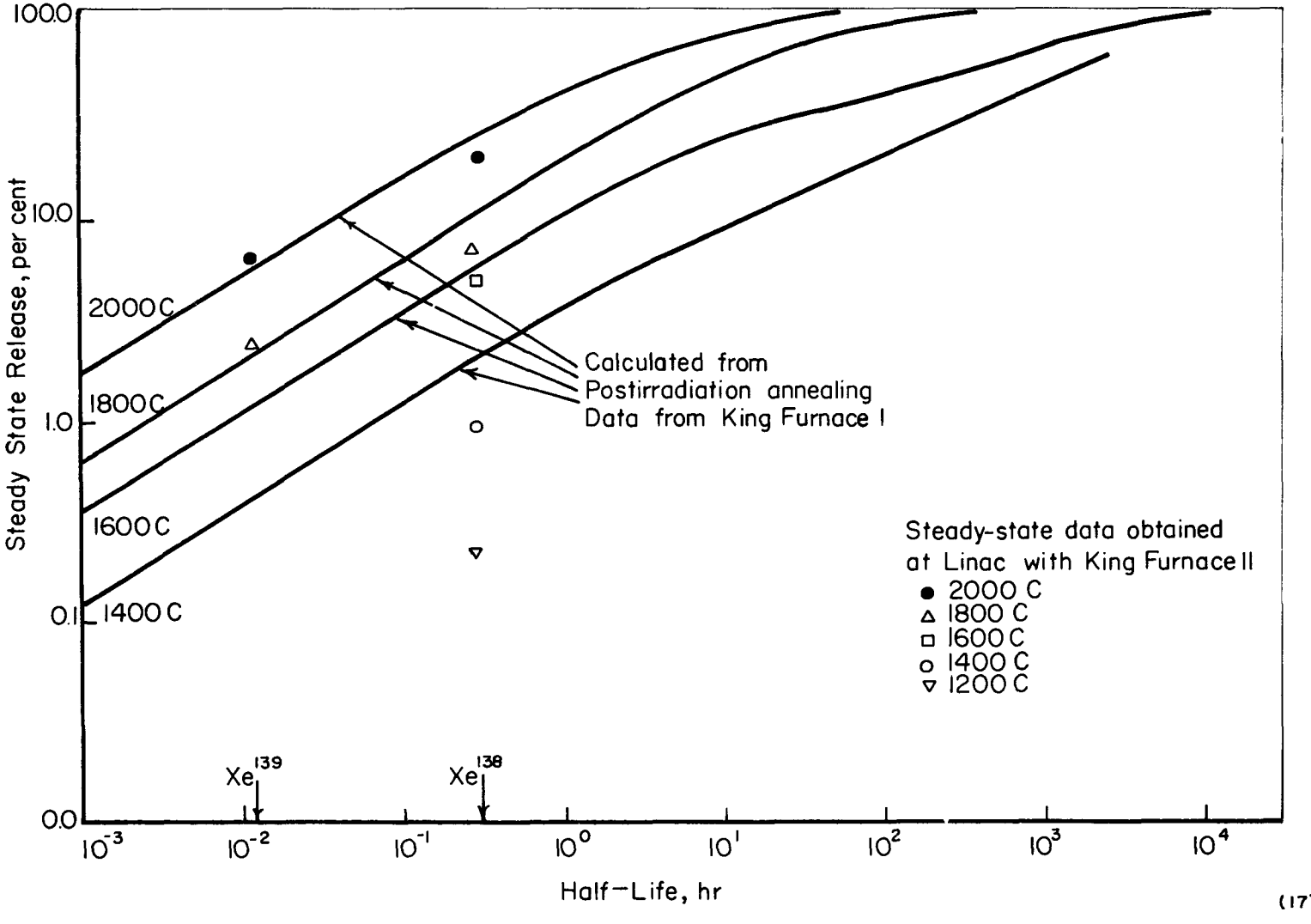

FIGURE G2b(1). XENON RELEASE FROM UNCOATED (U,Th) C_2 PARTICLES IN GRAPHITE-MATRIX FUEL BODIES[17]

AEA-43227

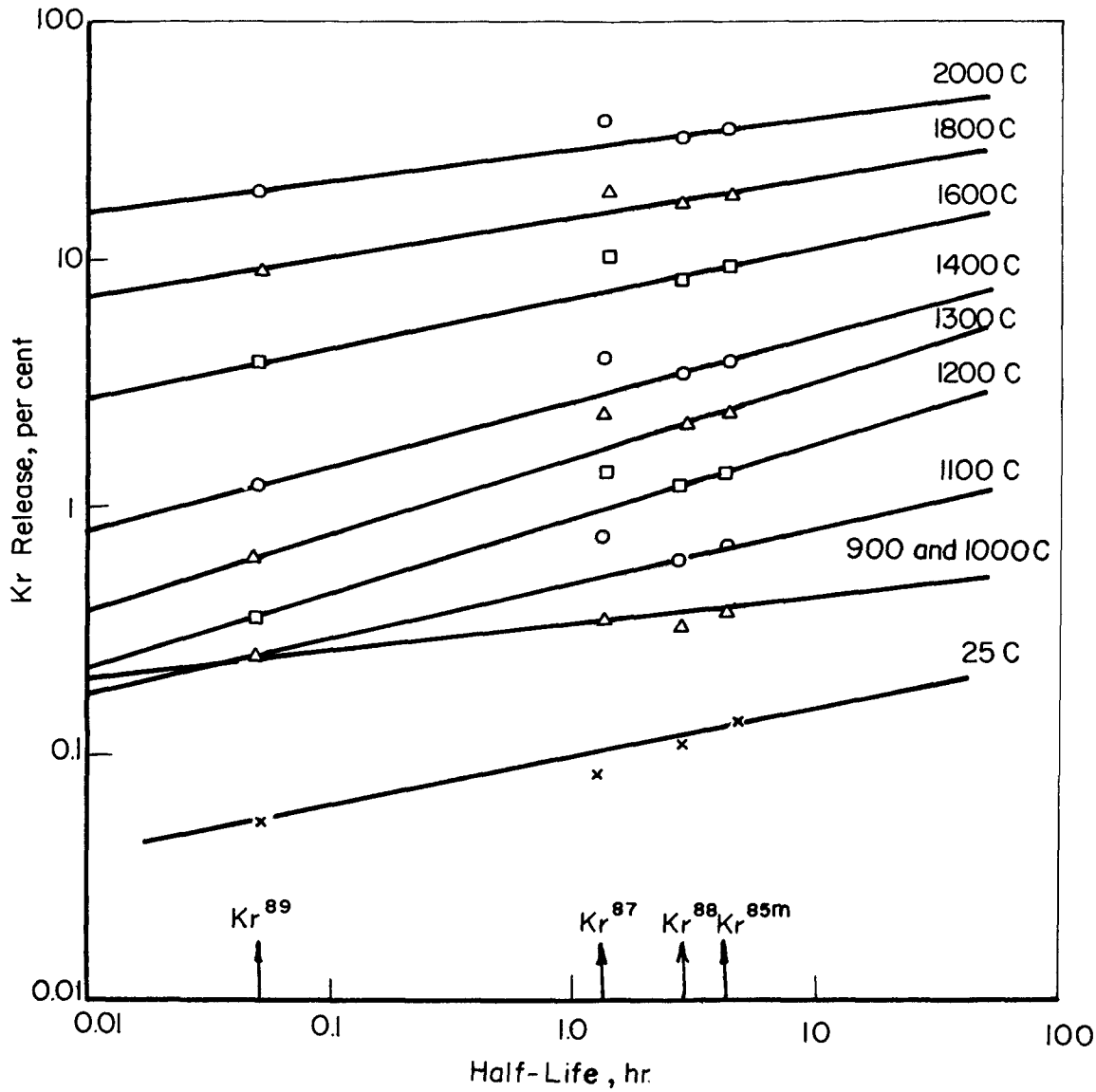

FIGURE G2b(2). STEADY STATE KRYPTON RELEASE FROM UNCOATED CARBIDE PARTICLES IN GRAPHITE-MATRIX FUEL BODIES[17]

AEA-43228

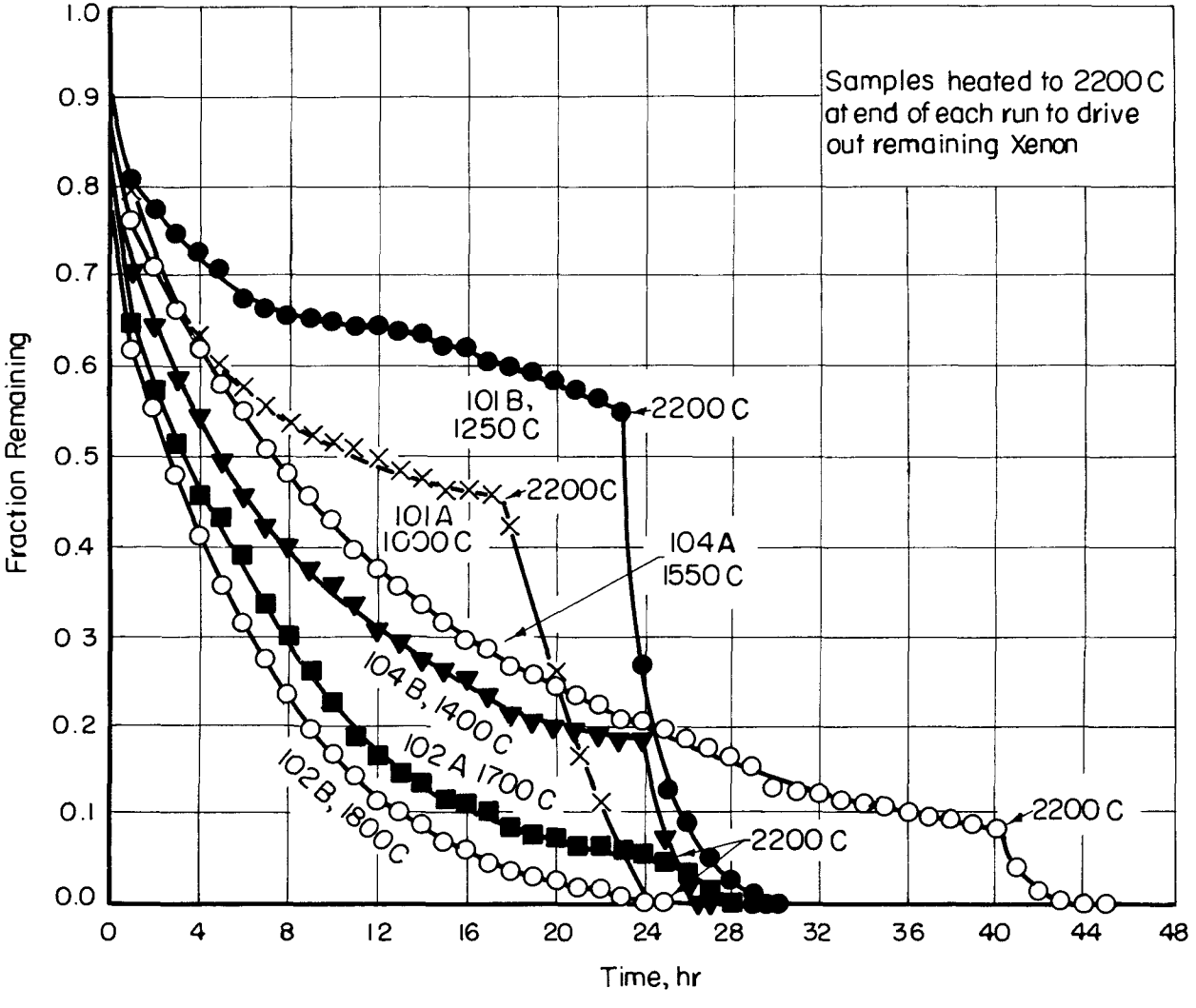

FIGURE G2b(3). Xe^{133} RELEASE FROM TURRET-TYPE UO_2-IMPREGNATED COMPACTS AT VARIOUS TEMPERATURES[18]

AEA-43229

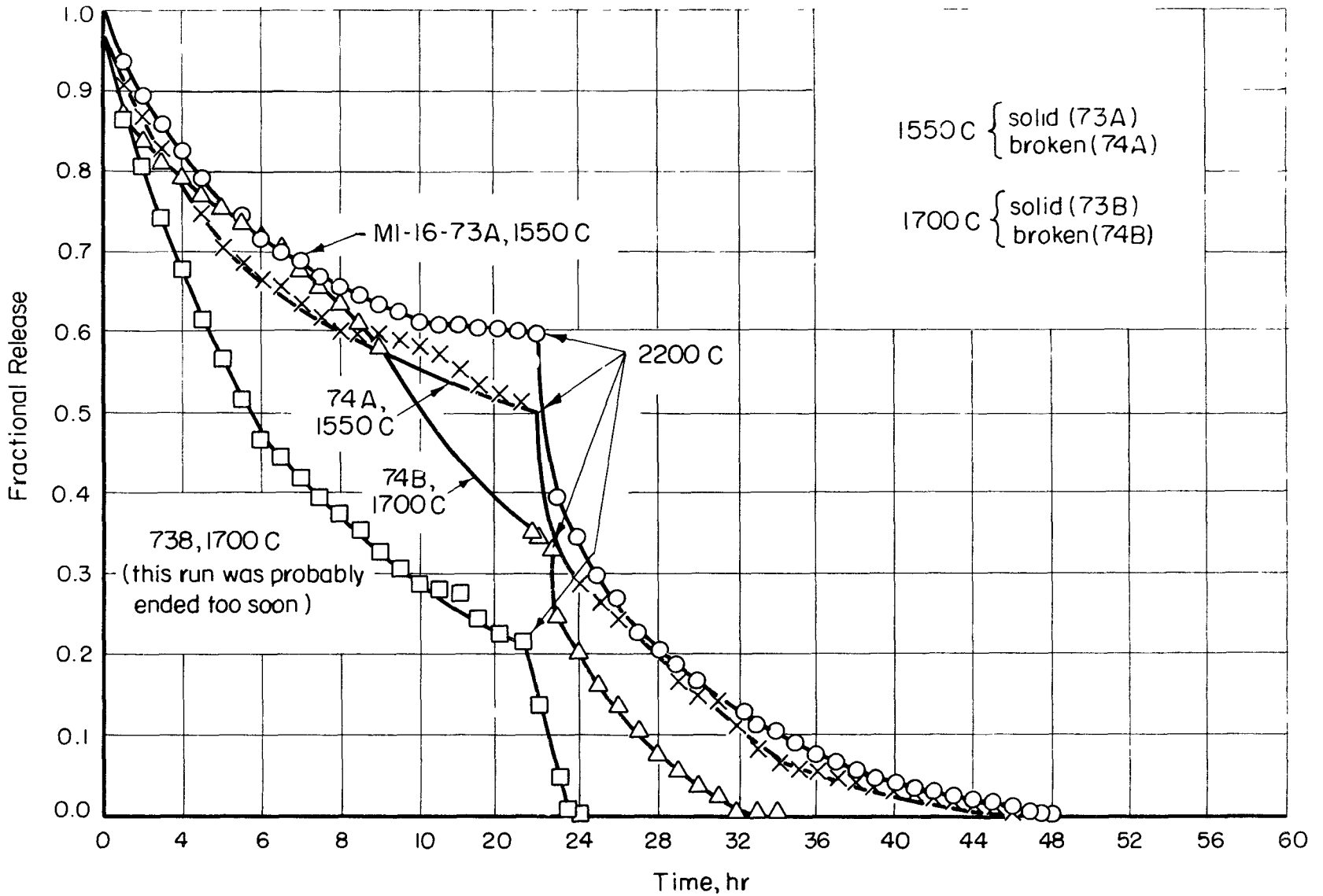

FIGURE G2b(4) XENON RELEASE FROM SOLID AND BROKEN FUEL COMPACTS AT 1550 AND 1700 C[18]

specimens to determine the effect of specimen size on release. No explanation was presented for the anomalous result of Specimen 74B (broken). Investigations by Cubicciotti[19] have indicated that the rate of xenon escape is independent of fueled-graphite sample size.

4. Unusual nuclear properties

No data available

5. Property changes as a result of irradiation

a. Durand, et al.,[20] and Hunter[21] have determined in-pile changes of the thermal conductivities of uranium-impregnated graphite as a function of exposure and temperature. Hunter found a ratio of K_o/K, where K_o is the preirradiation thermal conductivity, as high as 39 after an exposure of 6.3×10^{21} fissions per cm^3 at 780 C. Durand, et al., found less severe decreases in thermal conductivity at a comparable temperature and a ratio of K_o/K of only 1.3 after an exposure of 9.2×10^{21} fissions per cm^3 at 1300 C. Figure G5a, from Durand et al.,[20] compares data obtained by Hunter, Durand, et al. and Heterick et al.

b. The changes in properties of fueled graphites depend upon the percentage of fission fragments recoiling into the matrix, as well as upon temperature of irradiation and fuel burnup. Theoretical treatments[22] of the effect of fuel-particle size on fission-fragment damage have indicated that at a particle diameter of 100 μ the damage would be less than 5 per cent of the homogeneous case. Experimental studies[23,24] of radiation damage as a function of UO_2 fuel-particle size have been reported. Figure G5b illustrates the relative changes in electrical resistivity found for different UO_2 particle sizes after an integrated flux of 1.8 to 1.9×10^{18} nvt at maximum temperatures of 66 to 88 C and after pulse annealing for 1 hr at successive 25 C intervals.[5]. A subsequent anneal of these specimens at 425 C for 18 hr had little further effect on the resistivity. An additional 12-hr anneal at 725 C lowered the resistivity slightly.

II. References

(1) National Carbon Company, "Summary Report – Phase II, Graphite-Matrix Nuclear Fuel Elements", Newsletter No. 3, pp 54, 56, 66 (October 31, 1960).

(2) National Carbon Company, "Summary Report – Phase I, Graphite-Matrix Nuclear Fuel Elements", ORO-240, Vol. 1 (December 22, 1959), p 70.

(3) "Gas-Cooled Reactor Project Quarterly Progress Report", ORNL-3015 (November 11, 1960), p 75.

(4) Wagner, P., Driesner, A. R., and Kmetko, E. A., "Some Mechanical Properties of Graphite In the Temperature Range 20 to 3000°C", Proceedings of the Second United Nations International Conference on the Peaceful Uses of Atomic Energy, Geneva (1958), A/Conf. 15/P/702, Vol. 7, 379.

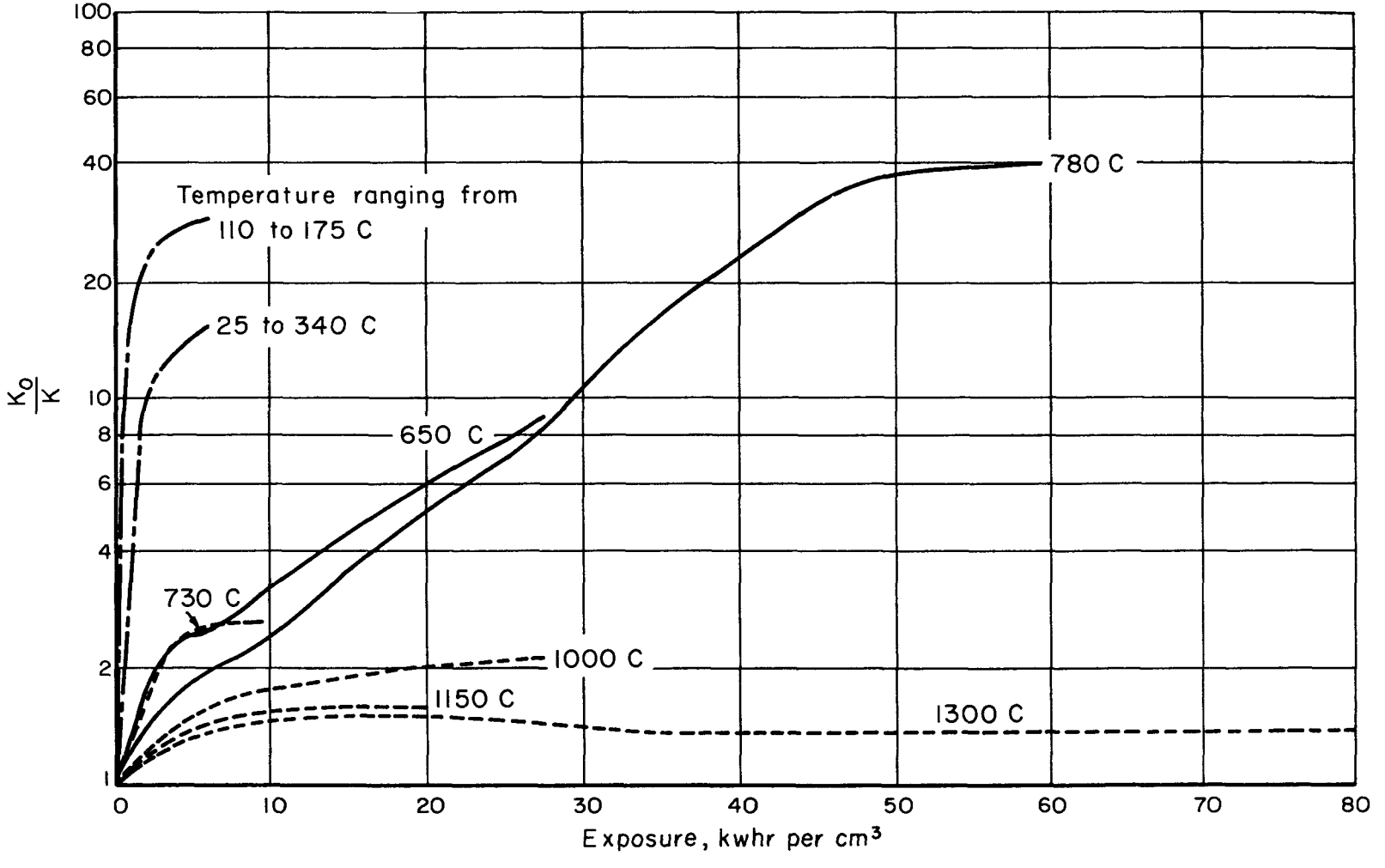

FIGURE G5a. IN-PILE THERMAL CONDUCTIVITY OF URANIUM-IMPREGNATED GRAPHITE AS MEASURED BY VARIOUS INVESTIGATORS AT DIFFERENT TEMPERATURE [20]

AEA-43224

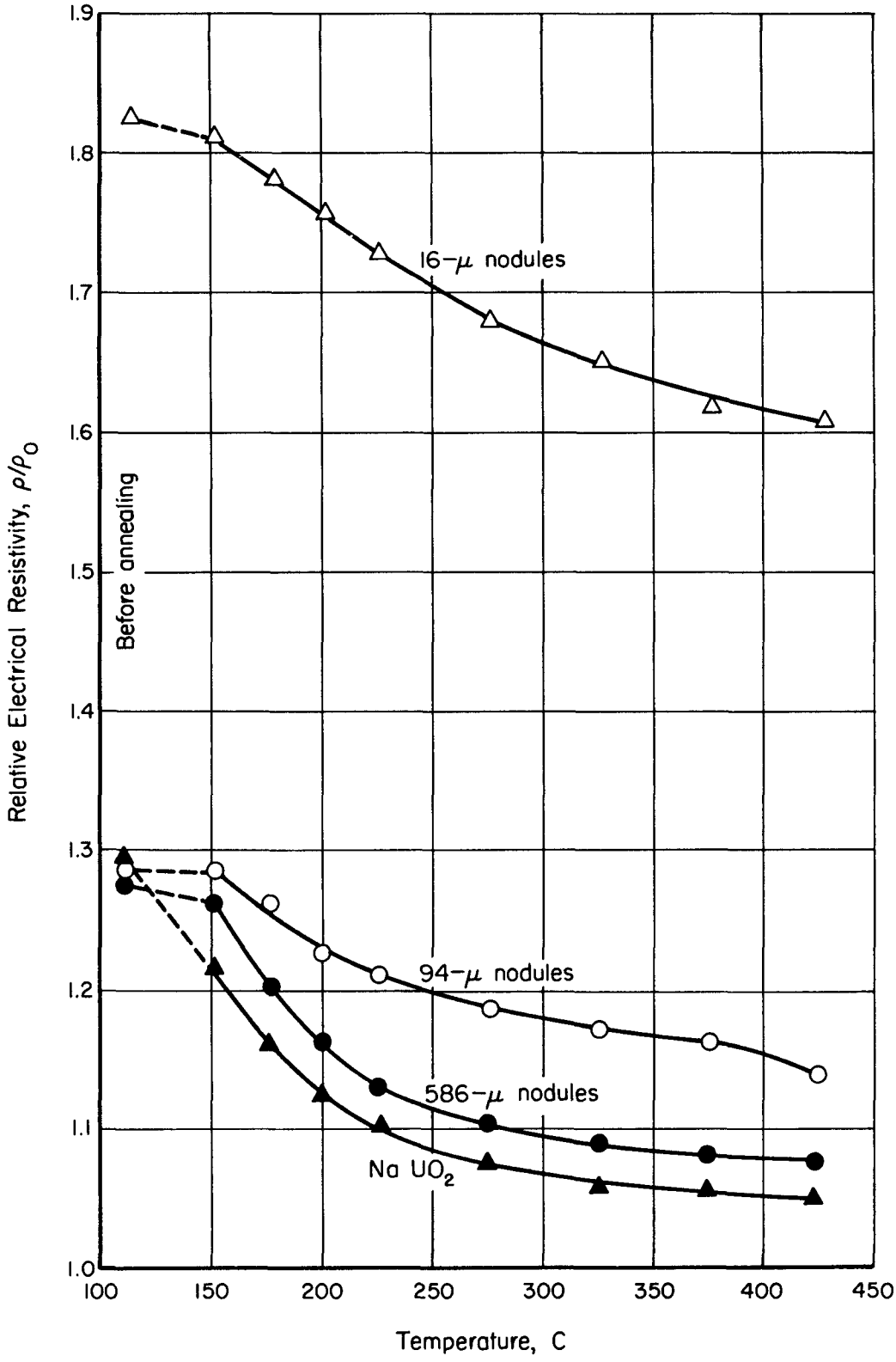

FIGURE G5b RADIATION—DAMAGE ANNEALING IN UO_2-GRAPHITE BODIES[5]

AEA-43232

(5) Eatherly, W. P., Janes, M., Mansfield, R. L., Bourdeau, R. A., and Meyer, R. A., "Physical Properties of Graphite Materials for Special Nuclear Applications", Proceedings of the Second United Nations International Conference on the Peaceful Uses of Atomic Energy, Geneva (1958), A/Conf. 15/P/708, Vol. 7, p 389.

(6) Green, L., Jr., Stehsel, M. L., and Waller, C. E., "Measurements of Mechanical Properties of Pure and Uranium-Loaded Graphites at Elevated Temperatures", AGC-1537 (December 23, 1958).

(7) Handwerk, J. H., and Lied, R. C., "The Manufacture of the Graphite-Urania Fuel Matrix for TREAT", ANL-5963 (January, 1960), p 21.

(8) Zumwalt, L. R., Burnette, R. D., and Riedinger, A. B., "Carbon Transport and Corrosion in High-Temperature Gas-Cooled Reactors", GA-2630 (April 12, 1962).

(9) Albaugh, F. W., "Reactor and Fuels Research and Development Operation", HW-72590A (January, 1962), p A38 (unclassified section).

(10) Clark, T. J., "Thermal and Microwave Oxidation of Various Reactor-Grade Graphites", TID-7597 (March 3, 1961), pp 207-228.

(11) Gill, J. J., "Sodium-Graphite Interactions and Graphite Protective Coatings", NAA-SR-6094 (May 1, 1961).

(12) Loch, L. D., "Graphite", Reactor Handbook, Vol I, Materials, 2nd Edition, Interscience Publishers, Inc., New York (1960), pp 893-894.

(13) Carpenter, R., and Del Grosso, A., "Army Gas-Cooled Reactor Systems Program Summary Report on Materials for the GCRE-II", IDO-28564 (December 30, 1960), p 54.

(14) "Gas-Cooled Reactor Project Quarterly Progress Report", ORNL-3102 (May 26, 1961), p 177-178.

(15) Goeddel, W. V., "The Development And Evaluation of Graphite-Matrix Fuel Compacts for the HTGR", GA-2289 (August 8, 1961).

(16) Morgan, J. G., "Irradiation Effects on UC_2 Dispersed in Graphite (ORNL-MTR-48-1), Interim Report No. 1., CF-60-6-78 (August 18, 1960).

(17) Anderson, E. E., "Steady-State Release Function of Krypton and Xenon Fission Products at High Temperatures From (U,Th)C_2-Graphite Fuel Matrix In Out-of-Pile Experiments, GA-3211 (June 15, 1962).

(18) "40-MW(E) Prototype High-Temperature Gas-Cooled Reactor Research and Development Program, Quarterly Progress Report for Period Ending September 30, 1960", GA-1774 (September 30, 1960).

(19) Cubicciotti, D., "The Diffusion of Xenon From Uranium-Carbide Impregnated Graphite at High Temperatures", NAA-SR-194 (October 13, 1952).

(20) Durand, R. E., Klein, D. J., and Nykiel, F. R., "Effect of Reactor Irradiation on the Thermal Conductivity of Uranium Impregnated Graphite at Elevated Temperatures", NAA-SR-836 (August 15, 1954).

(21) Hunter, L. P., "Effect of Fission Recoil Fragments on the Thermal Conductivity of Graphite", J. Appl. Phys., 30 (12), (December, 1959).

(22) Faris, F. E., "Uranium-Bearing Graphite for Fuel Elements", TID-2004, Reactor Sci. Technol., 2(4), 95-112 (1952).

(23) Loch, L. D., Slyh, J. A , and Duckworth, W H., "Studies of Graphite for Fuel Elements", BMI-954 (October 13, 1954).

(24) Kernohan, R. H., "Effect of Fissionable Particle Size on Fission Damage in Graphite", ORNL-1722 (July 14, 1954).

STAINLESS STEEL-UO_2 DISPERSION FUEL

Compiled by D. L. Keller and D. L. Stoltz

A1. Chemical composition

Stainless steel-UO_2 dispersion fuels containing 10 to 50 w/o UO_2 in the core have been fabricated successfully. Even higher loadings can be prepared but these are most generally called "cermet" fuels.

2. Phase diagram

Phase diagrams of the particular stainless steel and UO_2 are not applicable since little or no reaction occurs between constituents.

3. Effect of impurities

The effect of impurities on stainless steel is well known, so high-quality commercial steel powders are used in fuel fabrication. The total impurity level of the UO_2 should be maintained below 500 ppm to avoid harmful contamination of the matrix. Most important is avoidance of oxygen pickup by the stainless steel and this is achieved by using a UO_2 very low in "excess" oxygen content.

B1. Density (room temperature)

Density of UO_2 x volume per cent UO_2 + density of stainless steel x volume per cent stainless steel = density of dispersion.

3. Uranium content

0.881 x w/o UO_2 x density = uranium content of dispersion (see Fuel Comparison Table).

7. Thermal expansion (linear)[1]

The mean linear-thermal-expansion coefficients have been measured for various UO_2-stainless steel dispersions clad with stainless steel. In Table B7, the thermal-coefficient of expansion of various fuel plates is compared to commercial Type 318 stainless steel.

TABLE B7. THERMAL-EXPANSION DATA FOR STAINLESS STEEL AND FOR STAINLESS STEEL-UO_2 DISPERSION FUEL PLATES[1]

Material	Mean Coefficient of Thermal Expansion (20-925 C), 10^{-6} per C
Commercial Type 318 stainless steel	10.7
Fuel plate: 31-mil 25 w/o UO_2 prealloyed Type 318 stainless core, 7-mil Type 318 stainless cladding	10.7
Fuel plate: 31-mil 25 w/o UO_2 elemental Fe-18 w/o Cr-14 w/o Ni-2.5 w/o Mo alloy core, 7-mil Type 318 stainless cladding	11.0

8. Recrystallization temperature range

Effective recrystallization temperature of stainless steel matrix is raised due to interference of UO_2 particles.

C1. Hardness (room temperature)

The hardness of a 30 w/o UO_2-Type 316 stainless steel dispersion ranged from 81-90 Rockwell B. These values were dependent upon the type of UO_2 particles used and the density reached.

3&4. Ultimate tensile strength and yield strength[2]

Ultimate tensile strength, yield strength, and elongation of dispersions having various loadings of UO_2 in Type 316 stainless steel-matrix core materials are listed in Table C3. These cores have been cold pressed, sintered, and coined, and the values given are based on an average of samples. When these core materials are clad with stainless steel and fabricated into fuel plates, the cores are elongated extensively. During the fabrication, new variables are introduced which effect the ultimate tensile strength. The most useful measure of strength for these fuel plates is the transverse tensile strength. In this test, the tensile stresses are applied perpendicular to the rolling plane and do not involve the cladding. Table C4 contains ultimate transverse tensile-strength values for various w/o UO_2-stainless steel matrix dispersions.

5. Compressive strength

No data available

6. Creep strength[3]

Fuel plates with 25 w/o UO_2 in both elemental 18-14-2.5 alloy and prealloyed Type 318 stainless steel matrices have been fabricated by optimum fabrication techniques and have had creep-rupture tests performed at 900 C. Figure C6 summarizes these data.

7. Young's modulus

No data available

8. Shear modulus

No data available

9. Bulk modulus

No data available

10. Poisson's ratio

No data available

11. Elongation

See Table C3.

D2. Thermal conductivity[4]

See Figure D2.

TABLE C3. MECHANICAL PROPERTIES OF SOME UO_2-TYPE 316 STAINLESS STEEL DISPERSIONS[1]

UO_2, w/o	Density, per cent of theoretical	Room-Temperature Values			Values at 1600 F		
		Ultimate Strength, psi	0.2 Per Cent Offset Yield Strength, psi	Elongation in 1 In., per cent	Ultimate Strength, psi	0.2 Per Cent Offset Yield Strength, psi	Elongation in 1 In., per cent
25	98	46,700	31,800	10	12,400	11,400	14
30	96.2	43,200	31,800	6	14,400	13,700	9
30.64	96.5	43,400	29,600	7	13,500	12,300	8
35	96.6	37,700	29,800	6	12,900	12,100	5

TABLE C4. ULTIMATE TRANSVERSE TENSILE STRENGTHS OF VARIOUS UO_2 STAINLESS STEEL MATRIX DISPERSIONS[2]

UO_2, w/o	Fuel Matrix	Ultimate Transverse Tensile Strength, psi
20	Iron	33,500
25	Iron	28,500
30	Austenitic stainless	26,000[a]
35	Austenitic stainless	16,000
37	Austenitic stainless	14,500
40	Austenitic stainless	11,000
45	Austenitic stainless	8,000
50	Austenitic stainless	4,000

(a) Elevated-temperature values for austenitic stainless-30 w/o UO_2 dispersions:

Temperature, C	Ultimate Strength, psi
531	13,000
641	12,000
760	8,500

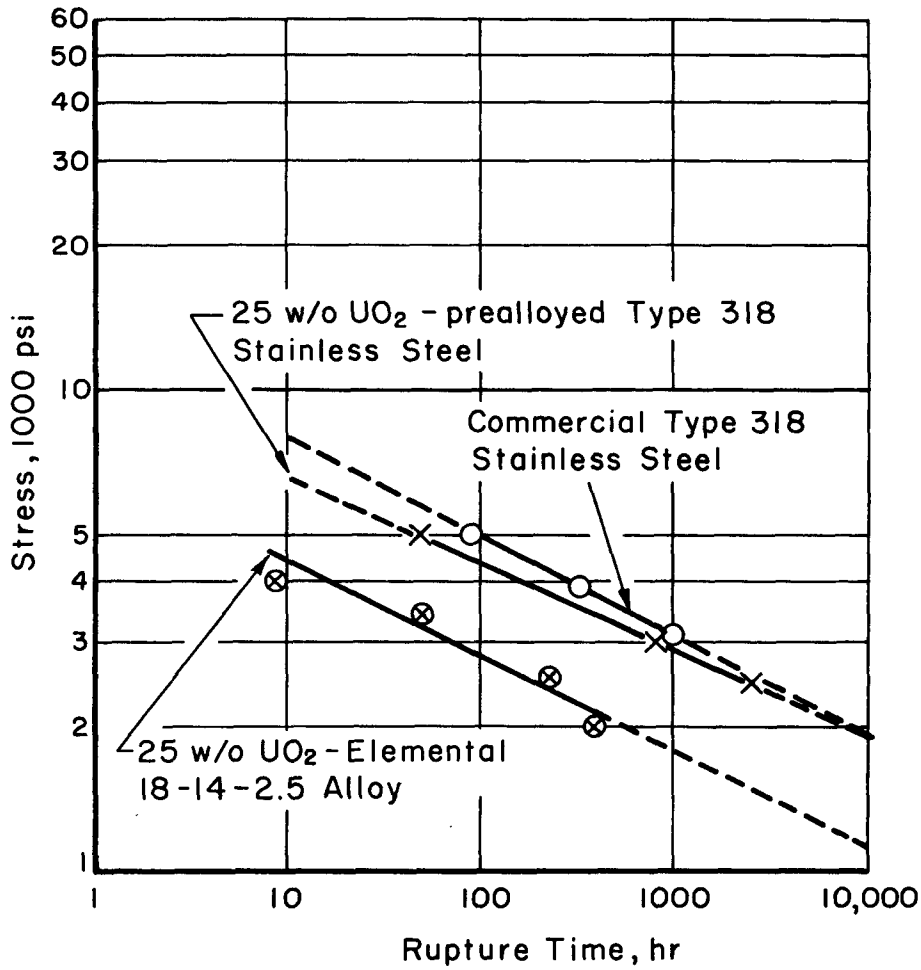

FIGURE C6. COMPARISON OF STRESS-RUPTURE CURVES OF UO_2 - STAINLESS STEEL FUEL PLATES WITH COMMERCIAL SHEET AT 900 C [3]

AEA-43233

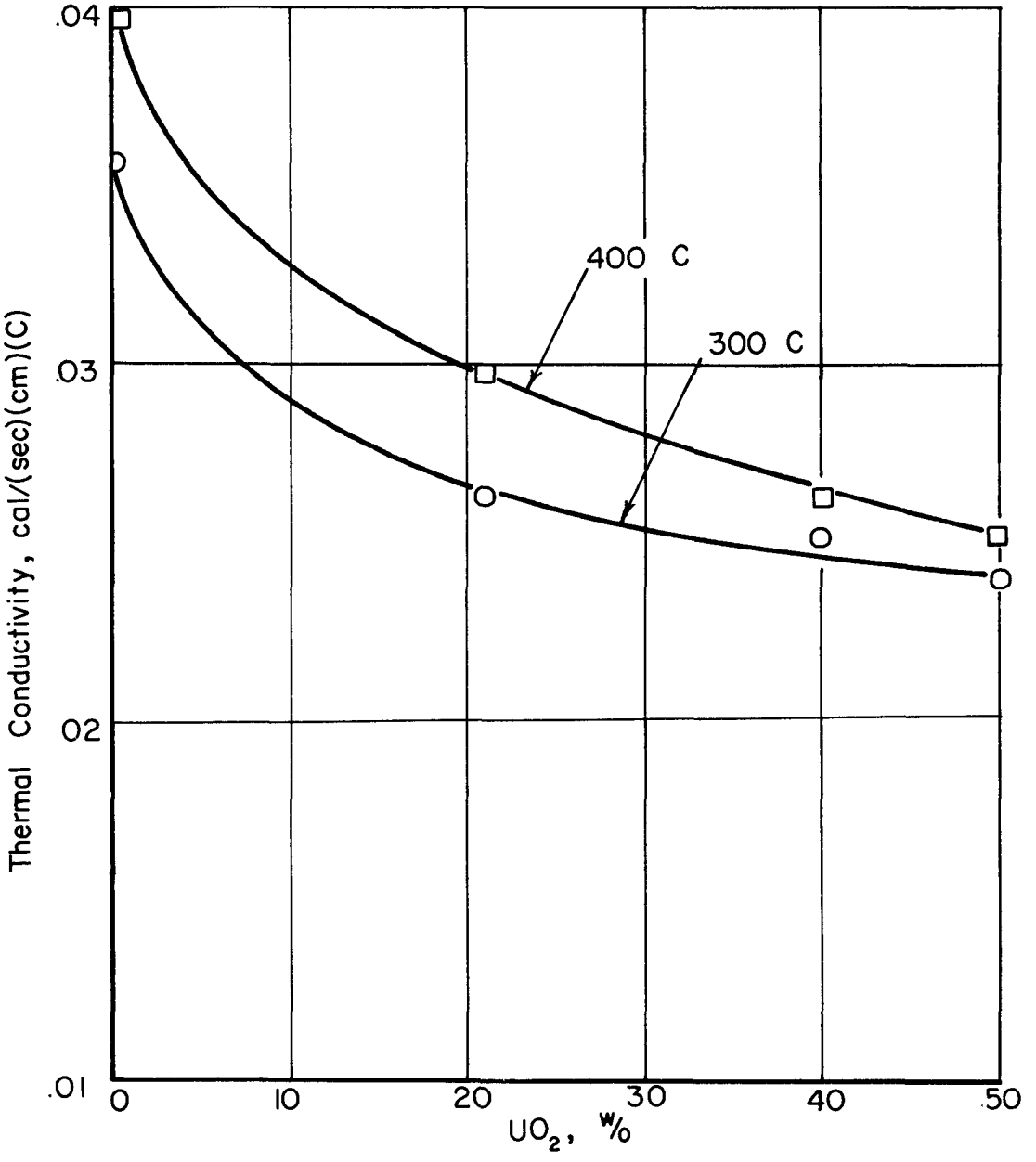

FIGURE D2. THERMAL CONDUCTIVITY FOR UO_2 – STAINLESS STEEL[4]

AEA-43219

E1. Electrical resistivity[5]

A fuel plate consisting of a 12-mil 30 w/o UO_2-elemental iron-18 w/o chromium-9 w/o nickel alloy core, and a 4-mil Type 347 stainless steel cladding has an electrical-resistivity value of 96.52 microhm-cm at 30 C.

F. Chemical properties[1]

a. The corrosion resistance of UO_2-stainless steel dispersions is greatly affected by the distribution of the UO_2 in the stainless steel matrix. Thus, if the fuel particles are dispersed uniformly in a continuous matrix of highly corrosion resistant material, a pinhole defect in the fuel plate's cladding would only result in a few UO_2 particles being attacked by the corrosive coolant.

b. Complete corrosion data are not available, but loadings of 25 and 30 w/o UO_2 in matrices of Types 347, 302, 304, 316, and 310 stainless steels have been tested in 731 C supercritical water at 5000 psi. No significant weight change was noted after 2 weeks of exposure of elements edge sheared to expose the core in two directions. Other tests were made on similar samples for 4 months in 260, 310, and 360 C static demineralized water with additional oxygen and hydrogen saturation. All samples revealed weight changes of only up to 0.116 mg/(cm^2)(month).

G1. Dimensional stability during irradiation[6]

Fuel plates containing various loadings of UO_2 dispersed in different types of stainless steel matrices have been examined for dimensional stability after irradiation. Table G1 summarizes these data.

2. Fission-gas-release data[7]

The postirradiation examination of fuel plates which had a Type 347 stainless steel cladding with a core containing 26 w/o UO_2 dispersed in a matrix of prealloyed Type 347 stainless steel showed that some specimens had been ruptured. Using both mass and gamma-ray spectrographic techniques, a measured quantity of 4.8×10^{-10} cm^3 of fission gas at STP was determined for the unruptured specimens. For those specimens which had been ruptured, values of 2.3×10^{-3} cm^3 and 1.0×10^{-2} cm^3 of krypton-85 were determined.

3. Swelling-temperature data[8]

Data available were used in the preparation of Figure G6.

4. Unusual nuclear properties

No data available

5. Property changes as a result of irradiation[1]

Postirradiation-annealing studies were carried out on stainless steel-UO_2 fuel materials. In Figure G5, the hardness of these materials is shown after irradiation and postirradiation annealing.

TABLE G1. DIMENSIONAL CHANGE OF FLAT-PLATE

Fuel		Matrix		Core-to-Cladding Ratio			Irradiation Temperature, F		Uranium Burnup,
Type[a]	Amount, w/o	Stainless Type	Amount, w/o	Length	Width	Thickness	Peak	Average	a/o
S UO_2	26	347	74	2	7	3	750[b]		
H UO_2	26	347	74	2	7	3	750[b]		45
H UO_2	26	347	74	2	7	3	750[b]		45
H UO_2	26	347	74	2	7	3	750[b]		45
H UO_2	26	347	74	2	7	3	750[b]		45
S UO_2	26	347	74	2	7	3	750[b]		45
S UO_2	25.9	347	74.1	2	7	3	750[b]		40
H UO_2	26.1	347	73.9	2	7	3	750[b]		40
H UO_2	26	347	74	2	7	3	750[b]		40
H UO_2	26	347	74	2	7	3	750[b]		40
S UO_2	26	347	74	2	7	3	750[b]		40
H UO_2	26	347	74	2	7	3	750[b]		40
H UO_2	24.2	347	75.8	2	7	3	750[b]		40
S UO_2	26	347	74	2	7	3	750[b]		40
S UO_2	26	347	74	2	7	3	750[b]		40
S UO_2	26	347	74	2	7	3	750[b]		40
S UO_2	25.9	347	74.1	2	7	3	750[b]		40
H UO_2	24.2	347	75.8	2	7	3	750[b]		40
S UO_2	26	347	74	2	7	3	750[b]		40
S UO_2	26	347	74	2	7	3	750[b]		40
S UO_2	26	347	74	2	7	3	600[b]		40
H UO_2	26	347	74	2	7	3	600[b]		40
S UO_2	26	347	74	2	7	3	600[b]		40
S UO_2	26	347	74	2	7	3	600[b]		40
S UO_2	26	347	74	2	7	3	600[b]		40
H UO_2	26	347	74	2	7	3	600[b]		40
H UO_2	25	318[c]	75	2	2.7	2.2	--	--	5.4
H UO_2	30	318	70	2	2.7	2.2	--	--	6.1
H UO_2	25	318	75	2	2.7	2.2	--	1500[d]	5.4
H UO_2	30	318	70	2	2.7	2.2	--	1529[d]	7.2
H UO_2	25	318	75	2	2.7	2.2	--	1248[d]	13.4
H UO_2	30	318	70	2	2.7	2.2	--	1390[d]	17.5
H UO_2	25	318	75	2	2.7	2.2	--	1477[d]	16.2
H UO_2	30	318	70	2	2.7	2.2	--	1325[d]	15.6
H UO_2	25	318	75	2	2.7	2.2	--	1280[d]	24.5
H UO_2	25	318	75	2	2.7	2.2	--	1238[d]	24.7
H UO_2	25	318	75	2	2.7	2.2	--	1055[d]	22.2
H UO_2	30	318	70	2	2.7	2.2	--	~1600[d]	3.1
H UO_2	25	318	75	2	2.7	2.2	--	~1600[d]	3.2
H UO_2	25	318	75	2	2.7	2.2	--	~1600[d]	3.8
H UO_2	30	318	70	2	2.7	2.2	--	~1600[d]	3.6
S UO_2	30	318	70	2	2.7	2.8	1375	1239[d]	15.1
H UO_2	30	318	70	2	2.7	2.8	1335	1186[d]	15.4
S UO_2	30	318	70	2	2.7	2.8	1325	1128[d]	14.2
H UO_2	30	318	70	2	2.7	2.8	1120	967[d]	17.1

DISPERSION FUEL SPECIMENS DURING IRRADIATION(6)

Over-All Specimen Dimensions, in.			Dimensional Change, per cent				Density Loss,	
					Thickness			
Length	Width	Thickness	Length	Width	Maximum	Average	per cent	Specimen Condition
1.506	0.570	0.040	--	--	--	--	--	Blistered
1.506	0.570	0.040	0.07	0.09	--	5.3	1.9	Good condition, no blistering or warpage
1.506	0.570	0.040	0.15	0.07	--	6.0	2 2	Ditto
1 506	0.570	0.040	0.79	0 19	--	2.6	2.7	Ditto
1.506	0 570	0.040	0.11	0.09	--	4.8	2.5	Ditto
1 506	0 570	0 040	0 04	0 09	--	4.5	2.5	Ditto
1.506	0.570	0.040	0.17	0 34	--	5.0	1.4	Ditto
1.506	0.570	0.040	--	0.12	--	6.3	2.7	Ditto
1.506	0.570	0.040	0.17	0.38	--	5.5	2.9	Ditto
1.506	0.570	0.040	--	0.35	--	5.4	2.6	Ditto
1.506	0.570	0.040	0.15	0.17	--	5.8	3.1	Ditto
1.506	0.570	0.040	--	0.14	--	6.6	2.9	Ditto
1.506	0.570	0.040	0.19	--	--	4.8	2.4	Ditto
1.506	0.570	0.040	0.09	0.04	--	4.2	2.2	Ditto
1.506	0.570	0.040	0.26	0.21	--	4.2	2.0	Ditto
1.506	0.570	0.040	--	0.14	--	4.5	1.8	Ditto
1.506	0.570	0.040	0.36	0.19	--	3.6	1.7	Ditto
1.506	0.570	0.040	0.75	0.86	--	3.9	1.9	Ditto
1.506	0.570	0.040	0.24	0.09	--	3.6	1.8	Ditto
1.506	0.570	0.040	--	--	--	--	--	Blistered, fused
1.506	0.570	0.040	--	0.12	--	6.4	2.2	Good condition, no blistering or warpage
1.506	0.570	0.040	0.09	0.09	--	2.9	2.1	Ditto
1.506	0.570	0.040	0.05	0.09	--	3.6	1.6	Ditto
1.506	0.570	0.040	0.05	0.09	--	5.5	1.8	Ditto
1.506	0.570	0.040	0.12	0.23	--	1.7	1.4	Ditto
1.506	0.570	0.040	0.86	0.31	--	2.7	0.9	Ditto
1.5	0.687	0.045	-1.56	0.07	12.42	0.57	0.00	Good surface but warped
1.5	0.687	0.045	-0.96	0.20	73.58	13.32	2.23	Large blister
1.5	0 687	0.045	--	0 19	10.92	3.71	1.04	Good
1.5	0.687	0.045	-0.14	0.13	18.16	2.63	1.15	Small blister
1.5	0.687	0.045	--	0.00	2.17	1.52	0.86	Good
1.5	0.687	0.045	-0.20	0.08	10.94	5.79	-2.09	Small blister
1.5	0.687	0.045	-0.10	0.00	5.49	4.18	1.72	Good
1.5	0.687	0.045	--	0.00	25.27	6.26	1.84	Ruptured
1.5	0.687	0.045	-0.12	0.19	23.04	7.61	3.70	Large blister
1.5	0.687	0.045	--	--	--	--	--	Small blister
1.5	0.687	0.045	--	--	--	--	--	Blistered, ruptured
1.5	0.687	0.045	0.00	0.00	0.00	0.00	0.00	Good, no blistering or warpage
1.5	0.687	0.045	-0.11	0.00	0.00	0.00	0.00	Ditto
1.5	0.687	0.045	0.00	0.00	0.00	0.00	0.00	Ditto
1.5	0.687	0.045	-0.12	0.06	0.06	0.68	0.00	Ditto
1.5	0.687	0.045	0.00	0.00	--	2.6	0.8	Good, no blistering or warpage
1.5	0.687	0.045	0.00	0.00	--	2.0	0.7	Ditto
1.5	0.687	0.045	0.00	0.00	--	2.2	0.7	Ditto
1.5	0.687	0.045	0.00	0.00	--	2.0	0.5	Ditto

TABLE G1.

Fuel		Matrix		Core-to-Cladding Ratio			Irradiation Temperature, F		Uranium Burnup,
Type[a]	Amount, w/o	Type	Amount, w/o	Length	Width	Thickness	Peak	Average	a/o
H UO_2	30	318	70	2	2.7	2.8	1565	1355[d]	11.8
S UO_2	30	318	70	2	2.7	2.8	1620	1402[d]	11.8
H UO_2	30	318	70	2	2.7	2.8	--	--	11.5
S UO_2	30	318	70	2	2.7	2.8	1300	1155[d]	10.4
UN	24	318	76	2	2.7	2.8	--	1600[d]	5.4
UC	24	318	76	2	2.7	2.8	--	1710[d]	6.6
UN	24	318	76	2	2.7	2.8	--	1800[d]	7.7
UC	24	318	76	2	2.7	2.8	--	1800[d]	7.8
UN	24	318	76	2	2.7	2.8	--	1490[d]	2.2
UC	24	318	76	2	2.7	2.8	--	1600[d]	2.1
UN	24	318	76	2	2.7	2.8	--	1720[d]	--
UC	24	318	76	2	2.7	2.8	--	1490[d]	3.4
UN	24	318	76	2	2.7	2.8	--	1390[d]	--
UN	24	318	76	2	2.7	2.8	--	1625[d]	12
UC	24	318	76	2	2.7	2.8	--	1600[d]	12
UC	24	318	76	2	2.7	2.8	--	1460[d]	--
							Max.	Min.	
H UO_2	30	318	70	2	2.7	2.8	1880	1500[d]	3.6
UN	28	318	72	2	2.7	2.8	>1800[e]	1575[d]	4.8
UN	28	318	72	2	2.7	2.8	>1850[e]	1590[d]	5.0
UN	28	318	72	2	2.7	2.8	>1750[e]	1470[d]	4.3

(a) H = hydrothermal, S = spherical UO_2.
(b) Specimen surface temperature.
(c) Elemental blend of iron, chromium, nickel, and molybdenum powders in all Type 318 stainless steel matrices.
(d) Central core temperature.
(e) Thermocouples were inoperative last two cycles of the reactor. Specimens may have reached 1900 to 2000 F.

(Continued)

Over-All Specimen Dimensions, in.			Dimensional Change, per cent				Density Loss,	Specimen Condition
					Thickness			
Length	Width	Thickness	Length	Width	Maximum	Average	per cent	
1.5	0.687	0.045	0.00	0.00	--	2.4	0.4	Good, no blistering or warpage
1.5	0.687	0.045	0.00	0.00	--	2.4	0.6	Ditto
1.5	0.687	0.045	0.00	0.00	--	2.2	0.7	Ditto
1.5	0.687	0.045	0.00	0.00	--	2.0	0.4	Ditto
1.5	0.687	0.045	--	--	--	1.3	0.37	Ditto
1.5	0.687	0.045	--	--	--	1.7	2.88	Blister
1.5	0.687	0.045	--	--	--	2.3	2.16	Blister
1.5	0.687	0.045	--	--	--	1.5	6.12	Blister
1.5	0.687	0.045	--	--	--	0.9	0.28	--
1.5	0.687	0.045	--	--	--	0.4	0.08	--
1.5	0.687	0.045	--	--	--	0.2	Nil	--
1.5	0.687	0.045	--	--	--	0.2	0.28	--
1.5	0.687	0.045	--	--	--	1.3	1.71	--
1.5	0.687	0.045	--	--	--	3.1	0.8	Good, no blistering or cracking
1.5	0.687	0.045	--	--	--	3.2	2.15	Blister
1.5	0.687	0.045	--	--	--	3.2	2.04	Blister
					Blister			
1.5	0.687	0.045	--	--	30	0.00	1.2	Small blister, no warpage
1.5	0.687	0.045	--	--	29	0.00	1.3	Small blister, no warpage
1.5	0.687	0.045	--	--	25	0.00	1.5	Small blister, no warpage
1.5	0.687	0.045	--	--	23	0.00	0.6	Small blister, no warpage

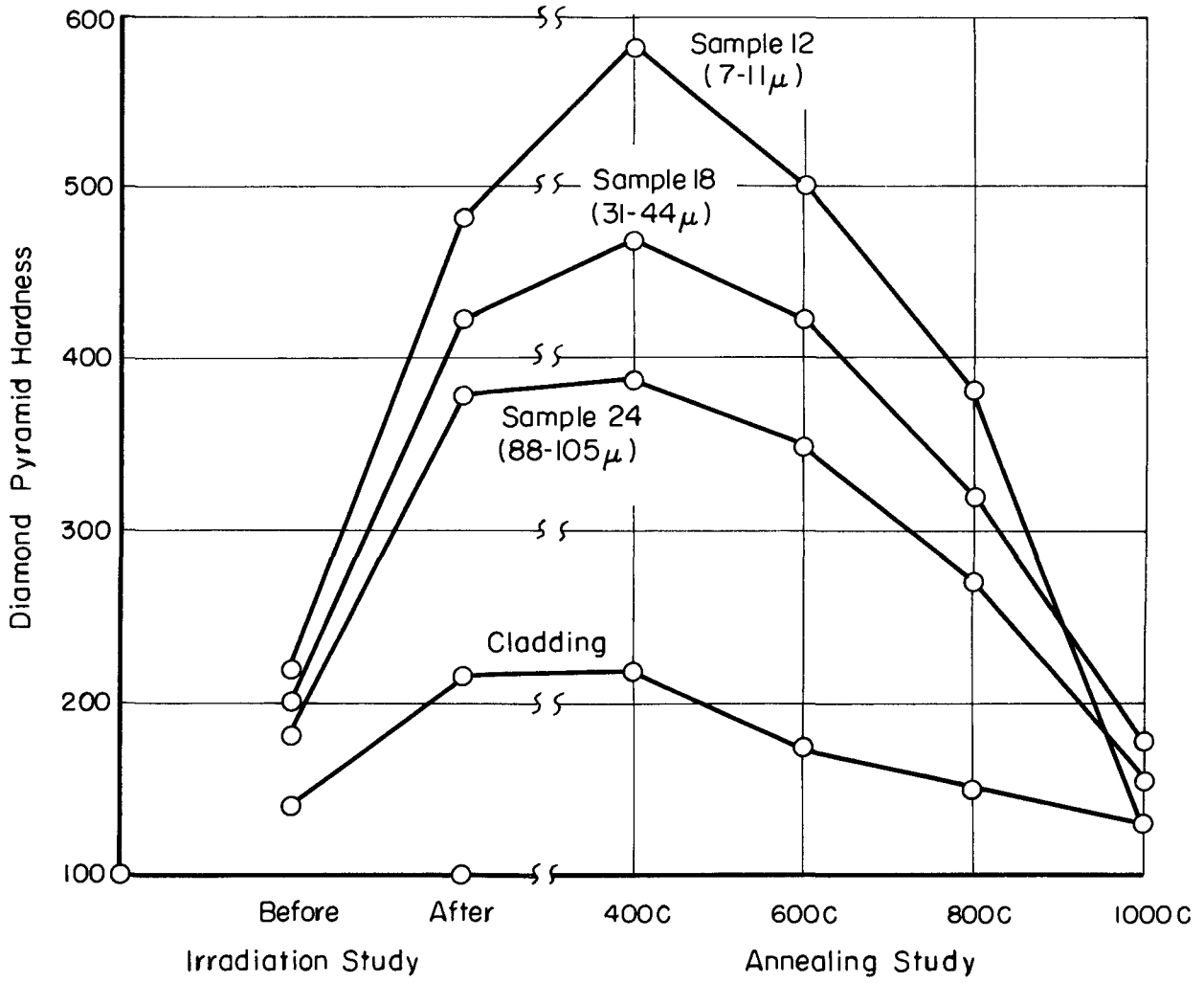

FIGURE G5. SUMMARY OF POSTIRRADIATION ANNEALING STUDIES ON STAINLESS STEEL-UO_2 FUEL MATERIALS[1]

AEA-43235

6. Failure versus temperature data[8-11]

Figure G6 and Table G6 summarize the results of many capsule irradiations of UO_2-stainless steel fuel-element specimens.

H. References

(1) Keller, D. L., "Dispersion Fuels", Reactor Handbook, Volume 1 Materials, Interscience Publishers, Inc., New York (1960), pp 304-330.

(2) Cunningham, J. E., Beaver, R. J., Thurber, W. C., and Waugh, R. C., "Fuel Dispersions in Aluminum-Base Elements for Research Reactors", Fuel Elements Conference, Paris, November 18-23, 1957, TID-7546 (March, 1958), pp 269-297.

(3) Paprocki, S. J., Keller, D. L., and Fackelmann, J. M., "Properties of Uranium Dioxide-Stainless Steel Dispersion Fuel Plates", BMI-1339 (April, 1959).

(4) Meny, L., Buffet, J., and Sauve, C., "Powder Sintering and Extrusion for the Fabrication of U-Al and UO_2-Stainless Steel Dispersion", 4th Plansee Seminar, Austria, June 20-24, 1961.

(5) Keeler, J. R., and Cuddy, L. J., "Properties of Stainless Steel-Uranium Dioxide Fuel Plates", BMI-913 (May, 1954).

(6) Lozier, D. E., BMI, Unpublished Data.

(7) Paprocki, S. J., Dickerson, R. F., Cunningham, G. W., Murr, W. E., and Lozier, D. E., "Fabrication and Irradiation of SM-2 Core Materials", BMI-1528 (July 12, 1961).

(8) Keller, D. L., "Predicting Burnup of Stainless-UO_2 Cermet Fuels", Nucleonics, 19 (6), 45-48 (June, 1961).

(9) Haynes, V. O., Neill, F. H., and Schafler, L. D., "Summary of UO_2-Stainless Steel Dispersion Irradiation Experiments", ORNL-CF-58-2-71 (March 18, 1958).

(10) Keller, D. L., Hulbert, L. E., and Dunnington, B. W., "A Method of Correlating Irradiation Effects in Dispersion Fuels", BMI-1408 (January 20, 1960).

(11) Saling, J. H., BMI, Unpublished Data.

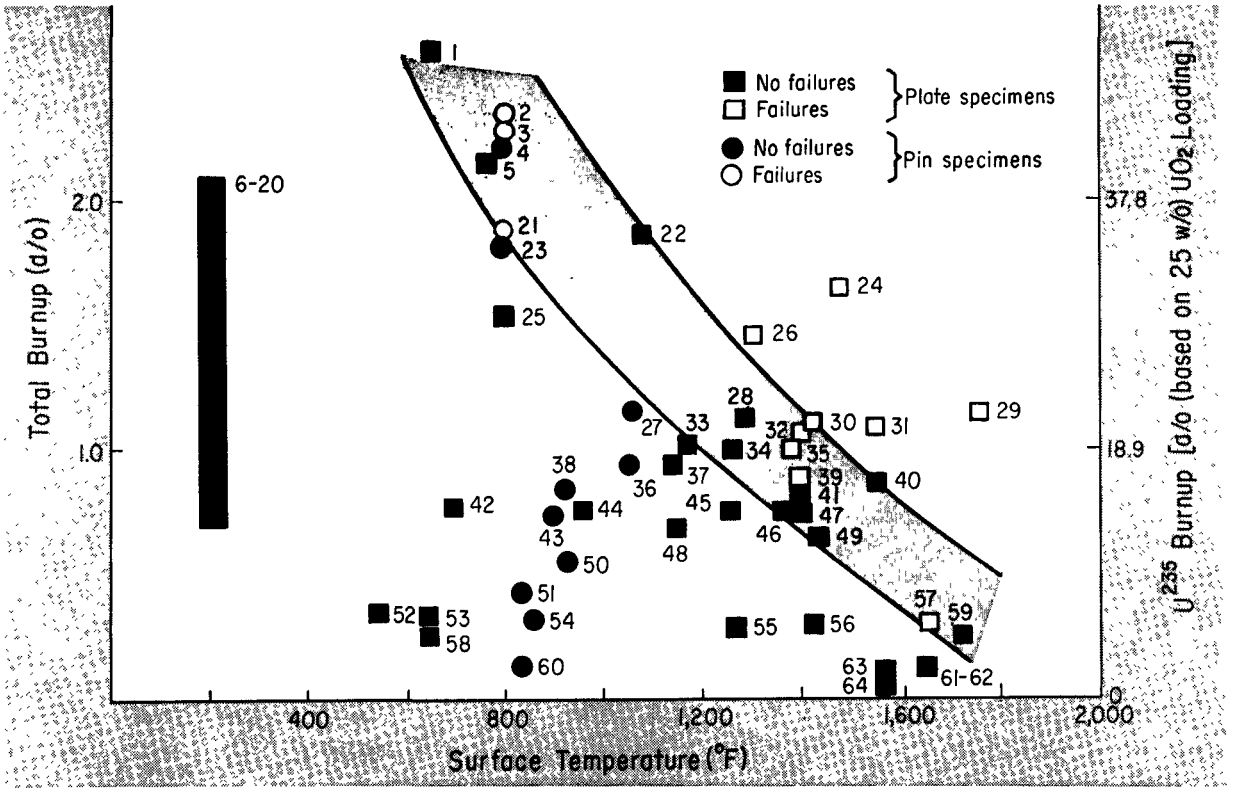

FIGURE G6. BURNUP PERFORMANCE OF STAINLESS-STEEL-UO_2 CERMET FUEL SPECIMENS HAVING 18-30 W/O UO_2

(Numbers next to data points are specimen numbers shown in Table G6). These data indicate that when a specimen temperature and burnup are below shaded area, a "typical" fuel element will not crack or blister (as seen visually or microscopically) or release radioactive products. Fuels exposed above shaded zone would fail; performance of fuels irradiated within shaded area is difficult to predict.[8]

AEA-43236

TABLE G6. IRRADIATION DATA ON STAINLESS STEEL-UO_2-DISPERSION FUEL SPECIMENS

Matrix	Cladding	Specimen Characteristics: UO_2 Loading, w/o	UO_2 Particle Size, μ	Cladding Thickness, mils	Irradiation Conditions: Surface Temperature, F	Irradiation Time, hr	Burnup, a/o: U^{235}	Burnup, a/o: Total[+]	Results	Identification in Figure G6	Reference
					Plates						
Type 304	Type 304L	17 92	--	5	190	--	52.5	1.93	No failures	6-20	(9)
		17 92	--	5	190	--	40.0	1.48	Ditto	6-20	(9)
		17.92	--	5	190	--	45.4	1.68	Ditto	6-20	(9)
		17.92	--	5	190	--	10.5	0.39	Ditto	6-20	(9)
		17 92	--	5	190	--	40.0	1.48	Ditto	6-20	(9)
		17.92	--	5	190	--	53.5	1.98	Ditto	6-20	(9)
		17.92	--	5	190	--	51.2	1.89	Ditto	6-20	(9)
		17.92	--	5	190	--	13.1	0.48	Ditto	6-20	(9)
		17.92	--	5	190	--	56.9	2.10	Ditto	6-20	(9)
		17.92	--	5	190	--	53.1	1.96	Ditto	6-20	(9)
		17.92	--	5	190	--	48.1	1.78	Ditto	6-20	(9)
		17.92	--	5	190	--	29.2	1.08	Ditto	6-20	(9)
		18.75	--	8	212	400	16.0	0.7	Ditto	6-20	(9)
		22.18	--	10	212	400	18.0	0.9	Ditto	6-20	(9)
		26.89	--	12	212	400	12.0	0.8	Ditto	6-20	(9)
Fe-18Cr-14Ni-2.5Mo (elemental)	Type 318	25	75-150	6	1725	32.7	5.4	0.29	No failures	59	(10)
		25	75-150	6	1430	47.5	12.7	0.67	Ditto	49	(10)
		25	75-150	6	1550	47.5	16.6	0.88	Ditto	40	(10)
		25	75-150	6	1400	85.2	20.4	1.08	Large blister	32	(10)
		25	75-150	6	1417	85.2	20.7	1.10	Small blister	30	(10)
		25	75-150	6	1650	52.7	2.2	0.12	No failures	61	(10)
		25	75-150	6	1650	52.7	2.6	0.14	Ditto	62	(10)
		30	75-150	6	1655	32.7	4.9	0.32	Small blister	57	(10)
		30	75-150	6	1533	47.5	17.5	1.15	Ditto	31	(10)
		30	75-150	6	1395	47.5	15.6	1.04	Ruptured	35	(10)
		30	75-150	6	1475	85.2	25.1	1.66	Ditto	24	(10)
		30	75-150	6	1300	85.2	22.2	1.47	Ditto	26	(10)
Fe-18Cr-9Ni (elemental)	Type 347	30	>44	6	550	610	5.3	0.35	8 pieces, 0 failed	52	(9)
		30	>44	4	650	425	4.4	0.29	Ditto	58	(9)
		30	>44	4	650	412	5.4	0.36	Ditto	53	(9)
		30	>44	4	700	1038	12.1	0.79	Ditto	42	(9)
		30	>44	4	650	2550	39.7	2.6	Ditto	1	(9)
		30	>44	4	800	--	23.5	1.54	Ditto	25	(9)
		30	>44	4	766	4015	33.3	2.17	Ditto	5	(9)
		30	>44	4	1080	2415	28.6	1.86	Ditto	22	(9)
		30	>44	4	1400	1889	12.9	0.84	8 pieces, 2 cracked	39,41	(9)
		30	>44	4	1765	880	17.4	1.14	8 pieces, all failed	29	(9)
Type 310	Type 310	30	>105	5	1260	370	4.6	0.30	2 pieces, 0 failed	55	(9)
		30	>105	5	1420	420	4.8	0.31	Ditto	56	(9)
		30	>105	5	1560	370	1.8	0.12	Ditto	63	(9)
		30	>44	4	1550	288	1.1	0.09	Ditto	64	(9)

TABLE G6. (Continued)

Matrix	Cladding	UO_2 Loading, w/o	Specimen Characteristics: UO_2 Particle Size, μ	Specimen Characteristics: Cladding Thickness, mils	Irradiation Conditions: Surface Temperature, F	Irradiation Conditions: Irradiation Time, hr	Burnup, a/o: U^{235}	Burnup, a/o: Total+	Results	Identification in Figure G6	Reference
					Plates (Continued)						
Fe-23Cr-17Ni (elemental)	Type 318	30	>44	4	1290	815	17	1.12	No failures	28	(9)
Fe-18Cr-14Ni-2.5Mo (elemental	Type 318	30	75-150	6	1240	2250	15.1	1.00	No failures	34	(11)
		30	75-150	6	1190	2250	15.4	1.02	Ditto	33	(11)
		30	75-150	6	1130	2250	14.2	0.94	Ditto	37	(11)
		30	75-150	6	970	2250	12.0	0.79	Ditto	44	(11)
		30	75-150	6	1360	1474	11.8	0.78	Ditto	46	(11)
		30	75-150	6	1400	1474	11.8	0.78	Ditto	47	(11)
		30	75-150	6	1270	1474	11.5	0.76	Ditto	45	(11)
		30	75-150	6	1140	1474	10.4	0.69	Ditto	48	(11)
					Pins						
Type 347	Type 347	23	--	10	860	790	6.7	0.33	No failures	54	(9)
		24	--	10	930	--	16	0.82	Ditto	38	(9)
		24	--	10	842	--	3	0.15	Ditto	60	(9)
		24	--	10	842	--	8.2	0.42	Ditto	51	(9)
		30	--	10	930	1000	8.9	0.58	Ditto	50	(9)
Fe-18Cr-12Ni (elemental)	Type 304	24.5	--	10	1060	2790	18	0.94	No failures	36	(9)
		28.5	--	10	1060	2790	18	1.13	Ditto	27	(9)
		28.5	--	10	900	--	12	0.75	Ditto	43	(9)
		30	44-74	10‡	800	1662	28	1.85	2 pieces, 1 failed	21,23	(9)
		30	44-74	10	800	2520	34	2.24	Ditto	3,4	(9)
		30	44-74	10	800	3310	35	2.31	Ruptured	2	(9)

* This table includes data only from experiments in which temperatures were carefully monitored and burnup was measured either radiochemically or isotopically
+ The conversion to a/o burnup is based on a U enrichment of 93% in all cases.
‡ Type-347ss cladding.

CERMETS

UC CERMETS

Compiled by D. E. Kizer

A1. Chemical composition

Cermets of UC have been successfully fabricated containing 60 to 80 volume per cent UC (67 to 92 w/o) dispersed in molybdenum.[1]

3. Effect of impurities

No data available

B1. Density (room temperature)

Calculated densities (external dimension divided by weight) range from 12.27 to 12.95 g per cm^3 over a 60 to 90 volume per cent UC loading in the molybdenum cermet.

2. Density versus temperature

No data available

3. Uranium content

0.952 x w/o UC x density (see Fuel Comparison Table)

4. Liquidus temperature

No data available

5. Solidus temperature

No data available

6. Vapor pressure

No data available

7. Thermal expansion (linear)[2]

The mean linear thermal expansion for a 80 volume per cent UC-molybdenum cermet having a density 95 per cent of theoretical over the temperature range 20 to 950 C was found to be 7.2 to 7.6 x 10^{-6} per C. A 60 volume per cent UC-molybdenum cermet of 97 per cent of theoretical density was found to have a coefficient of 6.4 to 6.8 x 10^{-6} per C over the 20 to 950 C temperature range.

C1. Hardness (room temperature)

No data available

2. Hot hardness

No data available

3. Ultimate tensile strength

No data available

4. Compressive yield strength[3]

See Table C4.

TABLE C4. COMPRESSIVE MECHANICAL PROPERTIES FOR UC-MOLYBDENUM CERMETS[3]

UC Content, volume per cent	Density, per cent of theoretical	Ultimate Compressive Strength, 10^3 psi	Young's Modulus, 10^6 psi	Yield Strength, 10^3 psi	
				0.1 Per Cent Offset	0.2 Per Cent Offset
60	95	139.5	28.8	114.5	113.8
60	98	111.7	25.5	73.9	80.0
80	95	95.1	27.8	93.5	--

5. Compressive strength[3]

See Table C4.

6. Creep strength

No data available

7. Young's modulus[3]

See Table C4.

8. Shear modulus

No data available

9. Bulk modulus

No data available

10. Poisson's ratio

No data available

11. Elongation

No data available

D1. Specific heat

No data available

2. Thermal conductivity[3,4]

See Figure D2.

E1. Electrical resistivity[5]

See Figure E1.

F. Chemical properties

No data available

G. Irradiation properties

No data available

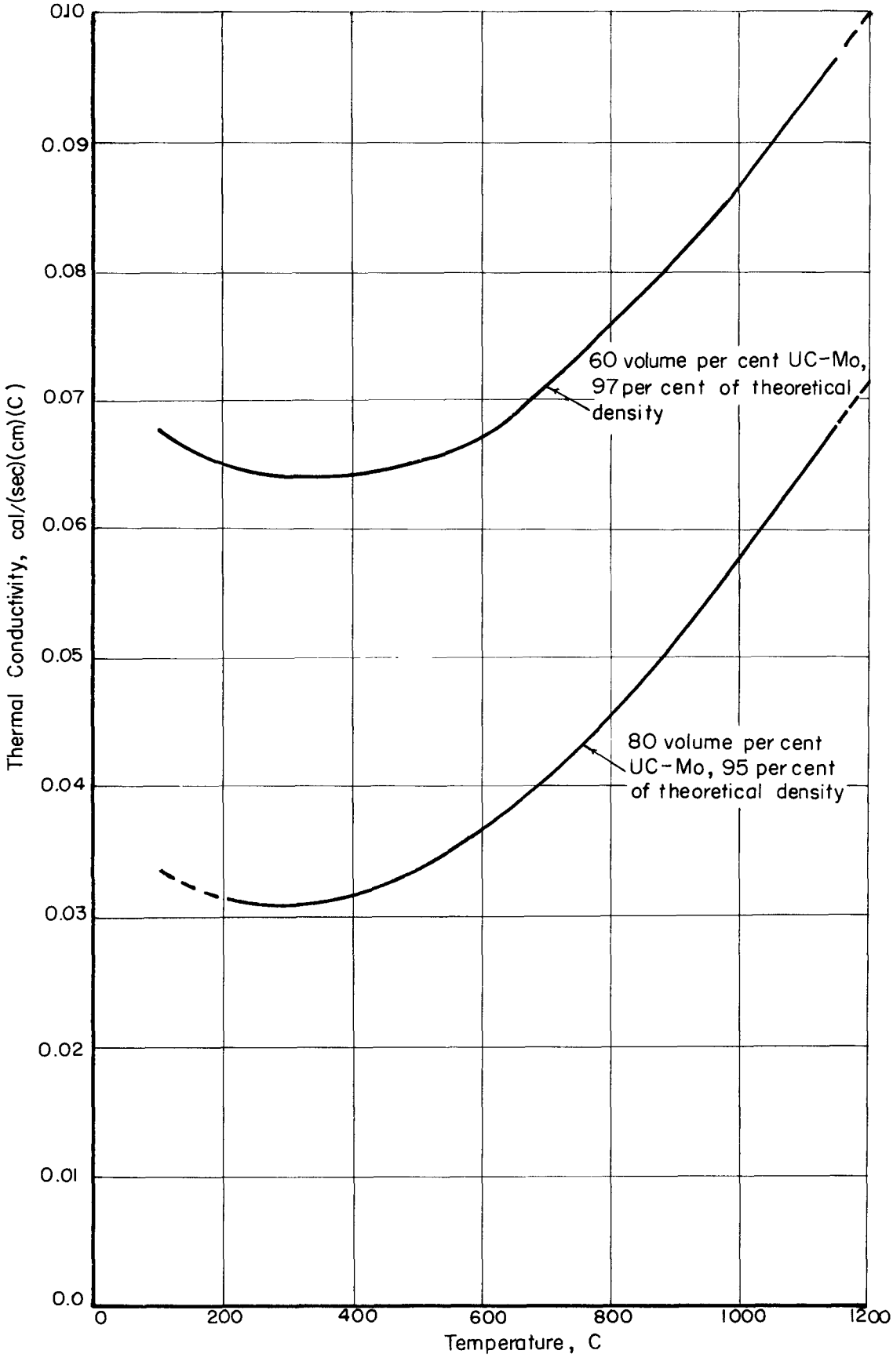

FIGURE D2. THERMAL CONDUCTIVITY OF UC CERMETS[3,4]

AEA-43220

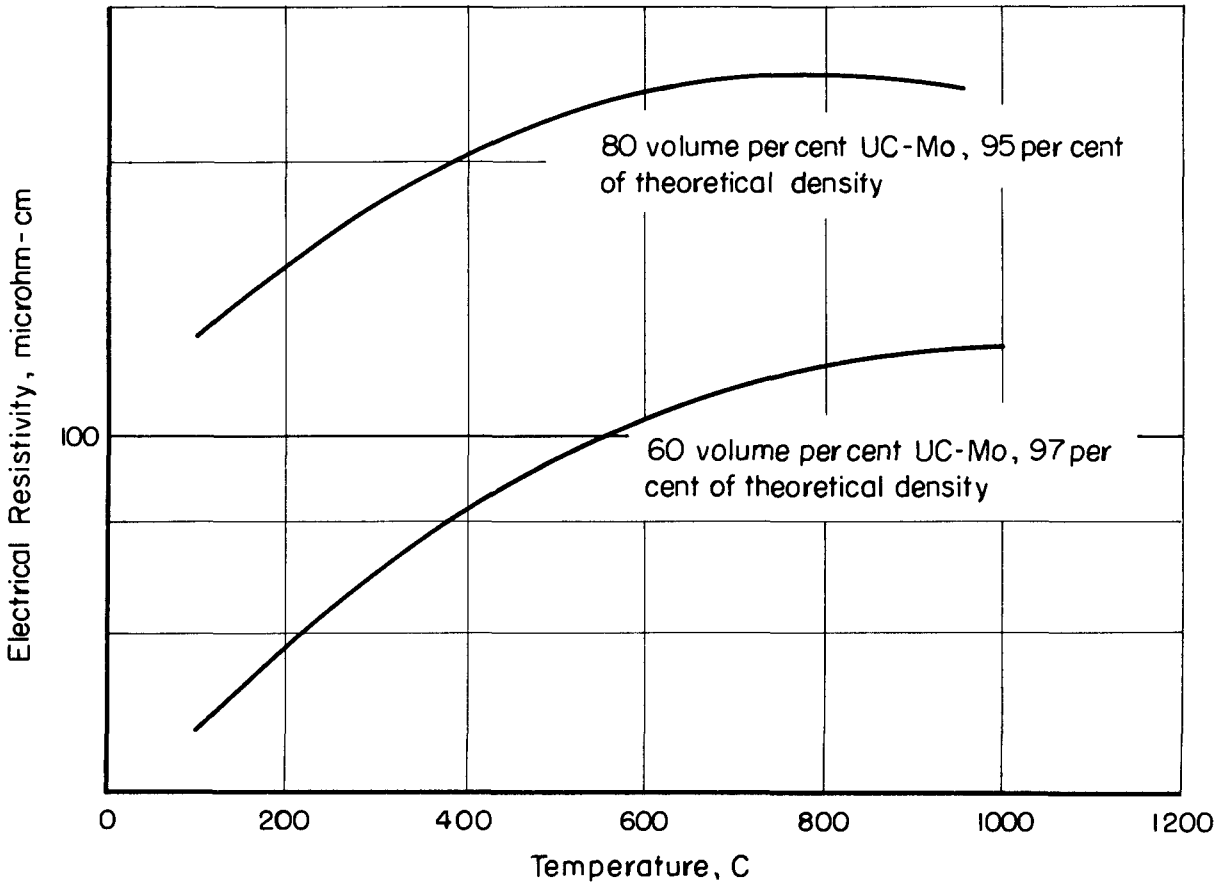

FIGURE E1. ELECTRICAL RESISTIVITY OF UC CERMETS[5]

AEA-43210

H. References

(1) Dayton, R. W., and Dickerson, R. F., "Progress Relating to Civilian Applications During March, 1962", BMI-1574 (April 1, 1962).

(2) Dayton, R. W., and Dickerson, R. F., "Progress Relating to Civilian Applications During July, 1962", BMI-1589 (August 1, 1962).

(3) Dayton, R. W., and Dickerson, R. F., "Progress Relating to Civilian Applications During June, 1962", BMI-1583 (July 1, 1962).

(4) Dayton, R. W., and Dickerson, R. F., "Progress Relating to Civilian Applications During May, 1962", BMI-1581 (June 1, 1962).

(5) Kizer, D. E., BMI, Unpublished Data.

UN CERMETS

Compiled by D. E. Kizer

A1. Chemical composition[1]

UN cermets have been successfully fabricated containing 60 to 90 volume per cent UN dispersed in molybdenum, chromium, and Type 304 stainless steel, resulting in weight loadings ranging from 67 to 94 w/o, depending on the matrix material used.

3. Effect of impurities

No data available

B1. Density (room temperature)

Calculated densities range from 11.57 to 13.5 g per cm^3, depending on the volume loading of UN and matrix material used. Below are calculated densities of 80 volume per cent UN cermets with the three matrix materials used.

Matrix Metal	Calculated Density, g per cm^3
Molybdenum	13.5
Type 304 stainless steel	13.0
Chromium	12.9

2. Density versus temperature

No data available

3. Uranium content

0.944 x w/o UN x density (see Fuel Comparison Table)

4. Liquidus temperature

No data available

5. Solidus temperature

No data available

6. Vapor pressure

No data available

7. Thermal expansion[1]

The mean linear thermal-expansion coefficient measured for an 80 volume per cent UN-molybdenum cermet with a density 90.9 per cent of theoretical was 9.1 to 9.5 x 10^{-6} per C over the temperature range 20 to 950.

C1. Hardness (room temperature)

No data available

2. Modulus of rupture[2]

See Table C2.

TABLE C2. MECHANICAL-PROPERTY VALUES OBTAINED ON MOLYBDENUM AND CHROMIUM CERMETS CONTAINING 80 VOLUME PER CENT UN[2]

Composition, volume per cent	Density, per cent of theoretical	Dynamic Modulus, 10^6 psi	Modulus of Rupture, psi	Compressive Properties		
				Static Modulus, 10^6 psi	0.2 Per Cent Offset Yield Strength, psi	Ultimate Strength, psi
Cr-80UN	90.1	25.19	18,100	27.2	104,800	131,000
Mo-80UN	93.9	30.24	26,200	33.1	118,000	152,000
--	93.9	29.66	24,900	30.2	110,000	140,000

4. Compressive yield strength[2]

See Table C2.

5. Compressive strength[2]

See Table C2.

6. Creep strength

No data available

7. Young's modulus[2]

See Table C2.

8. Shear modulus

No data available

9. Bulk modulus

No data available

10. Poisson's ratio

No data available

11. Elongation

No data available

D1. Specific heat

No data available

2. Thermal conductivity[3,4]

See Figure D2.

E1. Electrical resistivity[1,4]

See Figure E1.

F. Chemical properties

No data available

G. Irradiation properties

No data available

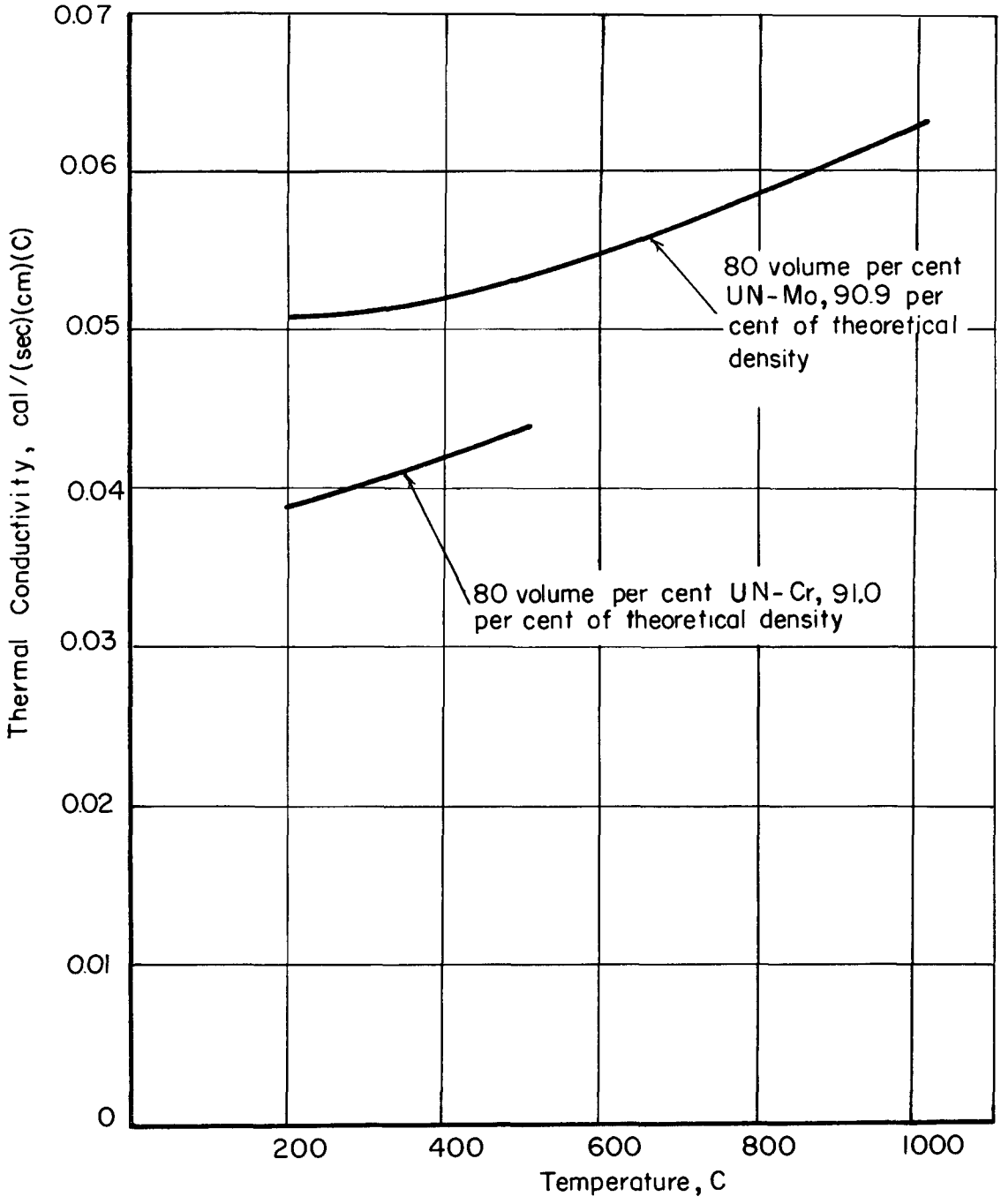

FIGURE D2. THERMAL CONDUCTIVITY OF UN CERMETS AEA-43234

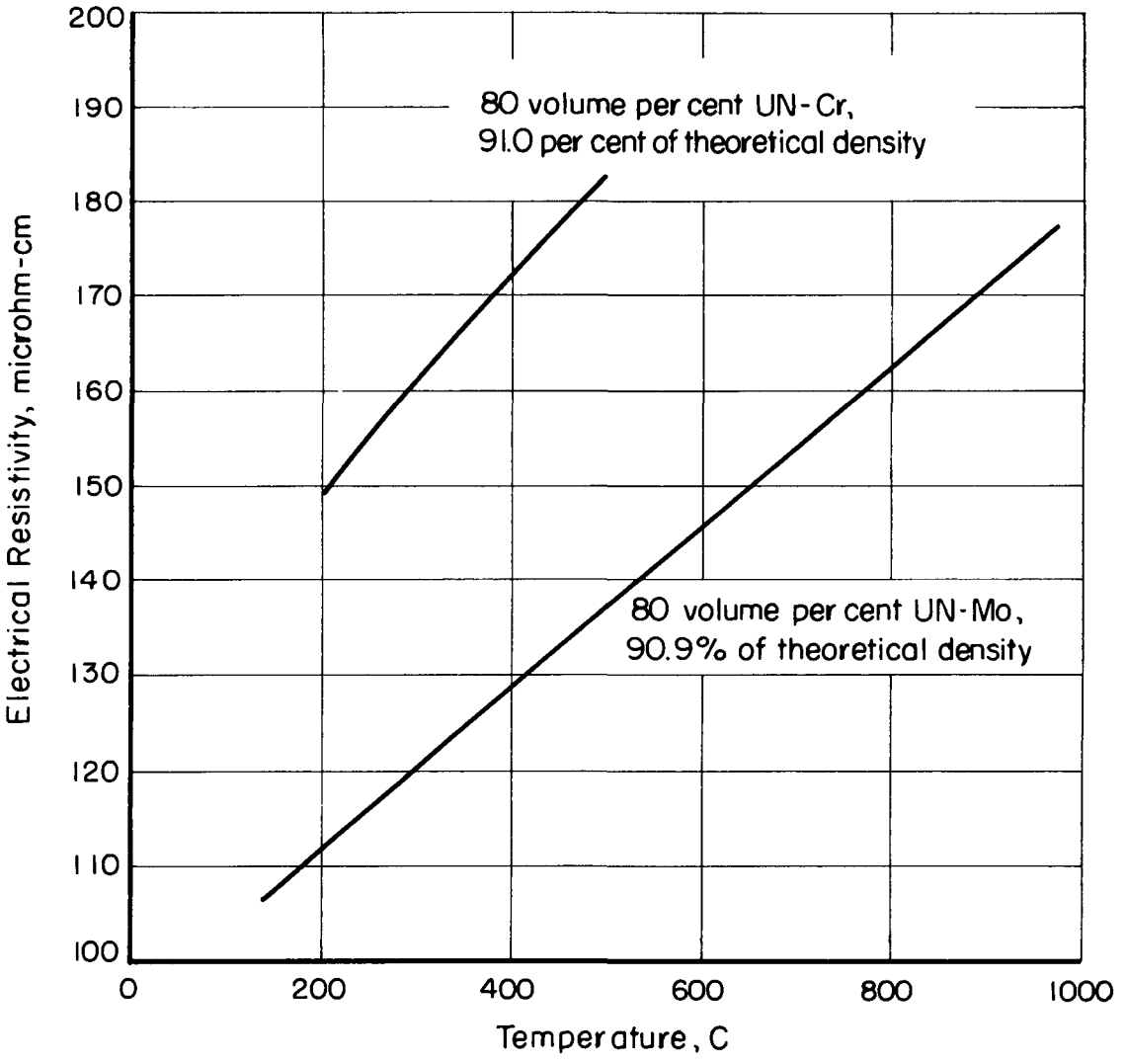

FIGURE E1. ELECTRICAL RESISTIVITY[1,4]

AEA-43212

K. References

(1) Kizer, D. E., BMI, Unpublished Data.

(2) Dayton, R. W., and Dickerson, R. F., "Progress Relating to Civilian Applications During April, 1962", BMI-1577 (May 1, 1962).

(3) Dayton, R. W., and Tipton, C. R., Jr., "Progress Relating to Civilian Applications During May, 1961", BMI-1518 (June 1, 1961).

(4) Dayton, R. W., and Tipton, C. R., Jr., "Progress Relating to Civilian Applications During August, 1961", BMI-1541 (September 1, 1961).

UO_2 CERMETS

Compiled by D. Kizer

A1. Chemical composition[1]

Cermets of UO_2 have been successfully fabricated containing 60 to 90 volume per cent UO_2 dispersed in matrix materials of molybdenum, chromium, niobium, and Type 302B stainless steel, resulting in a weight loading of UO_2 between 61 and 94 w/o, depending on the matrix material used.

3. Effect of impurities

No data available

B1. Density (room temperature)

Calculated theoretical densities range from 9.44 to 10.81 g per cm^3, depending on the volume loading of UO_2 and the matrix material used. Below are calculated densities of 80 volume per cent UO_2 cermets with the four matrix materials.

Matrix Metal	Calculated Density, g per cm^3
Molybdenum	10.81
Niobium	10.47
Chromium	10.20
Type 302B stainless steel	10.24

2. Density versus temperature

No data available

3. Uranium content

0.882 x w/o UO_2 x density (see Fuel Comparison Table).

4. Liquidus temperature

No data available

5. Solidus temperature

No data available

6. Vapor pressure

No data available

7. Thermal expansion[1]

Thermal-expansion data have been reported for chromium-, molybdenum-, and Type 302B stainless steel-UO_2 cermets:

Nominal UO_2 Content, Volume per cent	Matrix Metal	Cermet Density, per cent of theoretical	Thermal-Expansion Coefficient (20-950 C), 10^{-6} per C
80	Molybdenum	94.4	8.8 to 9.2
80	Chromium	97.1	10.2 to 10.4
80	Type 302B stainless	98.4	11.2 to 11.5
70	Type 302B stainless	97.0	11.3 to 11.7
70	Molybdenum	91.7	7.9 to 8.3

C1. Hardness

No data available

2. Hot hardness

No data available

3. Modulus of rupture[1]

Modulus of rupture has been measured on chromium-, molybdenum-, and Type 302B stainless-80 volume per cent UO_2 cermets:

Matrix Metal	Cermet Density, per cent of theoretical	Modulus of Rupture, psi
Molybdenum	91.6	12,000
	90.7	13,800
	88.5	12,100
Type 302B stainless	96.5	18,100
	97.4	17,200
	94.4	13,300
Chromium	96.5	22,500
	97.0	20,600
	95.5	21,600

4. Compressive yield strength[1]

See Figures C4a, C4b, and C4c.

5. Compressive strength[1]

See Figures C4a, C4b, and C4c.

6. Creep strength

No data available

7. Young's modulus[1]

See Figures C4a, C4b, and C4c.

8. Shear modulus

No data available

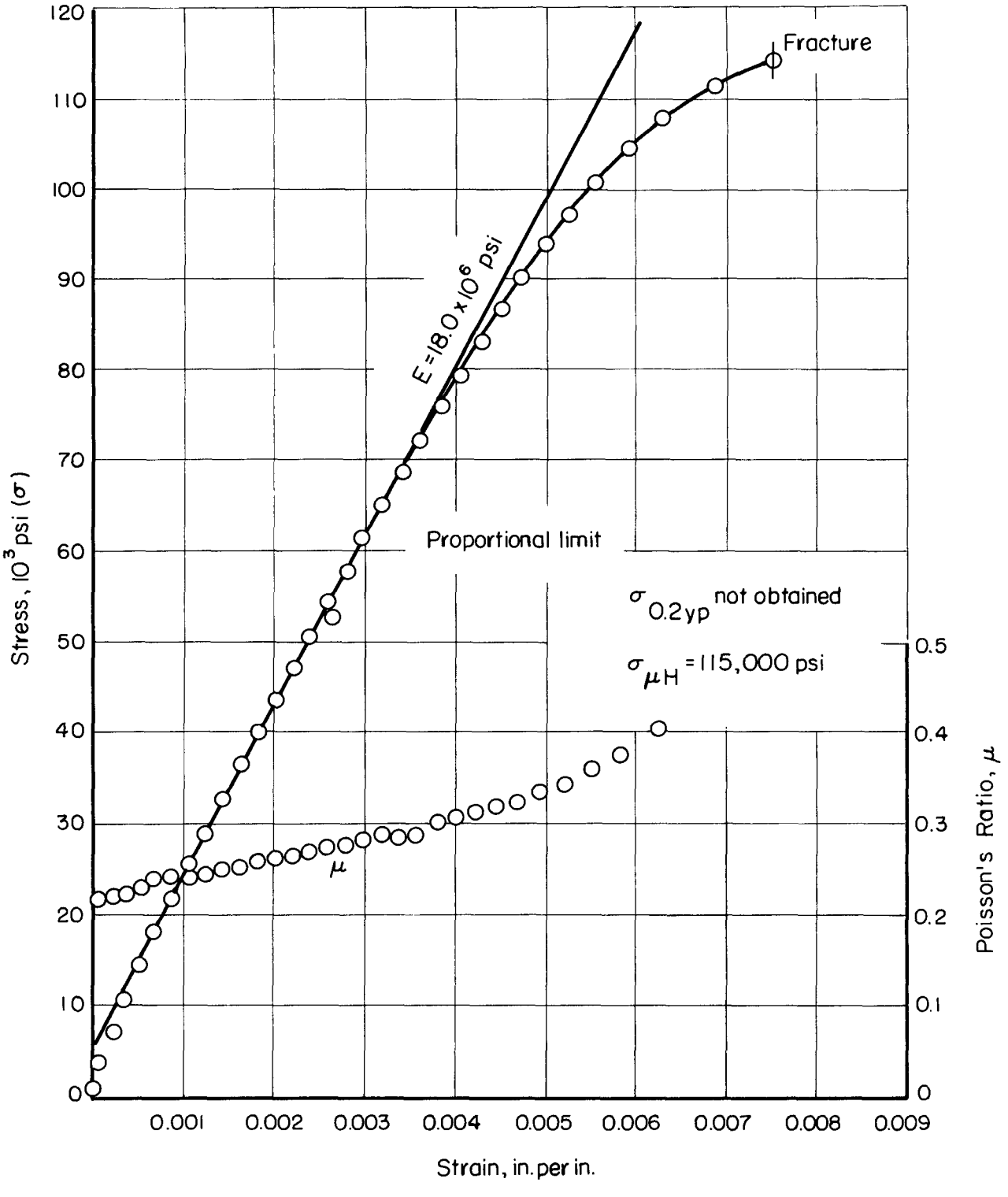

FIGURE C4a. COMPRESSIVE TEST ON AN 80 VOLUME PER CENT UO_2-STAINLESS STEEL CERMET WITH A DENSITY 96.5 PER CENT OF THEORETICAL DENSITY

AEA-43215

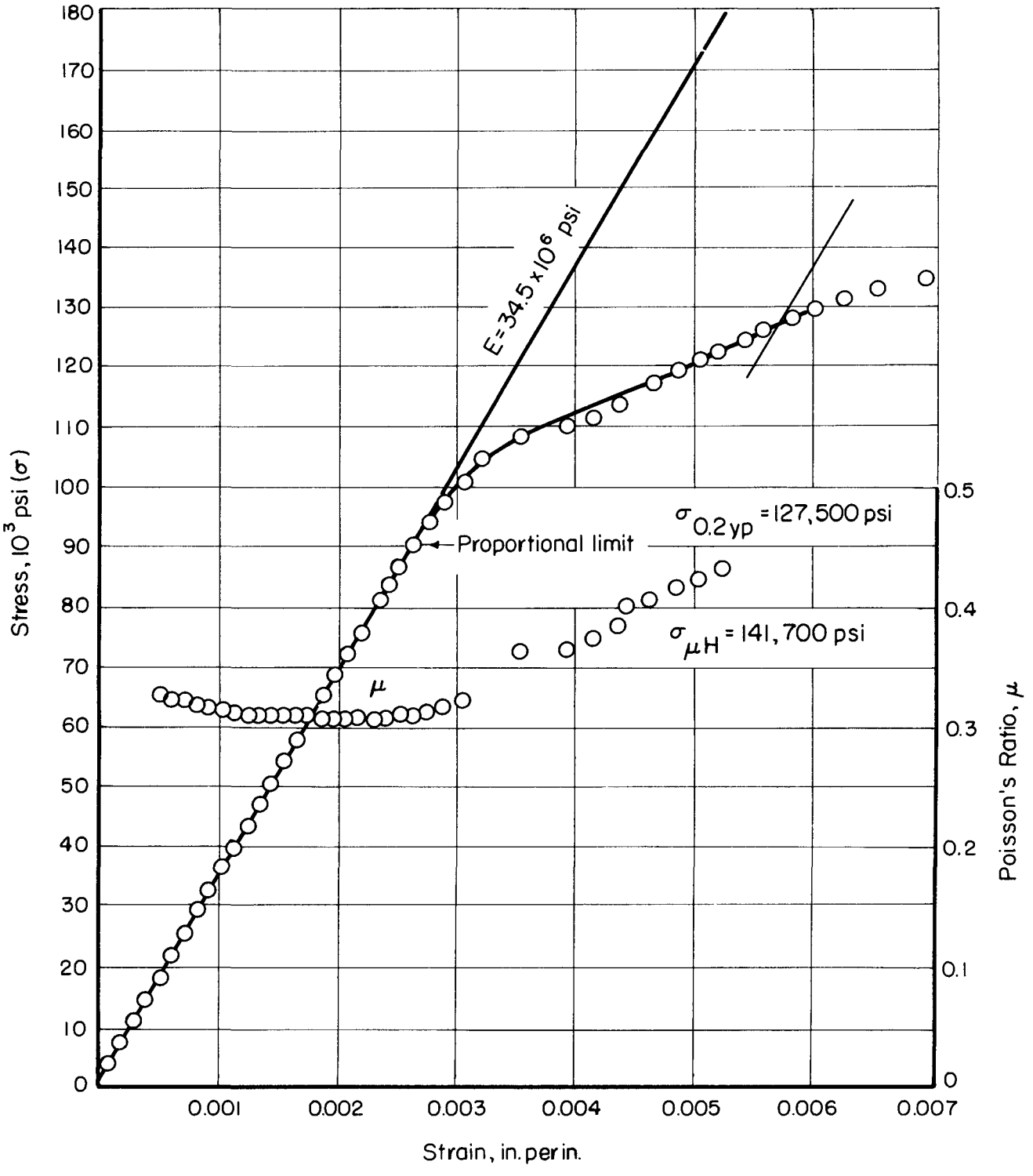

FIGURE C4b. COMPRESSIVE TEST ON AN 80 VOLUME PER CENT UO_2-CHROMIUM CERMET WITH A DENSITY 97.0 PER CENT OF THEORETICAL[1]

AEA-43216

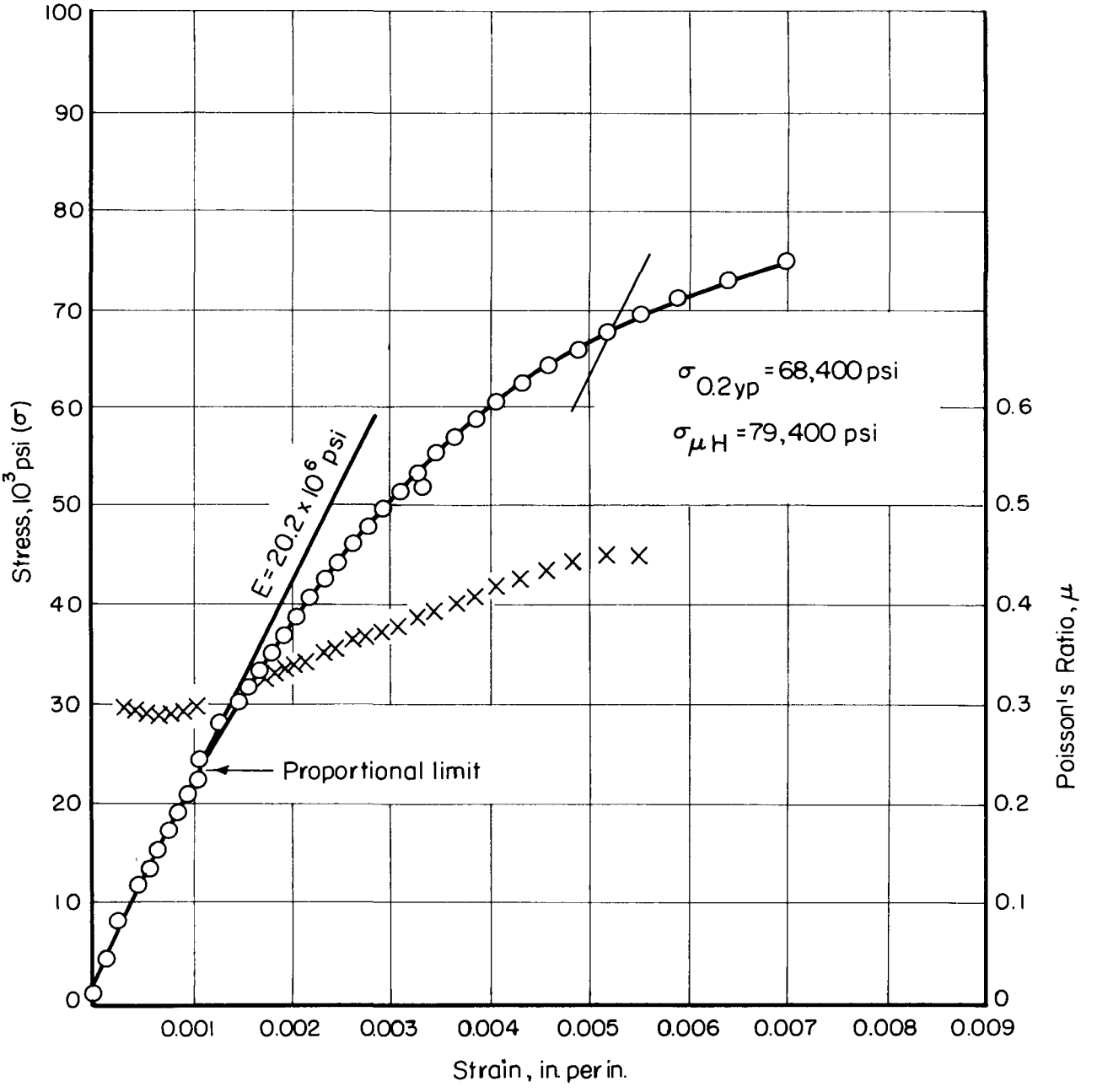

FIGURE C4c. COMPRESSIVE TEST ON AN 80 VOLUME PER CENT UO_2-MOLYBDENUM CERMET WITH A DENSITY 90.7 PER CENT OF THEORETICAL[1]

AEA-43217

9. Bulk modulus

No data available

10. Poisson's ratio[1]

See Figures C4a, C4b, and C4c.

11. Elongation

No data available

D1. Specific heat

No data available

2. Thermal conductivity[1]

See Figure D2.

E1. Electrical resistivity[1]

See Figure E1.

F1. Reaction of base material[2,3]

a. If the structure is not defected one would expect the reaction to be similar to the reaction with the base metal used until such time as the UO_2 was exposed.

b. A 0.006-in. cladding-defected hole has been drilled into a capsule of UO_2 and a capsule of chromium-80 volume per cent UO_2 to compare oxidation at 1750 F in air. Both cores were of equal volume and had densities approximately 96 per cent of theoretical. Following is a tabulation of the oxidation of UO_2 determined after 24 and 144 hr at temperature.

	Oxidation of UO_2, per cent	
	After 24 Hr	After 144 Hr
UO_2	48.2	60.6
Chromium-80 volume per cent UO_2 cermet	2.5	7.7

2. Reactions with claddings or structural materials

Any cladding that is compatible with UO_2 and the matrix metal used should be suitable from a compatibility standpoint.

G1. Dimensional stability[4]

A 95 to 96 per cent dense 80 volume per cent UO_2-niobium cermet clad with niobium irradiated at an average surface and center temperature of 925 and 1400 C (peak 1000 and 1500 C), respectively, to a burnup of approximately 3 per cent of the total uranium atoms (7.0×10^{20} fissions per cm^3) showed a 1.4 per cent decrease in density and 0.2 per cent growth in length and 0.7 per cent in diameter.

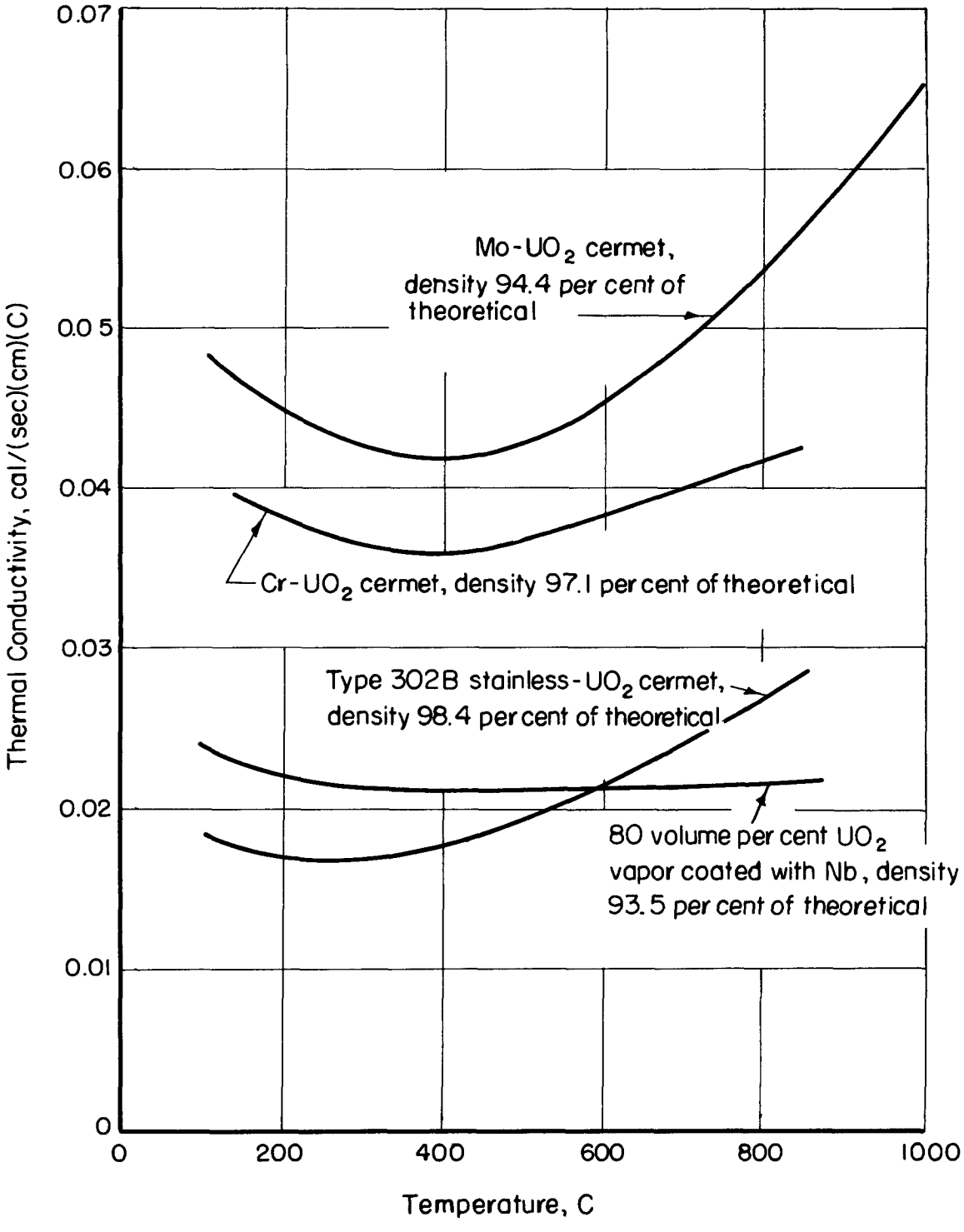

FIGURE D2. THERMAL CONDUCTIVITY OF UO_2 CERMETS [1]

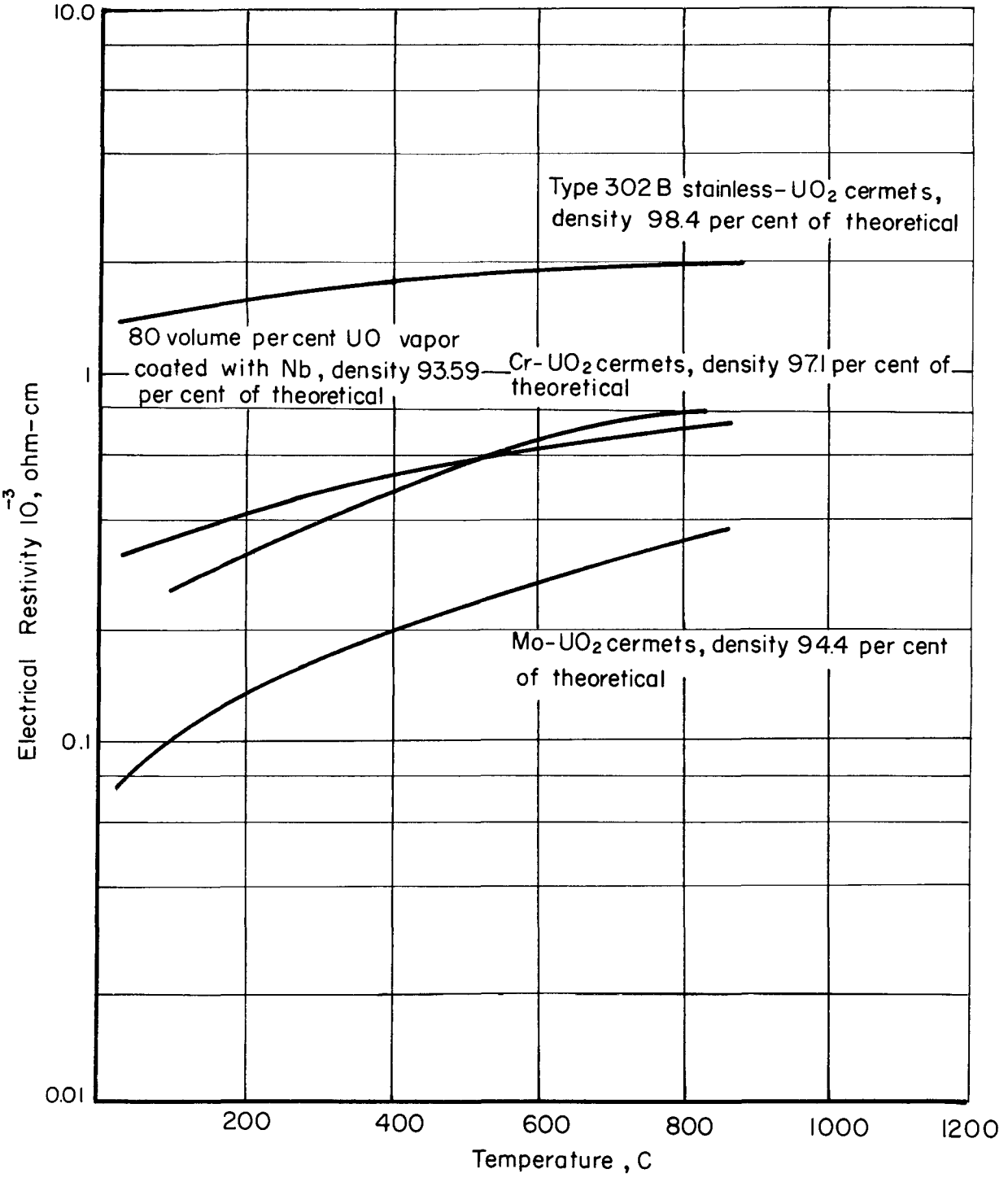

FIGURE E1. ELECTRICAL RESISTIVITY OF 80 VOLUME PER CENT UO_2 CERMETS[1]

AEA-43211

2. **Fission gas release**

No data available

3. **Swelling temperature data**

See G1.

4. **Unusual nuclear properties**

No data available

5. **Property changes as a result of irradiation**

No data available

H. References

(1) Paprocki, S. J., Keller, D. L., Cunningham, G. W., and Kizer, D. E., "Preparation and Properties of UO_2 Cermet Fuels", BMI-1487 (December 19, 1960).

(2) Paprocki, S. J., Keller, D. L., and Pardue, W. M., "Study of Experimental Fuel Bodies Made From Alumina-Coated UO_2 Particles", BMI-1586 (July 16, 1962).

(3) Kizer, D. E., BMI, Unpublished Data.

(4) Lozier, E. D., BMI, Unpublished Data.

COATED-PARTICLE FUELS

COATED-PARTICLE FUEL MATERIALS

Compiled by J. H. Oxley

Extensive property data on coated-particle fuels are unavailable owing to the relatively recent development of these materials. However, since this type of fuel holds considerable promise for gas-cooled reactors, it does appear desirable to summarize and tentatively interpret the limited data available. Therefore, the current status on the manufacture, properties, and performance of these new fuels is discussed in this section.

Sufficient information has been obtained for preliminary design purposes.

Preparation and Properties of Coated-Particle Fuels

M. F. Browning

Coatings of Al_2O_3, pyrolytic carbon, BeO, and MgO on UO_2 particles are being evaluated to determine their utility as fission-product and reaction barriers. Pyrolytic-carbon coatings on UC_2 and UC particles are also being evaluated for this purpose.

Chemical vapor-deposition reactions in fluidized beds of the particles are being used to apply coatings to particles 50 to 600 μ in diameter. Larger particles up to 1/8 in. in diameter and materials difficult to fluidize have been agitated by vibrating and/or tumbling during the coating operation. Although present experience has been limited mainly to the coating of particles in the 50-μ to 1/8-in.-diameter size range, there is reason to believe that this range can be extended. In general, the maximum coating thickness which can be applied is governed only by economic considerations.

Alumina and beryllia are formed by the hydrolysis of their respective chlorides with either steam or a CO_2:H_2 mixture as the hydrolyzing agent. The steam hydrolysis of MgI_2 is used for depositing MgO. In addition, the formation of these oxides by the thermal decomposition of metal organics has received limited attention. Pyrolytic carbon is formed generally by the decomposition of C_2H_2 and CH_4, but the use of other hydrocarbons has been investigated.

Alumina coatings of near theoretical density deposited at a temperature of 1000 C have good integrity and consist of small crystallites of alpha alumina with an average size of 0.3 μ dispersed in an amorphous matrix. Coatings deposited at temperatures from 500 to 700 C are porous, of lower density, and completely amorphous, but become crystalline on heat treating at temperatures of about 1000 C and above. Coatings prepared at 1400 C are highly crystalline, but exhibit a coating integrity inferior to that of the 1000 C coatings. The hardness of the coatings prepared at 1000 C and above is equal to or higher than that of sapphire (2200-2500 KHN, 50-g load).

The oxygen/uranium ratio of both porous and dense UO_2 substrates coated with Al_2O_3 under various conditions has tentatively been found to be 2.002, even though the ratio before coating was as high as 2.039.

Beryllia coatings prepared at 1400 C are of near theoretical density, are very crystalline, and exhibit good integrity. Coatings deposited at temperatures between 800 and 1100 C are less crystalline and porous. The hardness of the 1400 C coatings is essentially equal to that of single-crystal BeO (1200-1400 KHN, 50-g load).

Magnesia coatings deposited at 1400 C are relatively transparent, dense, and void-free. Coatings prepared at 1100 and 800 C are less transparent and appear to contain submicron pores. The hardness of the coatings is not significantly affected by coating temperature and is slightly less than that of fused MgO (925-975 KHN, 50-g load). The differential between the thermal expansion of UO_2 and MgO can result in cracked coatings, but this problem has been essentially overcome by the use of porous UO_2 or the incorporation of an annular void in the particle. All MgO coatings have failed to withstand oxidation at 1100 C. Recent investigations have tentatively indicated that oxygen diffusion is the major cause of failure.

Pyrolytic-carbon coatings with good integrity have been applied to fuel particles at temperatures of 950 to 2000 C. The PyC structure of a 1400 C coating varies from columnar to laminar, depending on the deposition rate. Coatings applied at under 10 μ per hr are definitely columnar and those deposited above 30 μ per hr are decidedly laminar. The density of the PyC coatings prepared by the fluidized-bed techniques decreases from 1.99 g per cm^3 at a coating temperature of 950 C to a minimum value of approximately 1.50 g per cm^3 at 1500 C and then increases to a density of 1.94 g per cm^3 at a temperature of 1800 C. The crystallite size of PyC coatings prepared in a fluidized bed varies with coating temperature and type (columnar or laminar). The c-axis crystallite size of laminar coatings deposited at 1400 C and below is about 25 A and increases to 150 A at a coating temperature of 1800 C. Columnar coatings prepared at below 1400 C have a crystallite size of about 40 A.

Graphite-Matrix Elements Containing Coated-Particle Fuels

M. C. Brockway

The development of coated-particle fuels is current, thus property data on dispersions of such fuel in graphite are very limited. However, certain generalizations concerning expected properties are possible. Many properties of fueled graphite should be similar whether coated or uncoated fuel is the dispersed phase. This will be true if comparison is made on the basis of equal volume loading, since particle coatings can add appreciably to the fuel volume. The primary differences expected of graphite fueled with coated-particle fuel versus uncoated fuel are: (1) high fission-product retention, (2) absence of fission-fragment damage to the matrix, (3) altered nuclear properties dependent upon the type and amount of coating material, and (4) operating-temperature limits dependent upon the type of coating as well as the fuel. For a given fuel loading, composite properties will be altered by the replacement of matrix volume with coating. Also, matrix properties or geometries may differ from those of uncoated fuel dispersions because of fabrication requirements imposed by coated fuel, as discussed in the following paragraph.

Graphite fueled with coated-particle fuel promises outstanding fission-product retention, but only if the fuel is undamaged during dispersion in the matrix graphite. Early work by several investigators[1-3] has shown that coated-particle fuels may be

readily damaged through impact or localized stresses. The dispersion and forming methods usually employed with uncoated fuels are damaging to coated-particle fuels. However, studies directed toward the solution of this dispersion problem have been successful. A hot-press technique[4] has been sufficiently successful in minimizing fuel damage during forming of graphite compacts fueled with PyC-coated $(Th,U)C_2$ that it is being used to prepare HTGR prototype fuel elements. A second method[5], fuel dispersion by matrix pelletizing, has permitted the dispersion of Al_2O_3-coated UO_2 in graphite without evidence of fuel damage. Such pelletizing also permits a closer approach to an ideal fuel-particle dispersion than previously possible.

Property data typical of HTGR graphite-matrix fuel compacts are given in Table 1. The values listed represent the most complete property data presently available for graphite matrices in which coated-particle fuels have been successfully incorporated. It should be noted that in these HTGR fuel compacts it is not essential that the dispersed fuel be completely free from damage. The property variations as a function of coated-particle fuel loading were not reported except that fuel particle size (50 to 500 μ) and fuel loading (0 to 22 w/o thorium plus uranium) had little, if any, effect on the thermal expansion of fueled compacts. These data should not be interpreted as being generally representative of properties of all graphite matrices in which coated-particle fuels may be incorporated.

TABLE 1. TYPICAL PROPERTIES OF GRAPHITE-MATRIX FUEL COMPACTS[4]

Graphite density	1.90-1.95 g per cm^3
Crushing strength	
Transverse	8500 psi
Longitudinal	7500 psi
Thermal expansion at 1000 C	
Transverse	7.5×10^{-6} per C
Longitudinal	2.25×10^{-6} per C
Thermal conductivity at 2000 C (radial)	0.3 w/(cm)(C) [0.07 cal/(cm)(sec)(C)]
Electrical resistivity	3.5×10^{-3} ohm-cm
Permeability (He at 1 atm)	2×10^{-3} cm^2 per sec
Pore structure	<1 per cent of porosity due to pores >1 μ in diameter
Radiation stability	$\leq$0.1 per cent contraction after 6×10^{19} fissions per cm^3 at 1100-1500 C

In-Pile Evaluations of Coated Particle Fuels

N. E. Miller and R. L. Ritzman

Ceramic-coated oxide- and carbide-base fuel particles prepared by Battelle are being evaluated for fission-gas-release characteristics[6], and coated carbide fuel particles supplied by commercial suppliers are being evaluated by ORNL[7]. Irradiation

studies of pyrolytic-carbon-coated $(U,Th)C_2$ particles are also being carried out by General Atomic. However, the primary purpose of the GA coatings is to prevent hydrolysis of the fuel during fabrication, and fission-product retention is of secondary importance. Table 2 contains a summary of the fission-gas-release data from sweep-capsule experiments conducted on these types of fuel materials at temperatures below 1200 C.

Alumina-coated UO_2 particles have shown a high degree of fission-gas retention at temperatures between 500 and 1100 C. At temperatures below 500 C, however, a rapid and severe coating failure occurs. The performance of the Lot BMI-715A material in the CFP-S-9 capsule experiment illustrates the temperature dependence of fission-gas-release characteristics of the alumina-coated fuels. In this experiment the R/B (ratio of the release rate to production rate) for xenon-133 rapidly changed from the order of 10^{-9} to 10^{-4} as the temperature was reduced from 645 C to 470 C and increased still more as the temperature was changed to 295 C.

In the one experiment conducted with beryllia-coated UO_2 at low temperature, the initial release fractions were in the order of 10^{-5} and showed little change up to 2 per cent uranium burnup. It is not definite whether this sample contained particles with cracked coatings prior to the irradiation or whether cracking occurred during the first few minutes of the irradiation.

The pyrolytic-carbon-coated UC_2 and UO_2 particles prepared by Battelle have shown initial good gas retention with a gradual increase in fission-gas release occurring as the irradiation proceeds. The CFP-S-9 experiment showed no apparent relation between coating failure and operating temperature. The overlay of pyrolytic carbon in the Lot 736B material resulted in cracking the Al_2O_3 coating, so the data from the CFP-S-10 experiment are representative of release from pyrolytic-carbon coatings protected from fission recoils from the fuel-particle surface.

Carbon-coated UC_2 particles prepared by NCC, HTM, and 3M are being evaluated at ORNL in sweep-capsule experiments at 820 C and compared with uncoated UC_2 particles. Of these experimental materials, the NCC sample has shown better fission-gas-retention characteristics than any carbon-coated particles evaluated.

Postirradiation Evaluation of Coated-Particle Fuels

R. J. Burian and R. L. Ritzman

Various types of coated particles have been evaluated after irradiation to determine the fission-product-retention properties of the coatings. Different combinations of pyrolytic carbon and high- and low-density Al_2O_3 coatings have been deposited on high- and low-density UO_2 and UC_2 particles. Parameters studied include the size, porosity, and material of the fuel particle, the thickness, porosity, and material of the coating, and the effect of heat treatment before irradiation, the irradiation temperature, the fuel burnup, and the support from a matrix on the performance of the coatings.

TABLE 2. SUMMARY OF FISSION-GAS-RELEASE DATA FROM COATED-PARTICLE FUELS IN SWEEP-GAS EXPERIMENTS

Specimen Description						CFP Irradiation Capsule	Nominal Irradiation Temperature, C	Accumulated Irradiation Time, hr	Uranium Burnup, a/o	R/B[b]		
	Fuel		Coating[a]							Kr^{85m}, Kr^{87}, and Kr^{88}[c]	Xe^{135}	Xe^{133}
Lot	Size, μ	Kind	Thickness, μ	Kind	Matrix							
BMI-4E	127	UO_2	42	Al_2O_3	Graphite	CFP-S-5	1070	47	0.2	4×10^{-6}	1×10^{-6}	5×10^{-6}
							1070	256	0.8	3×10^{-6}	4×10^{-6}	2×10^{-6}
BMI-715A	127	UO_2	42	Al_2O_3	None	CFP-S-7	100	11	0.0	--	3×10^{-4}	2×10^{-4}
							100	479	1.5	4×10^{-5}	4×10^{-5}	2×10^{-4}
							100	856	2.7	3×10^{-5}	3×10^{-5}	8×10^{-5}
BMI-715A	127	UO_2	42	Al_2O_3	None	CFP-S-9	815	18	0.1	4×10^{-9}	4×10^{-9}	4×10^{-9}
							645	94	0.3	4×10^{-9}	4×10^{-9}	4×10^{-9}
							470	170	0.5	3×10^{-6}	2×10^{-6}	1×10^{-4}
							295	421	1.3	3×10^{-5}	1×10^{-4}	3×10^{-4}
							815	597	1.9	4×10^{-5}	6×10^{-5}	3×10^{-4}
BMI-715A-HT	127	UO_2	42	Al_2O_3	None	CFP-S-11	100	8	0.0	--	--	1×10^{-4}
BMI-725D	127	UO_2	56	Al_2O_3	Graphite	CFP-S-6	1070	43	0.2	8×10^{-9}	6×10^{-9}	5×10^{-9}
							1070-440	208	0.6	3×10^{-6}	2×10^{-7}	1×10^{-6}
							750	1100	3.4	5×10^{-7}	1×10^{-6}	3×10^{-6}
BMI-736B	127	UO_2	16	Al_2O_3	Graphite	CFP-S-10	1050	42	0.2	3×10^{-8}	2×10^{-8}	6×10^{-8}
							800	421	1.3	8×10^{-6}	2×10^{-5}	4×10^{-4}
			27	Lam PyC			700	1871	5.8	--	2×10^{-4}	9×10^{-4}
BMI-845E	127	UO_2	60	BeO	None	CFP-S-3	100	4	0.0	5×10^{-5}	2×10^{-5}	5×10^{-6}
							100	758	2.4	1×10^{-5}	4×10^{-5}	2×10^{-4}
BMI-918A	200	UC_2	55	PyC	Graphite	CFP-S-2R	1070	73	0.2	1×10^{-8}	2×10^{-8}	3×10^{-8}
							1070	81	0.3	2×10^{-4}	1×10^{-4}	3×10^{-3}
							1070	227	0.7	5×10^{-3}	5×10^{-4}	5×10^{-3}
BMI-918A	200	UC_2	55	PyC	None	CFP-S-9	815	18	0.1	3×10^{-9}	3×10^{-9}	3×10^{-9}
							645	220	0.7	3×10^{-6}	2×10^{-6}	2×10^{-5}
							815	597	1.9	5×10^{-5}	6×10^{-5}	3×10^{-4}
BMI-1010A	127	UO_2	66	PyC	Graphite	CFP-S-8	1050	9 19	0.1	3×10^{-8}	4×10^{-8}	5×10^{-8}
							1050	349	1.1	2×10^{-5}	1×10^{-5}	4×10^{-5}
							850	1409	4.4	3×10^{-5}	5×10^{-5}	3×10^{-4}

TABLE 2. (Continued)

Specimen Description						CFP Irradiation Capsule	Nominal Irradiation Temperature, C	Accumulated Irradiation Time, hr	Uranium Burnup, a/o	R/B(b)		
	Fuel		Coating(a)									
Lot	Size, μ	Kind	Thickness, μ	Kind	Matrix					Kr^{85m}, Kr^{87}, and Kr^{88}(c)	Xe^{135}	Xe^{133}
HTM-1	200	UC_2	90	Col-PyC	None	B9-7	820	1000	12.0	4×10^{-5}	6×10^{-5}	3×10^{-4}
3M-SP-2	200	UC_2	90	Lam-PyC	None	C1-7	820	500	15.0	3×10^{-4}	2×10^{-4}	5×10^{-4}
NCC-AD	200	UC_2	90	Duplex-PyC	None	B9-8	820	480	14.7	9×10^{-6}	2×10^{-5}	7×10^{-5}
3M-101-U	200	UC_2		None	None	C1-8	820	500	4.3	6×10^{-3}	8×10^{-3}	7×10^{-2}

(a) Listed in order of preparation in the case of multiple coatings.

(b) Rate of release of isotope divided by rate of generation, values listed are the release ratios at end of indicated time, except for the last four materials where values listed are average values over the indicated time period.

(c) Data are an average of the release fraction of the three krypton isotopes.

The coated particles were irradiated in static capsules containing a helium atmosphere. Postirradiation studies included analyses of samples of gases released from the particles irradiated in static helium atmospheres, leaching of the uranium from irradiated specimens with nitric acid to determine the number of particles with failed coatings, heat treatment to determine fraction of gas retained in particles with failed coatings, and metallographic examination to study structural changes in the particles.

Sixty specimens comprising 12 types of coated particles have been irradiated at Battelle. All but a few of these specimens were removed from the capsules after irradiation and were examined. The results of postirradiation examinations of all specimens and in some instances the results of in-pile gas measurements are presented in Table 3.

The 60 specimens were irradiated at 100 to 1070 C to burnups ranging up to 5.0 per cent of the uranium. The results of the postirradiation gas-release studies indicate, in general, that dense Al_2O_3 coatings experience nearly complete failure at 100 C but perform much better at 1070 C. Coatings with a porous Al_2O_3 layer between two dense Al_2O_3 layers perform better at 100 C than fully dense Al_2O_3 coatings, but their performance does not improve at the elevated temperature. Studies indicate that there is not a significant improvement in gas-retention ability of particles dispersed in a graphite matrix. The results of analyses of acid solutions used to leach the specimens indicate in a number of cases a greater degree of coating failure than was indicated by the postirradiation gas-release studies. An investigation into the source of the lack of agreement between these two techniques has not yet resolved this discrepancy.

The results of postirradiation examinations of gas release from pyrolytic-carbon-coated particles are less consistent than data from examinations of alumina-coated particles. However, in general, the data indicate that pyrolytic-carbon coatings fail more severely than Al_2O_3 coatings at 100 to 1070 C.

The investigations of coated particles conducted at Oak Ridge have been concerned with pyrolytic-carbon-coated UC_2 particles. The thickness of the coatings on the particles studied have been as large as 161 μ. Coated particles have been irradiated in both the unsupported condition and supported in a graphite matrix. Coated-particle specimens have been irradiated at temperatures ranging from 475 to 1425 C and to burnups as high as 7.2×10^{20} fissions per cm^3. After irradiation, gas release from the particles was measured at room temperature and at elevated temperatures as high as 2050 C.

The results of these studies indicate that gas release is independent of the irradiation exposure within the range investigated. However, the gas release is temperature dependent, gas release increasing with irradiation temperature. It was concluded that the fission-gas release from the pyrolytic-carbon-coated particles occurs by diffusion through the coatings. A diffusion coefficient of 1.41×10^{-10} cm^2 per sec was determined for the release of Xe^{133} through the coatings of Type HTM-1 particles. It was also observed that the crushing strength of these particles was increased during irradiation.

The studies being conducted by General Atomic have dealt primarily with pyrolytic-carbon-coated UC_2 particles irradiated in graphite matrices. Particles with coatings ranging in thickness from 10 to 60 μ have been irradiated in six capsules to

TABLE 3. SUMMARY OF RESULTS OF POSTIRRADIATION EXAMINATION OF COATED-PARTICLE SPECIMENS

Coated Fuel Lot	Fuel		Coating[a]		Irradiation Capsule	Matrix Support[b]	Irradiation Temperature, C	U^{235} Fission Burnup, per cent	Fractional[c] Xe^{133} Release, ppm	Uranium Removed in Leach, per cent
	Material	Diameter, μ	Material	Thickness, μ						
Specimens With Alumina Coatings										
BMI-4E	UO_2	127	d-Al_2O_3	8						
			p-Al_2O_3	6						
			d-Al_2O_3	28	CFP-4	None	100	2.9	8.1	28
					CFP-S-5	Graphite	1070	3.9	0.29	0.65
					CFP-S-5	Graphite	1070	3.8	--	--
BMI-715A	UO_2	127	d-Al_2O_3	42	CFP-1D	None	100	3.3	100	54
					CFP-1B	None	100	4.7	120	39
					CFP-4	None	100	3.0	100	>7
					CFP-S-7	None	100	3.9	50	5
					CFP-S-7	None	100	4.0	--	>82
					CFP-S-9	None	815-295[d]	--	--	68
					CFP-1C	None	1070	1.7	0.09	0.9
					CFP-1A	None	1070	3.2	0.02	0.2
					CFP-1D	Graphite	100	3.5	1.9	33
					CFP-1B	Graphite	100	5.0	0.7	43;38[e]
					CFP-1C	Graphite	1070	1.7	--	0.007
					CFP-1A	Graphite	1070	3.3	--	--
BMI-715A-HT	UO_2	127	d-Al_2O_3	42	CFP-S-7	None	100	3.9	0.01	95
					CFP-S-8	None	1070	4(est.)	87	--
					CFP-S-7	Graphite	100	3.6	0.39	93
					CFP-S-8	Graphite	1070	4(est.)	18,000	--
BMI-717B	UO_2	127	d-Al_2O_3	43	CFP-S-7	None	100	3.9	--	1.5
					CFP-S-8	None	1070	4(est.)	190	--
BMI-721C	UO_2	127	d-Al_2O_3	8						
			p-Al_2O_3	18						
			d-Al_2O_3	28	CFP-1D	None	100	3.4	1.8	88
					CFP-1B	None	100	4.6	15	5
					CFP-4	None	100	3.1	26	95
					CFP-1C	None	1070	1.7	4.0	3

TABLE 3. (Continued)

Coated Fuel Lot	Fuel Material	Fuel Diameter, μ	Coating[a] Material	Coating Thickness, μ	Irradiation Capsule	Matrix Support[b]	Irradiation Temperature, C	U^{235} Fission Burnup, per cent	Fractional[c] Xe^{133} Release, ppm	Uranium Removed in Leach, per cent
					Specimens With Alumina Coatings (Continued)					
					CFP-1A	None	1070	3.2	44	0.5
					CFP-1D	Graphite	100	3.4	--	44
					CFP-1B	Graphite	100	4.8	1.8	30
					CFP-1C	Graphite	1070	1.7	--	0.004
					CFP-1A	Graphite	1070	3.4	130	--
					CFP-1D	Carbon	100	3.0	--	33
					CFP-1B	Carbon	100	4.9	32	43
					CFP-1C	Carbon	1070	1.6	--	0.5
					CFP-1A	Carbon	1070	3.3	--	0.09
BMI-725D	UO_2	127	d-Al_2O_3	56	CFP-S-7	None	100	3.9	17	0.3
					CFP-S-6	None	1070	3(est.)	760	--
					CFP-S-6	Graphite	1070	3(est.)	34[f]	2.4
					CFP-S-6	Graphite	1070	3(est.)	--	1.8
BMI-733B	UO_2	127	d-Al_2O_3	47	CFP-S-7	None	100	3.9	--	3
					CFP-S-8	None	1070	4(est.)	28	--
					Specimens With Pyrolytic-Carbon Coatings					
BMI-918A	UC_2	200	Col PyC	55	CFP-4	None	100	3.1	190	93
					CFP-S-9	None	815-470[g]	--	--	--
					CFP-S-2	None	1070	Nil	--	--
					CFP-S-5	None	1070	3.8	5,200	21
					CFP-S-2	Graphite	1070	Nil	--	--
					CFP-S-2R	Graphite	1070	1.8	--	--
BMI-919A	UC_2	200	Lam PyC	70	CFP-4	None	100	3.2	14	--
					CFP-S-5	None	1070	3.7	7,500	55
					CFP-S-6	Graphite	1070	3(est.)	35[h]	5.7

TABLE 3. (Continued)

Coated Fuel Lot	Fuel Material	Fuel Diameter, μ	Coating[a] Material	Coating Thickness, μ	Irradiation Capsule	Matrix Support[b]	Irradiation Temperature, C	U^{235} Fission Burnup, per cent	Fractional Xe^{133} Release, ppm[c]	Uranium Removed in Leach, per cent
				Specimens With Pyrolytic-Carbon Coatings (Continued)						
BMI-920A	UO_2	127	Lam PyC	45	CFP-4	None	100	3.4	220	30
					CFP-S-7	None	100	3.7	70	3
					CFP-S-5	None	1070	3.8	19,000	66
					CFP-S-6	Graphite	1070	3(est.)	470	90
BMI-921	UO_2	127	d-Al_2O_3[i]	48						
			Mix PyC	32	CFP-1D	None	100	3.1	48	46
					CFP-1B	None	100	4.9	16	2.2
					CFP-1C	None	1070	1.6	0.13	7.2
					CFP-1A	None	1070	3.3	0.04	3.0
BMI-1010A	UO_2	127	Lam PyC	66	CFP-S-7	None	100	3.6	--	0.1
					CFP-S-8	None	1070	4(est.)	15,000	--
					CFP-S-8	Graphite	1070	4(est.)	--	--
3M-10695-47	UC_2	--	PyC	48-161	--	None	--	--	1825 C:.003%[j] 2050 C:29%[k] 1960:nil[l]	
3M-SP-2	UC_2	250	PyC	82	--	None	475-980	7.2×10^{20} f per cm^3	--	5% failed by visual exam
					LCP-2	None	1260-1315	3.8×10^{20} f per cm^3	2000 Kr-85 500-900 Xe-133	0.6 to 10
3M (Pellet 1080)	UC_2	--	PyC	--	MTR-48-5	Graphite	840-1425	17	--	--
HTM-1	UC_2	--	PyC	109	B9-7	None	815-900	1.56×10^{20} f per cm^3	--	--
					LCP-1	None	1065-1150	3.8×10^{20} f per cm^3	100 to 1000 Kr	2 to 22
NCC-AD	UC_2	--	PyC	100-103	--	None	815	--	--	--
GA	UC_2	--	PyC	10-15	GA-309-7	Graphite	1000-1700	0.82×10^{20} f per cm^3	--	--

TABLE 3. (Continued)

Coated Fuel Lot	Fuel Material	Fuel Diameter, μ	Coating[a] Material	Coating Thickness, μ	Irradiation Capsule	Matrix Support[b]	Irradiation Temperature, C	U^{235} Fission Burnup, per cent	Fractional[c] Xe^{133} Release, ppm	Uranium Removed in Leach, per cent
					Specimens With Pyrolytic-Carbon Coatings (Continued)					
GA	UC_2	--	PyC	25	GA-309-4, -5, -6	Graphite	850-1950	1.2×10^{20} f per cm^3	--	--
GA	UC_2	--	PyC	50-60	GA-309-8	Graphite	1200-2050	0.82×10^{20} f per cm^3	--	--
					GA-309-9	Graphite	1250-1600	0.82×10^{20} f per cm^3	--	--

(a) In order of deposition. Code used is as follows:
- d-Al_2O_3: Essentially fully dense Al_2O_3 layer.
- p-Al_2O_3: Relatively porous Al_2O_3 layer.
- Col PyC: Pyrolytic carbon with a columnar or radially oriented structure.
- Lam PyC: Pyrolytic carbon with a laminar or circumferentially oriented structure.
- Mix PyC: Pyrolytic carbon with a mixed columnar and laminar structure.

(b) Three conditions of matrix support existed:
1. None: no support from a matrix.
2. Graphite: support afforded by a relatively graphitized matrix.
3. Carbon: support afforded by a relatively ungraphitized matrix.

(c) Ratio of fission product detected to total amount present at time of sampling.

(d) Step-temperature capsule. Initial irradiation temperature was 815 C. This was lowered successively at about 2-day intervals to 645, 470, and 295 C.

(e) This specimen consisted of two fueled-graphite pellets. Leach of one pellet as recovered from the capsules yielded 43 per cent uranium recovery. Second pellet was heated to 815 C at which temperature 270 ppm of Kr^{85} was driven off. Subsequent leach of second pellet yielded 38 per cent of uranium recovery.

(f) This specimen consisted of two fueled-graphite pellets. Analysis of gases sampled from within the specimen can after irradiation indicated 30 ppm of Xe^{133} was released by both pellets. Subsequent heating of one pellet to 540 C drove off an additional 1.4 ppm of Xe^{133}.

(g) Step-temperature capsule. Initial irradiation temperature was 815 C. This was lowered successively at approximately 2-day intervals to 645 and 470 C.

(h) This specimen consisted of two fueled-graphite pellets. Analysis of gases sampled from within the specimen can after irradiation indicated 30 ppm of Xe^{133} was released by both pellets. Subsequent heating of one pellet to 540 C drove off an additional 33 ppm of Xe^{133}.

(i) Alumina coating was cracked prior to irradiation as a result of overcoating with pyrolytic carbon.

(j) Heat treated at 1825 C for 90 hr. When the temperature was increased to 2290 C, the gas release increased.

(k) Heat treated at 2050 C for 103 hr; gas release detected after 37 hr of heating.

(l) Heat treated at 1960 C for 140 hr.

burnups of 0.82×10^{20} to 1.2×10^{20} fissions per cm^3. Irradiation temperatures ranged between 850 and 2000 C. Only in-pile gas-release data have been reported. Within the limits tested, gas release varied from about 1 per cent at the beginning of irradiation to near 100 per cent at the end of irradiation. The gas release appeared to be temperature independent but there may be a delayed temperature effect. Activation energies for fission-gas release were calculated. They ranged from 24.1 to 29.1 kcal per mole for four krypton isotopes and from 33.4 to 45.8 kcal per mole for two xenon isotopes.

References

(1) "40MW(E) Prototype High-Temperature Gas-Cooled Reactor Research and Development Progress", GA-1982 (July 1961), p 7.

(2) Parker, W. E., "Development of Graphite Matrix Fuel Elements", Trans. Am. Nuclear Soc., 4 (2), 343 (November, 1961).

(3) "Interum Status Report Phase III Graphite-Matrix Nuclear Fuel Elements", National Carbon Company, ORO-481 (June 30, 1961), p 17.

(4) Goeddel, W. V., "The Development and Evaluation of Graphite-Matrix Fuel Compacts for the HTGR", GA-2289 (August 8, 1961).

(5) Dayton, R. W., and Dickerson, R. F., "Progress Relating to Civilian Applications During February, 1962", BMI-1569 (Del) 11 (March 1, 1962), p L-10.

(6) Dayton, R. W., and Dickerson, R. F., "Progress Relating to Civilian Applications During September, 1962", BMI-1593 (Del.) (September 1962).

(7) Harms, W. O., "Coated Particle Fuel Element Development Activity Letter for the Period March 15 to May 15, 1962", CF-62-6-75 (June 29, 1962).

CONVERSION EQUIVALENTS

CONVERSION EQUIVALENTS

Length

mm	cm	in.	ft
1	0.1	0.03937	0.003281
10	1	0.3937	0.03281
25.40	2.54	1	0.08333
304.8	30.48	12	1

Area

mm^2	cm^2	$in.^2$	ft^2
1	0.01	1.550×10^{-3}	1.0764×10^{-5}
100	1	0.1550	1.0764×10^{-3}
645.2	6.452	1	6.944×10^{-3}
92,900	929	144	1

Volume

mm^3	cm^3	$in.^3$	ft^2
1	0.001	6.102×10^{-5}	3.5314×10^{-8}
1,000	1	0.06102	3.5314×10^{-5}
16,387.2	16.3872	1	5.7870×10^{-4}
2.832×10^{7}	2.8320×10^{4}	1728	1

Note: 1 British dry butt = 0.5781 cubic meter.

Mass

1 g = 0.002205 lb (avoir)
1 lb = 453.59 g
1 ton, US (short) = 2000 lb (avoir) = 0.8929 ton long = 0.9072 metric ton or tonne

Density

g/cm^3	$lb/in.^3$	lb/ft^3
1	0.03613	62.43
27.68	1	1,728
0.01602	0.0005787	1

Pressure

atm	mm Hg	$lb/in.^2$
1	760	14.70
1.316	1000	19.34
0.06804	51.710	1

Energy

Joules	w-hr	Btu	g-cal
1	2.7778×10^{-4}	9.486×10^{-4}	0.239
3.6×10^{3}	1	3.415	860.445
1054	0.2928	1	252

CONVERSION EQUIVALENTS
(Continued)

Thermal Conductivity

g-cal/(sec)(cm^2) (C per cm)	w/(cm^2) (C per cm)	g-cal/(hr)(cm^2) (C per cm)	Btu/(hr)(ft^2) (F per in.)	Btu/(hr)(ft^2) (F per ft)
1	4.183	3600	2903.0	241.917
0.2391	1	860.6	694.0	57.833
2.78×10^{-4}	1.162×10^{-3}	1	0.8064	0.0672
3.445×10^{-4}	1.440×10^{-3}	1.240	1	0.08333
4.13×10^{-3}	0.0173	14.880	12	1

Resistivity

1 microhm-in. = 2.5400 microhm-cm
1 microhm-cm = 0.3937 microhm-in.

Fission Units

1 g of uranium fissioned = 0.919 megawatt-day (MWD)
1 a/o uranium burnup = 9190 MWD/metric ton (tonne) of uranium
1 a/o uranium burnup = 8360 MWD/U. S. ton of uranium
0.109 a/o uranium burnup = 1000 MWD/metric ton of uranium
0.120 a/o uranium burnup = 1000 MWD/U. S. ton of uranium

Cross Section

1 barn = 10^{-24} cm^2

$$\frac{\text{cm}^2}{\text{g}} = \left(\frac{\text{barns}}{\text{atom}}\right)\left(\frac{0.602}{\text{mol. wt.}}\right)$$